

Final Report for the

Study on the Modifications Required to Re-engine the Lockheed D-21 Drone

Purchase Order #H-31409D

22 October 1999

Prepared For:

George C. Marshall Space Flight Center
National Aeronautics and Space Administration
Marshall Space Flight Center, Alabama 35812

Prepared By:

Lockheed Martin Astronautics – Huntsville Operations
620 Discovery Drive
Lakeside II, Suite 200
Huntsville, Alabama 35806

TITLE: Study on the Modifications Required to Re-engine the Lockheed D-21 Drone

FOREWORD

This report was prepared by Lockheed Martin (LM) for the National Aeronautics and Space Administration (NASA) under Purchase Order Number H-31409D entitled "Study on the Modifications Required to Re-engine the Lockheed D-21 Drone". The purpose of this 45 day study contract was to investigate the feasibility of using the D-21 as a Rocket Based Combined Cycle engine test-bed. The new NASA engine is entitled "Demonstration of Rocket Combined Cycle Operations (DRACO)".

ACKNOWLEDGMENTS

The information contained in this report is the product of a research effort by Lockheed Martin in support of the NASA Marshall Space Flight Center (MSFC) Space Transportation Directorate. Special appreciation is given to Jim Turner, DRACO Program Manager and Norman Smith, the Contracting Officers Technical Representative (COTR) for providing the opportunity and the necessary resources to perform this effort. The special efforts of other NASA representatives during the course of the study are also appreciated. These NASA employees include John Cramer, D. R. Komar, Craig McArthur, Joe Lowery and Tom Brown of MSFC, Charles Trefney of Glenn Research Center (GRC) and Stephen Corda, Jake Vachon and Ross Hathaway of the Dryden Flight Research Center (DFRC)

The Lockheed Martin Team for this study included David L. Christensen (LM Astronautics-Huntsville office - Program Manager), Dimitri Thomas, (LM Skunk Works - Project Manager) and John Whittenbury (LM Skunk Works - Project Engineer). In addition, the computer modeling skills of Greg Saks (LMA-Huntsville office) and George Schnurer (LMSS) provided essential analytical support needed for this highly interactive study. Richard Webb (LMSS) provided key support needed for the cost analysis.

Executive Summary

The purpose of this study was to determine the feasibility and suitability of modifying the Lockheed Martin D-21 vehicle into a Rocket Based Combined Cycle (RBCC) engine test-bed vehicle. Four objectives were defined for the 45-day D-21 modification study contract. Provide an estimation of the:

- a) Modified vehicle performance
- b) Required engine performance
- c) Required vehicle modifications
- d) Modification cost and schedule

The study has revealed that a modified D-21, referred to as the D-21 DRACO, will be capable of demonstrating all of the operational modes (Ejector Ramjet or Air Augmented Rocket, Ramjet, and Rocket) of the RBCC engine in a single flight. The maximum ramjet ΔV achievable by the modified vehicle with the current NASA DRACO engine design is between 240 ft/s and 1,150 ft/s depending on the required duration of the final rocket mode phase. At a minimum, the vehicle is capable of achieving a maximum Mach number of 3.5. While the study has indicated that greater performance (higher Mach numbers) could be obtained, follow on work is required to substantiate these findings.

The optimal inlet design Mach number was not identified during the study. In the current NASA DRACO engine design, the inlet design Mach number is 5.0. The maximum velocities reached by the D-21 DRACO were between Mach 3.23 and 4.5. Determination of the optimal inlet design Mach number for the D-21 test-bed will increase the thrust to drag ratio of the vehicle. This will alleviate the thermal load seen by the vehicle, which is believed will be the limiting factor of the vehicle performance.

In its original form, the D-21 was a non-recoverable ramjet powered reconnaissance vehicle. Modification to a test-bed vehicle will require the addition of oxidizer tanks (mounted within the existing wet wing / fuselage fuel tanks), main landing skids, and a nose landing gear. Replacement of the original fixed geometry axis symmetric inlet with a translating axis symmetric inlet, and of course the replacement of the original ramjet engine with the NASA DRACO RBCC engine will also be required.

The Rough Order of Magnitude (ROM) estimated cost of a modification and flight test program (modifying two D-21 Drones and performing 5 test flights) is \$91.2 M (CY2000\$). This cost assumes that the D-21, DRACO engine, and B-52 mother craft are Government Furnished Equipment (GFE). The manufacturing cost for the modification of the second D-21 is estimated to be \$11.26 M, which is included in the \$91.2M estimate.

While the study has shown that a modified D-21 is capable of demonstrating in flight RBCC engine operation to a minimum Mach number of 3.5, this performance falls short of the desired speed goal of Mach 6.0. Further matching of the inlet design to the flight envelope of the modified vehicle should result in improved vehicle performance. Follow-on trajectory and engine analysis work is recommended.

Table of Contents

Forward	i
Acknowledgments	ii
Executive Summary	iii
Table of Content	iv
1.0 Introduction	1
2.0 Motivations for RBCC Engine Development	1
3.0 Study Background	1
4.0 Vehicle Performance	2
4.1 Analysis Methods	2
4.1.1 Aerodynamic Envelope Extension	3
4.1.2 Trajectory Analysis	3
4.1.2.1 OTIS Simulations	3
4.1.2.1.1 Modeling	3
4.1.2.1.1.1 Aerodynamic Performance	3
4.1.2.1.1.2 Engine Data	3
4.1.2.1.1.3 Vehicle Mass Properties	3
4.1.2.1.2 Constraints	4
4.1.2.1.3 Optimatization Goal	4
4.1.2.1.4 Results	5
4.1.2.1.4.1 Propellant Load-outs	6
4.1.2.1.4.2 Dynamic Pressure and Heating	6
4.1.2.1.4.3 Time in Modes	7
4.1.2.1.4.4 Sensitivities	8
4.1.2.2 FASTPASS	10
4.1.2.2.1 Modeling	10
4.1.2.2.1.1 Aerodynamic Performance	10
4.1.2.2.1.2 Engine Performance	11
4.1.2.2.1.3 Vehicle Mass Properties	11
4.1.2.2.2 Constraints	12
4.1.2.2.3 Optimatization Goal	13
4.1.2.2.4 Results	13
4.1.2.2.4.1 Propellant Load-outs	14
4.1.2.2.4.2 Dynamic Pressure and Heating	14
4.1.2.2.4.3 Time in Modes	16
4.1.2.2.4.4 Sensitivities	16
4.2 Results	17
4.2.1 Ramjet Delta V Performance	17
4.2.2 Propellant Performance Discrepancies	17
4.2.3 Trajectory Ramjet Dynamic Pressure Trends	18
5.0 Required Vehicle Modifications	19
5.1 Tank Modifications	19
5.2 Recovery Modifications	22
5.2.1 Conventional Landing	22
5.2.2 Parachute / Parafoil Landing	23
5.2.3 Selected Concept	24
5.3 Flight Termination System	24
5.4 Avionics Modifications	24
5.5 Electrical System Modifications	25
5.6 Actuation System Modifications	26
5.7 Environmental Control System Modifications	26
5.8 Hatch Modifications	26
5.9 NB-52B Modifications	27
6.0 D-21 DRACO Mass Properties	27
6.1 D-21 DRACO Maximum Vehicle Weight	27
6.2 D-21 DRACO Center of Gravity Travel Limits	28
6.3 D-21 DRACO Mass Properties Sheet	28

7.0	Required Engine Performance	28
8.0	Recommended Modification Schedule and Flight Test Program	30
9.0	ROM Cost Estimate	30
10.0	Study Summary	33
10.1	Initial Assumptions	33
10.2	Actual Performance and Performance Limitations	34
10.3	Increased Performance	34
11.0	Recommended Follow-on Studies	34
11.1	Continued Performance Analysis Studies	34
11.2	Aerodynamic Studies	35
11.3	Power System Requirements and Power Generation Studies	35
11.4	Structural Modification Studies	35
12.0	Additional Test Bed Capabilities	35
Appendix		37
A:	Aerodynamic Data	
B:	NASA DRACO Engine Data	
C:	Minimum Modifications Propellant Tank Layout Drawing	
D:	Traditional Landing System Layout Drawing	
E:	OTIS Trajectory Results	
E1:	NASAE3GTLOXPRA	
E2:	NASAE3GTLOXJPA	
E3:	NASAE3GTH202JPA	
E4:	NASAE3CTLOXPRB4	
E5:	NASAE3CTLOXJPB4	
E6:	NASAE3CTH202JPB4	
E7:	NASAE3CTLOXPRC1	
E8:	NASAE3CTLOXJPC1	
E9:	NASAE3CTH202JPC1	
F:	FASTPASS Results	
F1:	NASAE3CTH202JP	
F2:	NASAE3CTLOXJP	
F3:	NASAE3CTLOXPR	
F4:	NASAE3GTH202JP	
F5:	NASAE3GTLOXJP	
F6:	NASAE3GTLOXPR	

1.0 Introduction

In order to achieve the NASA goal of reducing the cost of access to space, research in several advanced propulsion systems, including Rocket Based Combined Cycle (RBCC) engines, is now being performed. The Demonstration of Rocket Air-breathing Combined Cycle Operation (DRACO) is a new NASA RBCC engine program that requires ground and flight testing to gain a better understanding of this promising technology.

NASA selected Lockheed Martin to study the application of the D-21 Drone, a high-speed unmanned aircraft (no longer in service) as a potential flight-test vehicle for the DRACO engine demonstration. The D-21 Drone was developed by Lockheed Advanced Development Projects (“Skunk Works”) during the 1960’s and operated as a long range, high speed, high altitude reconnaissance system from 1966 to 1971. It was launched from both the MD-21 and the B-52 H aircraft during its operational phase. NASA has acquired several of the D-21 drones for potential research use and several more still reside in museums and storage.

2.0 Motivations for RBCC Engine Development

The continued quest for reduced launch cost requires the application of new technologies in the space transportation industry. RBCC engine development is just one of many new technologies that will enable significant launch cost reductions.

The NASA Spaceliner 100 initiative incorporates advanced technologies needed for future reusable space transportation systems with prime emphasis on safety and on lowering the cost of space access. System reliability, operability and responsiveness are also of prime interest to NASA and to our national space policy. Highly advanced, aircraft-like space transportation systems are envisioned which could operate across a broad range of operational conditions and provide rapid, on-time services for a variety of future missions and users. The technology requirements for the Spaceliner 100 initiative are now being identified and prioritized. Some technology development efforts are already underway, and new flight test vehicles are needed to demonstrate these selected technologies. A modified D-21 could fulfill many of the flight test requirements demanded by these new and emerging technologies.

Industry is also looking ahead to future aerospace launch systems. Lockheed Martin has been investigating utilizing the “ Bridge to Space “ concept as a means of greatly reducing the cost of access to space. An essential feature of this novel launch concept is the Sub-Orbital-Launch Vehicle (SOLV). The Sub-Orbital Launch Vehicle in conjunction with the orbiting space elevator exploit the natural physical phenomena of an orbiting tether to reduce the required ΔV of the sub-orbital launch vehicle to 18,000 ft/s. This reduction in the required ΔV imparted to space bound payloads, combined with the improved efficiency of the Rocket Based Combined Cycle Engine, is what allows an order of magnitude reduction in launch cost to be achieved.

3.0 Study Background

Four objectives were defined for the D-21 modification study. Provide an estimation of:

- Modified vehicle performance
- Required engine performance
- Required vehicle modifications
- Modification cost and schedule

To ensure that all of the study objectives were met, several study ground rules and initial assumptions were made in an effort to bound the study trade space and maintain focus on the key study parameters. The ground rules and initial assumptions for the study were as follows:

- Minimize structural modifications to the vehicle between fuselage stations 141 and 490
- Minimize modifications to the vehicle Outer Mold Line (OML)
- Utilize existing inlet flow path aft of fuselage section 141
- Vehicle will be air-launched from a B-52 at $M=.7$ and $h=40,000$ ft

- Vehicle gross weight not to exceed current B-52 carrier air craft weight limits
- Assume maximum operational altitude of 120,000 ft
- Assume maximum vehicle free flight weight limit is equivalent to original D-21 weight maximum free flight weight limit
- Assume maximum flight loads are equivalent to original D-21 maximum flight loads
- Assume cg travel limits are equivalent to original D-21 cg travel limits
- Assume maximum allowable dynamic pressure is equivalent to original D-21 maximum dynamic pressure
- Assume new avionics equipment will be required
- Assume new ground support equipment will be required
- Assume D-21, B-52, and NASA DRACO engine are GFE

4.0 Vehicle Performance

The focus of this study was to determine the feasibility of using the D-21 as an RBCC test bed. One of the main factors that will determine the suitability of the D-21 for this purpose is the performance of the modified vehicle. The performance goals for the modified vehicle were to demonstrate each of the RBCC engine operational modes (AAR, Ramjet, and Rocket) as well as validate the utility of each of the engine operational modes. In other words, demonstrate that accelerating in ramjet mode for a portion of the trajectory is superior (in terms of total vehicle mass required to achieve a desired final ΔV) to accelerating solely by means of the rocket mode.

4.1 Analysis Methods

Evaluation of the modified vehicle performance required extending the aerodynamic data base of the vehicle, assembling performance data for the new engine, and determining the optimal manner in which to operate the vehicle subject to the structural, thermal, and mass property limits of the modified vehicle.

4.1.1 Aerodynamic Envelope Extension

The aerodynamic database of the original D-21 covered the flight envelope from Mach 1.6 to Mach 3.5 for angles of attack from -2 degrees to 12 degrees. For this study, the original data was supplemented with low speed and higher speed data supplied by VORLAX ($0.1 < M < 1.6$) and APASS ($3.5 < M < 10.0$). Correlation between the analytical methods, which included the spike drag with the vehicle drag and the original wind tunnel data for regions of overlapping analysis, was good. This data was merged into a unitary aerodynamic database for the trajectory / performance analysis. Variation of Zero Lift Drag and Maximum Lift Coefficient with Mach number are shown below in Figure 4.1 and 4.2. The combined aerodynamic database is located in Appendix A.

Figure 4.1: C_{D0} vs Mach Number

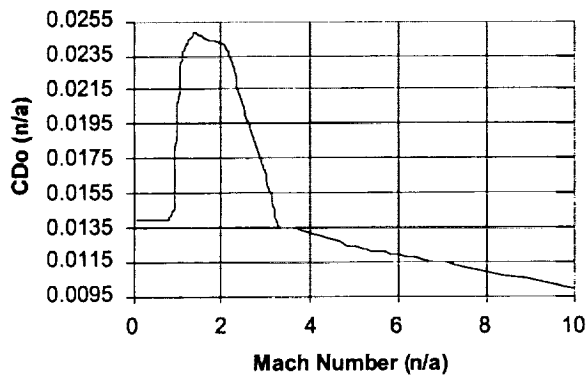
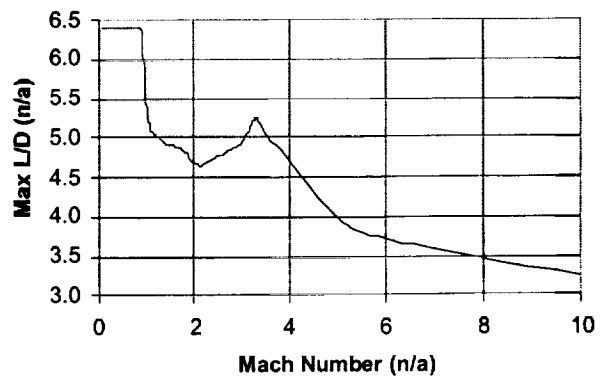


Figure 4.2: Maximum L/D vs Mach Number



4.1.2 Trajectory Analysis

Independent trajectory analysis was performed using OTIS (Optimal Trajectories by Implicit Simulation) and FASTPASS (Flexible Analysis for Synthesis, Trajectory, and Performance for Advanced Space Systems), such that a full exploration of the vehicle's potential was realized.

4.1.2.1 OTIS Simulations

OTIS (Optimal Trajectories by Implicit Simulation) was one of the two trajectory analysis tools used to evaluate the performance of the modified D-21. OTIS is capable of performing both 3 degree and 6 degrees of freedom simulations. Dynamic vehicle parameters that can affect the vehicle performance, such as center of gravity travel, can be modeled by the user and integrated into the analysis. The trajectories modeled in OTIS are divided into phases. This segmenting allows OTIS to model parameters that apply only too particular regions in the trajectory. Constraints can be applied to individual phases, or the entire flight regime. Optimization of desired performance parameters is performed subject to the user-defined constraints.

4.1.2.1.1 Modeling

4.1.2.1.1.1 Aerodynamic Data

The aerodynamic data supplied for the study was in the form of tabular data and can be found in Appendix A. Lift and drag coefficients were both supplied as functions of angle of attack and Mach number. OTIS determines conditions occurring between the supplied data points through linear interpolation.

4.1.2.1.1.2 Engine Data

Initial and Final RBCC engine decks were supplied by NASA during the study for three different propellant combinations: Liquid Oxygen (LOX) and Jet Propellant (JP), LOX and Propane, and Hydrogen Peroxide (H_2O_2) and JP. The NASA RBCC engine had three distinct operational modes: Ejector Ramjet or Air Augmented Rocket, Ramjet, and Rocket. The initial engine data was supplied for a spike to tail drag force accounting method. In the initial engine data, the ramjet mode thrust coefficient and specific impulse were supplied as a function of Mach number and the rocket performance was defined in terms of vacuum thrust and specific impulse. Ejector Ramjet data was not supplied with the initial engine data. Final engine data was supplied for a cowl to tail drag force accounting method and in terms of gross thrust. In the final engine data, the Ejector Ramjet and Ramjet engine thrust coefficients and specific impulses were supplied as functions of Mach number and altitude. The final rocket mode engine data was again defined in terms of vacuum thrust and specific impulse. The fuel flow rate for the Ejector Ramjet mode was determined by subtracting the primary oxidizer flow rate (assumed to be constant for both Ejector Ramjet and rocket modes) from the total propellant flow rate. Mass flow rate for the rocket mode was assumed to be constant (values for primary oxidizer and fuel flow rates for the given propellant combinations can be found in Appendix B). In addition to the supplied NASA data, intermediate engine data was generated from the initial NASA engine data, which defined the performance (both thrust and specific impulse) of the engine as a function of Mach number, altitude, fuel flow rate, and oxidizer flow rate. The complete engine decks can be found in Appendix B.

4.1.2.1.1.3 Vehicle Mass Properties

To run the trajectories, the separation weight and the dry weight of the vehicle had to be known. The starting point for all of the trajectories was an initial vehicle separation weight of 10,000 pounds (maximum original free flight design weight was 11,200 pounds) and a dry weight constraint of 5,500 pounds. To obtain a truly closed solution for the trajectories, the initial value for the separation weight would have to be iterated until the final vehicle weight matched the dry vehicle weight. The decision to continue to trade all propellant combinations through the end of the study made closing the trajectories impractical from a time perspective. Fortunately, for the final vehicle configurations, the dry mass constraint was approached or encountered during the simulations, thus negating the need to iterate to a closed solution.

4.1.2.1.2 Constraints

D-21 design limitations, RBCC engine characteristics, and the parameter to be optimized for the trajectory dictated the constraints placed on the trajectory simulations.

The design limitations of the D-21 set many of the global constraints. The vehicle was designed for a maximum dynamic pressure of 650 psi, so for the initial trajectories this was a global constraint (later trajectories required increasing this constraint to allow the vehicle to be flown without throttling). The maximum altitude reached by the D-21 was 95,000 ft. The ability of the vehicle's control surfaces to maintain effectiveness beyond that altitude was unknown. As a result, the absolute ceiling for the trajectories was limited to 120,000 ft. The maximum and minimum free flight maneuver load factors of the vehicle were 5.0 and -2.0 g respectively and these values were used as acceleration constraints. The fuel volume of the original D-21 was limited to 122 cubic feet. The requirement that the modified vehicle carry oxidizer as well as fuel reduced the available fuel volume to 59.8 cubic feet with a maximum oxidizer volume of 47.5 cubic feet.

The characteristics of the engine also placed constraints on the trajectories. The minimum operational Mach number for the engine in ramjet mode was determined to be Mach 2.3. Thus operation was restricted to Ejector Ramjet / Air Augmented Rocket for speeds below Mach 2.3. The minimum time to transition from ramjet to rocket was also a constraint applied to the trajectories. This value was allowed to vary between 5 and 20 seconds and did effect the final performance of the vehicle.

Finally, the trajectory optimization method coupled with the requirement to demonstrate all of the engine operating modes required additional constraints to be applied to the trajectory. Maximizing final vehicle weight required the addition of a minimum range or end velocity constraint to drive the vehicle away from the trivial solution. Maximizing final Mach number required definition of required engine operation modes to ensure operation in all modes. Maximizing Ramjet final velocity required definition of the minimum time required to operate in Rocket mode to ensure rocket mode operation. Table 4.1 summarizes the constraints applied to the final set of trajectories. The constraints applied to the remaining trajectories precede their results and can be found in Appendix E.

4.1.2.1.3 Optimization Goals

As mentioned above, several optimization goals were evaluated during the study. In theory, the goal of minimizing the vehicle separation weight with the constraint of achieving some maximum final velocity should have produced the desired results (demonstration of all engine-operating modes, with significant vehicle acceleration occurring in ramjet mode). To achieve the above goal, the trajectory tool must be capable of iterating on the separation weight through multiple trajectory runs. OTIS as a stand alone tool is not capable of optimizing separation weight over multiple trajectory iterations (for future studies this can be done by wrapping OTIS with Model Center, a rapid conceptual design tool). A similar approach, which OTIS is capable of implementing, is to maximize the final vehicle weight with the constraint of achieving some maximum final velocity. Both approaches require that the vehicle is capable of achieving the specified end velocity. In addition, the engine performance for each of the operating modes must be superior to the remaining modes during some point within the trajectory for the mode to be chosen. For the current engine design / engine decks, the performance of the engine in the ramjet mode is limited. Thus when optimizing final vehicle weight, care must be taken to set the final vehicle velocity constraint such that the velocity constraint can be met by the vehicle when operating with some time spent in ramjet mode.

Maximizing final vehicle velocity in theory should have also produced the desired demonstration results. However, this approach produced the same results as maximizing final weight: Ramjet mode was not selected without the application of additional constraints, such as limits on pure rocket mode operation time. To show the capability of the current engine design / engine decks, the optimization goal of maximizing ramjet final velocity was chosen, with the constraint of 20 seconds of rocket mode operation required.

Table 4.1: OTIS Final Trajectory Constraints:

Global Trajectory Constraints:		
Maximum Dynamic Pressure	850 lb/ft ²	Value raised to allow operations w/o throttling
Minimum Normal Acceleration	-2.0 g	Original design limit of D-21
Maximum Normal Acceleration	5.0 g	Original design limit of D-22
Minimum Axial Acceleration	-2.0 g	Original design limit of D-23
Maximum Axial Acceleration	5.0 g	Original design limit of D-24
Minimum Flight Path Angle	0.0 deg	Prevent vehicle from diving to obtain speed
Minimum Range	100 nmi	Arbitrary minimum range limit
Minimum Vehicle Weight	5,500 lb	Propellant limit
Phase One, Ejector Ramjet / AAR Constraints:		
Minimum Final Phase Mach Number	2.30 n/a	Minimum start velocity of ramjet
Maximum Final Phase Mach Number	3.25 n/a	Maximum desired transition speed
Phase Two, Ramjet Constraints:		
Minimum Initial Phase Mach Number	2.30 n/a	Minimum start velocity of ramjet
Maximum Initial Phase Mach Number	3.25 n/a	Maximum desired transition speed
Minimum Rate of change of Altitude	0.0 ft/s	Ensure vehicle is climbing
Minimum Final Phase Mach Number	3.25 n/a	Prevent vehicle from decelerating
Maximum Final Phase Mach Number	5.5 n/a	Allow acceleration in rocket mode
Phase Three, Rocket Constraints:		
Minimum Initial Phase Mach Number	3.25 n/a	Lowest desired transition speed
Maximum Initial Phase Mach Number	5.5 n/a	Allow acceleration in rocket mode
Minimum Time in Phase	5 sec	Lower bound for transition transients
Maximum Time in Phase	20 sec	Upper bound for transition transients
Minimum Final Altitude	85,000 ft	Bound heat rates
Maximum Final Altitude	120,000 ft	Control effector limit
Maximum Final Phase Mach Number	6.0 n/a	Maximum desired speed

4.1.2.1.4. Results

As mentioned above, with the current engine design the performance of the engine in the ramjet mode was not superior to the performance of the engine in the rocket mode (superior performance being defined as change in velocity per unit mass flow rate). Thus the optimization parameter applied for the final trajectories was to optimize ramjet ΔV . While the results, discussed below, show that the engine as designed is capable of providing positive ΔV while operating in ramjet mode, to truly be an effective demonstrator for the potential of the RBCC concept for launch vehicles, the engine should exhibit ramjet mode performance superior to that of the rocket mode performance over some portion of the trajectory. Potential modifications to the engine design to allow the demonstration of this philosophy within the flight regime of a modified D-21 are discussed in Section 7.

The results of the final trajectory runs, for the three propellant combinations are shown in Table 4.2. As the table shows, the propellant combination which achieves the largest ΔV in ramjet mode is LOX / Propane followed closely by LOX / JP and ending with H₂O₂ / JP. These results remain unchanged when different optimization methods are employed (see B4 and A1 results Appendix E). Note, there is considerable separation between the performance of H₂O₂ / JP and the remaining propellants. In fact, the limitation for the H₂O₂ / JP trajectory was the performance of the engine (the trajectory terminated because the vehicle could no longer accelerate) while the limitations for LOX / Propane and LOX / JP were their propellant loads (the trajectory terminated because the vehicles ran out of propellant). Another interesting observation is that all of the vehicles wanted to fly at low altitudes, the rocket phase termination altitude for all three propellant combinations is at the minimum altitude constraint: 85,000 ft. Initially this was thought to be the result of the optimization method chosen (initially, it was to maximize final mach number not ramjet final velocity), however this was not the case (the results for each optimization were similar). It appears to be a result of the engine performance characteristics. Thus, future studies will have to closely trade performance vs heating constraints (heating constraints being the reason for the minimum altitude constraint).

4.1.2.1.4.1 Propellant Load-outs

The maximum allowable fuel and oxidizer propellant volumes for the minimal modified vehicle tank configuration (see Section 5.1) were determined to be 47.5 ft³ and 59.8 ft³ respectively. The maximum allowable free flight propellant mass is 5,700 lb (assumes vehicle dry weight of 5,300 lb). As Table 4.2 shows, all of the trajectories meet both the volumetric and weight propellant constraints. It is also apparent from the table that there is significant margin between the required oxidizer volume and the available oxidizer volume (44% and 37% for LOX / JP and LOX / Propane respectively). This is fortuitous, in that there is ample margin available for oxidizer boil off. Since the design is free flight weight limited instead of volumetrically limited, the extra oxidizer required to allow for boil off can be carried internal to the D-21 without imparting a performance penalty to the vehicle.

Table 4.2: OTIS C1 Results

OTIS C1 Results	JP/LOX	JP/H2O2	Propane /LOX
Max. Ramjet ΔV (ft/sec)	1,025	456	1,155
Max. Heat Rate (BTU/ft ²)	4.65	2.57	4.76
Max. Temp (°F)	1,409	1,152	1,420
Down Range (nm)	222	110	230
Fuel Load (lbm)	2,603	2,065	2,357
Fuel Vol. (cu.ft)	52.2	41.1	47.2
Oxidizer Load (lbm,tanked)	1,898	2,373	2,144
Oxidizer Vol. (cu.ft, tanked)	26.4	33.1	29.9
Total Tanked Propellant (lbm)	4,501	4,438	4,501
Max, Min Axial Accel. (ft/sec ²)	1.55 / 0.08	1.63 / 0.09	1.40 / 0.09
Max, Min Normal Accel (ft/sec ²)	3.49 / -1.21	1.83 / -1.15	1.62 / -1.21
Ramjet, Mach No. Range	3.25-4.26	3.01-3.47	3.16-4.30
Rocket Termination Mach No.	4.48	4.03	4.50
Rocket Termination Alt (ft)	85,000	85,000	85,000

4.1.2.1.4.2 Dynamic Pressure and Heating

The original D-21 was designed to operate at a maximum dynamic pressure of 650 psf. While this value will most likely remain the maximum allowable design q, the limit for the final trajectories had to be raised to 850 psf to allow the trajectories to run. In previous runs (and the FASTPASS runs) where the engine was allowed to throttle, the optimizer was able to meet the dynamic pressure constraint. This implies that some throttle capability will be required in the final engine design. The dynamic pressure profiles for the three propellant combinations are shown in Figure 4.3. It is interesting to note that, according to OTIS, the vehicle achieves its optimal performance in the ramjet mode when it rides the q constraint line.

Figure 4.4 shows the heat rate at the nose of the vehicle and Figure 4.5 shows the temperature of the nose of the vehicle as functions of time for the final vehicle trajectories. As Figure 4.5 shows, the LOX / Propane and LOX / JP heat rates remain fairly low for the Ejector Ramjet phase, begin to rise continuously during the Ramjet phase, and sharply increases in the Rocket phase. In Figure 4.4, the effect of the heating rate trends on nose temperature are shown. The high heating rates encountered during the rocket phase result in modest (~ 200 °F) temperature increases due to the limited duration of operation in the rocket phase. In contrast, the steady heat rate increase encountered during the ramjet mode results in a large temperature change between the beginning of the mode and the end of the mode (~ 600 °F) due to the duration of the ramjet mode. The maximum vehicle design temperature (900 °F) is reached within ~ the first 200 seconds of the ~ 425 second long flight. Maintaining operations in this elevated temperature environment would add large amounts of weight to an ablative thermal protection system. This would in turn reduce the performance of the vehicle. Figure 4.6 illustrates that while the current engine design for LOX / Propane and LOX / JP are capable of producing a reasonable amount of ΔV in the ramjet mode, the duration of the velocity increase is unacceptable.

Figure 4.3: Final Trajectory Propellant Dynamic Pressure Profiles

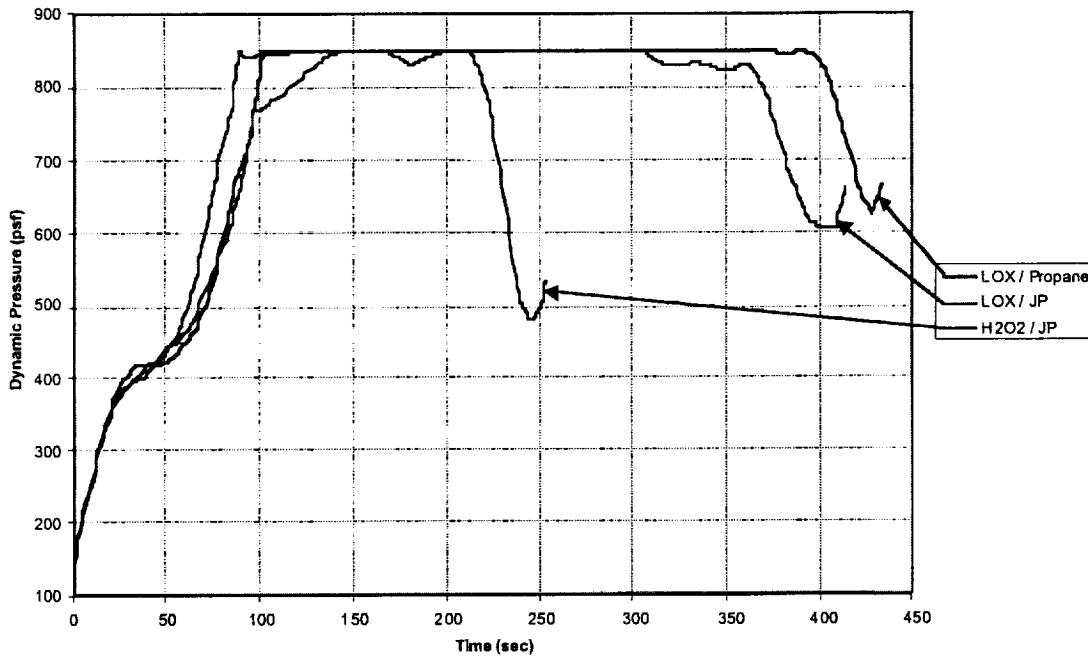
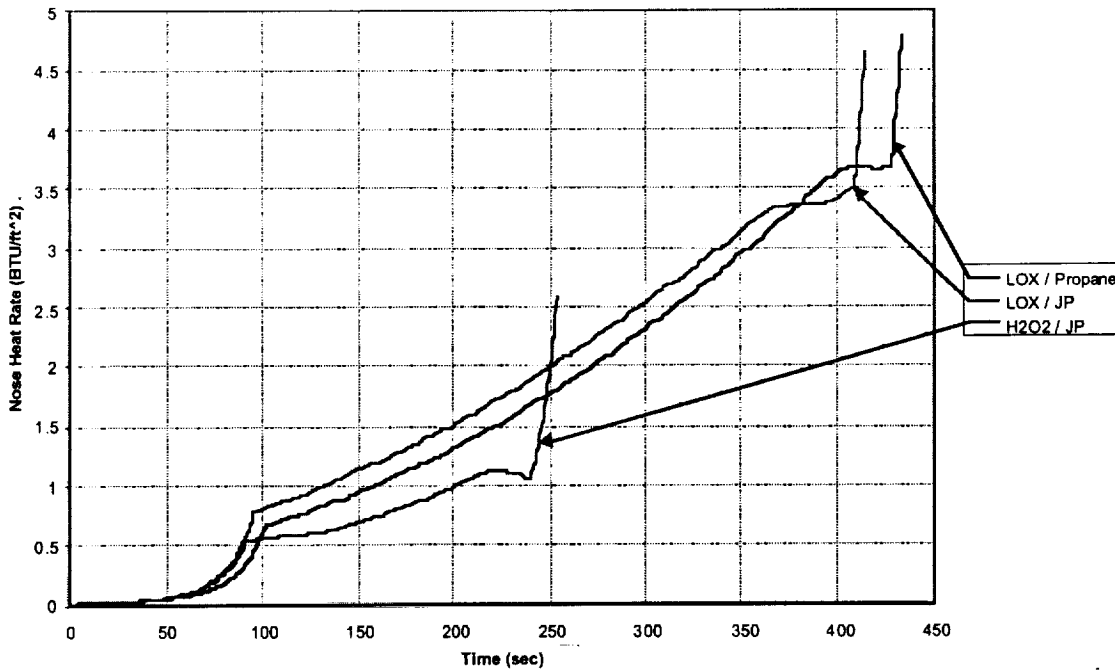


Figure 4.4: Final Trajectory Propellant Heat Rate Profiles



4.1.2.1.4.3 Time in Modes

Table 4.3 shows the time in each of the operational modes for each of the propellant combinations in the final trajectory. As mentioned above, if the D-21 is to be used as the RBCC test bed, the duration of the rocket, and especially the ramjet acceleration phases must be reduced: In other words, the thrust to drag ratio of the vehicle must be increased.

Figure 4.5: Final Trajectory Propellant Nose Temperature Profiles

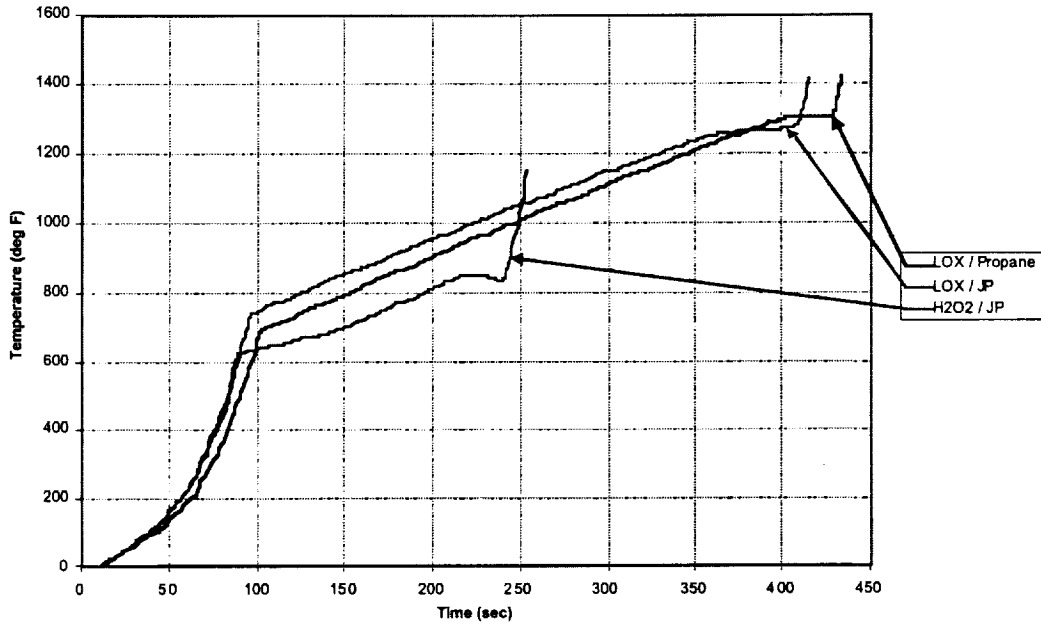


Table 4.3: Final Trajectory Time in modes.

	LOX / Propane	LOX / JP	H ₂ O ₂ / JP
AAR	101	96	89
Ramjet	327	313	151
Rocket	5	5	14

4.1.2.1.4.4 Sensitivities:

The final two trajectory runs (trajectories C1 and B4) exposed the sensitivity of the vehicle's performance to the time spent in rocket mode. The goal of both trajectory runs was to maximize velocity. Trajectory C1 had the constraint that the vehicle must be in rocket mode for 5 to 20 seconds. Trajectory B4 had the constraint that the vehicle must be in rocket mode for 20 seconds. Figure 4.6 shows the difference in vehicle performance between the two trajectory runs. Given the option, the optimizer chose to minimize the amount of time spent in rocket mode when trying to maximize the ramjet ΔV . The end result is that the vehicle in trajectory C1 achieves greater overall ΔV as well as greater ramjet ΔV , but it remains in the atmosphere much longer than the vehicle in trajectory B4 does.

Figure 4.7 shows how the total heat transferred (after the nose temperature has reached 900 degrees Fahrenheit) to the LOX / Propane vehicle varies for trajectories A1 (gross thrust engine performance), B4 (cowl to tail thrust engine performance w/ 20 seconds of rocket mode operation constraint), and C1 (cowl to tail thrust engine performance w/ 5 seconds of rocket mode operation). The figure shows that the rate at which heat is transferred to the vehicle is strongly dependent upon how quickly it accelerates through the atmosphere. Vehicle A1 has the greatest thrust to drag margin and as a result accelerates fast and has the lowest total heat transfer rate. The vehicles in trajectories C1 and B4 have the same engines, but the vehicle of trajectory B4 obtains most of its acceleration from the rocket mode, whose thrust to drag ratio is much higher than the ramjet modes thrust to drag ratio. As a result, vehicle B4 has the second lowest total heat transfer rate. The vehicle of trajectory C1 gets most of its acceleration from the ramjet mode. The low thrust to drag ratio of the engine in this mode cause the vehicle to spend a good amount of time accelerating; as a result, the vehicle of trajectory C1 has the highest total heat transfer rate. This vividly illustrates how sensitive total heat transfer to vehicle is with time spent in the atmosphere. The total heat transfer is an important figure of merit because it determines how much ablative material will have to be added to the vehicle in order for it to survive the flight.

Figure 4.6:
LOX / Propane Trajectory C1 and B4 Ramjet Delta V Performance

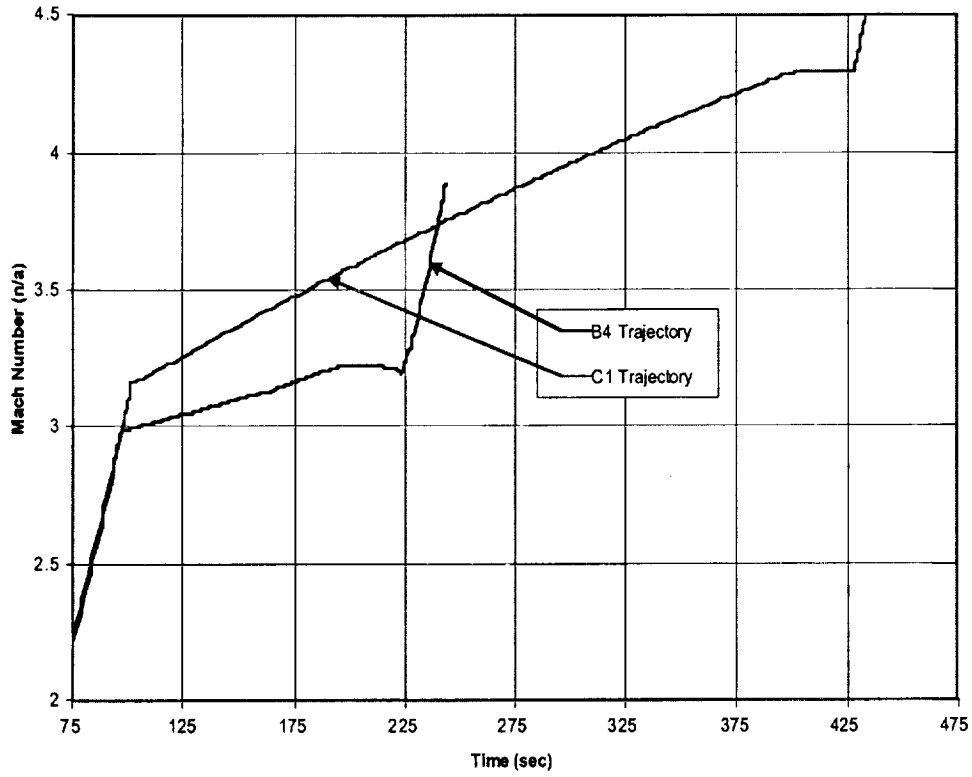
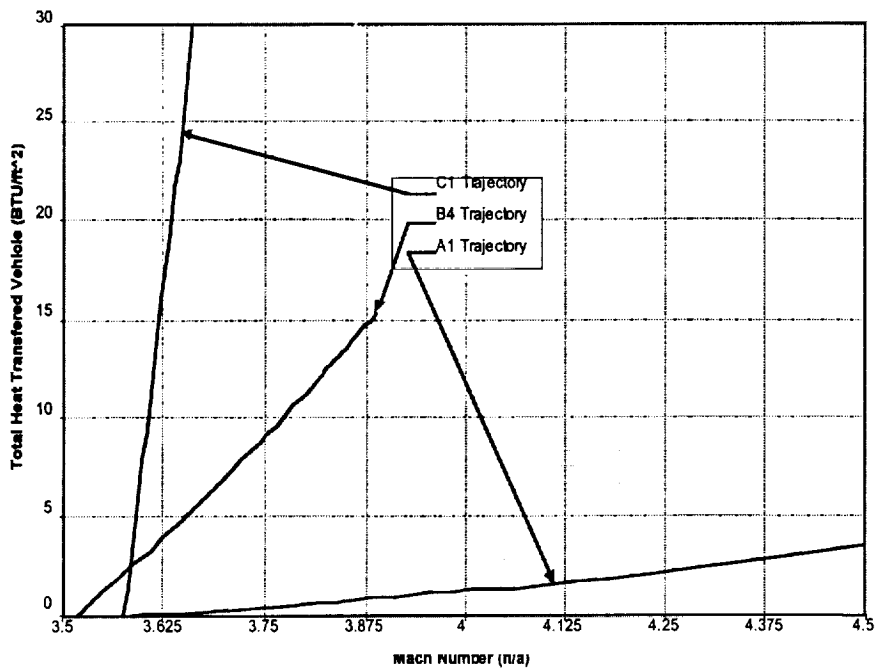


Figure 4.7:
LOX / Propane Total Heat Transferred to Vehicle
for skin Temperatures above 900 deg F vs Mach Number



4.1.2.2 FASTPASS Simulations

FASTPASS (Flexible Analysis for Synthesis, Trajectory, and Performance for Advanced Space Systems) is a preliminary design tool extensively used by the LMA Huntsville office. Primarily used for rocket-based launch vehicle design studies, it has the ability to simulate the trajectory and performance of most any vehicle configuration. The trajectory capability allows for flight simulation in 3 dimensions and 3 degrees of freedom (3 DOF). Trajectory profiles are broken down into flight segments, similar to POST, and the optimizer manipulates the flight control variables to achieve the final optimization goal. However, FASTPASS also has the ability to manipulate weights, propulsion parameters, aerodynamics and any other vehicle level quantity that contributes to vehicle performance. Performance equations can also be manually inputted by the user for the weights, propulsion, aerodynamics and any of the other design variables. The optimization of trajectory and performance is bounded by inputted constraints that can be dictated for the whole trajectory or for individual segments.

4.1.2.2.1 Modeling

Trajectory modeling in FASTPASS is similar to POST in the manner in which the flight plans are programmed. Building a trajectory model required use of historical trajectory information from similar test flights, as well as some assumed trajectory methods used to analyze RBCC vehicles. A trajectory was used that had enough flexibility to allow the optimizer to fly the vehicle for optimal performance, while keeping the trajectory bounded to a realistic flight plan. The sequence of trajectory event is summarized as follows:

- 1) Starting at Mach=0.8 and 40,000ft, separate from B-52 and drop for ~ 2.5 sec (similar to Pegasus drop).
- 2) After 2.5 sec, start a pitch-up maneuver
- 3) After another 2.5 sec, start the air-augmented rocket (AAR) mode
- 4) After another 2.5 sec, start the
- 5) At optimizer determined time, update pitch-up maneuver (do this 4 times)
- 6) At some optimizer determined propellant level, start AAR shutdown and ramjet startup.
- 7) After the ramjet reaches 100% throttle, the optimizer chooses a target angle of attack and flies the vehicle with angle of attack steering to hit the target alpha while maximizing the average q during this mode.
- 8) When ramjet propellant allotment is almost up, start transition to rocket and start another pitch-up maneuver.
- 9) When ramjet allotted propellant and throttle are zero, shut down ramjet
- 10) Update pitch profile
- 11) Shut down rocket when propellant loading is zero and be sure to be at a low flight path angle to insure low altitude return initiation.

The pitching of the vehicle in the AAR and rocket modes was based on current RBCC launch vehicle trajectories. Since the ramjet data was assumed for low angles of attack and the thrust/drag balance was uncertain, the idea was to allow the optimizer to pick its own path by allowing it to manipulate the angle of attack steering. This made it clearer how the performance effects the flight plan without preconceived trajectory determinations.

4.1.2.2.1.1 Aerodynamic Performance

FASTPASS can use aerodynamic data either in equation mode (as a function of other trajectory variables), or as a lookup table. The aerodynamic information for the D-21 was supplied as tables of lift and drag coefficients as a function of angle of attack and Mach number. There were also 2 separate pairs of tables: one set of Cd/Cl data when the ramjet is on and one set when the ramjet is off. These aerodynamic tables, as used in FASTPASS, are in Figures A and B. Whenever the trajectory flies a particular path asking for an angle or a Mach number between the prescribed data points, the program uses linear interpolation to calculate the values.

4.1.2.2.1.2 Engine Performance

The RBCC data supplied by NASA MSFC was sent in separate decks for each mode. The AAR and Ramjet information were sent as thrust coefficient and Isp tables as functions of altitude and Mach number. The rocket information supplied consisted of vacuum thrust and Isp values. Primary oxidizer flow rates and mixture ratios were supplied for the ejector and rocket modes. The thrust values given for the AAR and ramjet modes included the added performance due to fuel/air combustion. The Isp for these modes, however, accounts only for tanked propellant flow. Using the primary flow rates and mixture ratios, the exact flow rates of primary oxidizer, primary fuel and secondary (afterburning) fuel rates and loads can be calculated for AAR and ramjet (see Vehicle Mass Properties).

In order to account for transition periods between modes, a throttling schedule was implemented to simulate the overlapping startup and shutdown transients. The transition from air-augmented rocket to ramjet was done by throttling the AAR linearly from 100% to 0% over a period of time determined by the optimizer (between 5 and 7 seconds). Over the same period of time, the ramjet throttles up linearly from 0% to 100%. This was done to make sure that the secondary fuel injectors (used for both AAR and ramjet modes) never exceeded 100% throttle. Since the ramjet shutdown and rocket startup did not have any common firing components, they could be modeled separately as overlapping transitions. The ramjet shutdown throttling was determined by:

$$throttle_{RamjetShutdown} = 1 - \frac{\Delta t_{current}^2}{\Delta t_{Shutdown}^2}$$

Where $\Delta t_{Shutdown}$ is the calculated determined shutdown interval and $\Delta t_{current}$ is the time since shutdown initiation. The calculated ramjet shutdown interval is approximated by the equation:

$$\Delta t_{shutdown} = \frac{M_{RamjetStart}}{M_{RamjetStop}} \Delta t_{RamjetStart}$$

Where $M_{RamjetStart}$ is the Mach number when the ramjet mode started, $M_{RamjetStop}$ is the Mach number at the start of shutdown and $\Delta t_{RamjetStart}$ is the startup transition time between the AAR and ramjet modes. This ratio is used to account for higher Mach number effects on an airbreathing system shutdown time. The rocket mode was modeled by the throttling equation:

$$throttle_{RocketStartup} = \frac{\Delta t_{current}^2}{\Delta t_{RocketStartup}^2}$$

Where $\Delta t_{current}$ is the time interval since startup initiation and $\Delta t_{RocketStartup}$ is the historically estimated startup time of 5 seconds (based on Atlas centaur and SSME data).

4.1.2.2.1.3 Vehicle Mass Properties

The reference D-21 vehicle for these trajectories had a mass 5,300 lbm. To account for some added mass required for TPS, 200 lbm was added to the vehicle. This made the total dry mass 5,500 lbm. The dry mass was fixed in FASTPASS, which does not allow the simulation to burn up the vehicle when propellant is used up (without warning the user).

The propellant loads were determined for each propulsion mode separately. This is because the engine data was supplied separately for each mode, and FASTPASS is able to run multiple propulsion modules within a single trajectory. Each mode was treated like a separate engine, each with its own mixture ratio, performance data and flow rates. The total loads were then determined by integrating the sum of the separate "engine" flow rates over time. Using the density of the fuel and oxidizer, these totals were then used to calculate equivalent volumes, which were constrained by fixed tank volumes. The primary engine oxidizer flow rates for the AAR mode were provided and assumed fixed. Also, assuming a constant mixture ratio, the primary fuel flow rate for the AAR mode could be calculated. The total flowrate was determined by taking the thrust value and dividing by the Isp. Subtracting the total primary flow rate from the total engine flow rate gave the fuel flow rate from the afterburning injectors. The flow rate monitored during the ramjet mode was purely the fuel flow rate from those injectors. During the rocket mode, the thrust/Isp value was used along with the mixture ratio to determine the primary oxidizer and fuel flow rates. Separating out these rates, and integrating them, provided a good approximation of the propellant loading over the flight time.

4.1.2.2.2 Constraints

The constraints imposed on the vehicle were in most part defined by the capability and limits of the original D-21. This was done in order to provide trajectories that would require the least amount of modifications to the vehicle. Other constraints were imposed on the simulation in order to force the optimizer to alter the trajectory path in a desired direction. A summary of these constraints is in Table 4.4.

Table 4.4: FASTPASS Trajectory Constraints

AAR Off/Ramjet Start Constraints				
Min. AAR/Ram Transition Time (sec)	\geq	5	± 0.1	Conservative no. based on RL10/SSME historical data
Min. AAR/Ram Transition Time (sec)	\leq	7	± 0.1	Conservative no. based on RL10/SSME historical data
Max. Ramjet Altitude (ft)	\leq	90K	± 10	Leave room for rocket mode below 110kft
Q at Ramjet Starting Point (psf)	\leq	650	± 5	Upper limit imposed by original D21
Q at Ramjet Starting point (psf)	\geq	400	± 5	Prevent Simulation from seeking low q's
Ramjet Starting Mach No.	\geq	2.3	± 0.1	Try to push towards original D21 mach no.
Ramjet Starting Mach No.	\leq	3.3	± 0.1	Try to push towards original D21 mach no.
Flight Path Angle during Ramjet ($^{\circ}$)	\geq	0	± 0.1	Prevent vehicle from diving to gain speed
Ramjet Off/Rocket Start Constraints				
Q at Ramjet Termination Point (psf)	\leq	650	± 5	Upper limit imposed by original D21
Q at Ramjet Termination Point (psf)	\geq	400	± 5	Prevent Simulation from seeking low q's
Max Deviation from Average q (psf)	\leq	200	± 10	This is to prevent q's below 400 during mode
Ramjet ΔV	\geq	0	± 1	Force trajectory to use ramjet mode
Min. FPA during Ramjet ($^{\circ}$)	\geq	0	± 0.1	Prevent vehicle from diving prior to rocket mode
Rocket Shutdown				
Flight Path Angle @ Termination ($^{\circ}$)	\leq	1	± 0.1	Level out vehicle for return to site
Minimum Flight Path Angle ($^{\circ}$)	\geq	0	± 0.5	Prevent any diving of vehicle
Overall Trajectory Constraints				
Minimum normal acceleration (g)	\geq	-5	± 0.0	Prescribed by original D-21 limits
Maximum normal acceleration (g)	\leq	2	± 0.0	Prescribed by original D-21 limits
Minimum Axial Acceleration (g)	\geq	-2.5	± 0.0	Realistic limits
Maximum Axial Acceleration (g)	\leq	2.5	± 0.0	Realistic limits
Max. Dynamic Pressure (psf)	\leq	650	± 5	Upper limit imposed by original D21
Max. Temperature ($^{\circ}$ F)	\leq	2600	± 1	Avoid too much extra TPS
Oxidizer Volume (cu.ft.)	\leq	47.5	± 0.0	Dictated by LMSW tank design
Fuel Volume (cu.ft.)	\leq	59.8	± 0.0	Dictated by LMSW tank design
Final Latitude ($^{\circ}$)	\geq	35	± 0.1	Keep D21 within Dryden facility airspace
Final Longitude ($^{\circ}$)	\geq	-119	± 0.1	Keep D21 within Dryden facility airspace
Final Longitude ($^{\circ}$)	\leq	-117	± 0.1	Keep D21 within Dryden facility airspace

4.1.2.2.3 Optimization Goal

The optimization goal for FASTPASS was to maximize the ΔV achieved during the ramjet mode, not including any transition effects of AAR or rocket. This parameter was chosen, because the ramjet performance was the biggest uncertainty in the RBCC design concept. In order to assess the contribution of the ramjet as a potential launch vehicle propulsion mode, it was necessary to optimize on a figure of merit that could be compared to conventional rocket performance. The standard performance criteria used to gauge conventional rocket propelled launch vehicles is the ΔV a propulsion system is able to provide for the vehicle, which can be compared to the total required ΔV to achieve a particular orbit. Thus, maximizing the ramjet ΔV in the simulation, while optimizing the D-21 performance, also provides a clear indication of the potential of this mode for a launch system.

4.1.2.2.4 Results

The overall performance of the various propellant combinations were similar. Review of key results (see Table 4.5) provides a good overall picture on the capability of a modified D-21 RBCC test-bed vehicle. The low ΔV values realized in the ramjet phase show that the current engine design does not have a sufficient thrust to drag ratio during the ramjet mode. This lack of acceleration is also evident in the ramjet acceleration range data. The low ΔV 's also make it uncertain which propellant combination performance is best, since the values are so small that the differences fall within the noise of the simulation. This leads to the conclusion that although there is sufficient performance in the current engine design to allow the D-21 to model the various RBCC modes in flight, there is not enough performance for any real application beyond this demonstration. A redesign of the engine will be necessary to allow the modified D-21 to show feasibility of the RBCC engine as a potential launch vehicle propulsion system.

Table 4.5: FASTPASS Final Trajectory Key Results Summary

	JP7/LOX	JP7/H2O2	Propane/LOX
Maximum Ramjet ΔV (ft/sec)	226.0	249.8	239.2
Maximum Heat Rate (BTU/ft ²)	2.45	2.89	2.17
Maximum Nose Temperature (°F)	1,108.6	1,175.5	1,062.6
Maximum Axial Acceleration (ft/sec ² , g's)	56.1 (1.74g)	57.6 (1.79g)	46.3 (1.44g)
Minimum Axial Acceleration (ft/sec ² , g's)	-5.45 (-0.17g)	-5.6 (-0.18g)	-6.0 (-0.19g)
Maximum Normal Acceleration (ft/sec ² , g's)	1.28 (0.04g)	0	0.50 (0.02g)
Minimum Normal Acceleration (ft/sec ² , g's)	-73.12 (-2.27g)	-73.6 (-2.29g)	-77.31 (-2.40g)
Pure Ramjet Acceleration range in g's	0.101-0.146	0.115-0.138	0.120-0.171
Ramjet Mach No. Range (with mode transition included)	3.03 - 3.59	3.08 - 3.67	3.07 - 3.63
Ramjet Mach No. Range (without mode transition included)	3.18 - 3.39	3.27 - 3.47	3.23 - 3.46
Mach Number at Rocket Termination	4.5	4.6	4.4
Altitude at Rocket Termination (ft)	85,124	86,030	84,470
Down Range at Rocket Termination (nmi)	104.6	119.8	99.6
Max. Estimated Return Down Range (nmi) (at α that gives max L/D)	222.4	236.0	212.3
Max. Estimated Return Cross Range (nmi) (at bank angle = 45° and max L/D)	156.0	160.0	154.0

4.1.2.2.4.1 Propellant Load-outs

The total onboard propellant load was calculated by integrating the flow rates over the trajectory flight time. The total propellant loads and volumes for the various propellant combinations are summarized in Table 4.6.

Table 4.6: Propellant Load-outs

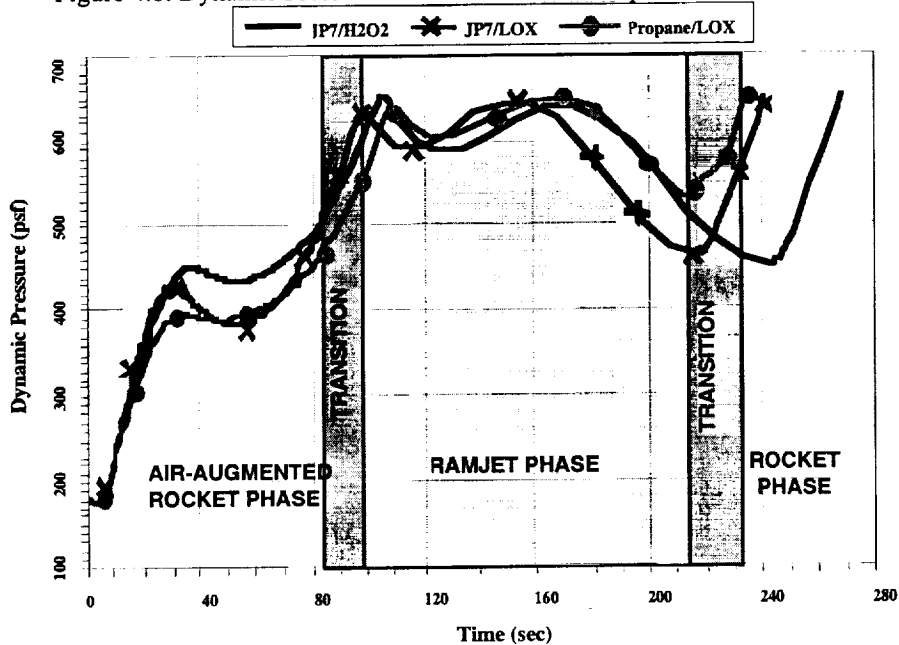
Vehicle Dry Weight = 5500 lbm	JP7/LOX	JP7/H2O2	Propane/LOX
Fuel Load (lbm)	1,527	1,133	1,364
Fuel Volume (cu.ft.)	30.91	22.95	36.88
Oxidizer Load (lbm)	2,706	3,817	2,944
Oxidizer Volume (cu.ft.)	39.50	44.75	42.96
Total Propellant Load (lbm)	4,233	3,950	4,308
Total Propellant Volume (cu.ft.)	70.41	67.70	79.84

The maximum allowable fuel and oxidizer tank volumes, based on a minimal vehicle modification approach, are 47.5 and 59.8 cubic feet respectively. The reason why the optimization chose not to use the full fuel/oxidizer capacity lies in the ability of the vehicle to maintain level flight (at the very least) or a climb. A higher propellant loading caused the vehicle to dive instead of climb, mostly because the ramjet performance was not able to generate enough speed to increase lift. However, with boiloff and ullage factored into the volume calculations (based on X-34 data), the results do show that a complete engine demonstration can be done with the propellant volume allotted.

4.1.2.2.4.2 Dynamic Pressure and Heating

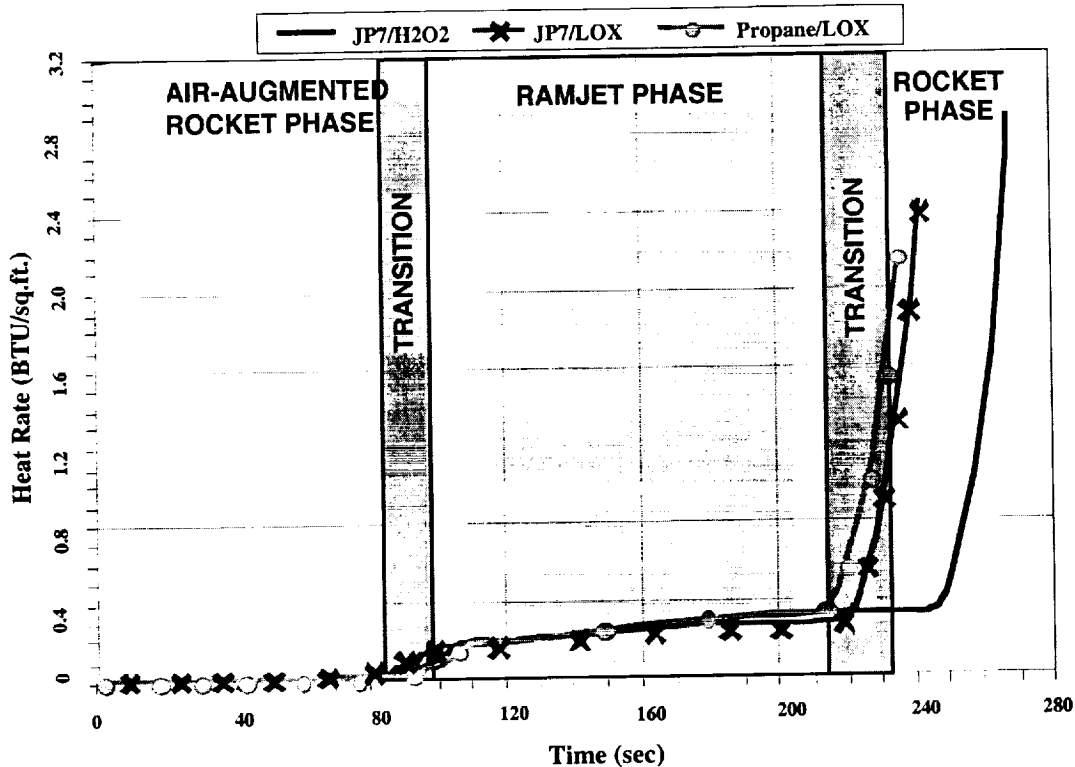
The maximum dynamic pressure the original D-21 was designed for was 650 psf. This was used as the upper limit for the trajectory runs to avoid structural modifications as a result of higher loads. The change in q over time is illustrated in Figure 4.8. It can be seen that the vehicle does not necessarily want to hit the q limit to achieve maximum performance. The FASTPASS trajectory methodology chosen for these simulations allowed the optimization to pick an angle of attack profile leading to a q -corridor that will give the best answer. The results show that this corridor may not necessarily be constant or want to push the upper q limit, which hints at a delicate balance between the increased performance at higher dynamic

Figure 4.8: Dynamic Pressure Profile for Various Propellant Combinations



pressures and the increased drag at higher dynamic pressures. The delicate balance can be linked to the low net thrust (engine thrust - drag) that the current RBCC engines provide. Another reason why the vehicle chooses to maintain its chosen q-corridor is so that it can reach a q high enough to provide performance, but low enough that the rocket mode can be initiated without breaking the 650 psf limit.

Figure 4.9: Comparison of Heat Rates Over Time



The aerodynamic heating on the D-21 shows low heat rates until the vehicle transitions into rocket mode (see Figure 4.9). The low heat rates encountered during the air-augmented rocket phase are likely attributed to the low acceleration pitchup during this phase. The transition from AAR to ramjet shows an increase in heating for all cases, but still below 0.4 BTU/ft² for the duration of the ramjet mode. The significant increase in heat rate occurs at the transition from rocket to ramjet. During this mode transition, the vehicle starts to accelerate prior to a pitchup, and with a faster change in dynamic pressure. Even with this sharp increase in heating, the maximum heat rate among all three cases does not exceed 2.9 BTU/ft². The change in nose temperature varies like the heat rate (see Appendix F). The temperatures during most of ramjet phase are below the 900°F limit, with the threshold not being broken until transition to the rocket phase. A summary of maximum temperature values for each mode is provided in Table 4.7.

Table 4.7: Minimum and Maximum Temperatures for Each Mode (Including Transition Time)

	JP7/LOX	JP7/H2O2	Propane/LOX
Min. AAR mode Temp (°F)	-70 (ambient temp)	-70 (ambient temp)	-70 (ambient temp)
Max. AAR Mode Temp (°F)	727	752	751
Min. Ramjet mode Temp (°F)	650	673	672
Max. Ramjet mode Temp (°F)	950	934	972
Min. Rocket mode Temp (°F)	850	884	878
Max. Rocket mode Temp (°F)	1498	1566	1453

4.1.2.2.4.3 Time in Modes

The time spent in each mode was similar amongst the different propellant combinations. For simulation purposes, all cases ran the rocket mode for 20 seconds. This was to insure sufficient gauging of rocket performance without causing the vehicle to violate altitude, heating and dynamic pressure constraints. Therefore, the variations in mode times were confined to the air-augmented mode, the ramjet modes and the transition between modes. Table 4.8 shows the timelines for the various propellant combinations.

Table 4.8: Time Duration in Each Eode for Reference Propellant Combinations

		JP7/LOX	JP7/H2O2	Propane/LOX
AAR Time	(sec)	88.9	96.4	99.5
AAR/Ramjet Transition	(sec)	6.3	6.4	6.4
Ramjet Time	(sec)	116.4	134.7	99.4
Ramjet Shutdown	(sec)	7.1	7.2	7.2
Rocket Startup	(sec)	5.0	5.0	5.0
Rocket Time	(sec)	20.0	20.0	20.0

4.1.2.2.4.4 Sensitivities

During the simulation process, different engine performance tables were provided. Each table accounted for a different amount of drag associated with an air-breathing vehicle. Since the aerodynamic model accounted for only the D-21 cone, body and wing drag, the remaining pressure drag had to be accounted in the engine tables (a cowl-to-tail engine model). The reference aero and engine tables (cowl-to-tail) provide drag and thrust profiles that result in only a 500 lbf average net thrust during the ramjet phase. This does not allow for useful acceleration of the vehicle, but allows for a cruising mode. This is characterized by very low ramjet ΔV s, which makes it hard to compare the propellant combinations and choose the best one based on performance.

Trajectories were run that used the engine tables *without* pressure drag consideration (a gross-thrust model), in order to simulate effect of increased thrust (far above drag values) on vehicle performance (see Appendix F). The results showed a very large increase in performance and a better dispersion of results that allows for a clearer comparison of the various propellant combinations. Although the ramjet ΔV s are still quite small compared with what a rocket could provide, the performance increase allows the vehicle to accelerate and gain altitude as opposed to cruising. The increased performance also came with less propellant loading. If the trajectory were modified to push some of the constraints so the gross-thrust cases could use the same propellant loading as the reference cases, even more ΔV would be possible. A performance comparison between the two types of engine data can be seen in Table 4.9, with more detail provided in Appendix F.

Table 4.9: Ramjet Mode Performance Sensitivity to Drag

Propellants	Engine Data with Pressure Drag (Cowl-to-Tail)			Engine Data without Pressure Drag (Gross Thrust)		
	JP7/LOX	JP7/H2O2	Propane/LOX	JP7/LOX	JP7/H2O2	Propane/LOX
Ramjet ΔV (fps)	226.0	249.8	239.2	1844	1799	1924
Max. axial accel. (g)	0.123	0.116	0.123	0.780	0.830	0.825
Starting Mach No.	3.18	3.27	3.23	3.12	3.15	3.19
Finishing Mach No.	3.39	3.47	3.46	4.95	4.93	5.09

This sensitivity shows that pressure and inlet drag during the airbreathing propulsion mode can severely affect performance, and engine design must minimize these drag effects while achieving maximum air capture.

Table 4.10: OTIS B4 Results

OTIS B4 Results	JP/LOX	JP/H2O2	Propane /LOX
Max. Ramjet ΔV (ft/sec)	187.5	135.9	238.9
Max. Heat Rate (BTU/ft ²)	2.38	3.13	2.12
Max. Temp (°F)	1,121	1,233	1,076
Down Range (nm)	100	100	100
Fuel Load (lbm)	2,121	1,990	1,860
Fuel Vol. (cu.ft)	42.5	39.9	37.3
Oxidizer Load (lbm,tanked)	2,066	2,570	2,357
Oxidizer Vol (cu.ft., tanked)	28.8	35.8	32.8
Total Tanked Propellant (lbm)	4,187	4,560	4,217
Max, Min Axial Accel. (ft/sec ²)	3.50 / -1.18	1.50 / 0.06	1.38 / 0.08
Max, Min Normal Accel (ft/sec ²)	1.54 / -0.08	2.00 / -1.08	2.95 / -1.08
Ramjet Mach No. Range	3.04-3.21	3.10-3.23	2.99-3.23
Ramjet, Mach No. Range	3.97	4.17	3.89
Rocket Termination Mach No.	85,000	85,000	85,000
Rocket Termination Alt (ft)			

4.2 Results

In the previous sections, the results from each of the independent trajectory analysis with OTIS and FASTPASS were presented. Mostly the findings from the two analyses were in agreement. However, for a few of the resulting trends they were not. In the following paragraphs the common conclusions, concerns, and discrepancies between the two analyses will be discussed.

4.2.1 Ramjet Delta V Performance

Strong correlation was shown between the final FASTPASS and OTIS (B4) trajectory runs (see Tables 4.2 Section 4.1.2.1.4 and Table 4.10). For these runs, the vehicle was constrained to operate in rocket mode for 20 seconds at the end of the flight. As discussed previously, with the current engine design, the sensitivity of the vehicle performance and total heat load is significantly affected by the rocket mode operating time constraint. Since the correlation in performance between the two analyses is good, the following conclusions about the vehicle performance, subject to the applied constraints, can be made:

- A modified D-21 operating with the current engine DRACO NASA RBCC design will not exhibit ramjet mode acceleration performance superior to the rocket mode acceleration performance over any portion of the trajectory.
- The maximum ramjet ΔV achievable by the vehicle with the current engine design is between 240 ft/s (20 seconds of rocket mode operation) and 1,150 ft/s (5 seconds of rocket mode operation). However, heating constraints will most likely prevent the vehicle from demonstrating the maximum ΔV value for the manner in which the trajectory was flown (low altitude).

4.2.2 Propellant Performance Discrepancies

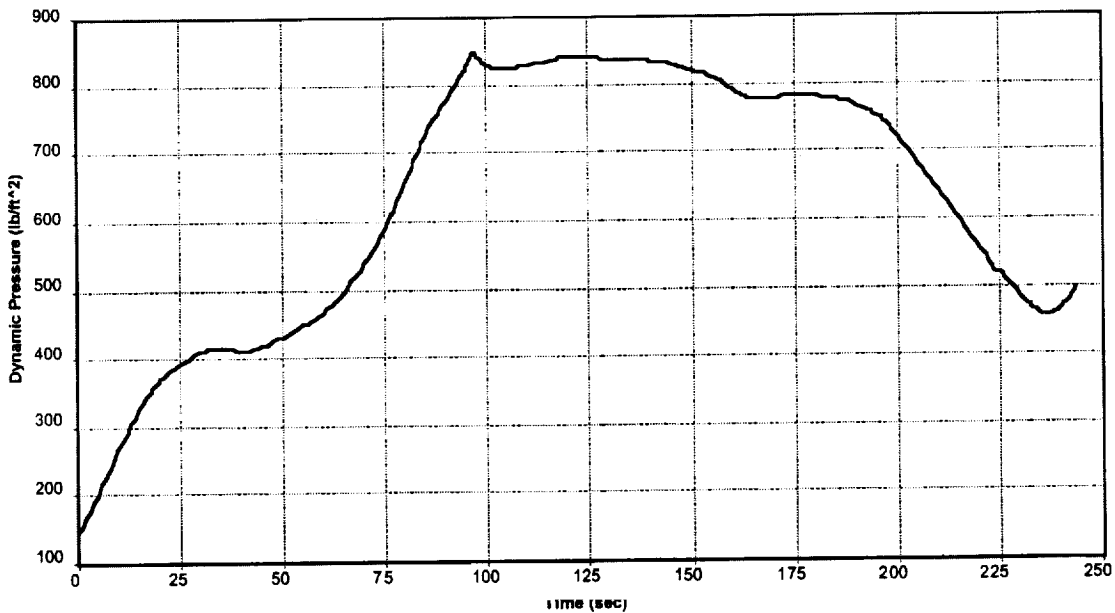
During the study, the relative performance rankings of each of the propellant combinations were constant throughout the OTIS trajectory runs. LOX / Propane always performed the best, and LOX / JP consistently performed better than H2O2 / JP. For the final set of FASTPASS trajectories, this trend was upset, H2O2 / JP performed better (had a larger ramjet ΔV) than LOX / Propane and LOX / JP. The difference between the ramjet ΔV s was 10.6 ft/s between H2O2 / JP and LOX / Propane and 23.8 ft/s between H2O2 / Propane and LOX / JP. The small difference between the ΔV values could be an explanation for the performance reversal. It is possible that the separation between the final performances fell within the noise of the criterion tolerance of the trajectory runs. The propellant performance trends seen with the engine gross thrust

FASTPASS runs seem to support this hypothesis. In these runs, the propellant performance matched the trends observed constantly throughout the OTIS trajectory runs. Therefore the conclusion reached by this study is that the greatest vehicle performance is obtained when LOX / Propane is chosen as the propellant. LOX / JP is a close second to LOX / Propane in ramjet ΔV performance. The LOX / JP ramjet ΔV values were between 100% and 78% of the LOX / Propane ramjet ΔV values, with the performance gap decreasing with increasing ramjet ΔV performance / increasing ramjet thrust to drag ratios.

4.2.3 Trajectory Ramjet Dynamic Pressure Trends

In the C1 OTIS trajectory final results, the vehicle hit the dynamic pressure constraint when transitioning between the Ejector Ramjet / ARR mode and the Ramjet mode and continued to ride this constraint through the ramjet portion of the flight (see Figure x, Section 4.1.2.1.4.2). In the FASTPASS final results (see Figure 4.8, Section 4.1.2.2.4.2) and the OTIS B4 final results (see Figure 4.10) the vehicle also hit the dynamic pressure constraint at the AAR ramjet mode transition. However, instead of riding the constraint, the vehicle then modulated the dynamic pressure for the remainder of the ramjet mode. The above trend is worthy note because the C1 and B4 trajectories bound the achievable vehicle performance. The trends indicate that dynamic pressure, as well as the previously mentioned heating concerns, will become a limiting factor for the modified D-21 when try to maximize ramjet ΔV .

Figure 4.10:
NASAE3CTLOX/ProB4
Dynamic Pressure vs Time

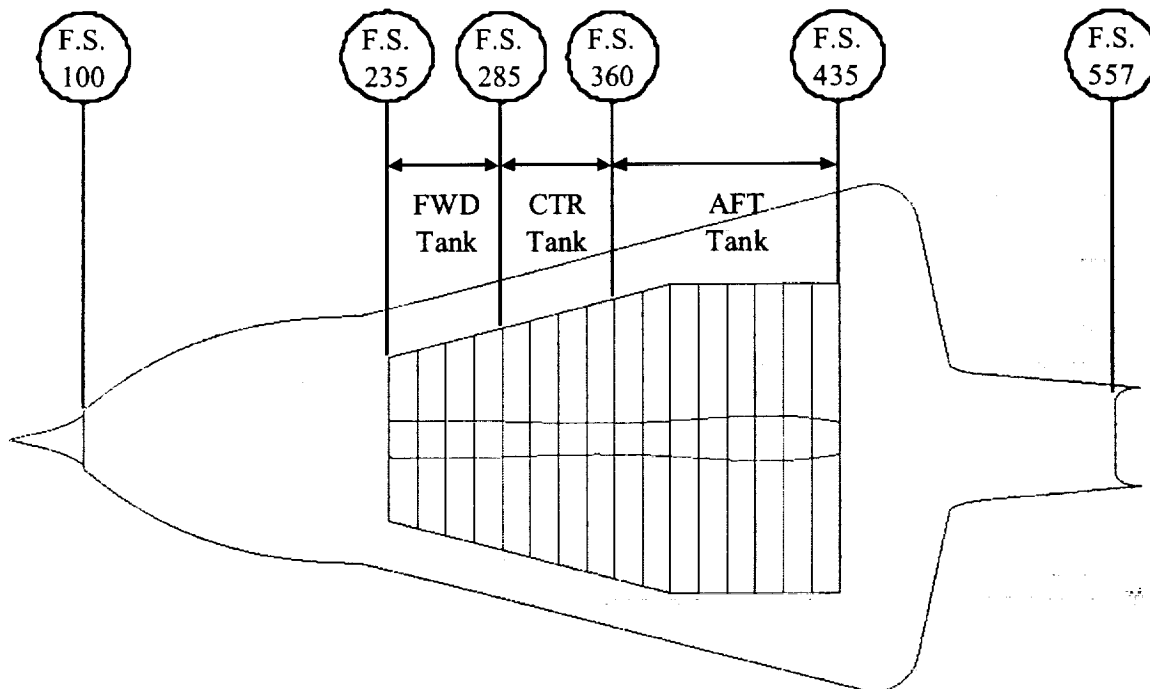


5.0 Required Vehicle Modifications

5.1 Tank Modifications

The D-21 was unique from other operational air vehicles in that it operated solely in the hypersonic flight regime. Although it operated as a hypersonic flight vehicle, portions of its design and construction are similar to conventional aircraft. The D-21 for example was purely an air-breathing vehicle. As a result, there are no provisions for carrying oxidizer on board the vehicle. Like most traditional aircraft, the fuel for the vehicle was stored in integral or “wet” wing / fuselage tanks. In other words, no dedicated fuel storage pressure vessels were part of the vehicle design. This is in contrast to the design philosophy applied to hypersonic vehicles today, which generally have dedicated pressure vessels for fuel and oxidizer storage.

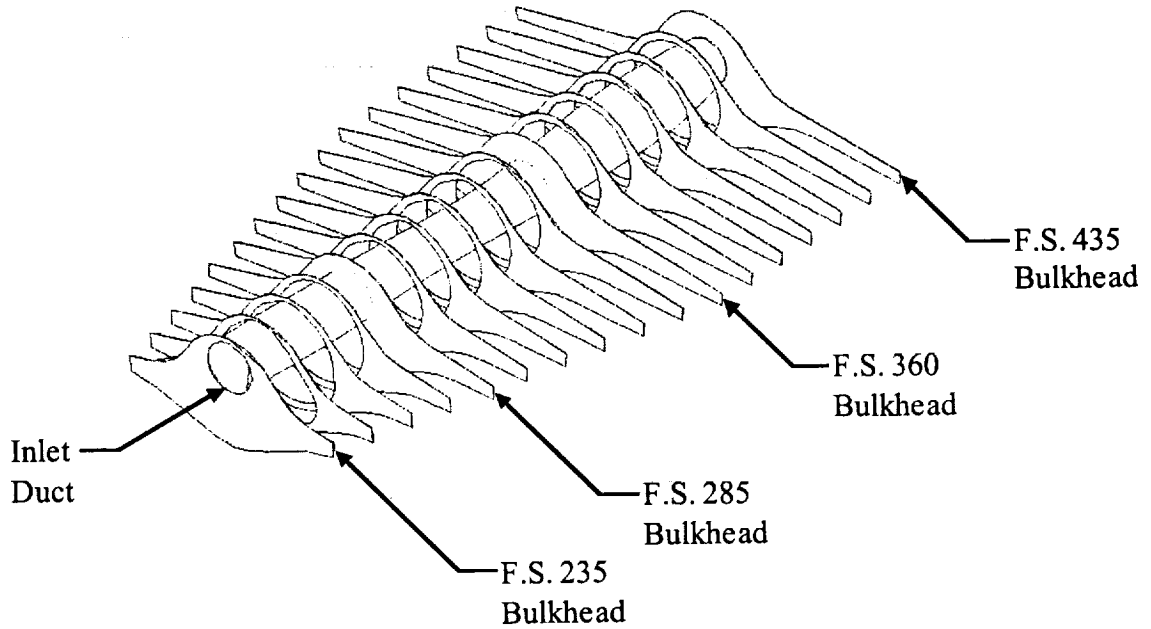
Figure 5.1: D-21 Fuel Tank Layout



Specifically, the D-21 has three integral fuel tanks (see Figure 5.1) designed to be pressurized to 1.5 psi above the current ambient conditions. The forward tank begins at the fuselage station (F.S.) 235 bulkhead and ends at the bulkhead at F.S. 285. Three fuselage frames are located between the F.S. 235 and 285 bulkheads and are integral structural components of the fuel tank. The center and aft fuel tanks are arranged similarly. The center fuel tank is bounded by the F.S. 285 and 360 bulkheads and also has three fuselage frames located between its bulkheads. The aft tank is bound by the F.S. 360 and 435 bulkheads and has seven fuselage frames located between its bulkheads. No fuel is able to pass between the tank bulkheads. In contrast the fuselage frames have large cutouts to allow fuel passage (see Figure 5.2).

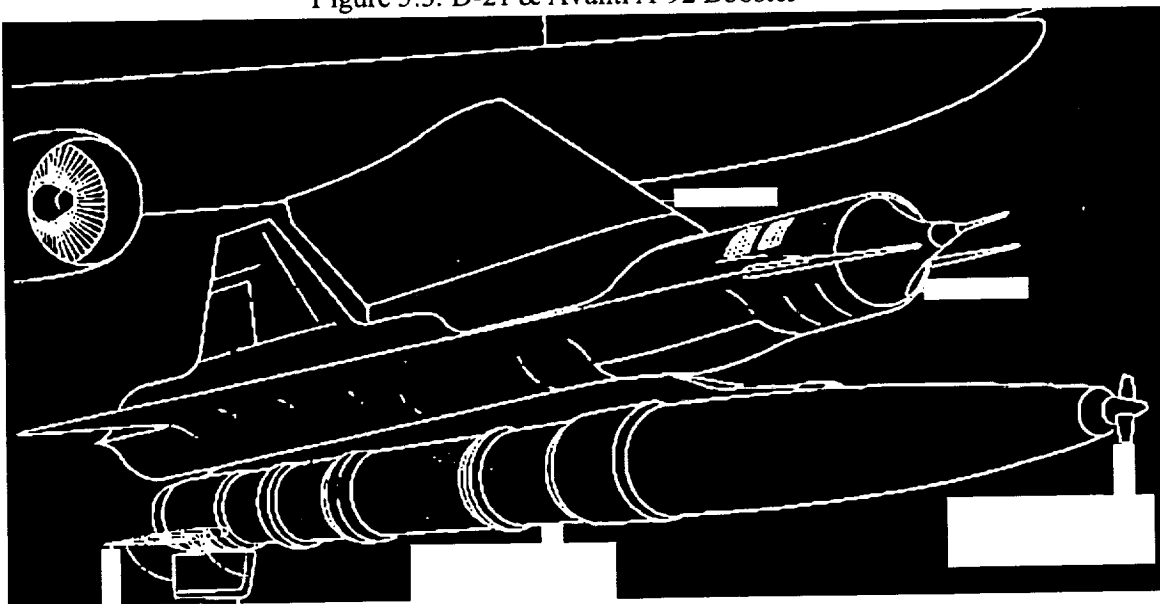
A requirement of a RBCC test bed vehicle would be the ability to carry both fuel and oxidizer. Not only would the vehicle have to carry the propellants, it would have to supply the propellants to the engine at the pressures defined by the engine design. For the engine design used in the study, the pressure delivery requirement for both the fuel and oxidizer were 30 psi at the engine interface. This requirement could either be met by having high-pressure tanks or by increasing the fuel or oxidizer delivery pressure with a boost pump.

Figure 5.2: D-21 Fuel Tank Bulkheads and Frames



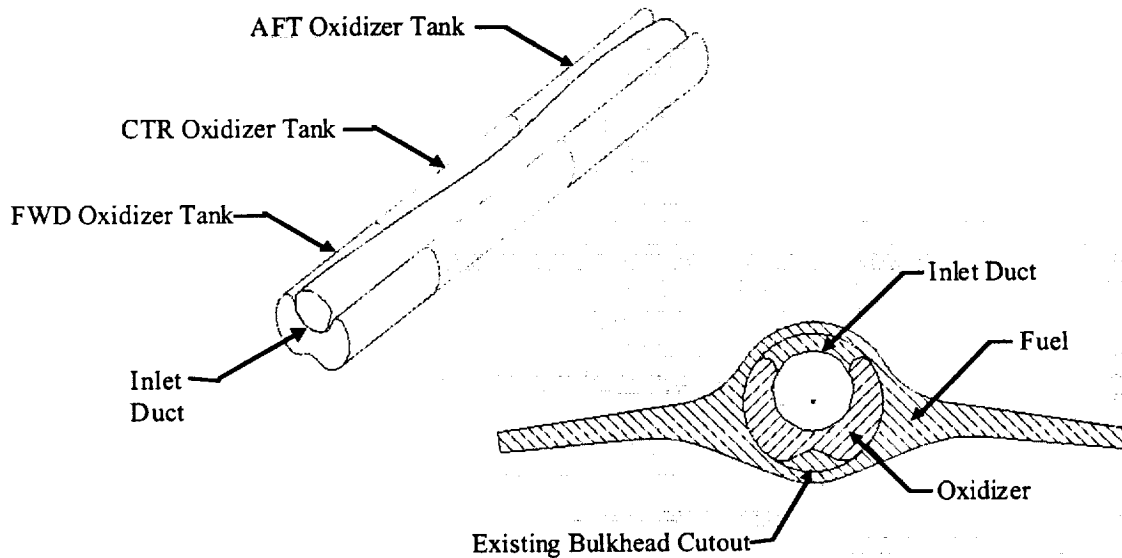
The required oxidizer could be carried either internally to the D-21 or externally in a propellant pod similar to the Avanti booster used by the D-21B during boost from the B-52 mother craft (see Figure 5.3). The trajectory analyses performed during the study have shown that reasonable performance (burnout speeds between Mach 4 and Mach 6) can be obtained with propellant volumes on the order of 100 cubic feet. Since suitable performance can be achieved with propellant volumes that are within the original design fuel volume of the D-21 (122 cubic feet), the path of storing both the oxidizer and fuel onboard the vehicle was taken.

Figure 5.3: D-21 & Avanti A-92 Booster



Substantial open area exists in the cutouts in the fuselage frames (see Figure 5.2). Oxidizer tanks located within each of the fuel tanks, designed to occupy / pass through the existing area in the fuselage frames, could obtain reasonable volumes with minimal modifications (the lower sections of the fuselage frames will have to be cut to allow installation of the oxidizer tanks) to the existing D-21 structure. This approach was adopted as the baseline method for the addition of pressurized oxidizer tanks to the vehicle (see Figure 5.4).

Figure 5.4: D-21 Minimum Modification Propellant Tank Design



The above method of oxidizer addition is extremely efficient, little volume beyond that which is added as oxidizer (only that due to oxidizer tank thickness) is lost from the original fuel tank volumes. As mentioned above, this remaining fuel volume is sufficient to achieve suitable test bed performance. In addition, no modification to the existing fuel system is required to satisfy the fuel delivery pressure requirement, since the original fuel system supplied the fuel to the engine at a rate of 10,000 lb/hr at 35 psig via a boost pump. In contrast if the fuel tanks were modified such that they could be pressurized to 30 psi or if pressurized fuel tanks added to the vehicle, significant structural modifications would be required. To modify the existing tanks into pressurized tanks would at a minimum require replacing all of the skin panels that bound the fuel tanks. The existing skin panels are the skin of the fuel tanks. They are currently only designed to see a gauge pressure of 1.5 psi. Increasing the pressure would require an increase in the skin thickness. The addition of pressurized fuel tanks would require additional structural modifications to the vehicle frames that occupy the fuel tank area. This approach would not only add unnecessary weight (the vehicle still has skin panels, but in addition it now has additional structure for tanks), in addition it would further reduce the volume available for fuel: an added pressurized tanks could not match the volume of a wet wing tank.

Table 5.1 and the Minimal Modification Oxidizer Tank Layout drawing (see Appendix C) summarize the propellant system characteristics for the baseline method of propellant system modification.

Table 5.1: Propellant Tank Characteristics

	FWD	CTR	AFT	Total
Oxidizer Tank Xcg (in)	260.0	321.5	397.9	n/a
Oxidizer Tank Volumes (ft ³)	14.0	18.6	14.9	47.5
Fuel Tank Xcg (in)	261.2	322.5	395.2	n/a
Fuel Tank Volume (ft ³)	13.0	25.1	21.7	59.8
Total Propellant Volume (ft ³)				107.3

5.2 Recovery Modifications

The D-21 airframe was never intended for recovery following mission completion, only the jettisonable hatch containing the reconnaissance payload and high-value avionics systems was recovered in the original system. After expending available fuel, the drone was programmed to descend at a constant equivalent airspeed of 300 knots until reaching an altitude of 60,000 feet at Mach 1.8, whereupon the payload/avionics hatch would be jettisoned. At 52,000 feet, a barometric switch activated an explosive charge to trigger structural break-up and flight termination.

Due to the limited number of remaining D-21s and the reality of program cost reductions through reuse, a recovery system and operational recovery plan must be defined for the modified D-21. Two options were explored in the present study: conventional lakebed landing using the elevons and rudder for aerodynamic control with extendable landing gear; and a ballistic parachute or parafoil system with extendable landing gear to achieve a near-vertical landing at low velocity.

5.2.1 Conventional Landing

The conventional landing concept employs the "aim point" method for landing vehicles possessing low L/D, such as the NASA/North American X-15 research aircraft. Following engine shutdown, the D-21 would begin an unpowered descent at constant equivalent airspeed towards the recovery lakebed, making turns as required for energy management and proper runway alignment. The vehicle would aim towards the intended touchdown point and perform a gradual flare to bleed airspeed and achieve the proper landing attitude. The landing gear, employing a steerable nosewheel and extendable main skids, would be lowered and locked into place. Following touchdown and landing rollout, the vehicle would be recovered using a suitable ground handling dolly.

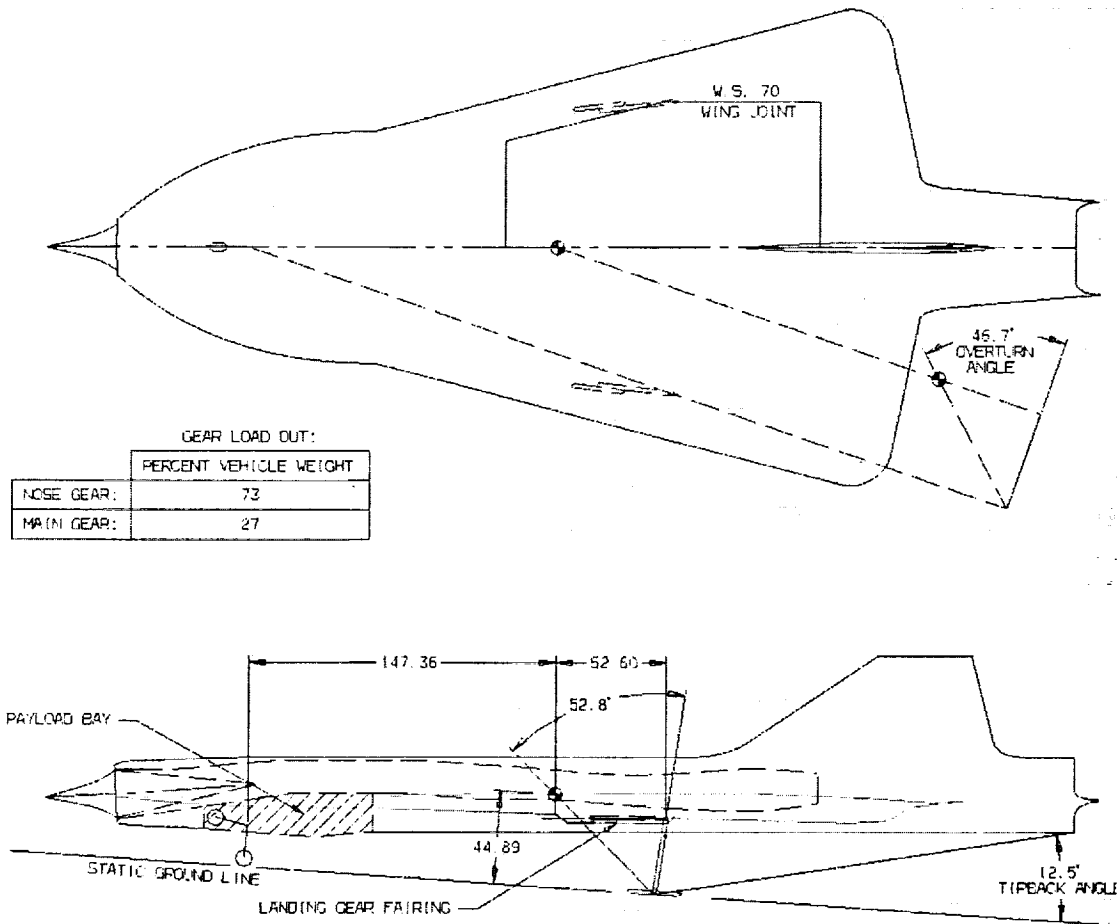
The major concern associated with the conventional landing concept is the suitability of the D-21 aerodynamic configuration and its associated low speed behavior. The low lift coefficient (between 0.10 and 0.125 at 4 degrees angle of attack) afforded by the low aspect ratio, highly swept, sharp leading edge wing results in excessive landing speeds (estimated to be between 230 and 260 knots) and strong bound vortices. A search of program files and discussions with the retired Lockheed ADP Chief Aerodynamicist revealed that no wind tunnel testing of the D-21 at low speed conditions and in ground effect were performed as there was no requirement to do so. It is recommended that such a test be performed in any follow-on study to reduce program risk.

Other proposed modifications associated with this approach include:

- Incorporating altitude gain scheduling for the flight control system laws
- Adding angle-of-attack and sideslip angle measurements to the air data system
- Differential GPS for runway alignment
- Radar altimeter for precision height
- Batteries to provide supplemental electrical power sufficient to operate air data/flight control system due to APU power output limitations from reduced air mass flow
- Extendable landing gear (steerable nosewheel and fixed orientation main skids)
- Hatch redesign to accommodate nose landing gear and transmit landing gear loads to primary structure

Figure 5.5 shows a conceptual design for the extendable landing gear and associated tip-back/tip-over angles. The main skids and housings are externally mounted close to the zero fuel weight center-of-gravity and tie in to the structural beams located at Wing Stations 70L/R. The nose gear is housed in the payload hatch area; gear loads are transmitted to the left and right lower longerons that span the payload bay. The landing gear would be extended using gravity and air loads to lock into place.

Figure 5.5: Conventional Landing Gear Layout



5.2.2 Parachute / Parafoil Landing

Concerns regarding the excessive landing speed and absence of low-speed aerodynamic data in ground effect lead to consideration of a parachute/parafoil recovery system. Pioneer Aerospace Corporation was consulted to evaluate this recovery method and its suitability for the D-21. No information proprietary to Pioneer Aerospace Corporation will be discussed in this report.

The ballistic parachute method is the simplest and lowest risk recovery method, and has been proven in multiple applications. However, there are several drawbacks to their use for this application. First, ballistic parachutes offer no control over the location of the landing impact point, and thus require careful coordination of the recovery initiation with winds aloft. Second, the estimated landing sink rate for the D-21 would exceed 10 feet per second, even with clustered multiple parachutes, which would ensure structural damage to the vehicle without some form of energy absorbing device (crushable skids or inflatable cushion).

Third, the weight and volume requirements for ballistic parachutes and their associated drogue/deployment chutes would significantly impact the volume available for on-board fuel, as would an inflatable cushion for softening the landing impact. For these reasons, a parafoil recovery system was explored.

The parafoil system offers the advantage of very low landing sink rates and control of the landing impact point. The inflated canopy acts as a low aspect ratio wing that is controlled by differential motion of the risers. This recovery system was selected for the X-38 research testbed. However, upon further examination the parafoil system was found to be of limited suitability for the D-21 application. First, the weight and volume requirements for the system are such that integration within the vehicle would require significant displacement of fuel and structural re-work. For example, a parafoil sized for a landing sink rate

between 2 to 5 feet per second would require approximately 20 cubic feet of packaging volume using current packing methods which, to date, have not been volumetrically constrained. Second, the lateral spacing of the D-21 upper longerons is considered insufficient to provide sufficient lateral spread for the parafoil risers, which is critical to achieving lateral stability and preventing weathercocking. Providing sufficient lateral spacing would require significant structural redesign of the vehicle, making the D-21 DRACO less of a modification and more of a new aircraft.

5.2.3 Selected Concept

Given the preceding discussion of the recovery method options, it was decided to select the conventional landing under aerodynamic control as the baseline recovery method. However, this method is still considered high risk until low speed aerodynamic data, in ground effect, can be obtained. Such data could be obtained using the Lockheed Martin Skunk Works Low Turbulence Wind Tunnel.

5.3 Flight Termination System

The original D-21 flight termination system consisted of an explosive charge set to activate at a pressure altitude of 52,000 feet following jettison of the payload/avionics hatch. This system is not suitable for the D-21 DRACO application for safety reasons. It is proposed that flight termination be accomplished by using the elevons to initiate a hardover maneuver leading to structural break-up of the vehicle within a narrow dispersion zone. The system would include dual-redundant receivers and processors to signal the flight control computer.

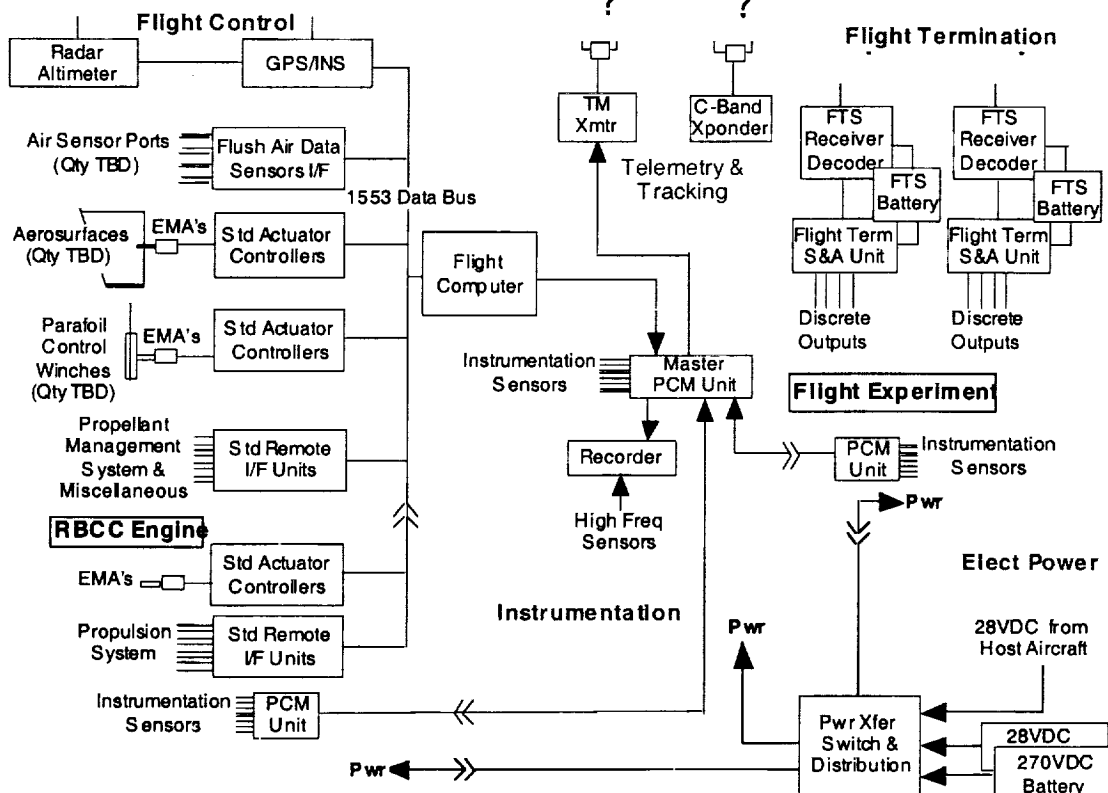
5.4 Avionics Modifications

The original D-21 avionics system included a three-axis, single channel, analog Automatic Flight Control System (AFCS) consisting of an air data computer, electronic component assembly, and rate gyro package; an Inertial Navigation System (INS) consisting of an inertial platform, gimbal control electronics, digital computer, and power supply; and a Telemetry System capable of transmitting 55 different signals via VHF antennas in the vertical fin and vehicle underside. Unfortunately, the whereabouts of these systems has not been positively determined. Due to a number of factors, it was not possible during the course of the study to lower the payload hatches of the NASA-controlled D-21s to determine if these components were in the vehicles. However, a Lockheed Martin Skunk Works Vice President believed that these systems were scrapped or salvaged following termination of the D-21 program in 1972.

Regardless of their final disposition, these systems are considered unsuitable for the D-21 DRACO application for a number of reasons. First, the systems represent early 1960s state-of-the-art and are therefore obsolete. Their functionality can be replicated in modern-day digital systems of greatly reduced volume, weight, and electrical power requirement. Secondly, these systems would require significant modification to support the expanded flight envelope of the testbed, particularly the low-speed descent/landing portion. For example, the fixed gain schedule in the AFCS would require altitude gain scheduling that would be difficult to incorporate. The analog air data computer would require addition of angle-of-attack and sideslip angle inputs. The Telemetry System hardware would require significant modification to monitor the desired data channels. Third, it is certain that these systems are no longer supportable by the original vendor.

Accordingly, a revised avionics system concept was developed, as shown in Figure 5.6. This employs a modern MIL-STD-1553B digital data bus for simplicity and to reduce wiring requirements. The flight control computer functions as the bus controller.

Figure 5.6: Conceptual Avionics Architecture



5.5 Electrical System Modifications

The present D-21 electrical system includes the following items:

- A 4 kVA, 120/208V, 400 Hz generator combined with a 100 A, 28VDC generator in the same housing driven at 12,000 RPM by the APU
- A 600 V-A solid-state inverter to provide 115/200 V power to the AFCS/INS, and payload
- A 28VDC, 25 Ampere-hour silver zinc battery to provide secondary power to the inverter and command/destroy systems

Because the D-21 was intended for one-time use, a number of simplifications were employed in the electrical system. These included “pig-tail” wiring connections instead of connectors; elimination of wiring terminal blocks; and elimination of circuit breakers. Spliced connections were made in the event a piece of equipment was removed and replaced. These practices are not suitable for the reusable D-21 DRACO testbed. For this reason and due to concerns of wiring condition following long-term storage, it is recommended that all existing wiring be removed from the vehicle and replaced as necessary. The addition of connectors and circuit breakers to protect system wiring will require the fabrication of new mounting panels and disconnect panels in accessible locations.

Electrical conduits are required to provide interface to the electromechanical actuators powering the rudder and elevons. Existing conduits that run through the fuel tanks will be modified and re-routed as necessary to provide proper clearance for the oxidizer tanks. The existing electrical umbilical box, located on top of the vehicle will be retained to provide interface to the NB-52B carrier aircraft.

A detailed electrical load breakdown as a function of mission phase must be performed to determine the adequacy of existing electrical power available. It is known that the proposed inlet spike actuator has a

maximum estimated power requirement of 5 kVA and an average estimated power requirement of 2.5 kVA. Due to the short free flight duration of the testbed, electrical power availability is not considered to be a major factor in determining overall feasibility of the D-21 DRACO concept.

5.6 Actuation System Modifications

The D-21, as presently configured, is equipped with a single hydraulic system for operating the elevon and rudder actuators. The system is pressurized to 3,200 psi using a pump driven by the APU during free flight conditions; a ram air turbine-driven generator on the A-92 rocket booster was used during boosted flight to Mach 3.3/80,000 feet. The only hydraulic fluid permitted for use in the system is that meeting specification MIL-H-27601, the same as that used in the SR-71 aircraft. The fluid, essentially de-waxed mineral oil, has an operating temperature range of -65 to +600 degrees Fahrenheit and is cooled by fuel through a heat exchanger.

Retention of the existing hydraulic system for the D-21 DRACO application poses several concerns. First, the system was designed and optimized for operation at steady-state conditions at a single cruise Mach number. The expanded flight envelope of the D-21 DRACO represents a significant departure from the original operating envelope. Major concerns in this regard include fluid operating temperatures at higher Mach numbers; the ability of the fuel to provide sufficient cooling; and thermal shock imposed by large temperature gradients as would occur during descent to landing following attainment of maximum Mach number. Second, the hydraulic system must be leak-checked on the ground by heating the fluid to operating temperature using a device nicknamed a "hot gig". The concern is whether the hot gig will be able to replicate hydraulic fluid temperatures at higher Mach numbers (a hazardous operation). Also, the location of the DG-15 hot gigs developed for the D-21 is unknown (though it may be possible to use the SR-71 hot gig). Third, it is uncertain whether the existing system components can be refurbished without assessing their condition, which was not possible during the study.

Accordingly, it is proposed that the existing surface actuators and hydraulic system in its entirety be replaced with electromechanical actuators (EMAs) operating from +28 or +270 VDC electrical power and signaled via the MIL-STD-1553B digital data bus. Such mechanization would considerably simplify the system architecture and reduce weight. The EMAs would operate the elevons, rudder, inlet spike, and nosewheel steering. Such actuators have been successfully employed on a variety of aerospace programs.

5.7 Environmental Control System Modifications

The D-21 Environmental Control System (ECS) provides conditioned airflow to the payload bay sufficient for equipment cooling at the Mach 3.3 steady-state cruise condition. High temperature inlet bleed air is pre-cooled through an air-to-fuel heat exchanger before being expanded and cooled through the APU, from which it is ducted to the payload bay. The temperature of the airflow leaving the APU is controlled by varying the fuel flow through the air-to-fuel heat exchanger. Of special significance to the D-21 modification study is the fact that all ECS components were sized and optimized to accommodate the thermal loads existent at the Mach 3.3 cruise condition only. Flight at higher Mach numbers, with correspondingly higher inlet airflow temperatures, is of concern. However, use of sub-cooled propane as the fuel (and heat sink) may mitigate this concern. It is possible that upon further examination, supplementary cooling may be required for the avionics and flight test instrumentation. Such determination requires a detailed thermal analysis that is beyond the scope of this study.

5.8 Hatch Modifications

The present payload/avionics hatch incorporates numerous features that are no longer required for the D-21 DRACO implementation. These include:

- Hatch power release system (including thrusters, latch pin actuators, safety valve, initiator, gas generator, altitude sensing switch)
- Recovery and stabilization parachutes and housing
- Watertight equipment protective covers
- Reconnaissance payload windows

- Hatch pivot hinges (aft end of hatch; used to permit hatch to swing away from airframe during jettison)
- Self-sealing doors on hatch umbilicals (electrical, air, and plumbing)

A major consideration for the hatch modification is the installation of the nose landing gear. Landing gear loads must be transmitted into the lower fuselage longerons that span the payload bay at Butt Lines 20L/R. At present, the hatch is locked into place using sliding steel pins and mating fittings on each side of the hatch. These pins are mechanically latched/unlatched for hatch installation/removal on the ground and were gas-actuated for hatch jettison in-flight. The structural suitability of the hatch latching mechanism to accommodate nose landing gear loads must be assessed in any follow-on study effort.

5.9 NB-52B Modifications

To accommodate D-21 carriage aboard the B-52H aircraft, a special pylon was designed and built by Lockheed ADP. This pylon was similar to that employed on the NASA NB-52B, except that it positioned the D-21 in such a way as to not require notching of the right inboard flap (thus making it inoperable). For comparison, the B-52H D-21 pylon was mounted 10 inches further outboard than the NB-52 X-15 pylon. Ground clearances were critical, however, due to the presence of the A-92 rocket booster carried underneath the D-21.

Carriage of the D-21 DRACO aboard the NASA NB-52B is considered feasible for the following reasons:

- The D-21 was successfully carried and released from the B-52 H, which mounted the D-21 in a very similar manner to that used on the X-15
- The D-21 DRACO is well within the published NB-52B launch weight limitations. Elimination of the A-92 rocket booster (not required for the D-21 DRACO) results in system weight savings of 13,000 pounds compared to the D-21/A-92 system launched from the B-52H and provides much greater ground clearance.

Carriage aboard the NASA NB-52B pylon will require the following modifications:

- Pylon adapter for picking up the existing D-21 structural mounting points/electrical disconnects/cooling air disconnects
- Cooling air provisions for the D-21 during captive carry
- Launch control officer monitoring systems and control panels
- Though LOX is proposed as the oxidizer for the D-21 DRACO, there is no requirement to re-install a LOX top-off system on board the NB-52B because there is sufficient LOX volume aboard the D-21 to permit boil-off and still meet mission performance goals.

6.0 D-21 DRACO Mass Properties

The mass properties of the modified DRACO vehicle are constrained by carrier aircraft constraints as well as several of the design constraints of the original D-21.

6.1 D-21 DRACO Maximum Vehicle Weight

The maximum weight that can be supported by the B-52H including the pylon and adapter is 45,000 lb. This maximum weight limit constraint is not expected to be reached by the D-21 DRACO. However, vehicles weighing less than 10,000 lb have less extensive dynamic analysis requirements. Since meeting this weight constraint could provide cost savings, the free flight weight for the D-21 DRACO in the OTIS trajectories was limited to 10,000. The structural design of the original D-21 limited the maximum free flight weight of the vehicle to 11,200 lb. This is slightly greater than the 10,000 lb dynamic analysis weight imposed by the B-52. Thus if improved performance can be achieved by the increase in vehicle separation weight; this would represent the absolute upper bound.

6.2 D-21 DRACO Center of Gravity Travel Limits

The free flight center of gravity of the original D-21 was required to be located between fuselage stations 320 (encountered at the start of free flight) and 300 (encountered at end of the flight). These center of gravity constraints will also apply to the D-21 DRACO vehicle. As previously discussed the D-21 DRACO will have segmented fuel and oxidizer tanks. This propellant tanking scheme is similar to original D-21 tanking scheme (the fuel tanks were segmented). The original D-21 managed its cg by distributing fuel to the center propellant tank (which feed the engine) from its forward and aft tanks. The symmetry of the D-21 DRACO propellant tank design allows it to manage its cg travel in the same manner: Pressure regulation between the forward, center, and aft oxidizer tanks will allow oxidizer management. Fuel management will be maintained as it was on the original vehicle.

6.3 D-21 DRACO Mass Properties Sheet

The weight and longitudinal center of gravity impacts of the vehicle modifications discussed in Section 5 are shown in Table 6.1. The net result of the proposed modifications is an increase in vehicle dry weight of about 200 lb and a cg shift of approximately 25.5 inches aft. This aft cg shift places the dry weight cg at fuselage station 325.5, 5.5 inches aft of the aft separation limit. Should more detailed design studies reveal that the dry weight cg is indeed at this location, ballast (~100 lb at fuselage station 55) will have to be added to move the dry weight cg with the separation limits. Tables 6.2 gives the separation mass properties for the three propellant combinations, LOX / Propane, LOX / JP, and H₂O₂ / JP. As the table shows the separation weights of the vehicle essentially match the assumed separation weights used in the trajectory analysis (percentage difference between calculated weights and assumed weights for OTIS C1 trajectories are 0.1%, 0.1%, 0.5% respectively).

7.0 Required Engine Performance

As discussed in Section 4, a modified D-21 utilizing the current NASA RBCC engine design is capable of demonstrating positive ΔV s between 240 ft/s (20 seconds of rocket mode operation) and 1,150 ft/s (5 seconds of rocket operation) in the ramjet engine mode and achieving maximum speeds between Mach 4.0 and Mach 4.25. However, as discussed in section 4.1.2.1.4.4, the time spent in the atmosphere during the acceleration phase for the higher ΔV trajectories significantly increased the total heat transferred to the vehicle (see Figures 4.4 and 4.9). As a result thermal constraints will most likely hinder realization of the higher ΔV s.

Trajectories run with the gross thrust engine performance achieved higher speeds, and more importantly lower total heat transfer rates (see Figure 4.4 and 4.9). The importance of this trend should not be under emphasized: The greater the acceleration, the lower the total flight time to a desired Mach number, and the lower the total heat transfer to the vehicle. The thermal design limits of the D-21 are reached at skin temperatures of approximately 900 degrees Fahrenheit. For the final trajectory runs (C1 and B4) the D-21 thermal design temperature was typically reached between Mach 3.5 and Mach 3.6. The maximum vehicle in flight separation limit, 11,200 lb, will limit the amount of additional thermal protection that can be added to the vehicle (currently 400 lb has been allocated for ablative TPS). Thus if flight speed significantly exceeding Mach 3.5 are a program requirement, then the engine ramjet mode thrust to drag ratio must be increased.

The optimal engine inlet design Mach number was not identified during the course of the study. The final engine decks were generated for an engine utilizing a mach 5.0 single cone inlet. As previously shown, the maximum mach numbers achieved by the D-21 DRACO vehicles were approximately Mach 4.5. Thus significant performance improvements can be obtained by better matching the inlet design Mach number to the actual trajectory flown by the vehicle.

To fly the vehicle in OTIS with the gross weight engine decks, the dynamic pressure constraints for the vehicle had to be increased. The dynamic pressures experienced during transition from Ejector Ramjet to Rocket mode were exceeding the maximum design limit for the original D-21. This constraint was not violated by the FASTPASS analysis due the incorporation of a throttling routine for the vehicle transition modes. While the trajectories flown with the cowl to tail thrust data did not encounter the dynamic pressure constraint, future trajectories flown with a better-matched inlet design Mach number might. Thus

future engine decks should provide the vehicle performance (thrust and specific impulse) as a function of Mach number, altitude, and throttle.

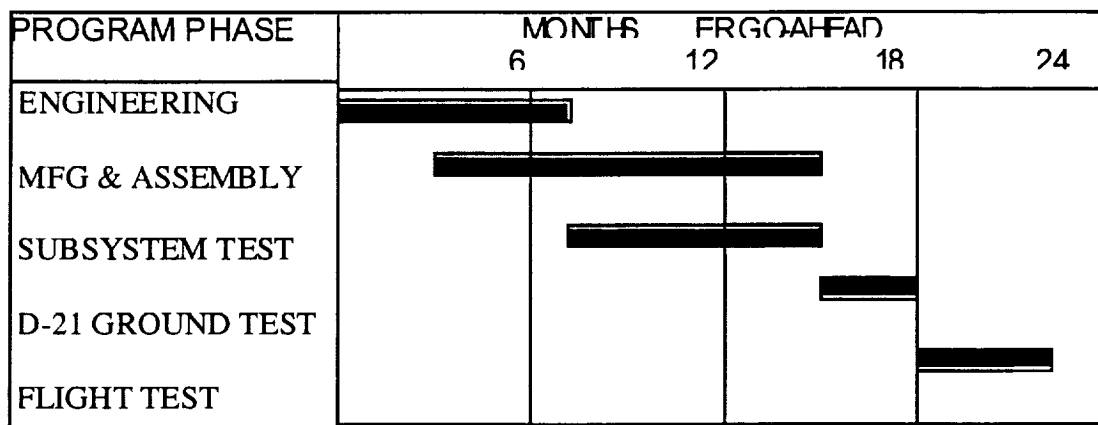
Table 6.1: Modified Vehicle Mass Properties

Component Description:		Component Weight (lb)	Component Xcg (in)
	D-21 Dry Weight Properties	5,300	300.0
	D-21 Separation Weight Properties	10,719	315.8
Electrical Group:	Battery	-14	227.2
	Primary Batteries	40	233.0
Environmental Control:	External Insulation	-375	315.8
	External Insulation	400	315.8
Hydraulic System:	Primary Hydraulic Pump	-4	233.0
	Hydraulic Package (Accumulator, Valving, & Controls)	-25	206.1
	Hydraulic Reservoirs (V=90 in ³)	-19	188.8
	Hydraulic Fluid Lines	-34	315.8
	Hydraulic Fluid (V=15 in ³)	-18	188.8
	Hydraulic System Heat Exchanger	-3	233.0
	Emergency Hydraulic Accumulator (V=35 in ³)	-15	341.2
	RHS Elevon Actuator & Transfer Valve Assy	-15	440.5
	LHS Elevon Actuator & Transfer Valve Assy	-15	440.5
	Rudder Elevon Actuator & Transfer Valve Assy	-13	486.0
	Rudder Electric Actuator	28	440.5
	RHS Elevon Electric Actuator	28	440.5
	LHS Elevon Electric Actuator	28	486.0
Propulsion System:	RJ-73, MA20S-4 Engine	-512	467.0
	NASA RBCC Engine	900	467.0
Propellant Storage & Feed System:	PSJ100 Fuel (FWD Tank)	-1,651	261.2
	PSJ100 Fuel (CTR Tank)	-2,425	322.5
	PSJ100 Fuel (AFT Tank)	-1,524	395.2
	Unusable Fuel	-33	305.6
	FWD Oxidizer Tank	30	260.0
	CTR Oxidizer Tank	50	321.5
	AFT Oxidizer Tank	50	397.9
Recovery System:	Recovery Hatch (Structure, Actuator, & Controls)	-227	189.2
	Recovery Electrical Systems	-26	171.2
	Parachute, Parachute Storage, & Dye Marker	-149	218.5
	Nose Landing Gear & Structure	90	185.0
	Aft RHS Landing Skid & Structure	60	402.0
	Aft LHS Landing Skid & Structure	60	402.0
Flight Controls System:	Automatic Flight Control System	-28	189.2
	Inertial Navigation System	-125	170.0
	Telemetry & Command Systems	-36	192.6
	Automatic Flight Control System	100	189.2
	Inertial Navigation System	90	170.0
	Telemetry & Command Systems	16	192.6
Flight Termination System:	Destructor Unit	-8	214.0
	Range Safety Systems	17	214.0
Air Data System	Air Data Computer	-12	188.4
Air Induction System:	Inlet Spike	-108	93.0
	Inlet Spike	150	93.0
Payload:	Cameras, Controls, & Window	-285	192.3
	Flight Test Instrumentation	350	192.3
Revised Vehicle Dry Properties:	Dry Weight	5,509	325.5

8.0 Recommend Modification Schedule and Flight Test Program

A notional schedule for the D-21 DRACO modification and test program is shown in Figure 8.1. The proposed program calls for commencement of flight tests 18 months after Authority to Proceed (ATP). The schedule is highly concurrent, in line with Lockheed Martin practices on similar development efforts. It is expected that the RBCC engine would be delivered approximately 12 months after ATP to enable system level checkouts prior to installation on the vehicle. Subsystem test would include such items as flight control system bench testing, LOX tank qualification, landing gear tests, and NB-52B fit checks. Ground tests would comprise the assembled vehicle with fully integrated on-board systems. The four-month flight test program would include one unpowered drop test and four powered flight tests to Mach 0.8, 1.5, 3.5, and the maximum obtainable vehicle Mach number.

Figure 8.1: Program Schedule (Notional)



9.0 ROM Cost Estimate

The Rough Order of Magnitude (ROM) cost estimate to perform the D-21 Drone Modification Program is \$91.2 Million (CY '00 \$'s). This ROM estimate is provided for budgetary and planning purposes only. The estimate, summarized in Figure 9-1, is the total cost to perform the program.

Figure 9-1. Drone Modification Cost Estimate Summary

Cost Categories	Total Cost (Mil '00 \$'s)
Engineering, Development, and Testing	50.2
Procurement, Fabrication, Manufacturing, and Assembly	26.5
Systems Ground Test	3.7
Vehicle Ground Test	5.7
Flight Test	5.1
Total	91.2

The baseline program estimate includes engineering, development, testing, procurement, fabrication, manufacturing assembly, systems ground test, and vehicle ground test for 2 drone modifications, B-52 wing pylon and other aircraft modifications, and one drop and four powered flight tests. The RBCC engine, the existing drones, and B-52 operations are assumed to be provided as Government Furnished Equipment (GFE) and are excluded from the estimate.

All costs were estimated in constant CY 2000 dollars. The propellant combination for the program is assumed to be JP-7 and liquid oxygen (LOX). The estimate is based on previous program cost history for

One of the key assumptions affecting cost, is the premise involving the context or “programmatic approach” within which the program is carried out. Skunk Works history has shown that a program of this type can be accomplished at a cost and within a schedule substantially less than is typically experienced using a traditional government contract method. The “Experimental Prototype” or “Skunk Works” approach is the programmatic approach context assumed for this estimate. This approach, epitomized by the Have Blue (F-117 prototype) program, can reduce cost by up to one-third that of programs carried out under more traditional approaches. Among the more important attributes associated with the Experimental Prototype approach are:

- Minimal drawing detail, red-line drawing changes, no drawing sign-offs by other engineering disciplines
- No parts list, no interchangeable parts
- Minimal engineering “-ilities” (e.g. reliability, producibility, etc.) support
- Soft tooling
- No static or fatigue testing
- Minimal quality assurance support
- Flight handbooks only
- No spares

Figure 9.2 provides a breakout of the estimated program cost by primary system element. Note Development Cost includes design, development, and testing and Production Cost include procurement, fabrication, manufacturing, and assembly. Figure 9.3 shows the proposed modification schedule. The manufacturing cost to modify the second drone is \$11.26M, which is included in the \$91.2M estimate. No learning curve is assumed between the first and second drone modifications. The primary cost contributor is Avionics and Software. It is assumed that the drone will require an entirely new avionics suite, autonomous flight software development and test, and a significant amount of developmental flight instrumentation (DFI) to capture the required flight test data. Based on previous LMSW experience on X-33, Tier3-, and JASSM in particular, this will involve a significant effort, with minimal amounts of commercial off-the-shelf (COTS) hardware and software available for use without substantial modification due to the extreme operating environments, packaging constraints, and unique system requirements.

The marginal cost to fly each additional test flight is driven primarily by the cost of the propellants and associated fluids and gasses, and the flight test crew labor cost. Based on the propellant combination of JP-7 and LOX and the estimated flight load of 1,667 lbs (JP-7) and 3,768 lbs (LOX) the cost per flight for propellants and gasses is less than \$1,000. This estimate is based on costs per pound of 15 cents for JP-7, 4 cents for LOX, a 10% factor for other fluids and gasses (e.g. purge gasses), and a boiloff factor of 74% for LOX. The marginal flight test labor cost is more difficult to quantify. It is LMSW’s experience that, barring an extraordinarily compressed or extended flight test program schedule, flight test labor cost is a function more of the flight test program duration than actual number of flight tests. The baseline flight test program estimate of \$5.07M assumes a four-month flight test program for the five tests: a drop test, a low speed flight (M~0.8), a transonic test (M~1.5), a high-speed test (M~3.5) and a maximum speed flight. The baseline flight test cost also including pre-first flight activation activities. Figure 9.4 shows total estimated flight test cost as a function of program duration.

Figure 9-2. Drone Modification Cost by Primary System Element

Cost Element	Development	Production	Test	Total	2nd Drone	Dry Weight (lbs)	Description
Wing	-	-	-	-	-	709	No change
Tail/Body	-	-	-	-	-	138	No change
Body	\$ 2.61	\$ 0.91	-	\$ 3.53	\$ 0.46	1,665	No change
Tanks	\$ 1.83	\$ 0.11	-	\$ 1.94	\$ 0.06	80	New LOX tanks (2); use existing fuel tanks
Landing Gear	\$ 0.25	\$ 2.27	-	\$ 2.52	\$ 1.13	228	New landing skids (nose 2 main); no tires, brakes
Flt Controls	\$ 0.17	\$ 0.78	-	\$ 0.95	\$ 0.39	84	Replace hydraulic actuators with EMAs
Elec Power	\$ 6.13	\$ 0.49	-	\$ 6.62	\$ 0.25	62	Replace hydraulic AP U with batteries (2); retain 1 AP U
MP S	-	-	-	-	-	900	Propellant feed, fill/drain, pressurization, and vent systems
Engine	\$ 0.01	\$ 0.99	-	\$ 1.00	\$ 0.49	177	Government furnished RBCC engine
Engine Install	\$ 0.02	\$ 1.02	-	\$ 1.04	\$ 0.51	200	New engine attachment/integration structure
Inlet Spike	\$ 28.77	\$ 11.29	-	\$ 40.06	\$ 5.65	666	New air inlet/spike hardware
Avionics & Software	\$ 3.23	\$ 0.67	-	\$ 3.23	\$ 0.34	-	New flight computer, INS, comm & telemetry, RS S, Test instrumentation
Design Support	-	-	\$ 1.72	\$ 1.72	\$ 0.86	-	Engineering analyses (aero, thermal, loads, stress, etc.)
Tooling	-	-	\$ 1.86	\$ 1.86	-	-	New tooling/handling fixtures for vehicle final ass'y, integ, & checkout
Quality Assurance	-	-	\$ 1.86	\$ 1.86	-	-	QA for all new and modified systems
Sys Eng & Integ	\$ 1.86	\$ 2.27	-	\$ 2.27	\$ 1.14	-	Systems engineering & analysis
Final Ass'y, Mfg Maint	\$ 2.92	-	-	\$ 2.92	-	-	Vehicle final assembly and checkout
Program Mgt & Supt	\$ 1.93	-	-	\$ 1.93	-	-	Program management, business operations, admin support
Special Test Equip	\$ 3.93	-	-	\$ 3.93	-	-	Special test equipment for all vehicle & ground support systems
B-52 Pylon/Mod	\$ 0.48	-	-	\$ 0.48	-	-	Design analysis, fab, ass'y, integ and test of B-52 wing pylon & mods
Ground Test	-	-	\$ 1.79	\$ 1.79	-	-	Wind tunnel, landing gear, controls proof, structural, component DET, etc.
Flight Test	-	-	\$ 5.07	\$ 5.07	-	-	5 flights: 1 drop test + 4 powered flights; fuel = JP-7, oxidizer = LOX
Ground Supt Equip	-	-	\$ 0.48	\$ 0.48	-	-	New and refurbished GSE
TOTALS	\$50.21	\$26.48	\$14.51	\$91.17	\$11.26	4,909	

Figure 9.3 Program Schedule

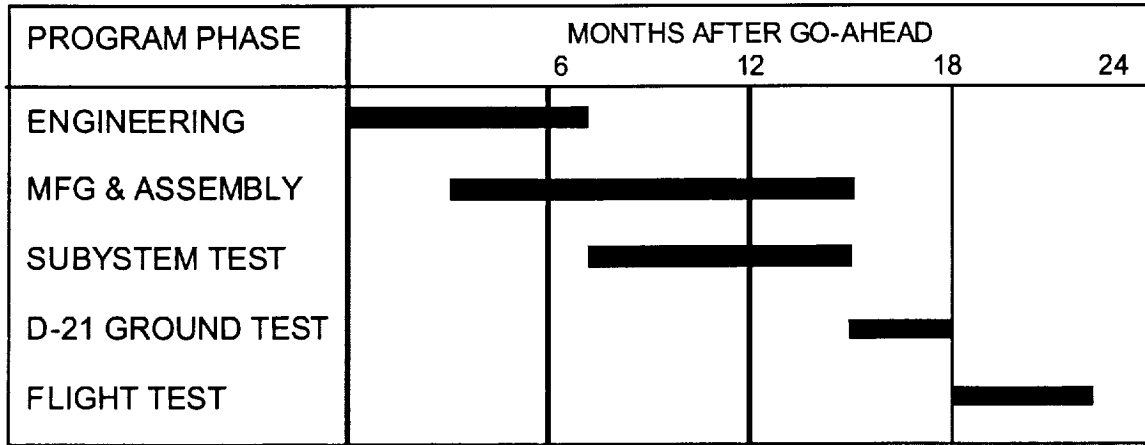
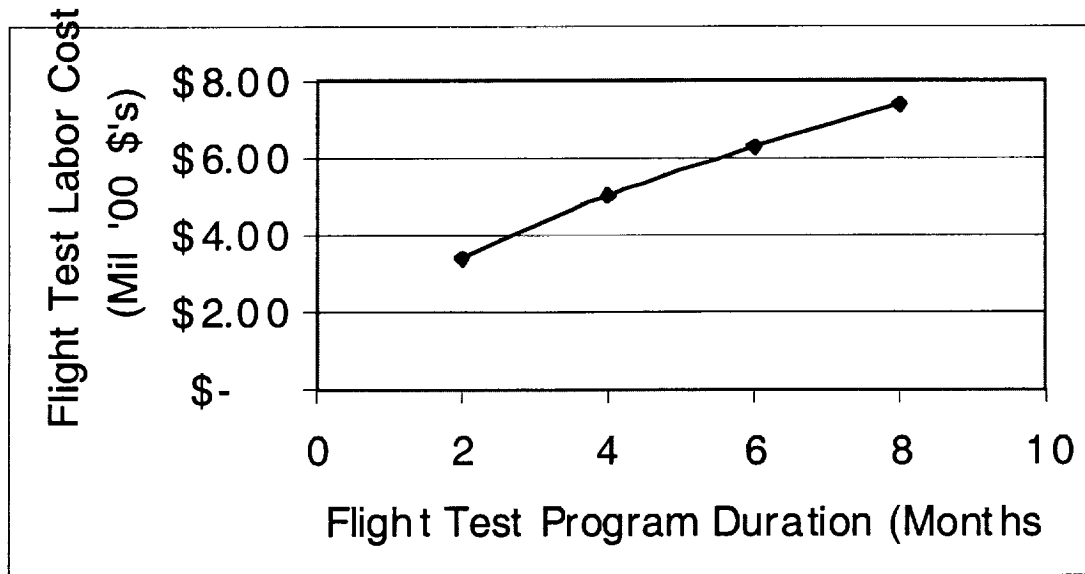


Figure 9.4. Flight Test Cost as a Function of Flight Test Program Duration



10.0 Study Summary

10.1 Initial Assumptions

Prior to the study, it was believed that a modified D-21 would not be capable of accelerating from Mach 0.7 at an altitude of 40,000, to Mach numbers approaching 3.5 at altitudes approaching 85,000 ft in a single flight solely with internally carried propellants. It was believed that insufficient propellant volume would exist within the vehicle. It was believed that staged flight test would have to be performed with external propellant tanks or solid boost motors added to the vehicle to propel it to a suitable initial condition for the desired engine mode demonstration. As the study has indicated, the performance of the vehicle has exceeded the performance envisioned prior to the study.

10.2 Actual Performance and Performance Limitations

As discussed in Section 4, the modified D-21 utilizing the current NASA engine design, is capable of achieving ramjet mode ΔV s between 240 ft/s (20 seconds of rocket mode operation) and 1,150 ft/s (5 seconds of rocket mode operation). The study has revealed that contrary to initial beliefs, the modified vehicle is weight limited instead of volume limited. In other words the vehicle reaches its maximum free flight weight limit (11,200 lb) before it runs out of fuel and oxidizer tank volume. Although the free flight weight limited has not been a limiting factor on the vehicle performance realized in this study (engine performance has), it has the potential to limit the vehicle performance in the future. If only small improvements in vehicle performance are realized through an improved inlet design Mach number, then the time spent accelerating in ramjet rocket mode will remain large. This will increase the required thermal protection system mass. Addition of this TPS mass will have to come at the expense of vehicle propellant such that the vehicle meets the maximum free flight weight limit. Should this situation occur, additional propellant could be added to the system via the methods discussed in the initial assumptions section.

10.3 Increased Performance

As previously stated, the maximum ramjet ΔV achievable by the vehicle with the current engine design is between 240 ft/s and 1,150 ft/s. Heating constraints will most likely prevent the vehicle from demonstrating the maximum ΔV value for the manner in which the trajectory was flown. If significant performance gains are achieved from further efforts to design the engine inlet such that it is optimally designed to the DRACO D-21 operating envelope then additional modifications will have to be made to the DRACO D-21.

The first obstacle to increased performance, external heating, has already been identified. Increased engine performance will reduce the time spent accelerating and hence the heat load transferred to the vehicle. This will reduce the thermal protection system requirements. For example, the X-15 flew to its maximum speed, Mach 6.7 at 102,100 ft in 170 seconds. With its current performance, the D-21 DRACO flies to Mach 4.5 at 85,000 ft in 240 to 425 seconds.

If it is assumed that the vehicle will be capable of meeting the desired maximum flight speed of Mach 6 on solely internally carried propellant once the inlet design optimization has been completed, then the following additional modifications to the vehicle would also be required:

- Increased ablative mass thickness (function of vehicle acceleration rate)
- Replacement of titanium inlet duct to accommodate higher inlet air stagnation temperature (will be required for speeds above Mach 3.5-5.0, depending on acceleration and altitude)
- Replacement of vehicle leading edges and control surfaces with material capable of accommodating higher stagnation temperatures (ablative material pressure limits will be exceeded for Mach number higher than 3.5 to 4.0)

11.0 Recommended Follow on Studies

11.1 Continued Performance Analysis Studies

The results obtained during the course of the 45 day study have shown that a modified D-21 is capable of demonstrating the NASA DRACO engines three engine operating modes while achieving a minimum burnout velocity of approximately 3,500 ft/s (Mach 3.5). While the study has indicated that greater performance could be obtained, follow on work is required to substantiate these findings.

As previously mentioned, the optimal DRACO engine inlet design Mach number was not determined over the course of the study. Further engine design studies coupled with further flight trajectory analysis will allow the determination of the optimal inlet design Mach number for the modified D-21 test bed.

The study has identified thermal loading as the biggest potential inhibitor to additional performance gains. An additional follow on study should include the development of an ablative thermal protection simulation module, which can be integrated with the trajectory analysis tools. This addition will allow the effects of the increased temperature environment to be accounted for in the trajectory optimization studies.

11.2 Aerodynamic Studies

The study has shown that a traditional recovery system out performs a parafoil recovery system in terms of cost, weight, and vehicle structural modification impacts. However obtaining closure on the ability the vehicle is to perform a traditional landing is not possible without conducting low speed wind tunnel testing. In addition, the incremental increase in drag due to the addition of the externally mounted landing skid pods must also be evaluated. Also, the effects of varying the leading edge radius of the wing on vehicle heating should also be evaluated.

11.3 Power System Requirements and Power Generation Studies

NASA engine power estimates have indicated that a peak engine power of 5 kW will be required with the average engine power requirements being on the order of 2.5 kW. The original D-21 utilized a 4 kW 120/208 V, 400 Hz generator and a 100 A, 28 VDC generator driven by the vehicle APU to provide primary vehicle power. Unfortunately, the design power levels would not be reached until the operational flight conditions of the original D-21 are reached. For this study it was assumed that batteries would supplement the APU over areas in the flight regime where the airflow was insufficient to allow the APU to provide the required vehicle power. A power schedule will have to be developed to determine if the approach taken during the study is indeed the best approach to providing vehicle power for flight conditions that do not supply sufficient airflow to drive the existing APU.

11.4 Structural Modification Studies

During the study, emphasis was placed on minimizing the number of structural modifications required to the vehicle. This preliminary study has indicated that two major structural modifications, the oxidizer tank and traditional landing system modifications, are required to modify the D-21 into an RBCC test bed. While efforts to minimize the impacts of these vehicle modifications were considered, no structural analyses were performed. If further evaluations on the suitability of utilizing the D-21 are to be performed, a structural analysis of the above modifications should be included.

12.0 Additional Test Bed Capabilities

The modularity designed into the D-21 makes it well suited to operate as an advanced technology test bed. The removable leading edge wing chines and wing sections and the lower mounted removable payload hatch are examples of this modular design philosophy. During the design modification phase an opportunity will exist to extend the modularity of the design by providing provisions to allow the installation of advanced components or subsystems for flight-testing. Examples of technologies that could be flight tested on a modified D-21 are discussed below:

- Advanced thermal protection systems. The modular design approach utilized in the wing chine and leading edge sections of the vehicle make it ideal for testing advanced thermal protection systems. New sections made of the advanced TPS materials can easily replace existing wing leading edge sections.
- High-density batteries, super capacitors, fuel cells, and compact, high efficiency electric motors and controllers are now being considered for use in advanced space vehicles and propulsion systems. Through a flexible design approach, these types of power units could be introduced as they become available for flight-testing. An all- electric system could also demonstrate numerous operational benefits due to simplified checkout and flight readiness procedures.
- The modular nature of avionic packages would allow a parallel and/or integrated approach for flight testing of advanced concepts. Automated flight safety systems, innovative thermal conditioning systems, advanced types of integrated health monitoring systems, and improved power and flight control concepts are likely candidates for demonstration in a flight test bed prior to introduction into fully operational vehicles.
- Advanced tank pressurant gas combinations using catalysts such as “Tridyne” can also be used for powering turbopumps, turboelectric generators and reaction control systems. LMA is now developing this technology under contract to NASA-MSFC.

- Advanced propulsion systems, such as Pulse Detonation Engines (PDE), could be installed (using similar mounting points) in place of the NASA DRACO RBCC engine to allow flight demonstration.

Appendix:

A: Aerodynamic Data

B: NASA DRACO Engine Data

C: Minimal Modification Propellant Tank Layout Drawing

D: Traditional Landing System Layout Drawing

E: OTIS Trajectory Results

E1: NASAE3GTLOXPRA
E2: NASAE3GTLOXJPA
E3: NASAE3GTH2O2JPA
E4: NASAE3CTLOXPRB4
E5: NASAE3CTLOXJPB4
E6: NASAE3CTH2O2JPB4
E7: NASAE3CTLOXPRC1
E8: NASAE3CTLOXJPC1
E9: NASAE3CTH2O2JPC1

F: FASTPASS Results

F1: NASAE3CTH2O2JP
F2: NASAE3CTLOXJP
F3: NASAE3CTLOXPR
F4: NASAE3GTH2O2JP
F5: NASAE3GTLOXJP
F6: NASAE3GTLOXPR

Appendix A: Aerodynamic Data

D-21 N/C Aerodynamic Data

Alpha	Mach # 0.1		Mach # 0.8		Mach # 0.9		Mach # 1		Mach # 1.1		Mach # 1.2	
	CL	CL	CL	CL	CL	CL	CL	CL	CL	CL	CL	CL
-2												
-1												
0	0.0000	0.0000	0.0000	0.0000	0.0000	0.0000	0.0000	0.0000	0.0000	0.0000	0.0000	0.0000
1	0.0259	0.0259	0.0287	0.0331	0.0341	0.0333						
2	0.0548	0.0548	0.0603	0.0690	0.0706	0.0690						
3	0.0868	0.0868	0.0950	0.1077	0.1097	0.1070						
4	0.1218	0.1218	0.1326	0.1492	0.1513	0.1475						
5	0.1599	0.1599	0.1733	0.1935	0.1955	0.1903						
6	0.2009	0.2009	0.2170	0.2405	0.2421	0.2355						
7	0.2451	0.2451	0.2636	0.2903	0.2913	0.2831						
8	0.2922	0.2922	0.3133	0.3429	0.3430	0.3330						
9	0.3425	0.3425	0.3659	0.3983	0.3972	0.3854						
10	0.3957	0.3957	0.4216	0.4564	0.4539	0.4401						
11	0.4520	0.4520	0.4803	0.5173	0.5132	0.4972						
12	0.5113	0.5113	0.5419	0.5810	0.5749	0.5567						

Alpha	Mach # 0.1		Mach # 0.8		Mach # 0.9		Mach # 1		Mach # 1.1		Mach # 1.2	
	CD	CD	CD	CD	CD	CD	CD	CD	CD	CD	CD	CD
-2												
-1												
0	0.0140	0.0140	0.0146	0.0201	0.0235	0.0241						
1	0.0143	0.0143	0.0150	0.0206	0.0240	0.0246						
2	0.0153	0.0153	0.0161	0.0221	0.0256	0.0261						
3	0.0172	0.0172	0.0184	0.0249	0.0285	0.0288						
4	0.0204	0.0204	0.0220	0.0293	0.0329	0.0330						
5	0.0250	0.0250	0.0272	0.0356	0.0392	0.0390						
6	0.0314	0.0314	0.0343	0.0440	0.0476	0.0468						
7	0.0398	0.0398	0.0437	0.0550	0.0583	0.0569						
8	0.0507	0.0507	0.0558	0.0687	0.0718	0.0696						
9	0.0644	0.0644	0.0708	0.0857	0.0883	0.0850						
10	0.0813	0.0813	0.0891	0.1063	0.1081	0.1035						
11	0.1018	0.1018	0.1113	0.1308	0.1316	0.1254						
12	0.1264	0.1264	0.1377	0.1598	0.1592	0.1511						

Appendix A: Aerodynamic Data

D-21 N/C Aerodynamic Data

Alpha	Mach # 1.3		Mach # 1.4		Mach # 1.5		Mach # 1.6		Mach # 1.8		Mach # 2.1	
	CL	CL	CL	CL	CL	CL	CL	CL	CL	CL	CL	CL
-2							-0.0850	-0.0850	-0.0775			
-1							-0.0450	-0.0450	-0.0450			
0	0.0000	0.0000	0.0000	0.0000	0.0000	0.0000	-0.0100	-0.0100	-0.0100			
1	0.0325	0.0330	0.0337	0.0337	0.0337	0.0337	0.0250	0.0250	0.0250			
2	0.0673	0.0680	0.0691	0.0691	0.0691	0.0691	0.0600	0.0600	0.0600			
3	0.1045	0.1050	0.1063	0.1063	0.1063	0.1063	0.1050	0.1000	0.0925			
4	0.1439	0.1440	0.1451	0.1451	0.1451	0.1451	0.1500	0.1475	0.1325			
5	0.1856	0.1850	0.1857	0.1857	0.1857	0.1857	0.1900	0.1850	0.1725			
6	0.2296	0.2280	0.2280	0.2280	0.2280	0.2280	0.2325	0.2275	0.2100			
7	0.2759	0.2730	0.2720	0.2720	0.2720	0.2720	0.2875	0.2725	0.2500			
8	0.3246	0.3200	0.3178	0.3178	0.3178	0.3178	0.3325	0.3175	0.2900			
9	0.3755	0.3690	0.3652	0.3652	0.3652	0.3652	0.3825	0.3625	0.3300			
10	0.4287	0.4200	0.4144	0.4144	0.4144	0.4144	0.4350	0.4050	0.3725			
11	0.4842	0.4730	0.4653	0.4653	0.4653	0.4653	0.4800	0.4525	0.4150			
12	0.5420	0.5280	0.5179	0.5179	0.5179	0.5179						

Alpha	Mach # 1.3		Mach # 1.4		Mach # 1.5		Mach # 1.6		Mach # 1.8		Mach # 2.1	
	CD	CD	CD	CD	CD	CD	CD	CD	CD	CD	CD	CD
-2							0.0276	0.0275	0.0268			
-1							0.0254	0.0252	0.0249			
0	0.0244	0.0249	0.0247	0.0247	0.0247	0.0247	0.0245	0.0243	0.0239			
1	0.0249	0.0253	0.0252	0.0252	0.0252	0.0252	0.0248	0.0246	0.0242			
2	0.0263	0.0268	0.0267	0.0267	0.0267	0.0267	0.0260	0.0259	0.0256			
3	0.0289	0.0294	0.0295	0.0295	0.0295	0.0295	0.0292	0.0287	0.0280			
4	0.0330	0.0334	0.0336	0.0336	0.0336	0.0336	0.0341	0.0340	0.0323			
5	0.0386	0.0390	0.0392	0.0392	0.0392	0.0392	0.0399	0.0395	0.0382			
6	0.0461	0.0464	0.0465	0.0465	0.0465	0.0465	0.0476	0.0473	0.0451			
7	0.0557	0.0557	0.0558	0.0558	0.0558	0.0558	0.0598	0.0574	0.0540			
8	0.0677	0.0673	0.0671	0.0671	0.0671	0.0671	0.0717	0.0692	0.0644			
9	0.0824	0.0813	0.0807	0.0807	0.0807	0.0807	0.0869	0.0828	0.0764			
10	0.1000	0.0980	0.0968	0.0968	0.0968	0.0968	0.1052	0.0973	0.0908			
11	0.1208	0.1176	0.1156	0.1156	0.1156	0.1156	0.1228	0.1155	0.1069			
12	0.1452	0.1404	0.1373	0.1373	0.1373	0.1373						

Appendix A: Aerodynamic Data

D-21 N/C Aerodynamic Data

Alpha	Mach # 2.5		Mach # 2.75		Mach # 3		Mach # 3.25		Mach # 3.3		Mach # 3.5	
	CL	CL	CL	CL	CL	CL	CL	CL	CL	CL	CL	CL
-2	-0.0675	-0.0625	-0.0550	-0.0525	-0.0525	-0.0525	-0.0525	-0.0525	-0.0525	-0.0525	-0.0500	-0.0500
-1	-0.0350	-0.0350	-0.0275	-0.0275	-0.0275	-0.0275	-0.0275	-0.0275	-0.0275	-0.0275	-0.0250	-0.0250
0	-0.0025	-0.0025	-0.0025	0.0000	0.0000	0.0000	0.0000	0.0000	0.0000	0.0000	0.0000	0.0000
1	0.0250	0.0250	0.0250	0.0275	0.0275	0.0275	0.0275	0.0275	0.0275	0.0275	0.0225	0.0225
2	0.0600	0.0600	0.0525	0.0550	0.0550	0.0550	0.0550	0.0550	0.0550	0.0550	0.0475	0.0475
3	0.0925	0.0850	0.0800	0.0800	0.0800	0.0800	0.0800	0.0800	0.0800	0.0800	0.0725	0.0725
4	0.1250	0.1150	0.1100	0.1100	0.1100	0.1100	0.1100	0.1100	0.1100	0.1100	0.0975	0.0975
5	0.1575	0.1450	0.1350	0.1350	0.1350	0.1350	0.1350	0.1350	0.1350	0.1350	0.1225	0.1225
6	0.1900	0.1775	0.1650	0.1625	0.1625	0.1625	0.1625	0.1625	0.1625	0.1625	0.1475	0.1475
7	0.2250	0.2075	0.1950	0.1925	0.1925	0.1925	0.1925	0.1925	0.1925	0.1925	0.1750	0.1750
8	0.2600	0.2400	0.2225	0.2200	0.2200	0.2200	0.2200	0.2200	0.2200	0.2200	0.2000	0.2000
9	0.2925	0.2700	0.2525	0.2475	0.2475	0.2475	0.2475	0.2475	0.2475	0.2475	0.2250	0.2250
10	0.3300	0.3025	0.2800	0.2750	0.2750	0.2750	0.2750	0.2750	0.2750	0.2750	0.2525	0.2525
11				0.3000	0.3000	0.3000	0.3000	0.3000	0.3000	0.3000	0.2800	0.2800
12				0.3250	0.3250	0.3250	0.3250	0.3250	0.3250	0.3250	0.3075	0.3075

Alpha	Mach # 2.5		Mach # 2.75		Mach # 3		Mach # 3.25		Mach # 3.3		Mach # 3.5	
	CD	CD	CD	CD	CD	CD	CD	CD	CD	CD	CD	CD
-2	0.0228	0.0205	0.0183	0.0155	0.0155	0.0155	0.0155	0.0155	0.0153	0.0153	0.0153	0.0153
-1	0.0210	0.0189	0.0169	0.0141	0.0141	0.0141	0.0141	0.0141	0.0139	0.0139	0.0140	0.0140
0	0.0203	0.0182	0.0164	0.0136	0.0136	0.0136	0.0136	0.0136	0.0134	0.0134	0.0136	0.0136
1	0.0207	0.0186	0.0168	0.0141	0.0141	0.0141	0.0141	0.0141	0.0139	0.0139	0.0139	0.0139
2	0.0223	0.0203	0.0181	0.0157	0.0157	0.0157	0.0157	0.0157	0.0155	0.0155	0.0152	0.0152
3	0.0250	0.0224	0.0204	0.0179	0.0179	0.0179	0.0179	0.0179	0.0178	0.0178	0.0173	0.0173
4	0.0288	0.0259	0.0240	0.0217	0.0217	0.0217	0.0217	0.0217	0.0216	0.0216	0.0204	0.0204
5	0.0338	0.0305	0.0278	0.0258	0.0258	0.0258	0.0258	0.0258	0.0258	0.0258	0.0243	0.0243
6	0.0399	0.0366	0.0334	0.0313	0.0313	0.0313	0.0313	0.0313	0.0313	0.0313	0.0291	0.0291
7	0.0478	0.0433	0.0402	0.0384	0.0384	0.0384	0.0384	0.0384	0.0386	0.0386	0.0355	0.0355
8	0.0570	0.0518	0.0474	0.0460	0.0460	0.0460	0.0460	0.0460	0.0463	0.0463	0.0422	0.0422
9	0.0667	0.0607	0.0563	0.0546	0.0546	0.0546	0.0546	0.0546	0.0550	0.0550	0.0498	0.0498
10	0.0794	0.0716	0.0654	0.0643	0.0643	0.0643	0.0643	0.0643	0.0647	0.0647	0.0593	0.0593
11				0.0739	0.0739	0.0739	0.0739	0.0739	0.0745	0.0745	0.0698	0.0698
12				0.0843	0.0843	0.0843	0.0843	0.0843	0.0851	0.0851	0.0813	0.0813

Appendix A: Aerodynamic Data

D-21 N/C Aerodynamic Data

Alpha	Mach #	Mach #	Mach #
	-2	5	6 10
-1	CL	CL	CL
0	-0.027742	-0.02342	-0.012634
1	-0.013864	-0.011699	-0.006513
2	0	0	0
3	0.013909	0.011747	0.006952
4	0.027922	0.023614	0.014389
5	0.042097	0.035673	0.022357
6	0.056494	0.047994	0.030902
7	0.071172	0.06065	0.04007
8	0.08619	0.073712	0.049907
9	0.101606	0.087252	0.06046
10	0.11748	0.10134	0.071774
11	0.13387	0.116049	0.083895
12	0.150837	0.131449	0.09687
	0.168437	0.147613	0.110744
	0.186732	0.164612	0.125565

Alpha	Mach #	Mach #	Mach #
	-2	5	6 10
-1	CD	CD	CD
0	0.013441	0.012857	0.010036
1	0.012666	0.012182	0.009895
2	0.012366	0.011909	0.00992
3	0.012563	0.012064	0.010162
4	0.01328	0.012674	0.010669
5	0.01454	0.013765	0.011493
6	0.016366	0.015362	0.012684
7	0.018781	0.017492	0.01429
8	0.021807	0.02018	0.016362
9	0.025468	0.023454	0.018951
10	0.029786	0.027339	0.022105
11	0.034785	0.031861	0.025874
12	0.040486	0.037046	0.03031
	0.046914	0.04292	0.035461
	0.054091	0.04951	0.041378

Appendix B1: NASA E1STLOXPR

NASA Ejector Engine Data: 8/18/99

Primary Thruster Scaling Model	Propane/LOX	
RBCC Engine Reference Area Aref (ft ²)	4.2773	Existing Cowl Projected Area
RBCC Engine Exit Area Aexit (ft ²)	7.0686	Existing RJ-43 Exit Area
Primary Chamber Pressure Pc (psia)	1000	Primary Thruster Design Requirement
Primary Mixture Ratio MR_pri	3.4	Primary Thruster Design Requirement
Primary Exit Pressure Pexit (psia)	14.7	Primary Thruster Design Requirement
Primary Chamber-to-Exit Pressure Pc/Pexit	68.0272	Primary Thruster Design Requirement
Primary Area Ratio c _{pri}	10.673	CEA Output (Equilibrium Composition Assumed)
Vacuum Specific Impulse Isp_vac (sec)	328.1	CEA Output (Equilibrium Composition Assumed)
Vacuum Thrust Coefficient Ct_vac	1.8087	CEA Output (Equilibrium Composition)
Vacuum Thrust F_vac (lbf)	8584.66	Iterate to obtain required F_sls
Primary Throat Area A*_pri (in ²)	4.7463	Scaled Primary Throat Area
Primary Exit Area A_pri (in ²)	50.6574	Scaled Primary Exit Area
Primary Exit Area A_pri (ft ²)	0.3518	Scaled Primary Exit Area
Required SLS Thrust F_sls (lbf)	7840.00	Match required D-21 F_sls
Total Primary Flowrate W_pri (lbm/s)	26.1648	Information Only
Total Primary Oxidizer Flowrate Wo_pri (lbm/s)	20.2182	Information Only
Total Primary Fuel Flowrate Wf_pri (lbm/s)	5.9465	Information Only

NASA Ramjet Engine Data: 8/18/99

Mach Number	Specific Impulse (sec)	Thrust Coefficient
2.0	917.9	0.4374
2.5	1165.0	1.1504
3.0	1271.4	1.1385
3.5	1289.8	1.0805
4.0	1271.2	1.0072
4.5	1230.8	0.9381
5.0	1174.7	0.8607
5.5	1102.2	0.7907
6.0	1027.7	0.7541
6.5	951.0	0.6878
7.0	870.6	0.6207

Force accounting system: Spike Tip-to-Engine Tail

Appendix B2: NASA E1STLOXJP

NASA Ejector Engine Data: 8/18/99

Primary Thruster Scaling Model	JP-5/LOX	
RBCC Engine Reference Area Aref (ft^2)	4.2773	Existing Cowl Projected Area
RBCC Engine Exit Area Aexit (ft^2)	7.0686	Existing RJ-43 Exit Area
Primary Chamber Pressure Pc (psia)	1000	Primary Thruster Design Requirement
Primary Mixture Ratio MR_pri	2.6	Primary Thruster Design Requirement
Primary Exit Pressure Pexit (psia)	14.7	Primary Thruster Design Requirement
Primary Chamber-to-Exit Pressure Pc/Pexit	68.0272	Primary Thruster Design Requirement
Primary Area Ratio c_pri	10.052	CEA Output (Equilibrium Composition Assumed)
Vacuum Specific Impulse Isp_vac (sec)	326.9	CEA Output (Equilibrium Composition Assumed)
Vacuum Thrust Coefficient Ct_vac	1.7867	CEA Output (Equilibrium Composition)
Vacuum Thrust F_vac (lbf)	8546.84	Iterate to obtain required F_sls
Primary Throat Area A*_pri (in^2)	4.7836	Scaled Primary Throat Area
Primary Exit Area A_pri (in^2)	48.0847	Scaled Primary Exit Area
Primary Exit Area A_pri (ft^2)	0.3339	Scaled Primary Exit Area
Required SLS Thrust F_sls (lbf)	7840.00	Match required D-21 F_sls
Total Primary Flowrate W_pri (lbm/s)	26.1451	Information Only
Total Primary Oxidizer Flowrate Wo_pri (lbm/s)	18.8826	Information Only
Total Primary Fuel Flowrate Wf_pri (lbm/s)	7.2625	Information Only

NASA Ramjet Engine Data: 8/18/99

Mach Number	Specific Impulse (sec)	Thrust Coefficient
2.0	825.2	0.4009
2.5	1064.1	1.1248
3.0	1177.7	1.1290
3.5	1200.1	1.0762
4.0	1186.1	1.0061
4.5	1151.2	0.9393
5.0	1101.6	0.8640
5.5	1036.6	0.7961
6.0	968.6	0.7608
6.5	900.5	0.6972
7.0	828.9	0.6326

Force accounting system: Spike Tip-to-Engine Tail

Appendix B3: NASA E1STH2O2JP

NASA Ejector Engine Data: 8/18/99

Primary Thruster Scaling Model	JP-5/ H2O2 (90%)	
RBCC Engine Reference Area Aref (ft ²)	4.2773	Existing Cowl Projected Area
RBCC Engine Exit Area Aexit (ft ²)	7.0686	Existing RJ-43 Exit Area
Primary Chamber Pressure Pc (psia)	1000	Primary Thruster Design Requirement
Primary Mixture Ratio MR_pri	7.0	Primary Thruster Design Requirement
Primary Exit Pressure Pexit (psia)	14.7	Primary Thruster Design Requirement
Primary Chamber-to-Exit Pressure Pc/Pexit	68.0272	Primary Thruster Design Requirement
Primary Area Ratio c_pri	9.855	CEA Output (Equilibrium Composition Assumed)
Vacuum Specific Impulse Isp_vac (sec)	323.5	CEA Output (Equilibrium Composition Assumed)
Vacuum Thrust Coefficient Ct_vac	1.7808	CEA Output (Equilibrium Composition)
Vacuum Thrust F_vac (lbf)	8534.26	Iterate to obtain required F_sls
Primary Throat Area A*_pri (in ²)	4.7924	Scaled Primary Throat Area
Primary Exit Area A_pri (in ²)	47.2289	Scaled Primary Exit Area
Primary Exit Area A_pri (ft ²)	0.3280	Scaled Primary Exit Area
Required SLS Thrust F_sls (lbf)	7840.00	Match required D-21 F_sls
Total Primary Flowrate W_pri (lbm/s)	26.3810	Information Only
Total Primary Oxidizer Flowrate Wo_pri (lbm/s)	23.0834	Information Only
Total Primary Fuel Flowrate Wf_pri (lbm/s)	3.2976	Information Only

Appendix B4: NASAE2GTLOXPR

Ejector Thrust Data

ALT	MACH							
	0.0	0.5	1.0	1.5	2.0	2.5	3.0	3.5
0.0	8622.8	9987.3	15334.1	29497.9	52919.0	98210.3	143260.0	198985.0
5000.0	8714.2	9829.7	14288.8	26133.2	45843.1	84134.7	122705.0	168666.0
10000.0	8761.1	9708.6	13403.4	23169.6	39727.6	72079.8	104044.0	142431.0
15000.0	8717.2	9527.1	12674.6	20764.5	34533.4	61441.5	87914.6	119701.0
20000.0	8630.6	9313.5	12004.2	18646.7	29936.9	52215.0	74196.7	100310.0
25000.0	8526.7	9107.6	11346.7	16816.7	26133.5	44328.9	62292.7	83743.8
30000.0	8425.3	8905.3	10777.4	15270.6	22795.5	37657.6	52291.8	69722.0
35000.0	8332.9	8731.8	10281.0	13976.0	20029.3	31959.6	43749.6	58113.1
40000.0	8224.2	8552.1	9814.0	12785.8	17583.9	27006.9	36360.1	47748.6
45000.0	8148.1	8408.0	9434.4	11766.9	15610.6	23019.5	30377.5	39359.8
50000.0	8098.9	8317.6	9146.9	11008.1	14034.5	19864.8	25664.0	32753.9
55000.0	8057.2	8228.2	8892.2	10396.2	12801.7	17379.0	21928.6	27563.1
60000.0	8055.1	8191.6	8715.1	9907.0	11802.8	15428.2	19010.3	23479.4
65000.0	8050.3	8160.8	8579.1	9519.9	11017.9	13879.0	16712.2	20246.0
70000.0	8050.5	8133.6	8463.7	9208.4	10395.6	12630.9	14860.0	17668.6
75000.0	8045.3	8111.8	8371.8	8959.5	9900.7	11670.7	13422.6	15602.4
80000.0	8042.2	8096.9	8298.9	8764.9	9509.9	10904.1	12296.5	14021.9

Ejector ISP Data

ALT	MACH							
	0.0	0.5	1.0	1.5	2.0	2.5	3.0	3.5
0.0	247.63	283.55	414.68	685.04	1041.07	1523.04	1891.64	2234.36
5000.0	252.62	282.78	394.91	634.29	959.61	1418.21	1776.96	2106.72
10000.0	256.40	281.42	376.73	585.31	881.16	1312.64	1651.79	1972.15
15000.0	259.01	280.20	360.92	543.85	807.04	1205.13	1523.04	1829.83
20000.0	259.88	278.04	347.10	504.40	734.47	1097.27	1395.40	1684.63
25000.0	259.74	275.46	334.16	468.14	669.08	992.45	1264.52	1536.56
30000.0	259.26	272.41	322.51	435.94	606.50	893.01	1138.72	1388.99
35000.0	258.64	269.72	311.92	407.82	551.25	797.99	1015.39	1245.75
40000.0	257.26	266.50	301.46	380.63	499.24	707.72	896.42	1100.76
45000.0	256.50	263.89	292.75	356.14	454.81	628.37	788.60	966.24
50000.0	256.23	262.53	286.11	337.58	417.47	560.60	695.14	847.23
55000.0	255.93	260.87	279.92	322.17	387.18	503.85	614.95	744.38
60000.0	256.66	260.63	275.73	309.56	361.74	457.12	548.34	656.86
65000.0	257.14	260.37	272.50	299.43	341.28	418.45	493.14	582.85
70000.0	257.66	260.08	269.69	291.15	324.73	386.20	446.63	520.65
75000.0	257.89	259.83	267.42	284.45	311.34	360.83	409.36	468.61
80000.0	258.10	259.70	265.60	279.17	300.62	340.09	379.38	427.36

Appendix B4: NASAE2GTLOXPR

Ramjet Thrust Data

ALT	MACH										
	2.0	2.5	3.0	3.5	4.0	4.5	5.0	5.5	6.0	6.5	7.0
40000.0	2.1241	2.5496	2.6270	2.6923	2.7464	2.7835	2.8591	2.9524	2.8084	2.6847	2.5760
45000.0	2.1224	2.5499	2.6263	2.6921	2.7482	2.7826	2.8578	2.9514	2.8086	2.6829	2.5773
50000.0	2.1224	2.5499	2.6263	2.6921	2.7482	2.7826	2.8578	2.9514	2.8086	2.6829	2.5773
55000.0	2.1224	2.5499	2.6263	2.6921	2.7482	2.7826	2.8578	2.9514	2.8086	2.6829	2.5773
60000.0	2.1224	2.5499	2.6263	2.6921	2.7482	2.7826	2.8578	2.9514	2.8086	2.6829	2.5773
65000.0	2.1224	2.5499	2.6263	2.6921	2.7482	2.7826	2.8578	2.9514	2.8086	2.6829	2.5773
70000.0	2.1206	2.5435	2.6200	2.6869	2.7413	2.7779	2.8551	2.9457	2.8031	2.6818	2.5742
75000.0	2.1157	2.5361	2.6160	2.6634	2.7361	2.7744	2.8501	2.9430	2.7959	2.6733	2.5693
80000.0	2.1281	2.5317	2.6080	2.6572	2.7310	2.7687	2.8452	2.9341	2.7902	2.6693	2.5646
85000.0	2.1235	2.5246	2.6001	2.6510	2.7250	2.7620	2.8406	2.9272	2.7878	2.6650	2.5607
90000.0	2.1189	2.5174	2.5967	2.6449	2.7170	2.7584	2.8362	2.9256	2.7825	2.6625	2.5569
95000.0	2.1169	2.5135	2.5898	2.6391	2.7159	2.7549	2.8320	2.9191	2.7765	2.6577	2.5526
100000.0	2.1291	2.5066	2.5828	2.6335	2.7074	2.7469	2.8240	2.9128	2.7737	2.6535	2.5490
105000.0	2.1245	2.4997	2.5796	2.6280	2.7031	2.7441	2.8199	2.9058	2.7678	2.6470	2.5453
110000.0	2.1143	2.4828	2.5603	2.6145	2.6873	2.7291	2.8132	2.8942	2.7540	2.6346	2.5338
115000.0	2.1349	2.4669	2.5470	2.5982	2.6773	2.7197	2.8039	2.8778	2.7410	2.6227	2.5234
120000.0	2.1258	2.4518	2.5304	2.5841	2.6647	2.7081	2.7927	2.8624	2.7288	2.6126	2.5098

Ramjet ISP Data

ALT	MACH										
	2.0	2.5	3.0	3.5	4.0	4.5	5.0	5.5	6.0	6.5	7.0
40000.0	2759.1	2666.5	2960.6	3188.6	3382.4	3554.7	3716.9	3873.6	4019.6	4162.7	4301.5
45000.0	2757.8	2667.5	2960.7	3189.3	3385.6	3554.5	3716.2	3873.6	4021.2	4161.2	4305.0
50000.0	2757.8	2667.5	2960.7	3189.3	3385.6	3554.5	3716.2	3873.6	4021.2	4161.2	4305.0
55000.0	2757.8	2667.5	2960.7	3189.3	3385.6	3554.5	3716.2	3873.6	4021.2	4161.2	4305.0
60000.0	2757.8	2667.5	2960.7	3189.3	3385.6	3554.5	3716.2	3873.6	4021.2	4161.2	4305.0
65000.0	2757.8	2667.5	2960.7	3189.3	3385.6	3554.5	3716.2	3873.6	4021.2	4161.2	4305.0
70000.0	2762.8	2668.0	2961.5	3191.6	3386.0	3557.4	3721.8	3877.3	4024.9	4171.6	4312.3
75000.0	2765.1	2668.4	2966.0	3194.7	3389.4	3563.2	3725.6	3886.4	4027.9	4172.2	4318.3
80000.0	2714.4	2671.8	2965.7	3196.7	3392.9	3566.0	3729.4	3887.4	4032.8	4179.6	4324.5
85000.0	2716.8	2672.4	2965.6	3198.7	3395.3	3567.4	3733.4	3890.9	4042.5	4186.4	4332.0
90000.0	2719.1	2672.8	2970.5	3200.7	3395.0	3572.7	3737.7	3901.3	4047.7	4196.0	4339.6
95000.0	2724.6	2676.5	2971.3	3203.0	3403.2	3578.1	3742.0	3905.1	4052.0	4201.8	4346.1
100000.0	2676.1	2677.1	2972.0	3205.3	3402.2	3577.5	3741.1	3909.0	4060.7	4208.5	4353.8
105000.0	2678.4	2677.6	2977.0	3207.7	3406.4	3583.6	3745.4	3912.1	4065.0	4211.5	4361.3
110000.0	2687.2	2681.0	2978.3	3216.5	3412.5	3590.6	3763.1	3930.6	4080.2	4228.6	4379.7
115000.0	2598.4	2684.9	2986.0	3221.1	3425.4	3604.2	3776.4	3942.0	4096.0	4245.9	4399.4
120000.0	2607.5	2689.2	2989.4	3227.9	3434.3	3614.3	3786.2	3954.1	4112.3	4265.3	4412.6

All-Rocket Mode Data:

Vacuum Thrust	9986.07
Exit Area	7.0686
Vacuum Isp	329.243

Appendix B5: NASAE2GTLOXJP

Ejector Thrust Data

ALT	Mach								
	0.0	0.5	1.0	1.5	2.0	2.5	3.0	3.5	
0	8638.72	9909.87	14909.70	28075.60	52070.70	97967.20	143277.00	199234.00	
5000	8738.39	9832.08	14000.70	24891.20	44866.90	84017.10	122948.00	169078.00	
10000	8882.86	9729.19	13243.60	22367.70	38826.70	72133.50	104387.00	142967.00	
15000	8989.11	9717.24	12607.20	20162.40	33769.30	61528.80	88403.30	120239.00	
20000	9083.33	9698.20	12038.20	18273.50	29263.20	52406.30	74569.60	101037.00	
25000	9095.42	9645.32	11651.50	16780.00	25695.30	44617.10	62855.30	84419.20	
30000	9069.69	9541.75	11333.60	15435.10	22676.10	38006.40	52873.20	70410.00	
35000	9037.86	9430.95	10938.50	14476.00	20154.70	32402.00	44409.20	58912.00	
40000	8977.11	9304.17	10545.00	13422.90	18083.30	27546.30	37037.80	48515.80	
45000	8935.60	9197.19	10209.70	12518.50	16253.60	23616.40	31081.40	40163.00	
50000	8919.21	9134.29	9918.55	11783.60	14756.90	20503.20	26385.60	33547.50	
55000	8893.15	9068.08	9715.54	11196.60	13549.70	18091.30	22703.60	28377.20	
60000	8896.41	9030.49	9549.60	10722.30	12589.90	16166.00	19784.30	24281.70	
65000	8895.11	9003.63	9414.37	10351.20	11823.50	14648.50	17489.30	21080.30	
70000	8898.50	8979.82	9304.25	10043.00	11213.90	13428.00	15675.90	18513.90	
75000	8894.85	8960.42	9216.21	9802.19	10723.90	12476.60	14249.60	16452.50	
80000	8893.34	8946.80	9146.67	9605.29	10344.40	11727.20	13118.50	14877.70	

Ejector ISP Data

ALT	Mach								
	0.0	0.5	1.0	1.5	2.0	2.5	3.0	3.5	
0	241.10	273.52	394.90	646.56	970.00	1425.50	1773.93	2096.52	
5000	245.88	273.89	377.06	598.82	901.95	1329.34	1670.10	1979.83	
10000	250.41	273.49	362.25	556.63	830.81	1233.49	1555.12	1856.52	
15000	254.26	273.95	348.85	517.23	763.74	1133.69	1437.73	1724.50	
20000	257.70	274.12	336.84	481.60	695.99	1034.94	1317.10	1592.69	
25000	261.08	274.88	327.59	450.26	635.34	939.10	1198.83	1454.53	
30000	263.01	275.05	319.53	422.23	580.62	847.64	1082.25	1317.79	
35000	264.38	274.54	312.70	399.53	530.45	761.16	969.21	1186.94	
40000	264.66	273.26	305.25	376.47	484.75	679.37	859.01	1051.68	
45000	265.13	272.07	298.58	357.01	446.05	606.92	759.33	927.50	
50000	265.99	271.76	292.42	340.53	413.54	544.88	672.80	816.61	
55000	266.28	271.00	288.27	327.00	386.14	494.03	599.53	721.43	
60000	267.22	270.84	284.79	315.78	363.62	451.24	537.49	639.65	
65000	267.85	270.80	281.88	306.88	345.15	416.13	486.16	571.58	
70000	268.48	270.68	279.48	299.32	330.15	386.90	443.91	513.93	
75000	268.79	270.57	277.52	293.36	317.86	363.54	409.51	465.57	
80000	269.07	270.53	275.97	288.40	308.24	344.73	381.43	427.28	

Appendix B5: NASA E2GTLOXJP

Ramjet Thrust Data

ALT	Mach										
	2.0	2.5	3.0	3.5	4.0	4.5	5.0	5.5	6.0	6.5	7.0
40000	2.04421	2.53206	2.61802	2.68755	2.74423	2.78396	2.86133	2.95671	2.81515	2.69324	2.58622
45000	2.04261	2.53231	2.61727	2.68742	2.74597	2.78301	2.86001	2.95618	2.81465	2.69152	2.58604
50000	2.04261	2.53231	2.61727	2.68742	2.74597	2.78301	2.86001	2.95618	2.81465	2.69152	2.58604
55000	2.04261	2.53231	2.61727	2.68742	2.74597	2.78301	2.86001	2.95618	2.81465	2.69152	2.58604
60000	2.04261	2.53231	2.61727	2.68742	2.74597	2.78301	2.86001	2.95618	2.81465	2.69152	2.58604
65000	2.04261	2.53231	2.61727	2.68742	2.74597	2.78301	2.86001	2.95618	2.81465	2.69152	2.58604
70000	2.04078	2.52591	2.61110	2.68215	2.73912	2.77832	2.85764	2.94955	2.80985	2.68971	2.58360
75000	2.03611	2.51868	2.60715	2.65875	2.73400	2.77482	2.85257	2.94754	2.80272	2.68118	2.57968
80000	2.03143	2.51426	2.59913	2.65226	2.72900	2.76864	2.84771	2.93866	2.79096	2.67708	2.57495
85000	2.04391	2.50733	2.59126	2.64621	2.72295	2.76234	2.84296	2.93182	2.79431	2.67271	2.57033
90000	2.03946	2.50038	2.58774	2.64013	2.71520	2.75856	2.83822	2.93008	2.78889	2.67014	2.56717
95000	2.03744	2.49631	2.58091	2.63433	2.71389	2.75513	2.83432	2.92352	2.78299	2.66588	2.56276
100000	2.03302	2.48952	2.57416	2.62887	2.70545	2.74712	2.82634	2.91716	2.78015	2.66175	2.55911
105000	2.02842	2.48271	2.57082	2.62330	2.70112	2.74478	2.82260	2.91060	2.77422	2.65510	2.55543
110000	2.03514	2.46605	2.55168	2.60979	2.68523	2.72970	2.81574	2.89838	2.76028	2.64273	2.54360
115000	2.03963	2.45029	2.53839	2.59345	2.67551	2.72006	2.80674	2.88271	2.74786	2.63069	2.53389
120000	2.03064	2.43534	2.52190	2.57959	2.66285	2.70843	2.79508	2.86726	2.73568	2.62169	2.52075

Ramjet ISP Data

ALT	Mach										
	2.0	2.5	3.0	3.5	4.0	4.5	5.0	5.5	6.0	6.5	7.0
40000	2705.98	2473.69	2756.17	2973.30	3157.16	3321.17	3474.84	3623.75	3763.91	3901.00	4034.15
45000	2704.68	2474.71	2756.20	2974.06	3160.09	3320.98	3474.20	3624.29	3764.48	3899.78	4035.18
50000	2704.68	2474.71	2756.20	2974.06	3160.09	3320.98	3474.20	3624.29	3764.48	3899.78	4035.18
55000	2704.68	2474.71	2756.20	2974.06	3160.09	3320.98	3474.20	3624.29	3764.48	3899.78	4035.18
60000	2704.68	2474.71	2756.20	2974.06	3160.09	3320.98	3474.20	3624.29	3764.48	3899.78	4035.18
65000	2704.68	2474.71	2756.20	2974.06	3160.09	3320.98	3474.20	3624.29	3764.48	3899.78	4035.18
70000	2709.62	2475.13	2757.11	2976.11	3160.44	3323.69	3479.85	3626.67	3768.97	3908.49	4043.09
75000	2711.76	2475.63	2761.32	2979.08	3163.84	3329.07	3483.29	3636.13	3771.80	3908.93	4050.25
80000	2713.82	2478.68	2760.99	2980.68	3167.15	3331.12	3486.88	3637.04	3776.35	3915.70	4056.05
85000	2658.26	2479.32	2760.88	2982.68	3169.28	3332.93	3490.50	3640.36	3785.04	3922.02	4061.93
90000	2660.49	2479.88	2765.33	2984.56	3169.35	3337.68	3494.02	3649.95	3789.90	3930.90	4070.02
95000	2665.82	2483.21	2766.16	2986.68	3176.83	3342.75	3498.46	3653.46	3794.00	3937.21	4076.06
100000	2667.98	2483.79	2767.00	2988.92	3175.88	3342.17	3497.74	3657.11	3802.19	3943.62	4083.21
105000	2669.87	2484.30	2771.44	2991.17	3179.71	3348.43	3502.17	3660.49	3806.15	3946.28	4090.30
110000	2623.38	2487.54	2772.75	2999.28	3185.38	3354.93	3518.49	3677.10	3820.25	3962.35	4107.10
115000	2576.57	2491.20	2779.99	3003.51	3197.71	3367.35	3531.32	3688.73	3835.84	3978.30	4126.67
120000	2585.31	2495.31	2783.17	3009.98	3205.88	3376.63	3539.91	3700.03	3851.17	3998.25	4140.03

All-Rocket Mode Data:

Vacuum Thrust	11000.7
Exit Area	7.0686
Vacuum Isp	337.095

Appendix B6: NASA E2GTH2O2JP

Ejector Thrust Data:

ALT	MACH							
	0.0	0.5	1.0	1.5	2.0	2.5	3.0	3.5
0.0	8605.6	9874.7	14917.2	28102.7	52101.7	97683.4	142965.0	198761.0
5000.0	8743.8	9792.1	14010.3	25033.9	45060.9	83638.6	122512.0	168629.0
10000.0	8851.6	9735.5	13219.2	22304.9	38919.4	71788.3	103893.0	142433.0
15000.0	8914.2	9650.1	12584.3	20163.5	33797.1	61216.7	87951.8	119822.0
20000.0	8963.2	9599.1	12045.2	18306.7	29451.2	52121.4	74189.6	100607.0
25000.0	8940.0	9492.7	11597.1	16759.0	25719.9	44290.1	62468.5	84022.8
30000.0	8888.8	9357.4	11151.8	15497.0	22750.9	37718.1	52505.3	70034.1
35000.0	8840.2	9236.3	10737.1	14340.5	20236.3	32094.9	44049.5	58481.9
40000.0	8783.1	9095.0	10324.8	13180.7	17911.8	27240.4	36668.1	48094.6
45000.0	8732.4	8992.1	9996.1	12273.2	16006.0	23332.4	30730.6	39750.9
50000.0	8722.1	8926.6	9702.8	11544.2	14491.6	20247.3	26039.6	33187.3
55000.0	8688.3	8854.2	9498.4	10963.0	13300.0	17805.5	22380.0	28031.5
60000.0	8695.1	8825.4	9342.3	10498.6	12347.9	15889.1	19480.1	23960.1
65000.0	8699.1	8807.6	9209.1	10129.8	11584.5	14372.2	17187.8	20743.8
70000.0	8704.0	8785.0	9102.9	9823.9	10978.6	13174.3	15393.6	18178.7
75000.0	8704.8	8769.0	9020.3	9590.2	10502.6	12233.6	13974.5	16148.5
80000.0	8704.3	8756.1	8952.6	9407.1	10124.1	11491.0	12864.8	14592.6

Ejector ISP Data:

ALT	MACH							
	0.0	0.5	1.0	1.5	2.0	2.5	3.0	3.5
0.0	218.80	248.90	360.41	597.89	910.50	1359.78	1704.38	2025.21
5000.0	223.74	248.55	344.41	552.74	841.06	1261.23	1596.66	1905.13
10000.0	227.55	248.93	330.22	511.51	771.56	1165.55	1479.17	1777.73
15000.0	229.94	248.10	317.29	474.32	706.79	1066.75	1361.47	1645.08
20000.0	233.66	248.25	306.57	440.74	643.40	969.71	1242.10	1511.74
25000.0	235.57	248.49	296.74	410.88	583.70	874.90	1124.68	1374.01
30000.0	236.42	247.52	289.04	385.43	532.37	786.60	1010.35	1238.59
35000.0	237.01	246.54	281.87	363.10	485.23	702.57	900.21	1108.74
40000.0	237.18	244.74	274.17	339.99	442.13	623.93	793.18	976.65
45000.0	237.20	243.58	267.94	321.48	404.68	555.21	697.71	856.42
50000.0	238.02	243.07	262.01	306.08	373.52	496.97	615.15	750.95
55000.0	237.97	242.09	258.00	293.50	348.14	448.14	546.10	660.39
60000.0	238.84	242.09	254.94	283.23	327.22	408.05	487.96	583.34
65000.0	239.50	242.22	252.23	274.94	310.00	375.11	439.73	518.68
70000.0	240.07	242.10	250.05	267.93	296.09	348.35	400.61	464.49
75000.0	240.43	242.04	248.35	262.55	285.00	326.81	368.63	419.97
80000.0	240.68	241.99	246.92	258.31	276.07	309.47	343.01	384.70

Appendix B6: NASAE2GTH2O2JP

Ramjet Thrust Data:

ALT	MACH										
	2.0	2.5	3.0	3.5	4.0	4.5	5.0	5.5	6.0	6.5	7.0
40000.0	2.0442	2.5321	2.6180	2.6876	2.7442	2.7840	2.8613	2.9567	2.8152	2.6932	2.5862
45000.0	2.0426	2.5323	2.6173	2.6874	2.7460	2.7830	2.8600	2.9562	2.8147	2.6915	2.5860
50000.0	2.0426	2.5323	2.6173	2.6874	2.7460	2.7830	2.8600	2.9562	2.8147	2.6915	2.5860
55000.0	2.0426	2.5323	2.6173	2.6874	2.7460	2.7830	2.8600	2.9562	2.8147	2.6915	2.5860
60000.0	2.0426	2.5323	2.6173	2.6874	2.7460	2.7830	2.8600	2.9562	2.8147	2.6915	2.5860
65000.0	2.0426	2.5323	2.6173	2.6874	2.7460	2.7830	2.8600	2.9562	2.8147	2.6915	2.5860
70000.0	2.0408	2.5259	2.6111	2.6822	2.7391	2.7783	2.8576	2.9496	2.8099	2.6897	2.5836
75000.0	2.0361	2.5187	2.6072	2.6588	2.7340	2.7748	2.8526	2.9475	2.8027	2.6812	2.5797
80000.0	2.0314	2.5143	2.5991	2.6523	2.7290	2.7686	2.8477	2.9387	2.7970	2.6771	2.5750
85000.0	2.0439	2.5073	2.5913	2.6462	2.7230	2.7623	2.8430	2.9318	2.7943	2.6727	2.5703
90000.0	2.0395	2.5004	2.5877	2.6401	2.7152	2.7586	2.8382	2.9301	2.7889	2.6701	2.5672
95000.0	2.0374	2.4963	2.5809	2.6343	2.7139	2.7551	2.8343	2.9235	2.7830	2.6659	2.5628
100000.0	2.0330	2.4895	2.5742	2.6289	2.7055	2.7471	2.8263	2.9172	2.7802	2.6618	2.5591
105000.0	2.0284	2.4827	2.5708	2.6233	2.7011	2.7448	2.8226	2.9106	2.7742	2.6551	2.5554
110000.0	2.0351	2.4661	2.5517	2.6098	2.6852	2.7297	2.8157	2.8984	2.7603	2.6427	2.5436
115000.0	2.0396	2.4503	2.5384	2.5935	2.6755	2.7201	2.8067	2.8827	2.7479	2.6307	2.5339
120000.0	2.0306	2.4353	2.5219	2.5796	2.6629	2.7084	2.7951	2.8673	2.7357	2.6217	2.5208

Ramjet ISP Data:

ALT	MACH										
	2.0	2.5	3.0	3.5	4.0	4.5	5.0	5.5	6.0	6.5	7.0
40000.0	2706.0	2473.7	2756.2	2973.3	3157.2	3321.2	3474.8	3623.8	3763.9	3901.0	4034.15
45000.0	2704.7	2474.7	2756.2	2974.1	3160.1	3321.0	3474.2	3624.3	3764.5	3899.8	4035.18
50000.0	2704.7	2474.7	2756.2	2974.1	3160.1	3321.0	3474.2	3624.3	3764.5	3899.8	4035.18
55000.0	2704.7	2474.7	2756.2	2974.1	3160.1	3321.0	3474.2	3624.3	3764.5	3899.8	4035.18
60000.0	2704.7	2474.7	2756.2	2974.1	3160.1	3321.0	3474.2	3624.3	3764.5	3899.8	4035.18
65000.0	2704.7	2474.7	2756.2	2974.1	3160.1	3321.0	3474.2	3624.3	3764.5	3899.8	4035.18
70000.0	2709.6	2475.1	2757.1	2976.1	3160.4	3323.7	3479.9	3626.7	3769.0	3908.5	4043.09
75000.0	2711.8	2475.6	2761.3	2979.1	3163.8	3329.1	3483.3	3636.1	3771.8	3908.9	4050.25
80000.0	2713.8	2478.7	2761.0	2980.7	3167.2	3331.1	3486.9	3637.0	3776.4	3915.7	4056.05
85000.0	2658.3	2479.3	2760.9	2982.7	3169.3	3332.9	3490.5	3640.4	3785.0	3922.0	4061.93
90000.0	2660.5	2479.9	2765.3	2984.6	3169.4	3337.7	3494.0	3650.0	3789.9	3930.9	4070.02
95000.0	2665.8	2483.2	2766.2	2986.7	3176.8	3342.8	3498.5	3653.5	3794.0	3937.2	4076.06
100000.0	2668.0	2483.8	2767.0	2988.9	3175.9	3342.2	3497.7	3657.1	3802.2	3943.6	4083.21
105000.0	2669.9	2484.3	2771.4	2991.2	3179.7	3348.4	3502.2	3660.5	3806.2	3946.3	4090.30
110000.0	2623.4	2487.5	2772.8	2999.3	3185.4	3354.9	3518.5	3677.1	3820.3	3962.4	4107.10
115000.0	2576.6	2491.2	2780.0	3003.5	3197.7	3367.4	3531.3	3688.7	3835.8	3978.3	4126.67
120000.0	2585.3	2495.3	2783.2	3010.0	3205.9	3376.6	3539.9	3700.0	3851.2	3998.3	4140.03

All-Rocket Mode Data:

Vacuum Thrust	11112
Exit Area	7.0686
Vacuum Isp	314.598

Appendix B7: NASAE2CTHLOXPR

Ejector Thrust Data:

ALT	MACH							
	0.0	0.5	1.0	1.5	2.0	2.5	3.0	3.5
0.0	8599.49	8568.98	11345.90	16963.90	26913.70	46063.80	62029.70	78708.30
5000.0	8714.83	8689.69	10979.20	15650.30	24131.50	40666.90	54709.20	68909.50
10000.0	8770.52	8784.79	10683.00	14532.20	21658.50	36081.00	47909.10	59942.90
15000.0	8741.58	8770.81	10456.10	13556.70	19578.00	31924.10	41981.60	52321.70
20000.0	8667.11	8715.48	10212.50	12725.80	17687.80	28207.20	36754.00	45529.40
25000.0	8573.84	8637.76	9917.21	11992.30	16159.90	24965.80	32207.50	39534.40
30000.0	8476.02	8546.59	9645.32	11375.10	14791.20	22186.60	28187.70	34376.30
35000.0	8390.32	8468.27	9403.21	10824.00	13714.50	19752.30	24701.80	29956.90
40000.0	8294.50	8364.94	9144.31	10279.80	12642.60	17426.10	21391.90	25604.10
45000.0	8217.23	8279.69	8929.23	9779.90	11750.40	15495.20	18623.30	21956.60
50000.0	8178.65	8237.79	8769.89	9468.06	11026.10	13968.90	16440.30	19080.90
55000.0	8133.41	8186.90	8618.83	9207.97	10447.10	12767.60	14720.20	16826.60
60000.0	8143.34	8181.40	8521.59	8995.14	9984.86	11818.40	13343.90	15072.50
65000.0	8141.07	8174.12	8448.42	8825.06	9612.55	11054.10	12280.00	13653.70
70000.0	8144.13	8165.65	8382.22	8683.01	9304.23	10445.80	11393.80	12500.70
75000.0	8140.54	8158.31	8328.71	8567.17	9061.26	9958.72	10713.90	11583.30
80000.0	8138.58	8154.69	8287.35	8477.26	8869.89	9586.19	10180.80	10884.70

Ejector ISP Data:

ALT	MACH							
	0.0	0.5	1.0	1.5	2.0	2.5	3.0	3.5
0.0	244.21	240.61	303.62	390.40	525.41	710.03	814.83	879.92
5000.0	249.17	246.50	300.19	376.27	501.01	680.99	787.79	856.52
10000.0	253.76	251.16	297.00	363.51	476.24	652.40	755.89	825.51
15000.0	256.74	255.01	294.46	351.45	453.38	621.38	722.38	795.05
20000.0	257.93	257.17	291.98	340.62	429.81	587.91	686.16	759.62
25000.0	258.09	258.19	288.73	330.23	409.61	554.07	648.63	720.20
30000.0	257.71	258.33	285.28	321.13	389.47	521.28	608.62	679.52
35000.0	257.28	258.45	281.93	312.26	373.42	488.40	568.13	636.81
40000.0	256.31	257.51	277.54	302.50	354.99	452.00	522.34	584.96
45000.0	255.51	256.69	273.74	292.53	338.47	418.49	478.58	533.87
50000.0	255.58	256.83	270.99	286.90	324.19	389.89	440.62	488.59
55000.0	255.16	256.37	268.00	281.91	312.26	365.99	408.30	449.66
60000.0	256.27	257.09	266.30	277.66	302.39	346.14	380.59	417.08
65000.0	256.82	257.57	265.05	274.19	294.17	329.38	358.20	388.67
70000.0	257.42	257.86	263.79	271.18	287.12	315.60	338.45	364.15
75000.0	257.70	258.07	262.75	268.65	281.47	304.21	322.89	343.84
80000.0	257.94	258.30	261.94	266.68	276.95	295.37	310.34	327.82

Appendix B7: NASAE2CTHLOXPR

Ramjet Thrust Data:

ALT	MACH										
	2.0	2.5	3.0	3.5	4.0	4.5	5.0	5.5	6.0	6.5	7.0
40000.0	0.94541	1.25160	1.22537	1.17138	1.10588	1.03166	0.96814	0.89172	0.74841	0.62507	0.51657
45000.0	0.94397	1.25179	1.22456	1.17109	1.10764	1.03062	0.96665	0.89069	0.74855	0.62318	0.51776
50000.0	0.94397	1.25179	1.22456	1.17109	1.10764	1.03062	0.96665	0.89069	0.74855	0.62318	0.51776
55000.0	0.94397	1.25179	1.22456	1.17109	1.10764	1.03062	0.96665	0.89069	0.74855	0.62318	0.51776
60000.0	0.94397	1.25179	1.22456	1.17109	1.10764	1.03062	0.96665	0.89069	0.74855	0.62318	0.51776
65000.0	0.94397	1.25179	1.22456	1.17109	1.10764	1.03062	0.96665	0.89069	0.74855	0.62318	0.51776
70000.0	0.94270	1.24488	1.21769	1.16527	1.09999	1.02494	0.96284	0.88456	0.74260	0.62167	0.51424
75000.0	0.93874	1.23694	1.21315	1.15367	1.09387	1.02044	0.95655	0.88129	0.73500	0.61274	0.50891
80000.0	0.94744	1.23198	1.20441	1.14673	1.08787	1.01368	0.95084	0.87396	0.72882	0.60829	0.50374
85000.0	0.94376	1.22430	1.19588	1.13977	1.08103	1.00594	0.94436	0.86663	0.72597	0.60352	0.49937
90000.0	0.93999	1.21662	1.19186	1.13298	1.07214	1.00127	0.93870	0.86457	0.72014	0.60058	0.49512
95000.0	0.93790	1.21212	1.18431	1.12651	1.07010	0.99676	0.93314	0.85757	0.71372	0.59527	0.49031
100000.0	0.94642	1.20469	1.17673	1.12009	1.06076	0.98769	0.92369	0.85076	0.71043	0.59060	0.48629
105000.0	0.94277	1.19727	1.17294	1.11382	1.05559	0.98383	0.91820	0.84338	0.70413	0.58364	0.48213
110000.0	0.93382	1.17882	1.15179	1.09834	1.03724	0.96576	0.90763	0.83048	0.68905	0.56997	0.46934
115000.0	0.94871	1.16132	1.13671	1.07997	1.02474	0.95318	0.89422	0.81280	0.67486	0.55692	0.45773
120000.0	0.94074	1.14466	1.11836	1.06381	1.00955	0.93848	0.87880	0.79618	0.66149	0.54557	0.44288

Ramjet ISP Data:

ALT	MACH										
	2.0	2.5	3.0	3.5	4.0	4.5	5.0	5.5	6.0	6.5	7.0
40000.0	1228.04	1308.94	1380.96	1387.27	1361.97	1317.49	1258.60	1169.93	1071.17	969.20	862.58
45000.0	1226.55	1309.55	1380.47	1387.35	1364.54	1316.54	1257.02	1168.96	1071.73	966.58	864.85
50000.0	1226.55	1309.55	1380.47	1387.35	1364.54	1316.54	1257.02	1168.96	1071.73	966.58	864.85
55000.0	1226.55	1309.55	1380.47	1387.35	1364.54	1316.54	1257.02	1168.96	1071.73	966.58	864.85
60000.0	1226.55	1309.55	1380.47	1387.35	1364.54	1316.54	1257.02	1168.96	1071.73	966.58	864.85
65000.0	1226.55	1309.55	1380.47	1387.35	1364.54	1316.54	1257.02	1168.96	1071.73	966.58	864.85
70000.0	1228.24	1305.84	1376.42	1384.12	1358.65	1312.57	1255.13	1164.29	1066.30	967.05	861.47
75000.0	1226.84	1301.50	1375.47	1383.79	1355.08	1310.56	1250.39	1163.81	1058.86	956.29	855.34
80000.0	1208.44	1300.17	1369.61	1379.56	1351.53	1305.60	1245.67	1157.91	1053.39	952.44	849.42
85000.0	1207.41	1295.96	1363.98	1375.25	1346.93	1299.28	1241.19	1151.92	1052.69	948.05	844.80
90000.0	1206.23	1291.71	1363.44	1371.07	1339.69	1296.87	1237.05	1152.90	1047.61	946.48	840.30
95000.0	1207.16	1290.75	1358.79	1367.22	1340.94	1294.61	1232.98	1147.22	1041.59	941.13	834.80
100000.0	1189.61	1286.64	1354.04	1363.27	1332.99	1286.34	1223.70	1141.75	1040.08	936.70	830.60
105000.0	1188.55	1282.49	1353.61	1359.54	1330.22	1284.80	1219.58	1135.43	1034.14	928.62	826.12
110000.0	1186.85	1272.91	1339.80	1351.24	1317.18	1270.63	1214.11	1127.88	1020.87	914.82	811.25
115000.0	1154.65	1263.94	1332.66	1338.89	1311.08	1263.18	1204.38	1113.38	1008.47	901.59	798.00
120000.0	1153.91	1255.53	1321.22	1328.81	1301.10	1252.49	1191.43	1099.85	996.86	890.69	778.65

All-Rocket Mode Data:

Vacuum Thrust	10112.5
Exit Area	7.0686
Vacuum Isp	329.243

Appendix B8: NASA E2CTHLOXJP

Ejector Thrust Data:

ALT	MACH							
	0.0	0.5	1.0	1.5	2.0	2.5	3.0	3.5
0	8591.52	8503.55	10922.40	15549.20	25481.90	45785.50	62087.70	79081.10
5000	8718.93	8678.27	10693.20	14390.80	22860.30	40634.90	54923.80	69243.90
10000	8892.80	8792.72	10526.90	13660.40	20576.80	36117.30	48246.20	60461.90
15000	9015.77	8964.00	10388.70	12954.60	18693.90	32011.60	42369.30	52848.80
20000	9121.22	9099.49	10244.40	12354.10	16949.90	28451.30	37261.00	46054.60
25000	9144.11	9176.64	10236.90	11911.80	15687.00	25291.40	32747.90	40180.40
30000	9127.03	9184.37	10205.50	11502.00	14653.20	22565.10	28810.40	35042.60
35000	9103.77	9168.14	10063.00	11246.70	13906.00	20164.90	25356.80	30700.20
40000	9049.53	9118.02	9869.70	10880.60	13132.60	17945.60	22067.70	26318.10
45000	9013.31	9071.73	9705.86	10536.00	12397.20	16090.70	19304.40	22719.60
50000	9002.05	9057.02	9545.16	10248.00	11737.00	14622.80	17162.90	19904.40
55000	8971.63	9021.22	9443.95	10011.90	11198.20	13483.20	15473.20	17663.80
60000	8986.99	9022.42	9358.84	9813.05	10763.90	12567.20	14139.10	15876.20
65000	8988.64	9020.20	9286.82	9650.01	10410.50	11828.00	13073.60	14489.70
70000	8986.81	9014.49	9226.30	9521.01	10124.30	11244.90	12213.10	13347.90
75000	8992.92	9010.49	9176.70	9404.13	9887.74	10768.40	11534.00	12436.00
80000	8984.40	9008.35	9137.91	9319.44	9707.30	10400.60	10996.70	11728.10

Ejector ISP Data:

ALT	MACH							
	0.0	0.5	1.0	1.5	2.0	2.5	3.0	3.5
0	236.58	232.23	286.37	354.92	475.07	662.48	765.05	828.79
5000	242.12	239.17	285.02	344.85	456.01	639.02	742.17	807.16
10000	247.99	244.51	284.93	336.71	436.69	613.55	714.64	781.21
15000	252.25	249.99	284.42	329.07	419.12	585.65	684.76	753.78
20000	255.97	254.42	283.59	322.31	399.46	557.61	653.66	721.57
25000	259.60	258.67	284.18	316.35	384.20	528.03	620.02	687.72
30000	261.73	261.82	284.62	310.58	371.51	498.95	585.08	651.14
35000	263.32	263.92	284.53	307.13	361.18	469.43	548.77	613.75
40000	263.79	264.78	282.54	301.89	348.42	438.41	507.26	565.75
45000	264.40	265.32	280.66	297.19	336.64	409.44	467.20	520.03
50000	265.40	266.39	278.23	292.88	325.39	384.65	433.36	479.99
55000	265.55	266.52	277.03	289.13	315.64	364.34	404.46	444.69
60000	266.84	267.50	275.92	285.74	307.45	347.03	380.13	414.00
65000	267.55	268.17	274.88	282.84	300.50	332.35	359.54	388.80
70000	268.02	268.60	273.95	280.53	294.71	320.42	342.10	366.59
75000	268.61	268.94	273.15	278.22	289.75	310.26	327.82	348.10
80000	268.68	269.24	272.52	276.61	285.95	302.29	316.18	333.12

Appendix B8: NASA E2CTHLOXJP

Ramjet Thrust Data:

ALT	MACH										
	2.0	2.5	3.0	3.5	4.0	4.5	5.0	5.5	6.0	6.5	7.0
40000	0.87106	1.23401	1.21636	1.16658	1.10373	1.03213	0.97083	0.89600	0.75516	0.63361	0.52676
45000	0.86963	1.23422	1.21554	1.16638	1.10538	1.03108	0.96889	0.89543	0.75461	0.63185	0.52653
50000	0.86963	1.23422	1.21554	1.16638	1.10538	1.03108	0.96889	0.89543	0.75461	0.63185	0.52653
55000	0.86963	1.23422	1.21554	1.16638	1.10538	1.03108	0.96889	0.89543	0.75461	0.63185	0.52653
60000	0.86963	1.23422	1.21554	1.16638	1.10538	1.03108	0.96889	0.89543	0.75461	0.63185	0.52653
65000	0.86963	1.23422	1.21554	1.16638	1.10538	1.03108	0.96889	0.89543	0.75461	0.63185	0.52653
70000	0.86836	1.22734	1.20884	1.16048	1.09778	1.02541	0.96539	0.88838	0.74939	0.62962	0.52367
75000	0.86449	1.21958	1.20427	1.14900	1.09180	1.02088	0.95901	0.88589	0.74180	0.62062	0.51928
80000	0.86058	1.21452	1.19554	1.14180	1.08586	1.01365	0.95283	0.87853	0.73557	0.61604	0.51407
85000	0.86886	1.20705	1.18706	1.13504	1.07894	1.00631	0.94676	0.87122	0.73246	0.61121	0.50898
90000	0.86521	1.19957	1.18292	1.12824	1.07032	1.00148	0.94068	0.86901	0.72658	0.60818	0.50535
95000	0.86305	1.19496	1.17547	1.12173	1.06813	0.99699	0.93543	0.86199	0.72022	0.60346	0.50048
100000	0.85940	1.18764	1.16810	1.11545	1.05881	0.98790	0.92608	0.85517	0.71693	0.59886	0.49637
105000	0.85555	1.18029	1.16412	1.10916	1.05360	0.98449	0.92094	0.84815	0.71054	0.59176	0.49223
110000	0.85855	1.16204	1.14315	1.09361	1.03521	0.96636	0.91016	0.83466	0.69536	0.57814	0.47914
115000	0.86087	1.14470	1.12813	1.07521	1.02295	0.95359	0.89708	0.81775	0.68173	0.56487	0.46818
120000	0.85285	1.12825	1.10989	1.05926	1.00770	0.93878	0.88120	0.80106	0.66834	0.55466	0.45382

Ramjet ISP Data:

ALT	MACH										
	2.0	2.5	3.0	3.5	4.0	4.5	5.0	5.5	6.0	6.5	7.0
40000	1153.05	1205.57	1280.55	1290.62	1269.81	1231.30	1178.39	1098.14	1009.66	917.75	821.68
45000	1151.51	1206.15	1280.07	1290.79	1272.09	1230.39	1176.96	1097.80	1009.26	915.49	821.59
50000	1151.51	1206.15	1280.07	1290.79	1272.09	1230.39	1176.96	1097.80	1009.26	915.49	821.59
55000	1151.51	1206.15	1280.07	1290.79	1272.09	1230.39	1176.96	1097.80	1009.26	915.49	821.59
60000	1151.51	1206.15	1280.07	1290.79	1272.09	1230.39	1176.96	1097.80	1009.26	915.49	821.59
65000	1151.51	1206.15	1280.07	1290.79	1272.09	1230.39	1176.96	1097.80	1009.26	915.49	821.59
70000	1152.95	1202.66	1276.44	1287.67	1266.64	1226.69	1175.59	1092.32	1005.20	914.92	819.50
75000	1151.36	1198.73	1275.49	1287.44	1263.46	1224.79	1171.05	1092.84	998.29	904.81	815.29
80000	1149.66	1197.34	1269.99	1283.18	1260.20	1219.59	1166.70	1087.31	993.14	901.07	809.76
85000	1130.01	1193.57	1264.76	1279.36	1255.79	1214.17	1162.40	1081.77	992.16	896.91	804.35
90000	1128.67	1189.73	1264.10	1275.43	1249.34	1211.72	1158.04	1082.51	987.37	895.34	801.18
95000	1129.23	1188.69	1259.84	1271.76	1250.34	1209.62	1154.62	1077.21	981.87	891.24	796.01
100000	1127.81	1184.91	1255.61	1268.23	1242.92	1201.89	1146.07	1072.08	980.48	887.27	791.98
105000	1126.10	1181.05	1254.97	1264.69	1240.27	1201.00	1142.67	1066.66	974.84	879.54	787.88
110000	1106.70	1172.16	1242.19	1256.82	1228.02	1187.70	1137.31	1058.92	962.39	866.82	773.66
115000	1087.49	1163.81	1235.50	1245.21	1222.60	1180.51	1128.66	1046.39	951.65	854.23	762.47
120000	1085.80	1156.03	1224.88	1236.00	1213.19	1170.38	1116.01	1033.72	940.86	845.89	745.35

All-Rocket Mode Data:

Vacuum Thrust	11130.2
Exit Area	7.0686
Vacuum Isp	337.095

Appendix B9: NASA E2CTH2O2JP

Ejector Thrust Data:

ALT	MACH							
	0.0	0.5	1.0	1.5	2.0	2.5	3.0	3.5
0.0	8604.57	8504.27	10935.10	15591.20	25701.20	45445.50	61649.80	78688.50
5000.0	8762.62	8682.44	10732.00	14538.90	23028.70	40333.10	54547.50	68870.40
10000.0	8857.40	8827.03	10524.70	13640.00	20677.80	35745.20	47899.20	60124.00
15000.0	8982.51	8938.98	10400.70	12980.20	18755.10	31678.80	42035.70	52541.10
20000.0	9036.12	9036.56	10312.30	12401.40	17072.90	28159.60	36837.00	45719.20
25000.0	9022.32	9057.16	10207.50	11927.60	15727.50	24998.90	32335.20	39857.60
30000.0	8981.74	9036.71	10061.00	11557.10	14780.00	22304.20	28419.80	34631.00
35000.0	8944.99	9003.76	9898.47	11168.30	13908.90	19920.50	24985.60	30288.40
40000.0	8885.03	8948.40	9694.76	10669.40	13013.80	17696.70	21699.30	25976.10
45000.0	8844.46	8900.30	9522.16	10331.20	12174.90	15832.60	19020.90	22390.40
50000.0	8835.90	8892.86	9362.41	10045.60	11519.40	14381.70	16859.40	19549.10
55000.0	8805.34	8852.46	9266.19	9815.08	10987.70	13224.60	15186.20	17325.30
60000.0	8822.17	8853.79	9182.42	9622.59	10560.20	12326.00	13840.80	15594.20
65000.0	8828.04	8856.85	9118.91	9469.97	10213.00	11602.20	12798.30	14175.60
70000.0	8833.53	8853.58	9061.05	9339.65	9929.31	11026.40	11963.20	13059.00
75000.0	8836.66	8853.77	9016.03	9235.99	9699.99	10563.90	11301.80	12171.50
80000.0	8838.39	8855.56	8982.77	9157.99	9524.84	10201.90	10784.20	11484.20

Ejector ISP Data:

ALT	MACH							
	0.0	0.5	1.0	1.5	2.0	2.5	3.0	3.5
0.0	215.57	211.25	261.58	327.62	444.58	627.49	729.86	797.00
5000.0	220.39	217.16	260.09	318.53	425.17	602.87	705.50	772.95
10000.0	224.32	222.37	259.13	308.66	405.21	574.87	676.31	744.96
15000.0	227.84	225.96	258.42	301.19	387.47	546.44	644.84	715.58
20000.0	232.01	230.20	258.02	294.42	368.26	518.24	610.73	680.97
25000.0	234.12	233.50	257.32	288.29	352.24	488.16	576.07	645.59
30000.0	235.22	235.38	256.86	283.30	341.17	459.52	540.77	606.17
35000.0	236.10	236.62	255.90	278.64	329.88	430.53	504.56	567.90
40000.0	236.19	237.05	253.49	271.11	316.64	399.96	463.49	521.28
45000.0	236.47	237.31	251.28	266.51	303.32	371.55	426.17	476.37
50000.0	237.32	238.34	248.87	262.26	292.49	347.98	392.83	436.55
55000.0	237.35	238.22	247.74	258.70	283.26	327.99	365.33	402.59
60000.0	238.49	239.02	246.63	255.54	275.56	311.85	341.68	374.31
65000.0	239.18	239.71	245.81	253.00	269.07	298.24	322.58	349.32
70000.0	239.76	240.10	244.95	250.71	263.62	287.09	306.65	328.74
75000.0	240.18	240.48	244.28	248.86	259.09	277.85	293.58	311.78
80000.0	240.49	240.83	243.81	247.48	255.63	270.48	283.10	298.14

Appendix B9: NASA E2CTH2O2JP

Ramjet Thrust Data:

ALT	MACH										
	2.0	2.5	3.0	3.5	4.0	4.5	5.0	5.5	6.0	6.5	7.0
40000.0	0.87106	1.23401	1.21636	1.16658	1.10373	1.03213	0.97083	0.89600	0.75516	0.63361	0.52676
45000.0	0.86963	1.23422	1.21554	1.16638	1.10538	1.03108	0.96889	0.89543	0.75461	0.63185	0.52653
50000.0	0.86963	1.23422	1.21554	1.16638	1.10538	1.03108	0.96889	0.89543	0.75461	0.63185	0.52653
55000.0	0.86963	1.23422	1.21554	1.16638	1.10538	1.03108	0.96889	0.89543	0.75461	0.63185	0.52653
60000.0	0.86963	1.23422	1.21554	1.16638	1.10538	1.03108	0.96889	0.89543	0.75461	0.63185	0.52653
65000.0	0.86963	1.23422	1.21554	1.16638	1.10538	1.03108	0.96889	0.89543	0.75461	0.63185	0.52653
70000.0	0.86836	1.22734	1.20884	1.16048	1.09778	1.02541	0.96539	0.88838	0.74939	0.62962	0.52367
75000.0	0.86449	1.21958	1.20427	1.14900	1.09180	1.02088	0.95901	0.88589	0.74180	0.62062	0.51928
80000.0	0.86058	1.21452	1.19554	1.14180	1.08586	1.01365	0.95283	0.87853	0.73557	0.61604	0.51407
85000.0	0.86886	1.20705	1.18706	1.13504	1.07894	1.00631	0.94676	0.87122	0.73246	0.61121	0.50898
90000.0	0.86521	1.19957	1.18292	1.12824	1.07032	1.00148	0.94068	0.86901	0.72658	0.60818	0.50535
95000.0	0.86305	1.19496	1.17547	1.12173	1.06813	0.99699	0.93543	0.86199	0.72022	0.60346	0.50048
100000.0	0.85940	1.18764	1.16810	1.11545	1.05881	0.98790	0.92608	0.85517	0.71693	0.59886	0.49637
105000.0	0.85555	1.18029	1.16412	1.10916	1.05360	0.98449	0.92094	0.84815	0.71054	0.59176	0.49223
110000.0	0.85855	1.16204	1.14315	1.09361	1.03521	0.96636	0.91016	0.83466	0.69536	0.57814	0.47914
115000.0	0.86087	1.14470	1.12813	1.07521	1.02295	0.95359	0.89708	0.81775	0.68173	0.56487	0.46818
120000.0	0.85285	1.12825	1.10989	1.05926	1.00770	0.93878	0.88120	0.80106	0.66834	0.55466	0.45382

Ramjet ISP Data:

ALT	MACH										
	2.0	2.5	3.0	3.5	4.0	4.5	5.0	5.5	6.0	6.5	7.0
40000.0	1153.05	1205.57	1280.55	1290.62	1269.81	1231.30	1178.39	1098.14	1009.66	917.75	821.68
45000.0	1151.51	1206.15	1280.07	1290.79	1272.09	1230.39	1176.96	1097.80	1009.26	915.49	821.59
50000.0	1151.51	1206.15	1280.07	1290.79	1272.09	1230.39	1176.96	1097.80	1009.26	915.49	821.59
55000.0	1151.51	1206.15	1280.07	1290.79	1272.09	1230.39	1176.96	1097.80	1009.26	915.49	821.59
60000.0	1151.51	1206.15	1280.07	1290.79	1272.09	1230.39	1176.96	1097.80	1009.26	915.49	821.59
65000.0	1151.51	1206.15	1280.07	1290.79	1272.09	1230.39	1176.96	1097.80	1009.26	915.49	821.59
70000.0	1152.95	1202.66	1276.44	1287.67	1266.64	1226.69	1175.59	1092.32	1005.20	914.92	819.50
75000.0	1151.36	1198.73	1275.49	1287.44	1263.46	1224.79	1171.05	1092.84	998.29	904.81	815.29
80000.0	1149.66	1197.34	1269.99	1283.18	1260.20	1219.59	1166.70	1087.31	993.14	901.07	809.76
85000.0	1130.01	1193.57	1264.76	1279.36	1255.79	1214.17	1162.40	1081.77	992.16	896.91	804.35
90000.0	1128.67	1189.73	1264.10	1275.43	1249.34	1211.72	1158.04	1082.51	987.37	895.34	801.18
95000.0	1129.23	1188.69	1259.84	1271.76	1250.34	1209.62	1154.62	1077.21	981.87	891.24	796.01
100000.0	1127.81	1184.91	1255.61	1268.23	1242.92	1201.89	1146.07	1072.08	980.48	887.27	791.98
105000.0	1126.10	1181.05	1254.97	1264.69	1240.27	1201.00	1142.67	1066.66	974.84	879.54	787.88
110000.0	1106.70	1172.16	1242.19	1256.82	1228.02	1187.70	1137.31	1058.92	962.39	866.82	773.66
115000.0	1087.49	1163.81	1235.50	1245.21	1222.60	1180.51	1128.66	1046.39	951.65	854.23	762.47
120000.0	1085.80	1156.03	1224.88	1236.00	1213.19	1170.38	1116.01	1033.72	940.86	845.89	745.35

All-Rocket Mode Data:

Vacuum Thrust	11293.2
Exit Area	7.0686
Vacuum Isp	314.598

Appendix C:

**D-21 Modification:
Minimal Modification Oxidizer Tank Layout**

12

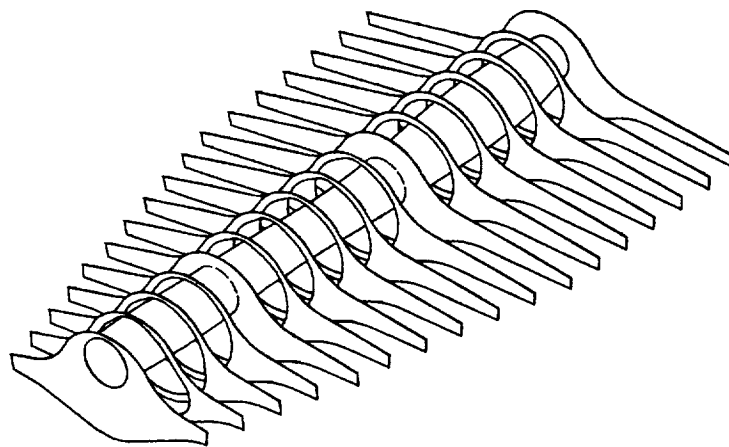
11

10

E



D



Tank Bulkhead 150

C

F.S.
100

F.S.
235

F.S.
285

F.S.
360

F.S.
435

FWD TANK

CTR TANK

AFT TANK

B

A

B

C

A

B

C

A

12.50
TYP

12

11

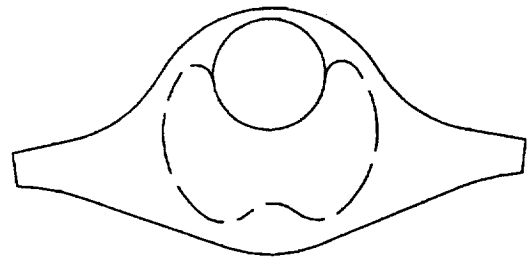
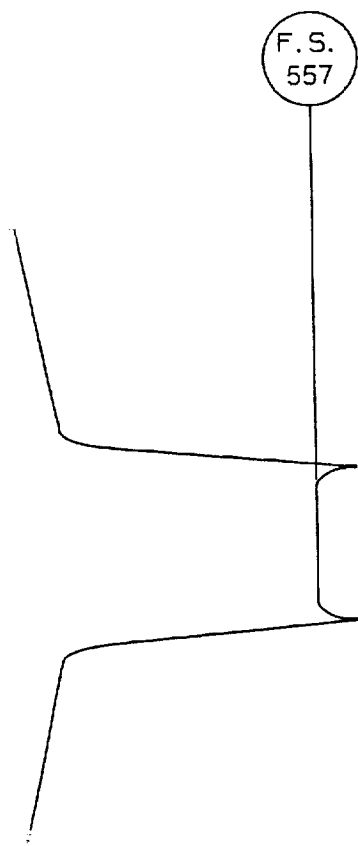
10

	9	8	7
--	---	---	---

CTR Oxidi.

FWD Oxidizer Tank

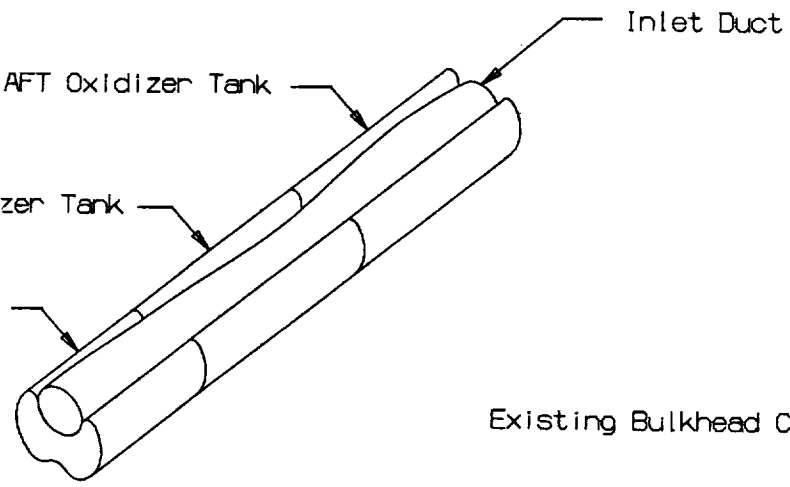
Oxidizer.



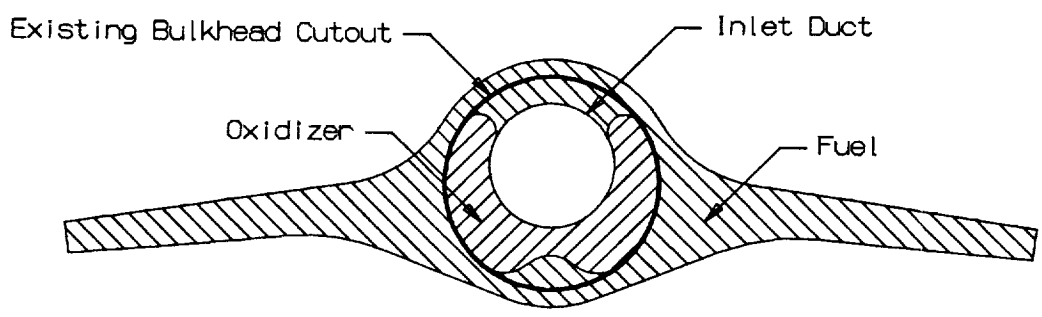
Section A-A
 Rotated CW 90 deg
 F.S. 235
 View Looking Aft

E:

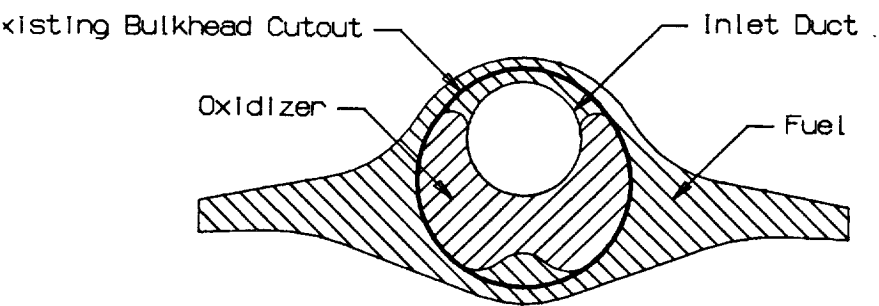
	DWG NO.	SH	REV		9	8	7
--	---------	----	-----	--	---	---	---



Tank & Inlet Duct ISO



Section C-C
 Rotated CW 90 deg
 F.S. 422.5
 View Looking Aft

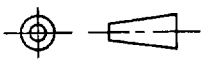


Section B-B
 Rotated CW 90 deg
 F.S. 272.5
 View Looking Aft

	FWD	CTR	AFT	Total
Oxidizer Tank X C.G.s (in)	260.0	321.5	397.9	N/A
Oxidizer Tank Volumes (ft ³)	14.0	18.6	14.9	47.5
Fuel Tank X C.G.s (in)	261.2	322.5	395.2	N/A
Fuel Tank Volumes (ft ³)	13.0	25.1	21.7	59.8
Total Propellant Volume (ft ³)				107.3

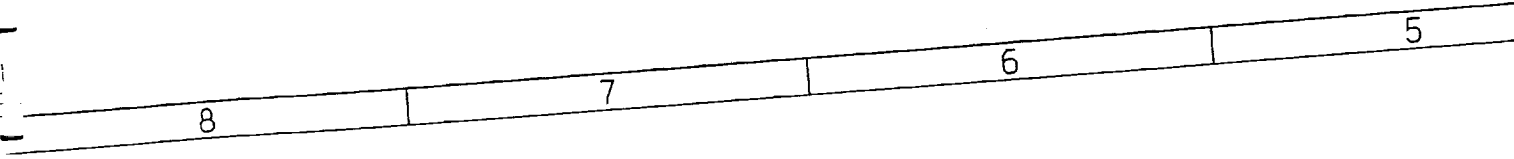
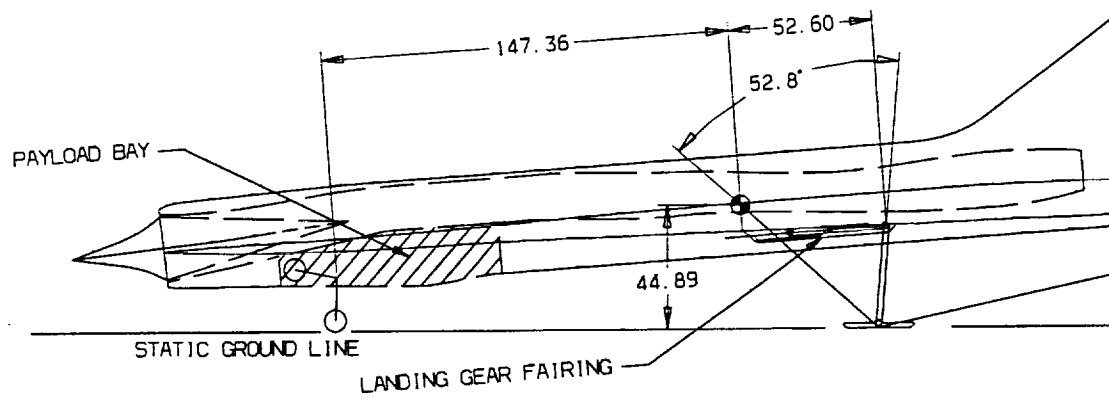
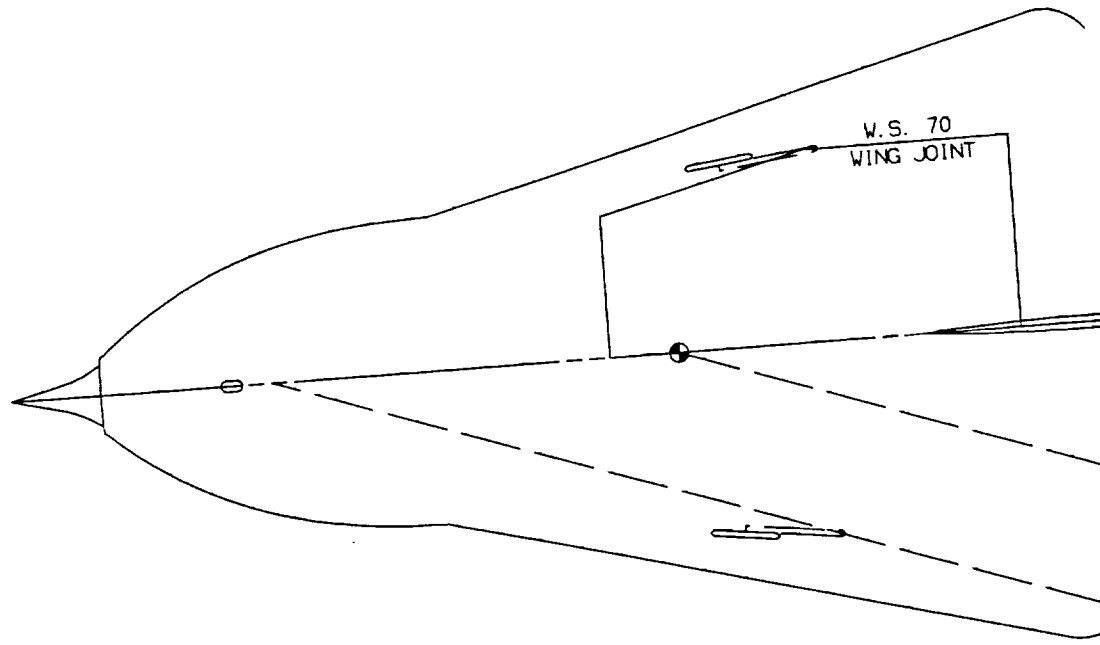
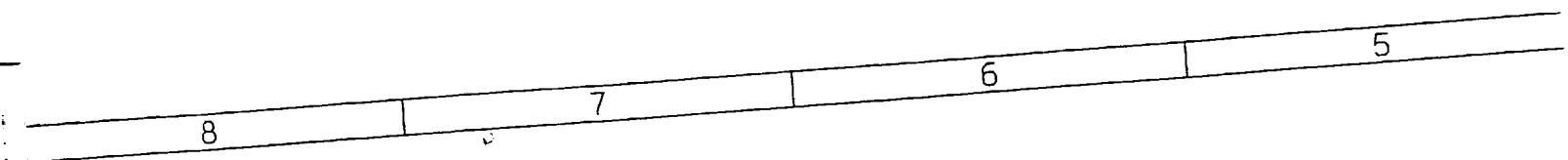
E
D
C
REV
SH
DWG NO
B
A
34X132

NOTE NUMBERS ENCLOSED IN A Δ (DELTA) ARE THE SAME AS PL. NOTE NUMBERS PREFIXED WITH AN ASTERISK (*). ALL SHEETS OF THIS DRAWING BEAR THE SAME REVISION. FOR PARTS LIST AND NOTES, SEE SEPARATE PARTS LIST.

 <p>THIRD ANGLE PROJECTION</p>	UNLESS OTHERWISE SPECIFIED DIMENSIONS ARE IN INCHES TOLERANCES EXCEPT AS NOTED			CONTR NO	LOCKHEED MARTIN CORPORATION SKUNK WORKS PALMDALE, CALIFORNIA			
	DECIMALS ANGLES			ENGR D. THOMAS	D-21 MODIFICATION: MINIMAL MODIFICATION OXIDIZER TANK LAYOUT			
.X ±.1	.XX ±.03	.XXX ±.010	±1°	SUPV				SIZE
				STRESS	J	92685		
				WEIGHT	SCALE:		CALC WT.	SHEET 1 OF
				MANUFACT	NEXT ASSEMBLY		ORIG. JOB NO.	
				SUBMITTAL CONTR NO.				

Appendix D:

D-21 Modification:
Traditional Landing System Layout Drawing



4

3

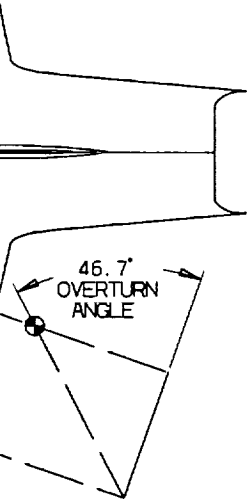
2

1

THIS MATERIAL CONTAINS PROPRIETARY INFORMATION OF LOCKHEED MARTIN SKUNK WORKS. DISCLOSURE TO OTHERS, USE OR COPYING WITHOUT EXPRESS WRITTEN AUTHORIZATION OF LOCKHEED MARTIN SKUNK WORKS IS STRICTLY PROHIBITED.
 © 1996 LOCKHEED MARTIN CORPORATION. UNPUBLISHED WORK. ALL RIGHTS RESERVED.

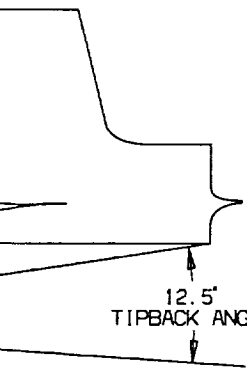
REVISIONS

ZONE	REV	DESCRIPTION	DATE	APPROVED
------	-----	-------------	------	----------



GEAR LOAD OUT:

	PERCENT VEHICLE WEIGHT
NOSE GEAR:	73
MAIN GEAR:	27



NOTE NUMBERS ENCLOSED IN A Δ (DELTA) ARE THE SAME AS PL NOTE NUMBERS PREFIXED WITH AN ASTERISK (*). ALL SHEETS OF THIS DRAWING BEAR THE SAME REVISION. FOR PARTS LIST AND NOTES, SEE SEPARATE PARTS LIST.

THIRD ANGLE PROJECTION 	UNLESS OTHERWISE SPECIFIED DIMENSIONS ARE IN INCHES			CONTR NO.
	TOLERANCES EXCEPT AS NOTED			ENGR D. THOMAS
	DECIMALS		ANGLES	SUPV
	.X	.XX	.XXX	STRESS
	±.1	±.03	±.010	WEIGHT
			±1'	MANUFACT
				NEXT ASSEMBLY
				SUBMITTAL CONTR NO.

LOCKHEED MARTIN CORPORATION SKUNK WORKS PALMDALE, CALIFORNIA			
D-21 MODIFICATION: TRADITIONAL LANDING SYSTEM LAYOUT DRAWING			
SIZE	CAGE CODE	DWG NO.	REV
J	92685		
SCALE:	CALC WT.	SHEET 1 OF	
		34X132	

4

3

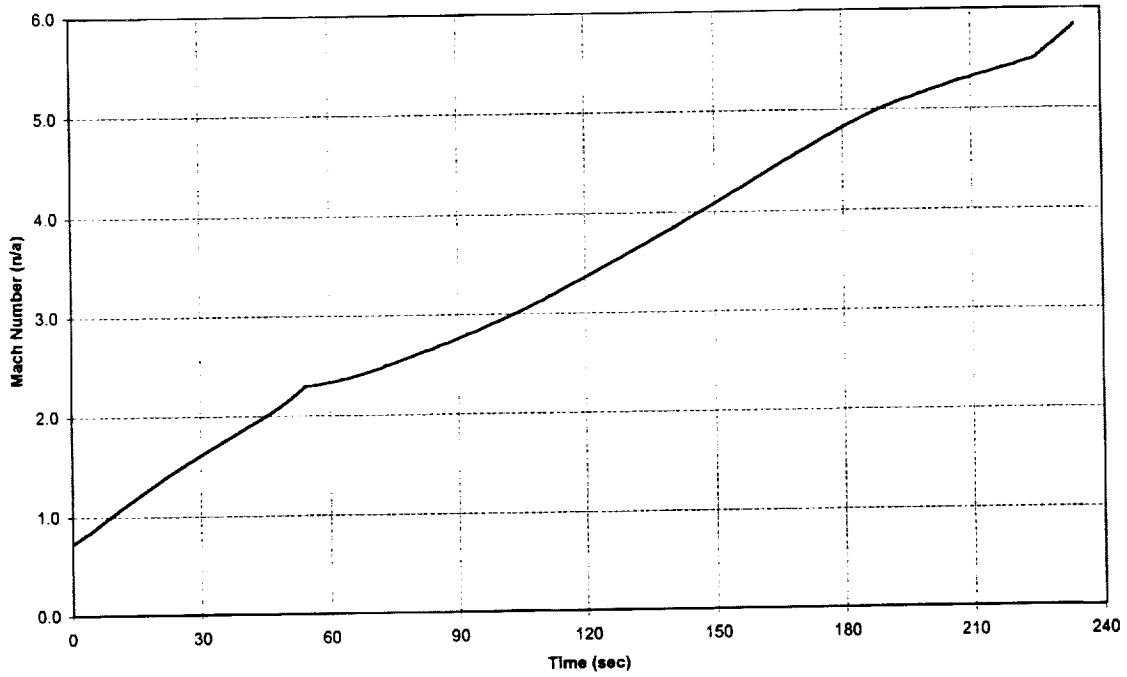
2

ORIG. JOB NO.

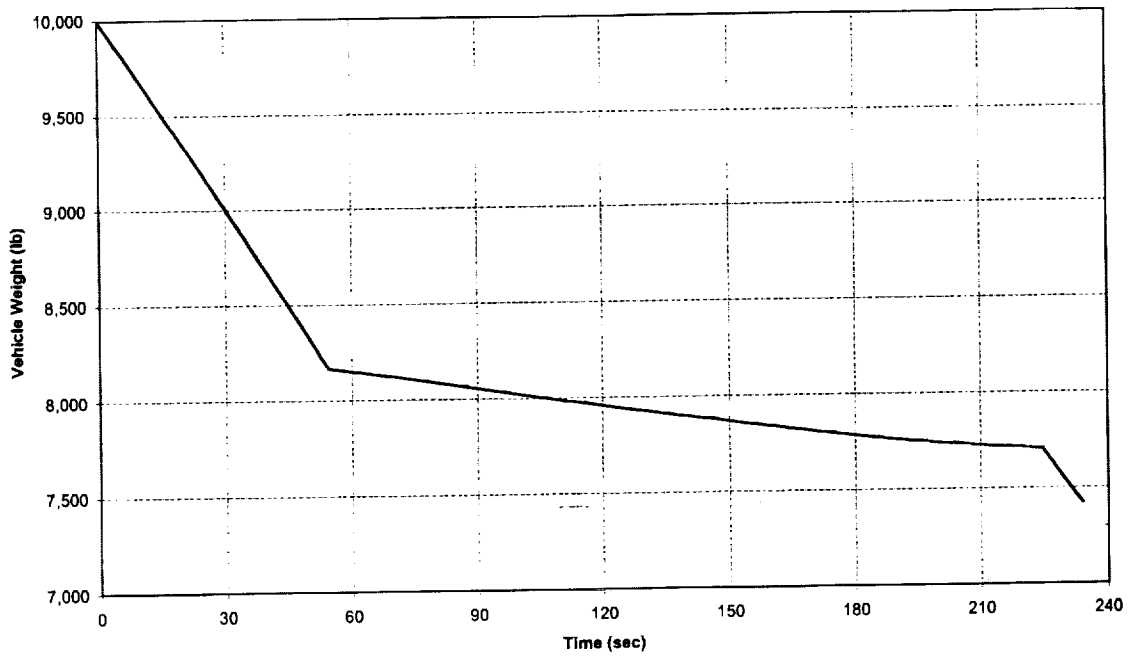
E
D
C
REV
SH
DWG NO
A

Appendix E1: NASA E3GTLOXPRA

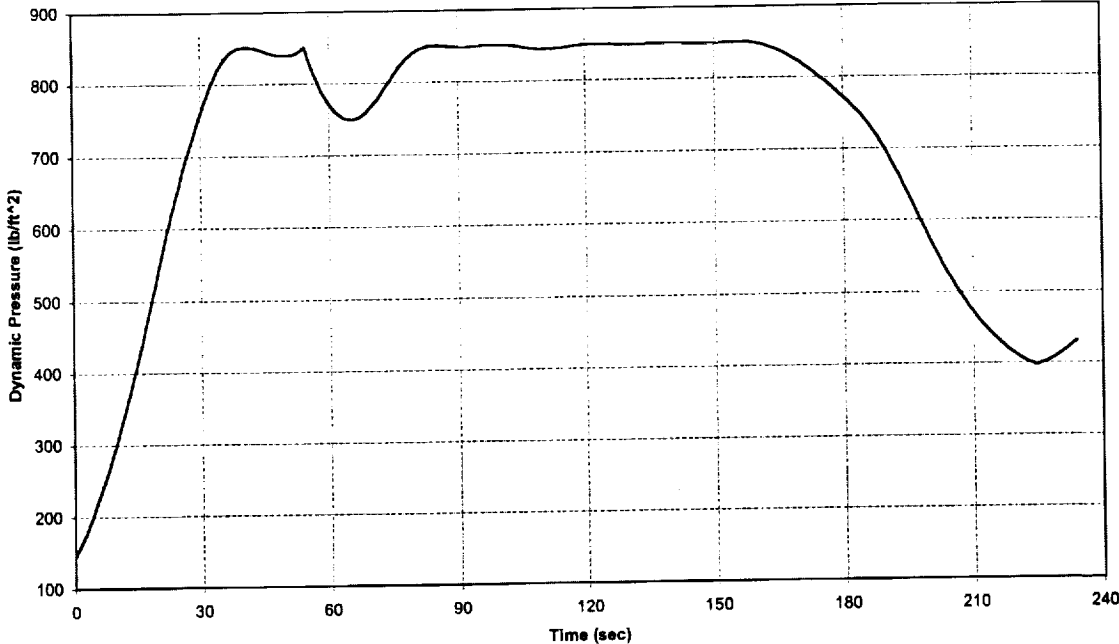
NASAE3GTLOX/PRA
Mach vs Time



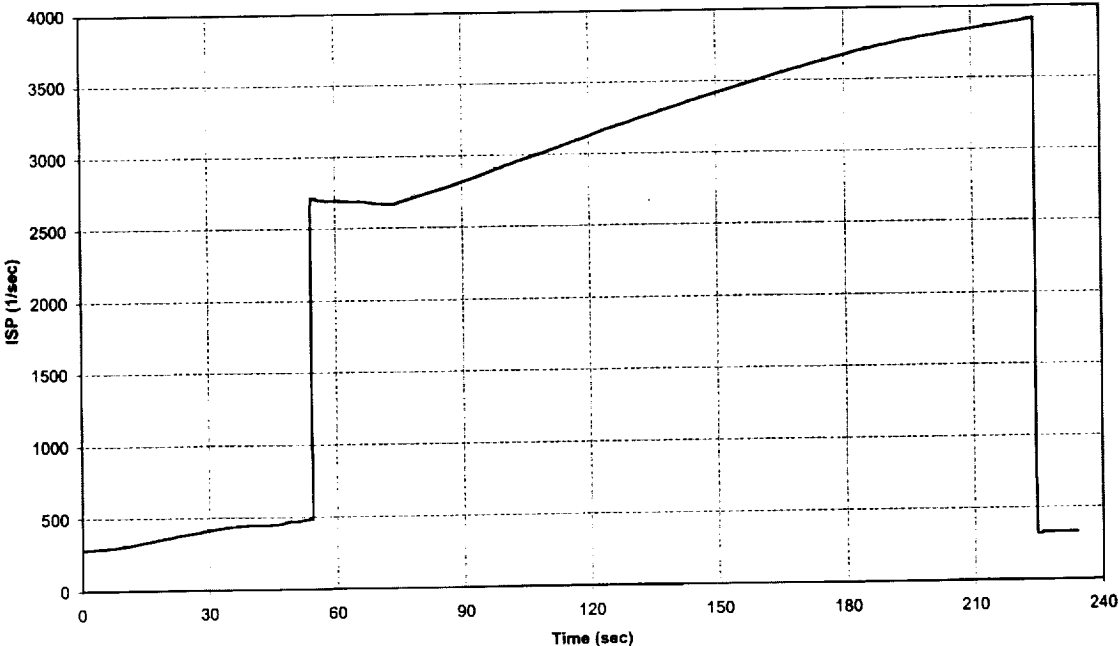
NASAE3GTLOX/PRA
Weight vs Time



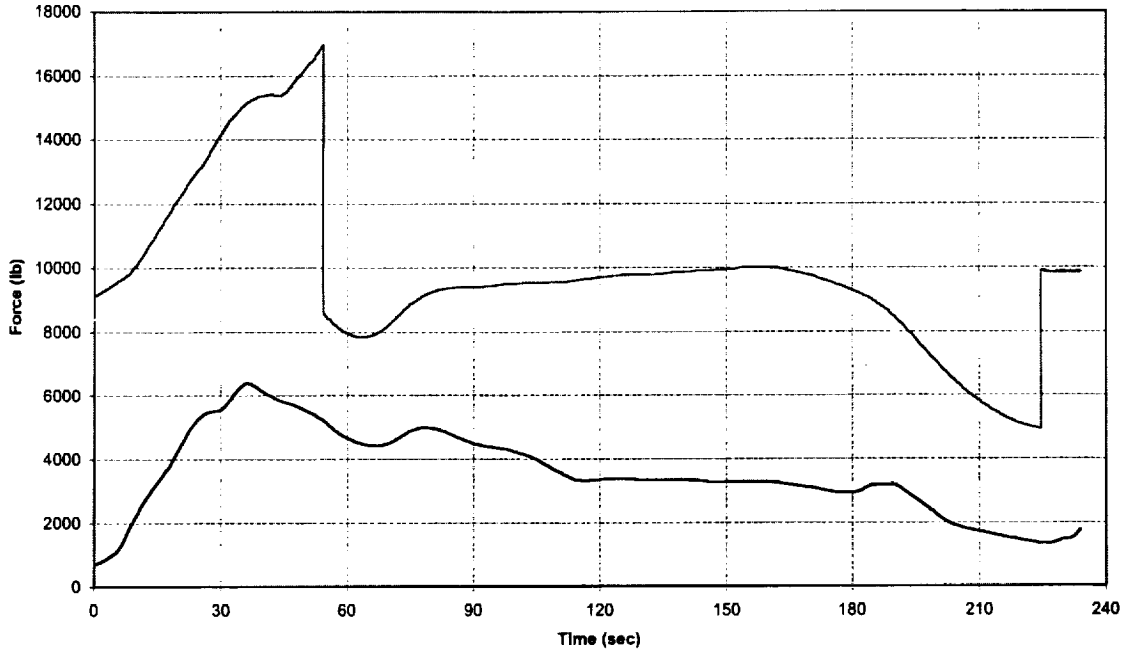
NASAE3GTLOX/PRA
Dynamic Pressure vs Time



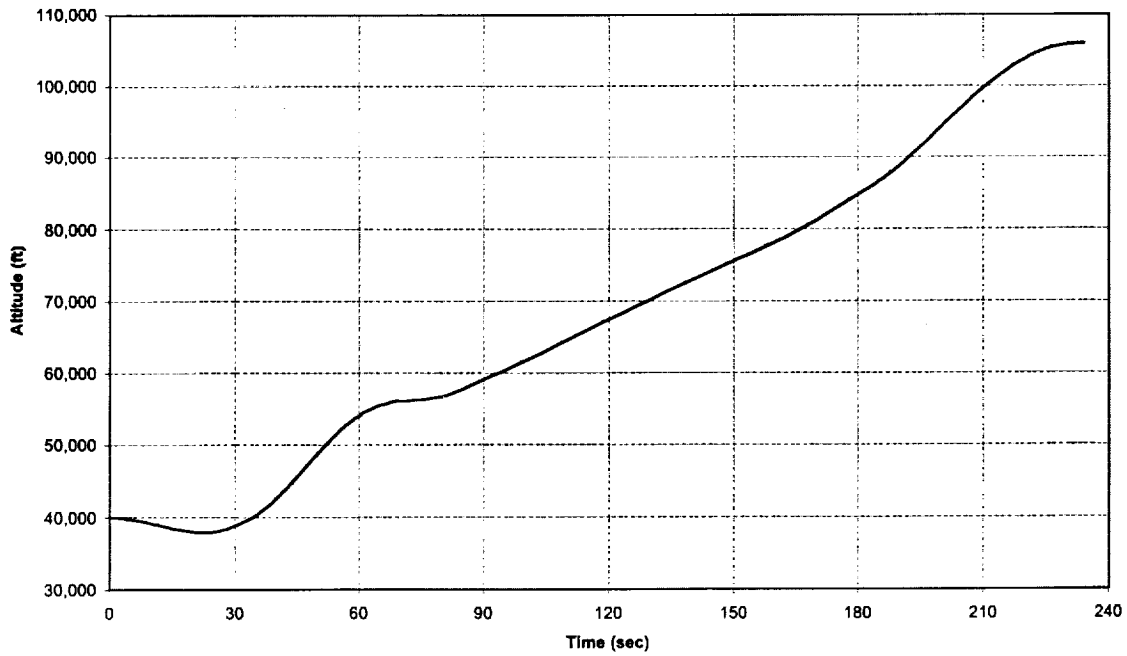
NASAE3GTLOX/PRA
Specific Impulse vs Time



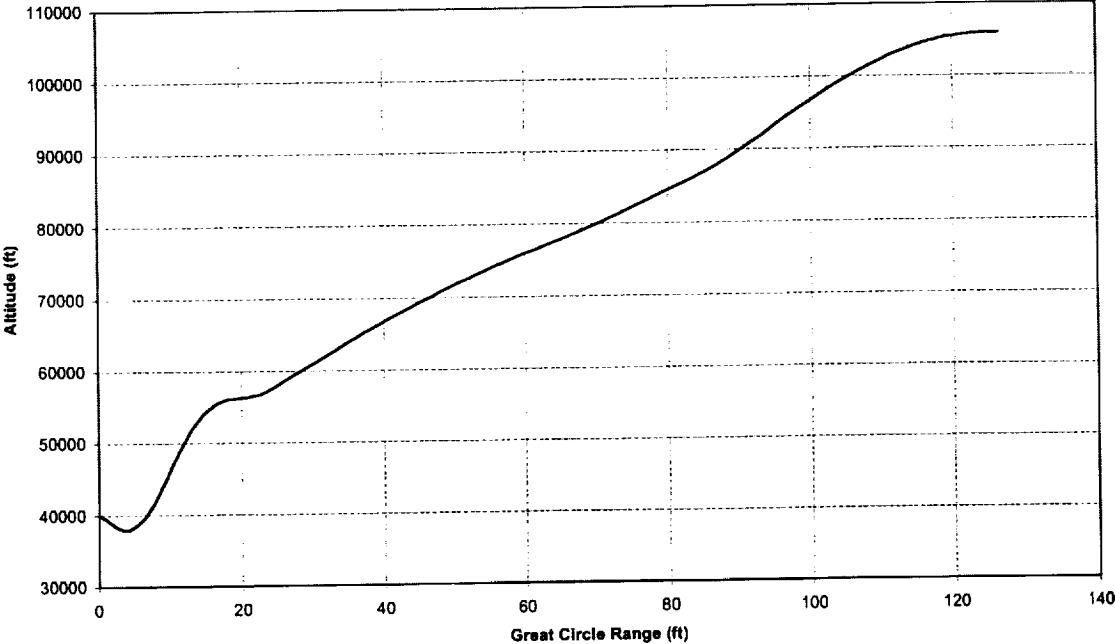
NASAE3GTLOX/PRA
Thrust & Drag vs Time



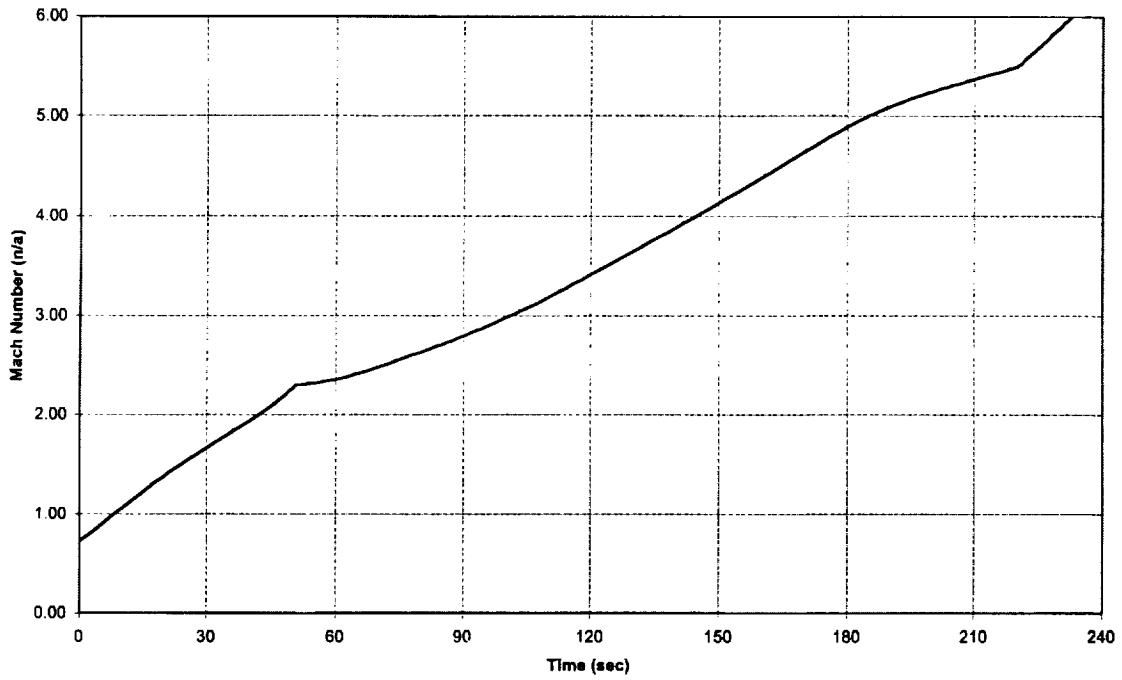
NASAE3GTLOX/PRA
Altitude vs Time



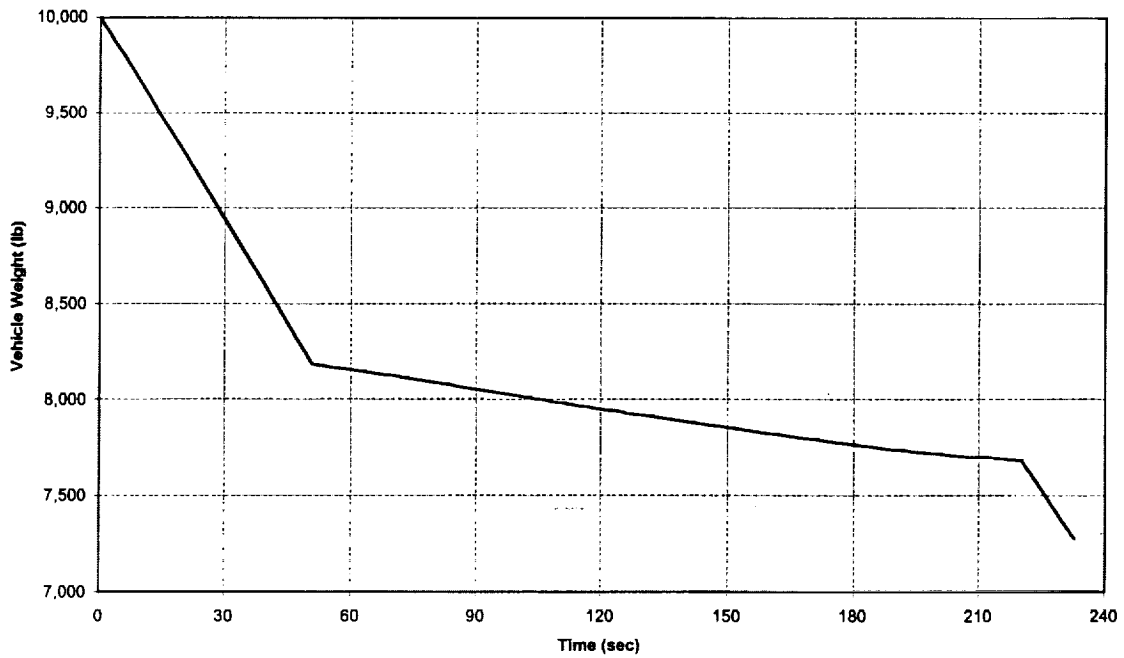
NASAE3GTLOX/PRA
Altitude vs Great Circle Range



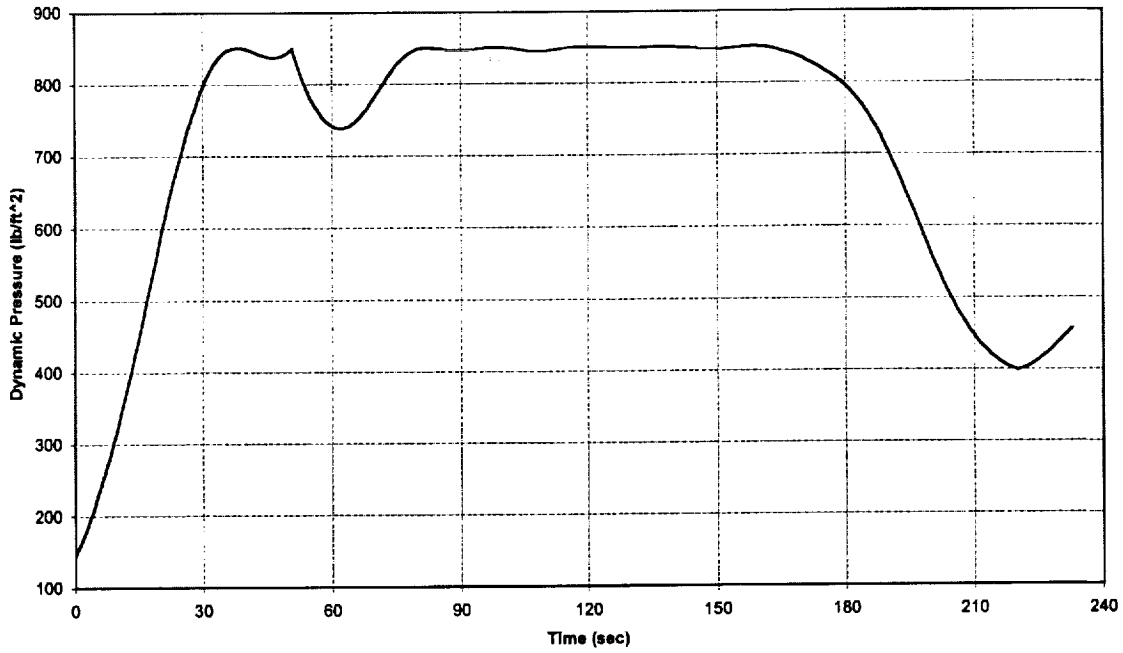
NASAE3GTLOX/JPA
Mach vs Time



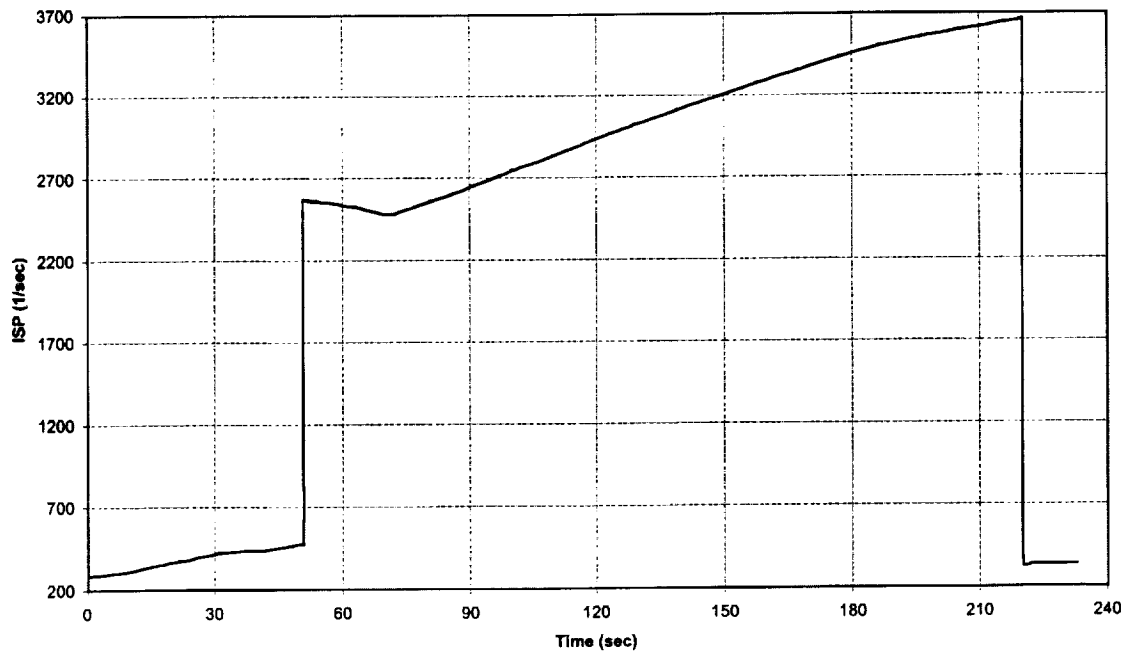
NASAE3GTLOX/JPA
Weight vs Time



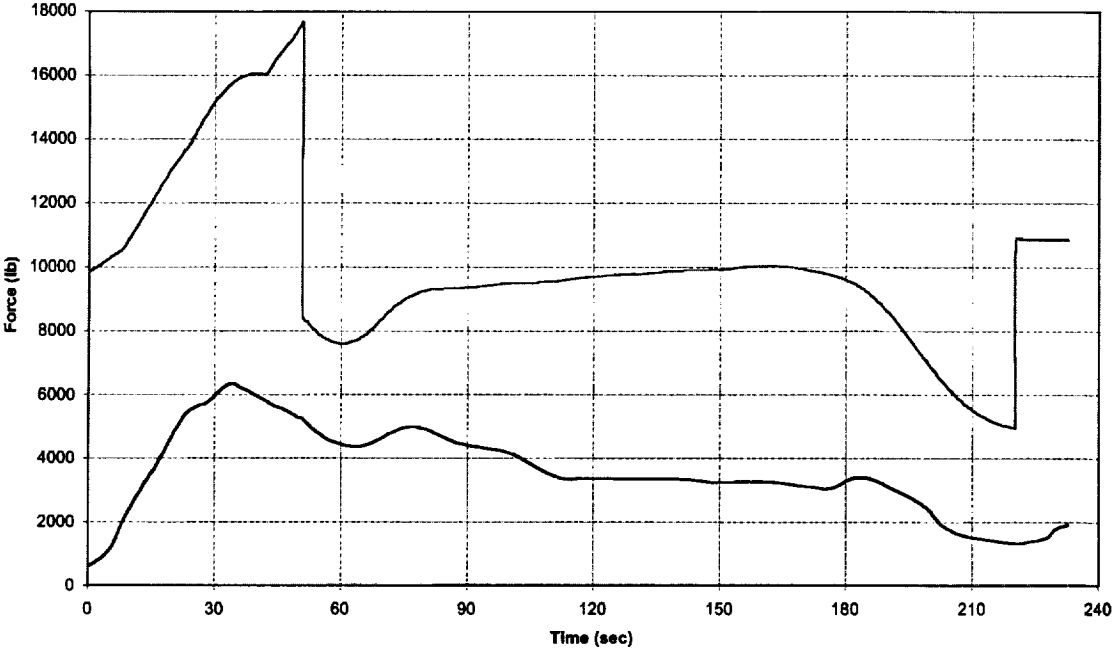
NASAE3GTLOX/JPA
Dynamic Pressure vs Time



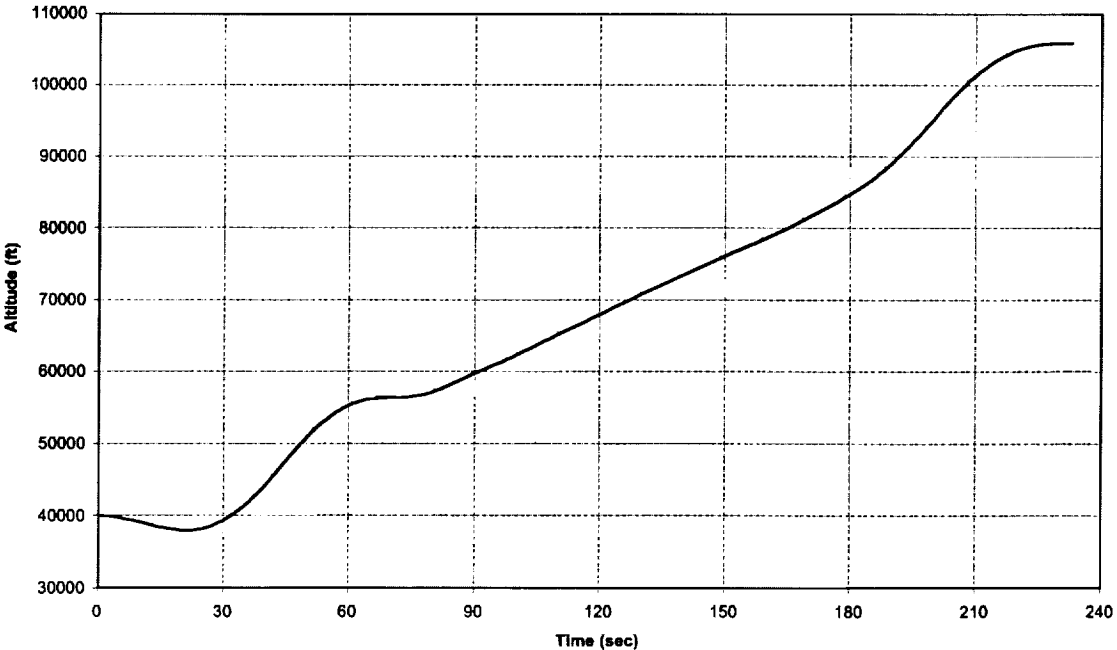
NASAE3GTLOX/JPA
Specific Impulse vs Time



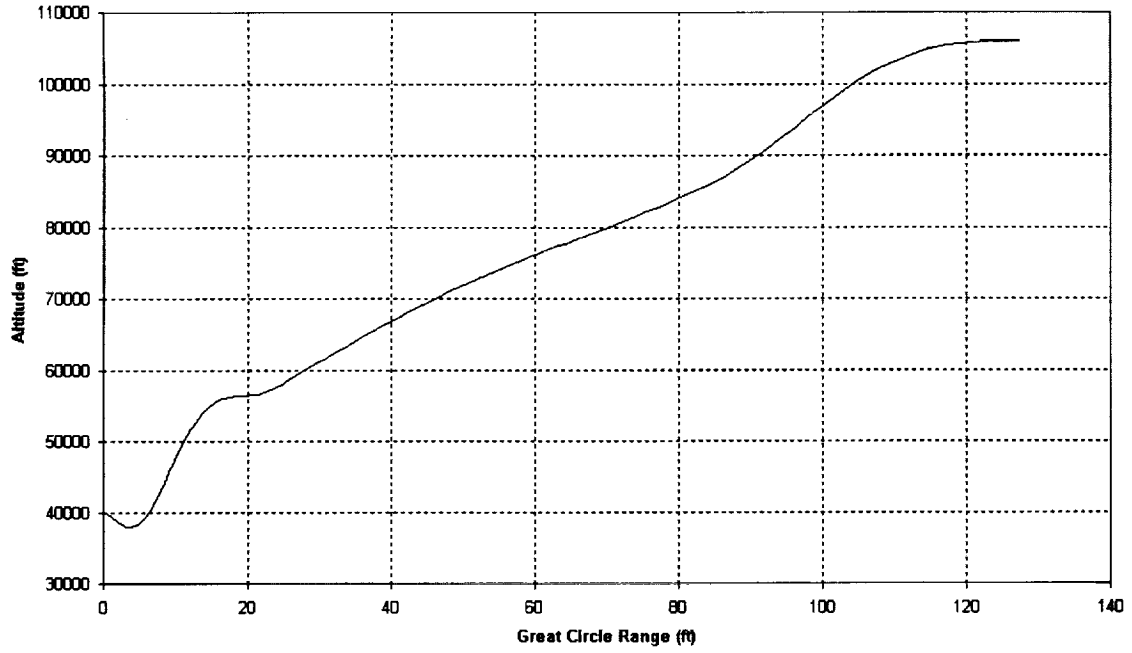
NASAE3GTLOX/JPA
Thrust & Drag vs Time



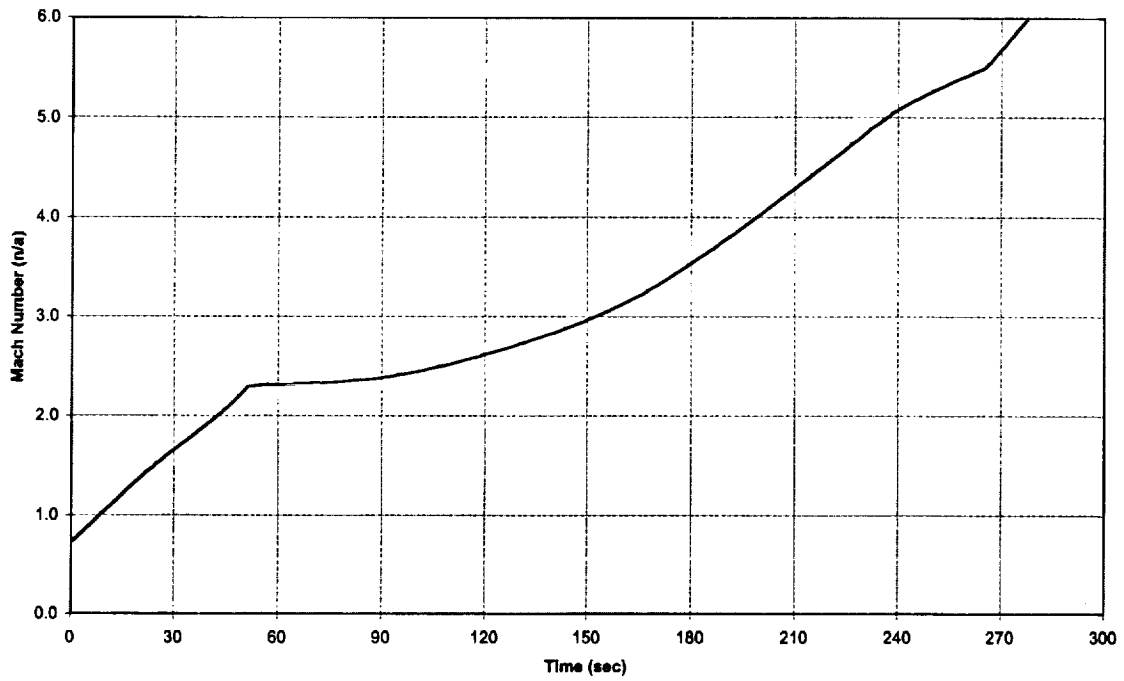
NASAE3GTLOX/JPA
Altitude vs Time



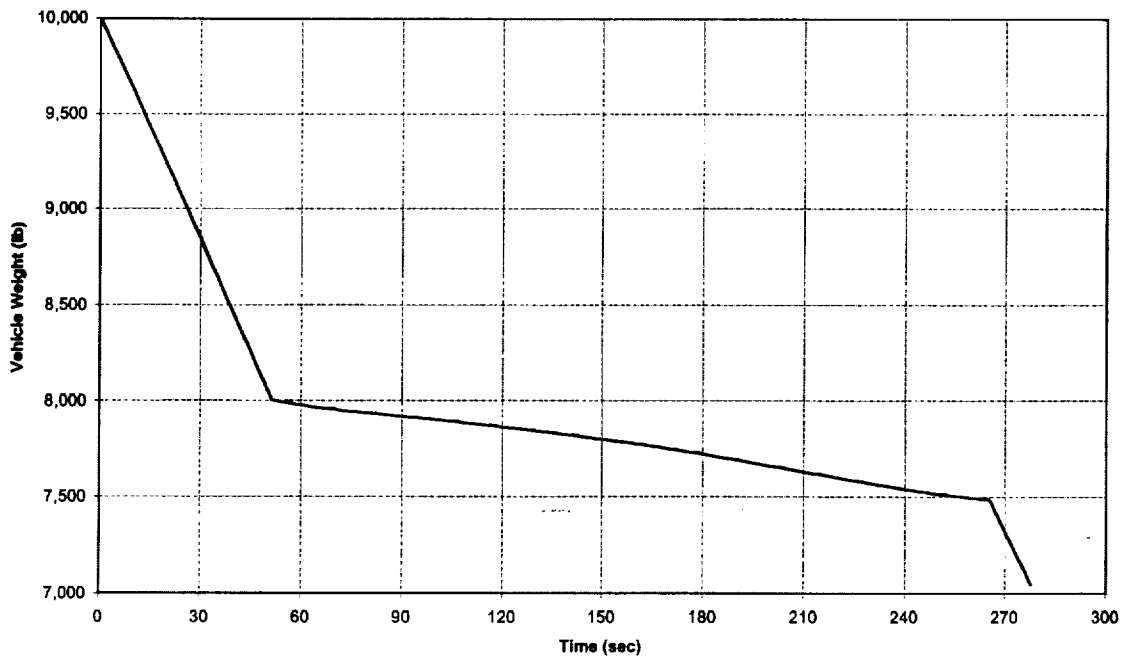
NASAE3GTLOXJPA
Altitude vs Great Circle Range



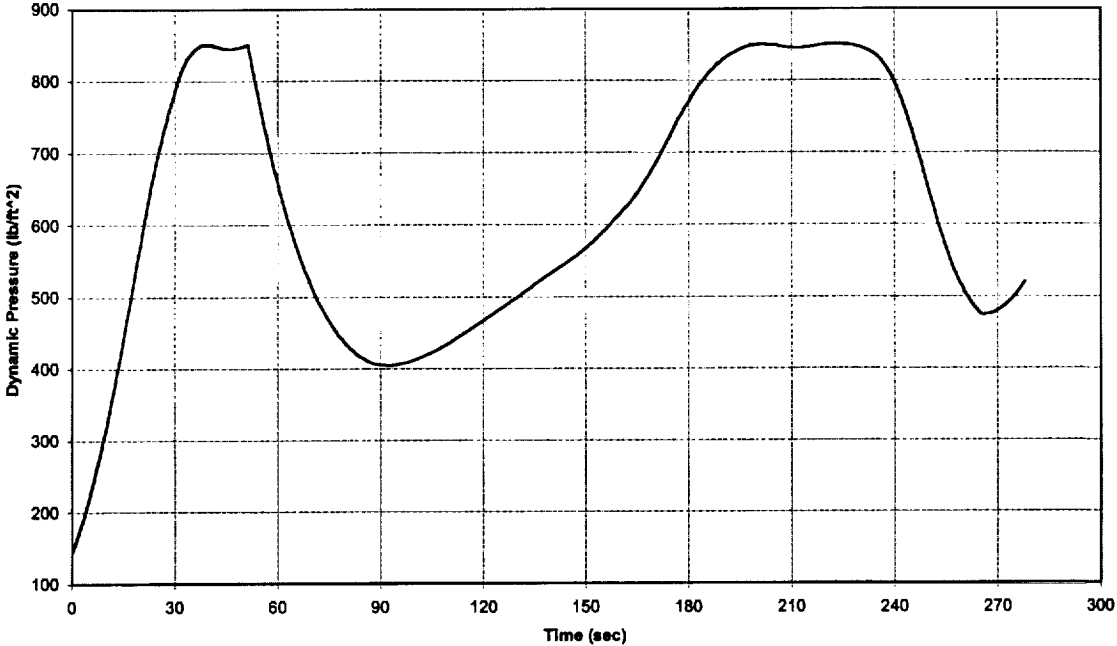
NASAE3GTH2O2/JPA
Mach vs Time



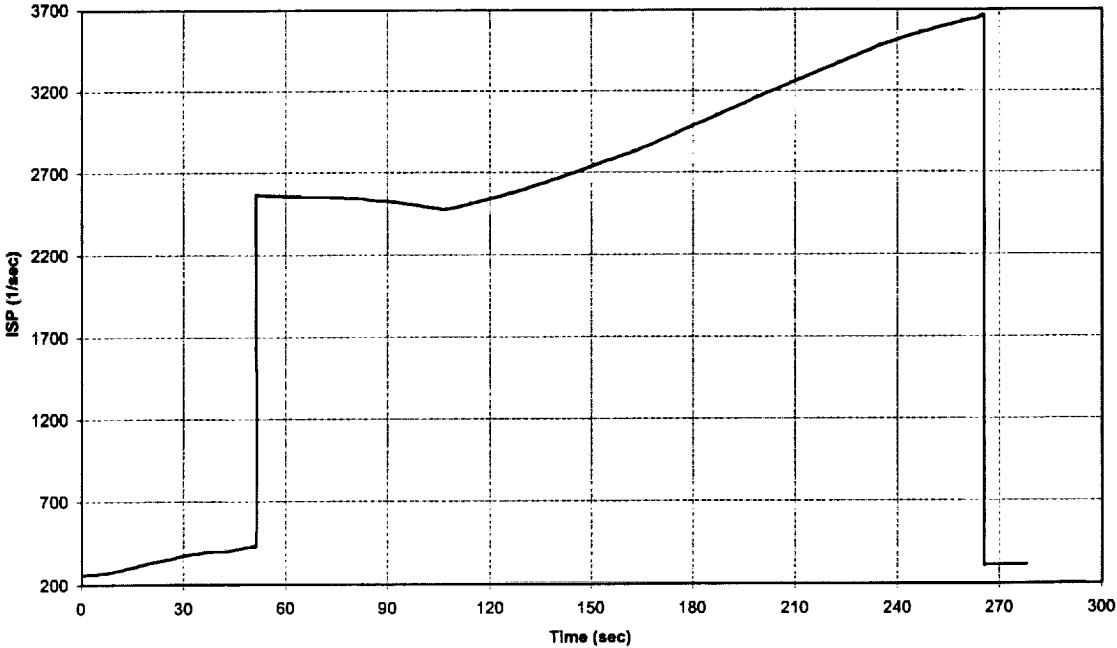
NASAE3GTH2O2/JPA
Weight vs Time



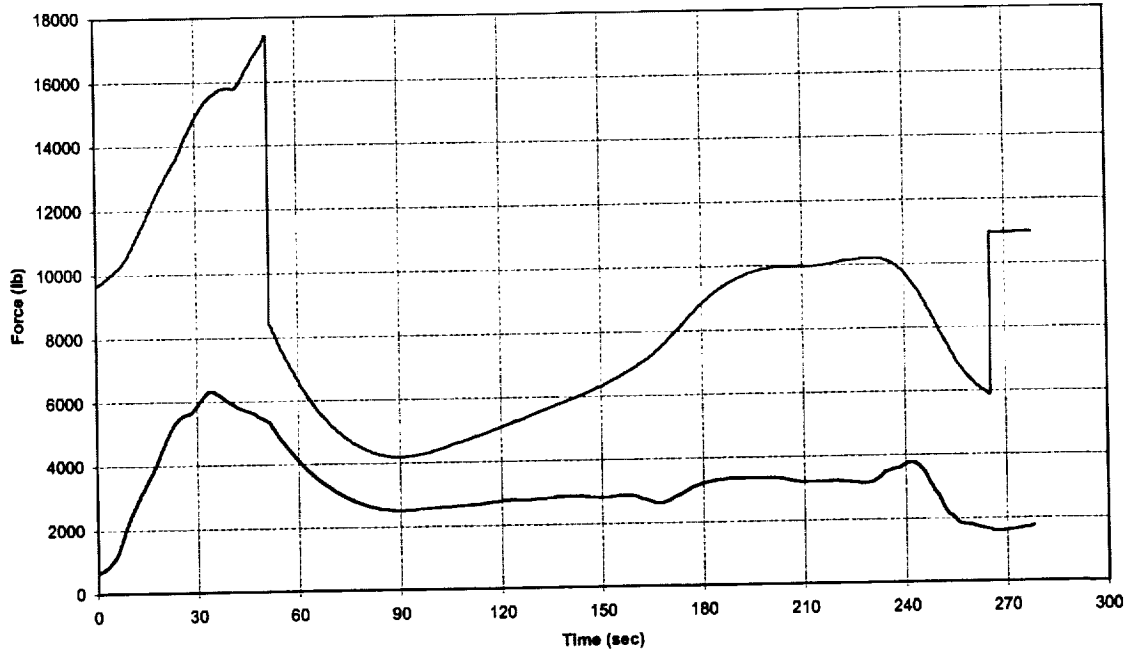
NASAE3GTH2O2/JPA
Dynamic Pressure vs Time



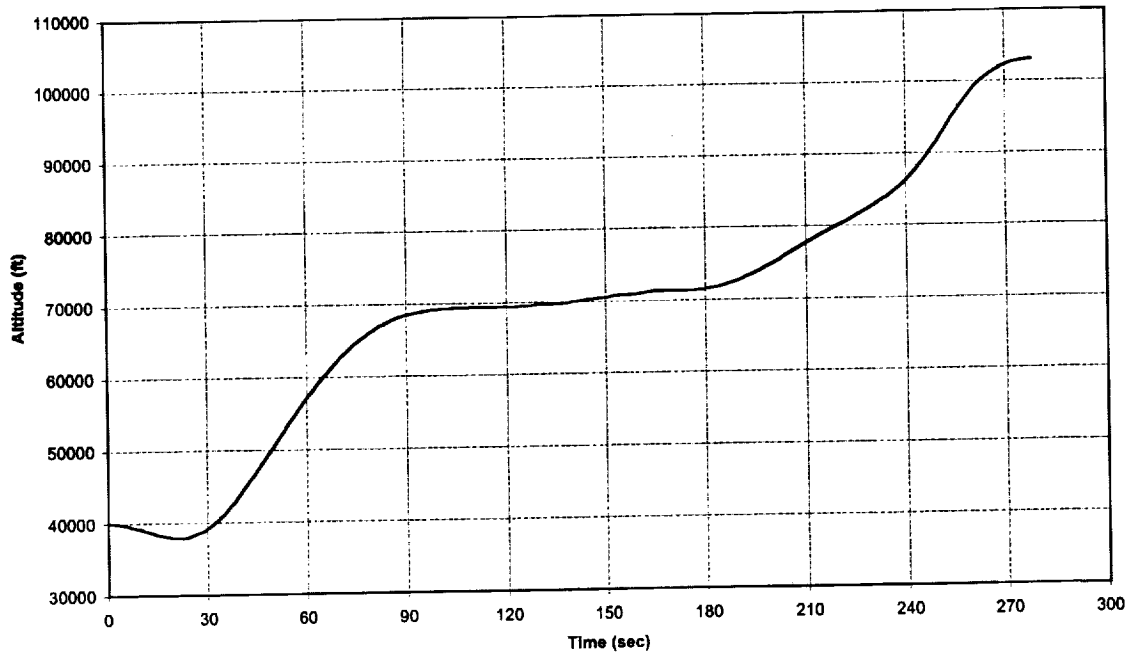
NASAE3GTH2O2/JPA
Specific Impulse vs Time



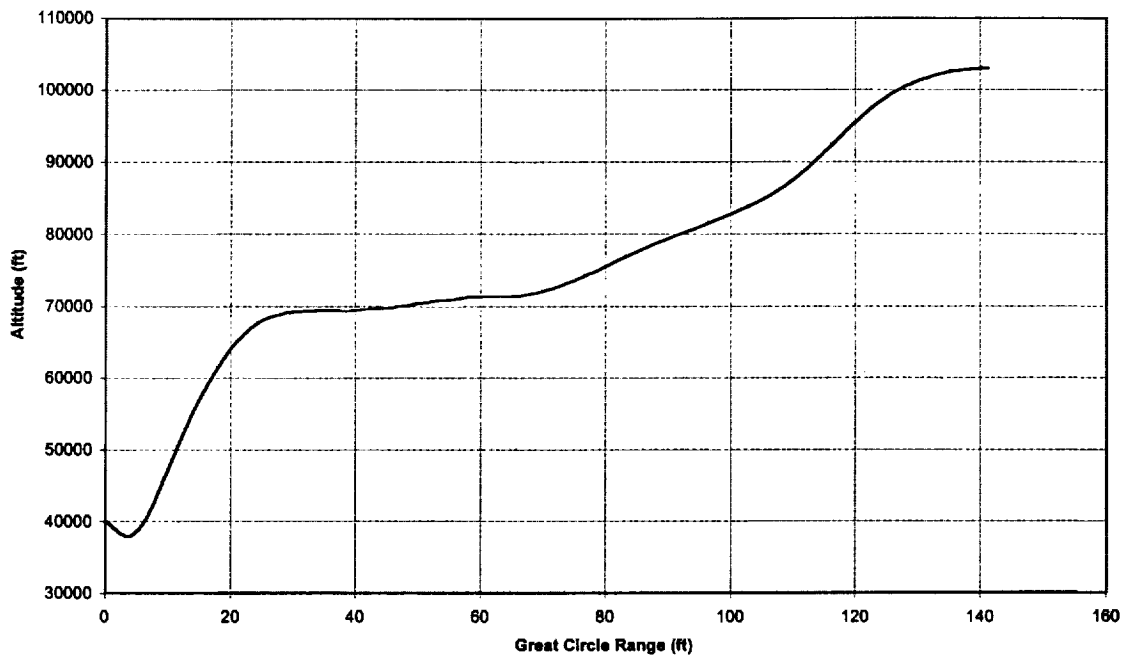
NASAE3GTH2O2/JPA
Thrust & Drag vs Time



NASAE3GTH2O2/JPA
Altitude vs Time

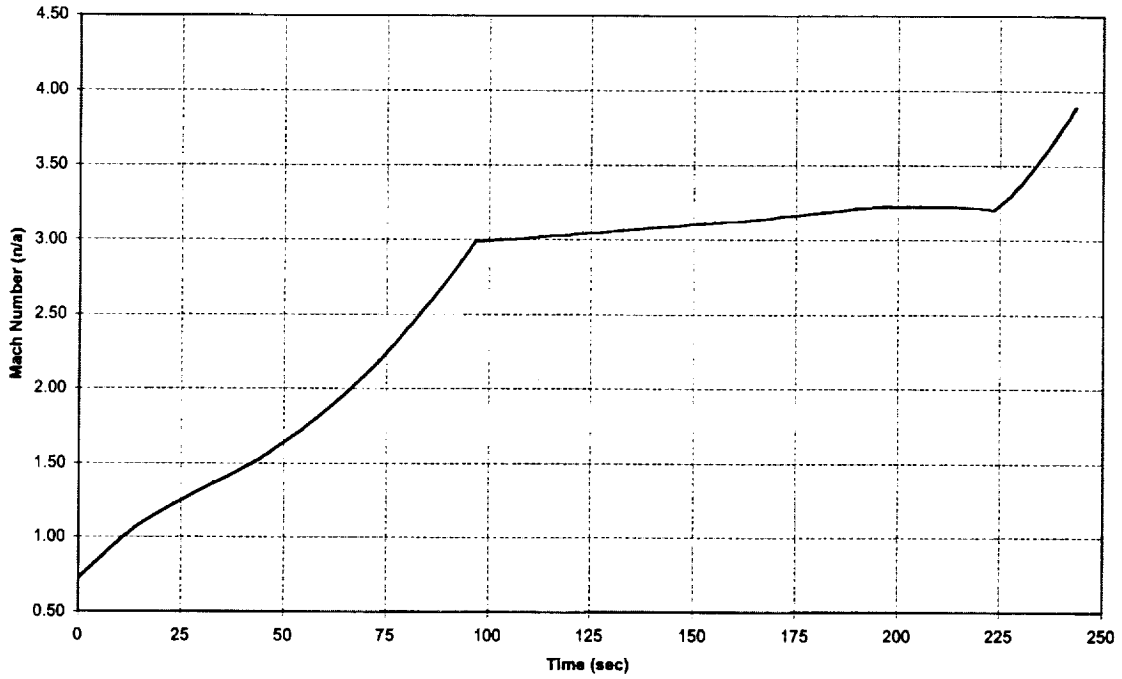


NASAE3GTH2O2/JPA
Altitude vs Great Circle Range

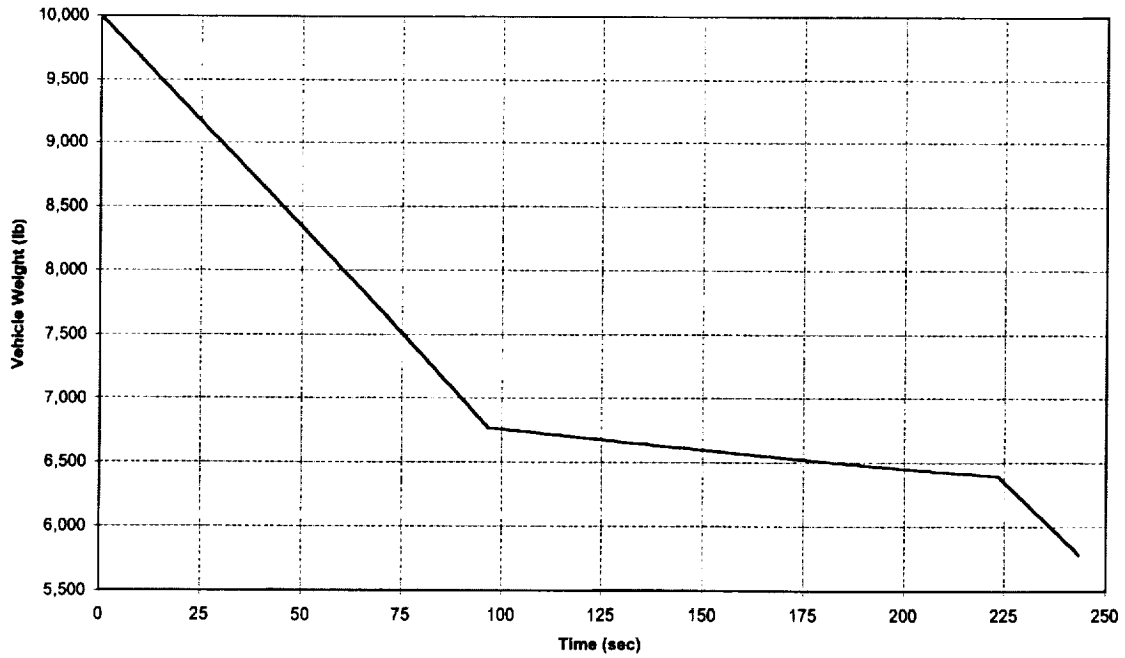


Appendix E4: NASA E3CTLOXPRB4

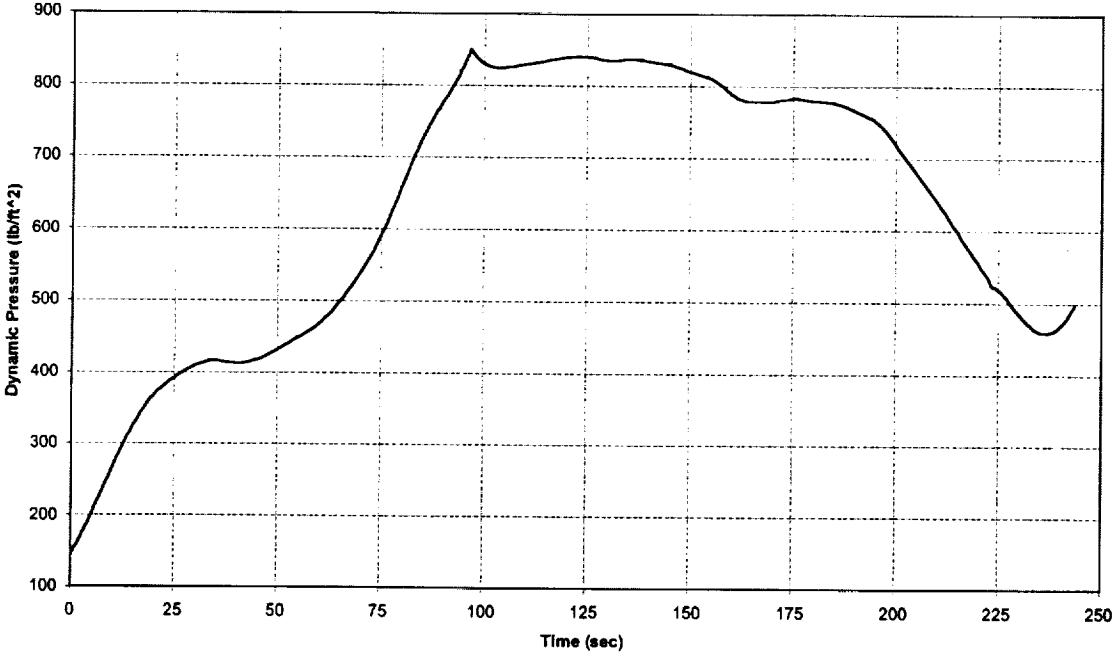
NASAE3CTLOX/ProB4
Mach vs Time



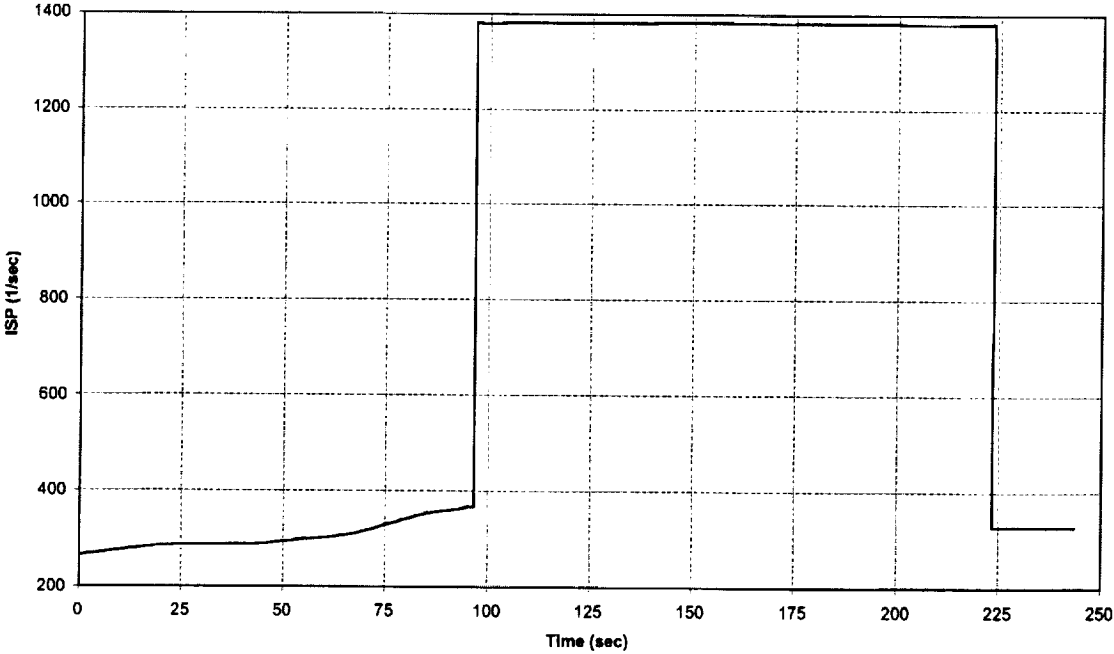
NASAE3CTLOX/ProB4
Weight vs Time



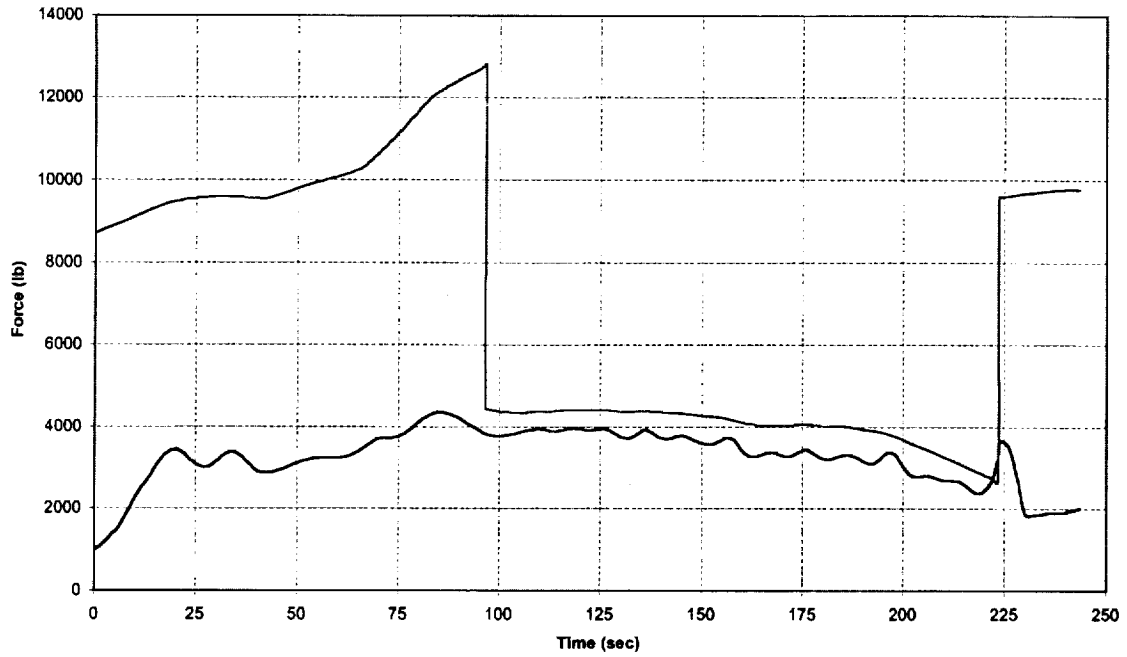
NASAE3CTLOX/ProB4
Dynamic Pressure vs Time



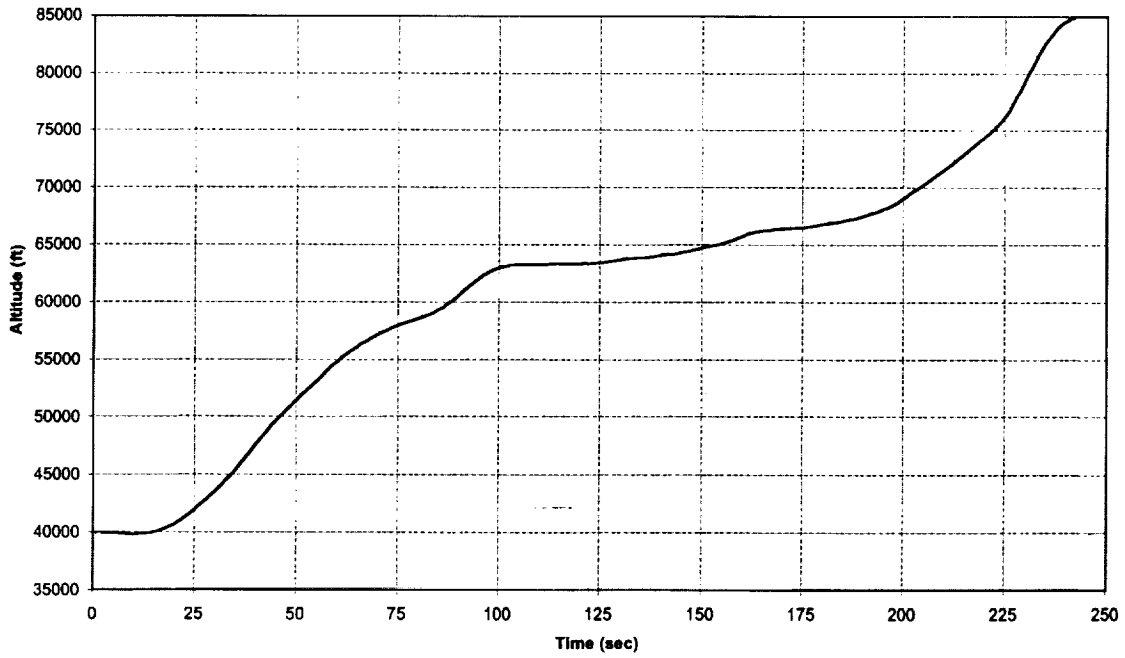
NASAE3CTLOX/ProB4
Specific Impulse vs Time



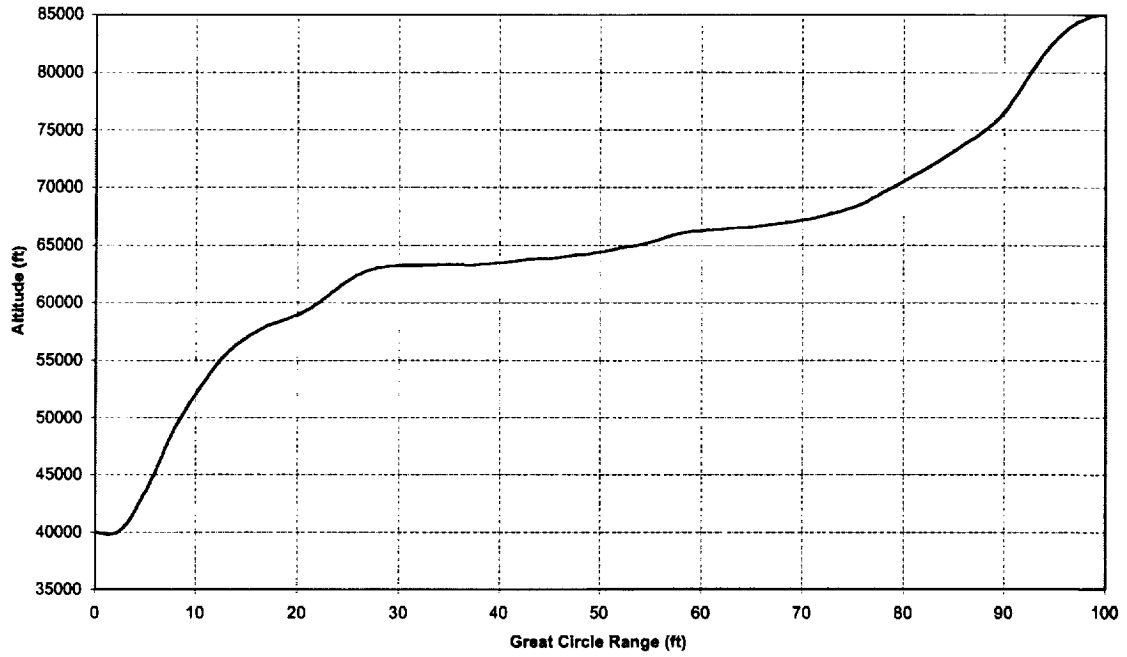
NASAE3CTLOX/ProB4
Thrust & Drag vs Time



NASAE3CTLOX/ProB4
Altitude vs Time

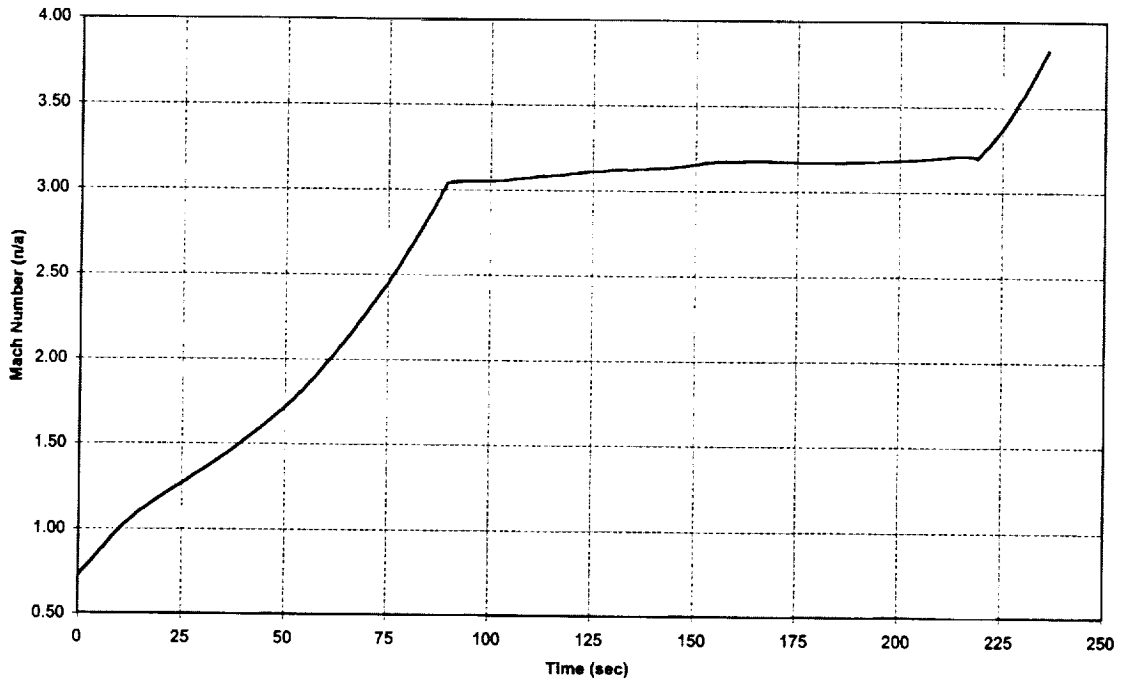


NASAE3CTLOX/ProB4
Altitude vs Great Circle Range

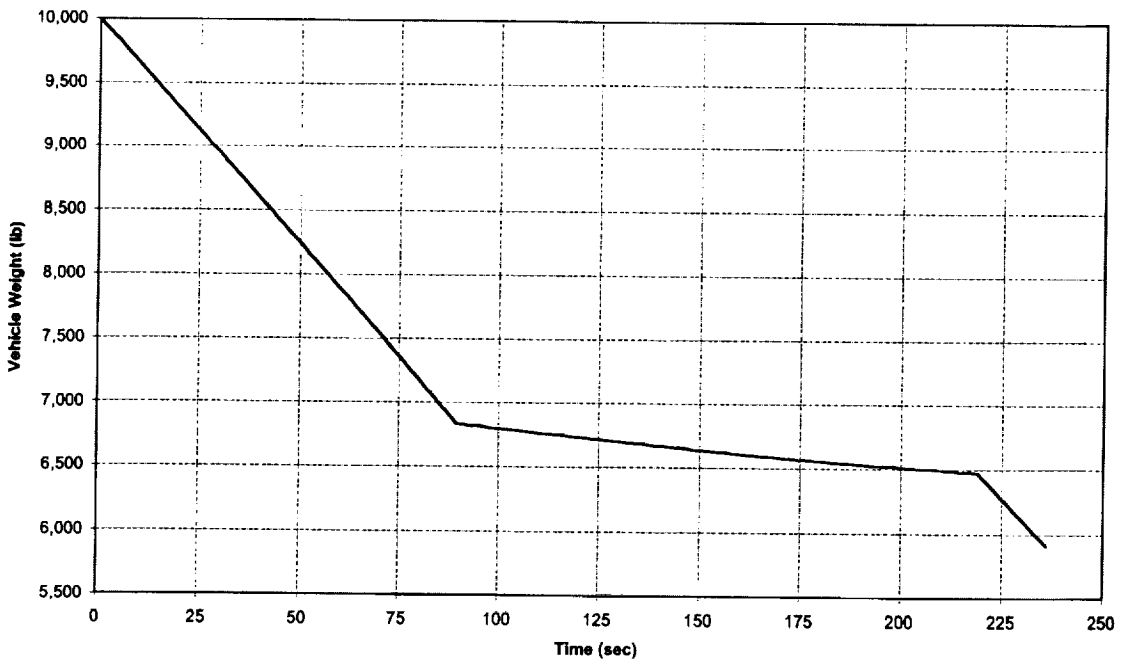


Appendix E5: NASA E3CTLOXJPB4

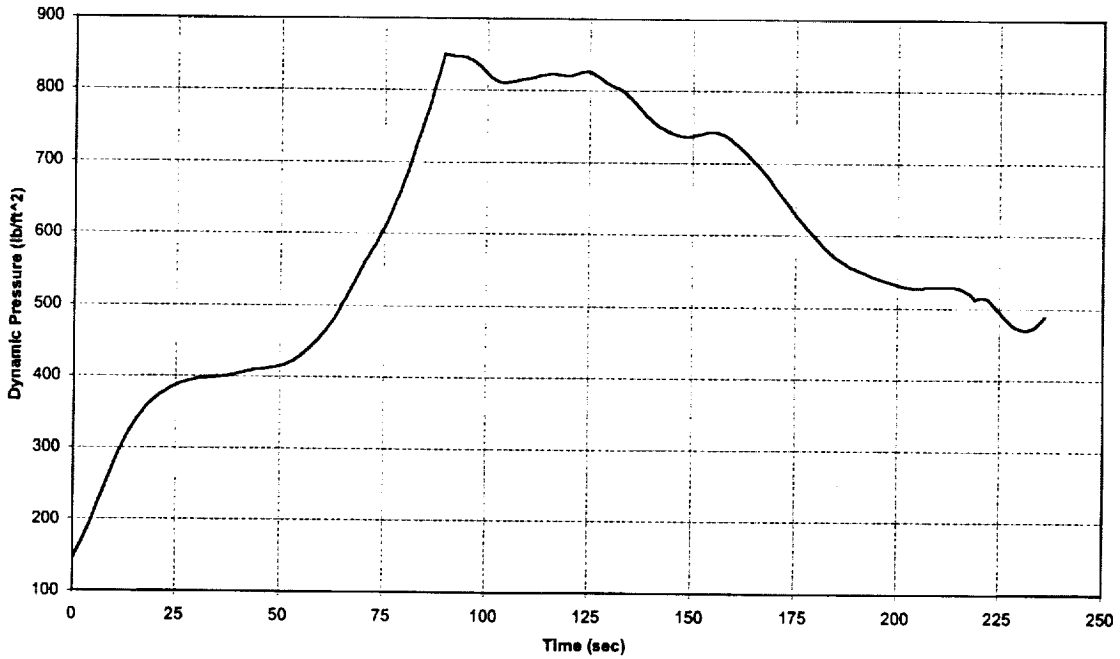
NASAE3CTLOX/JPB4
Mach vs Time



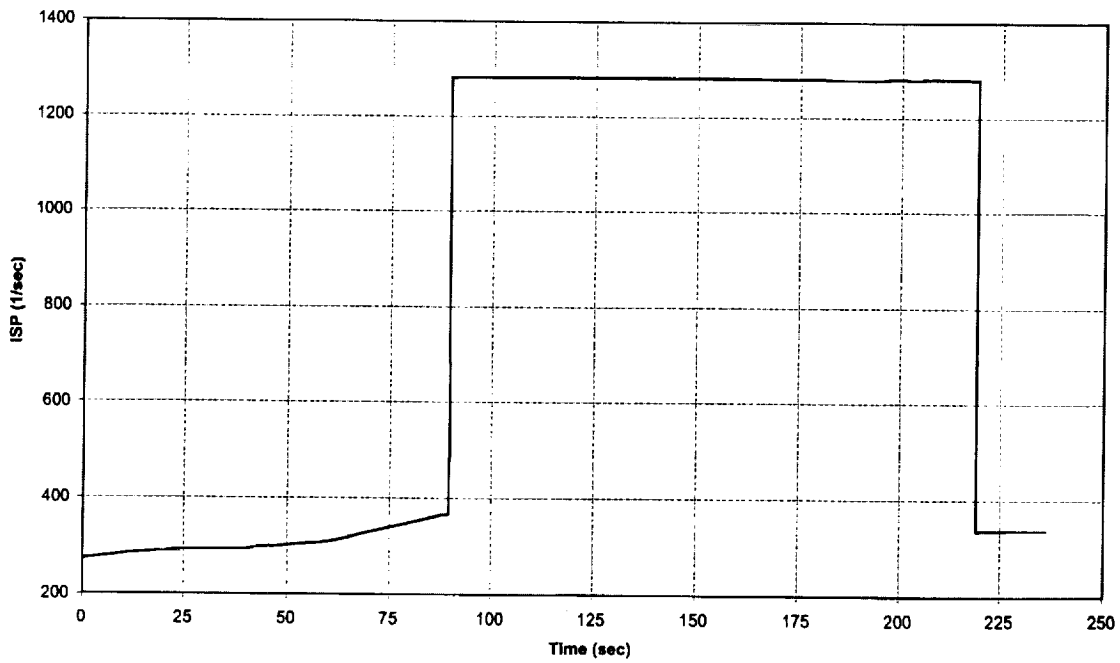
NASAE3CTLOX/JPB4
Weight vs Time



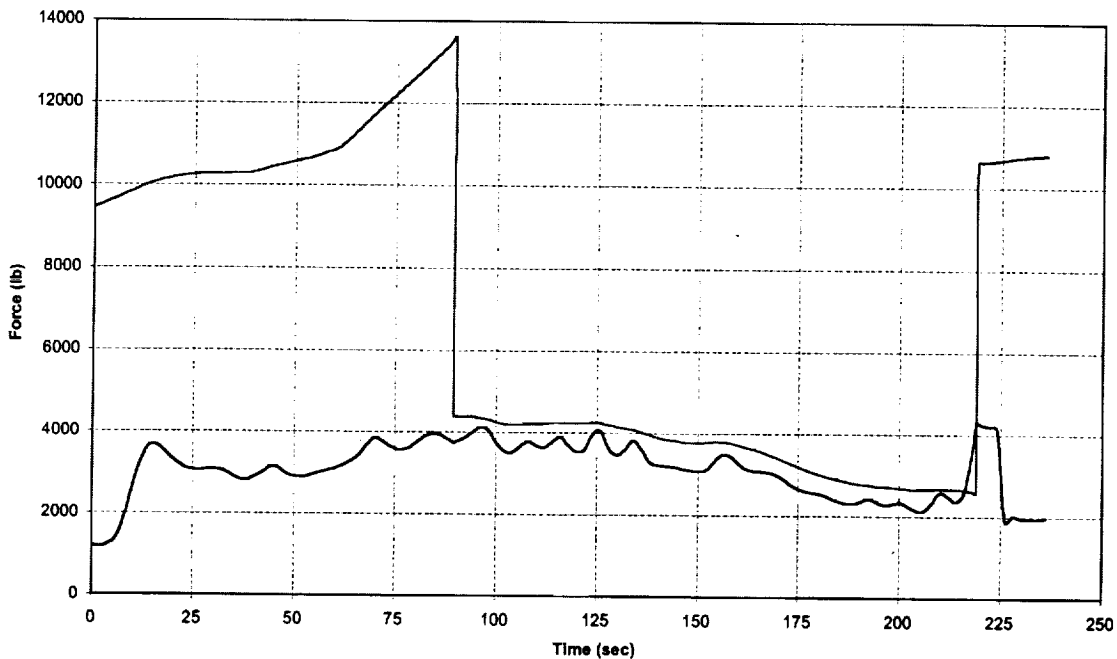
NASAE3CTLOXJPB4
Dynamic Pressure vs Time



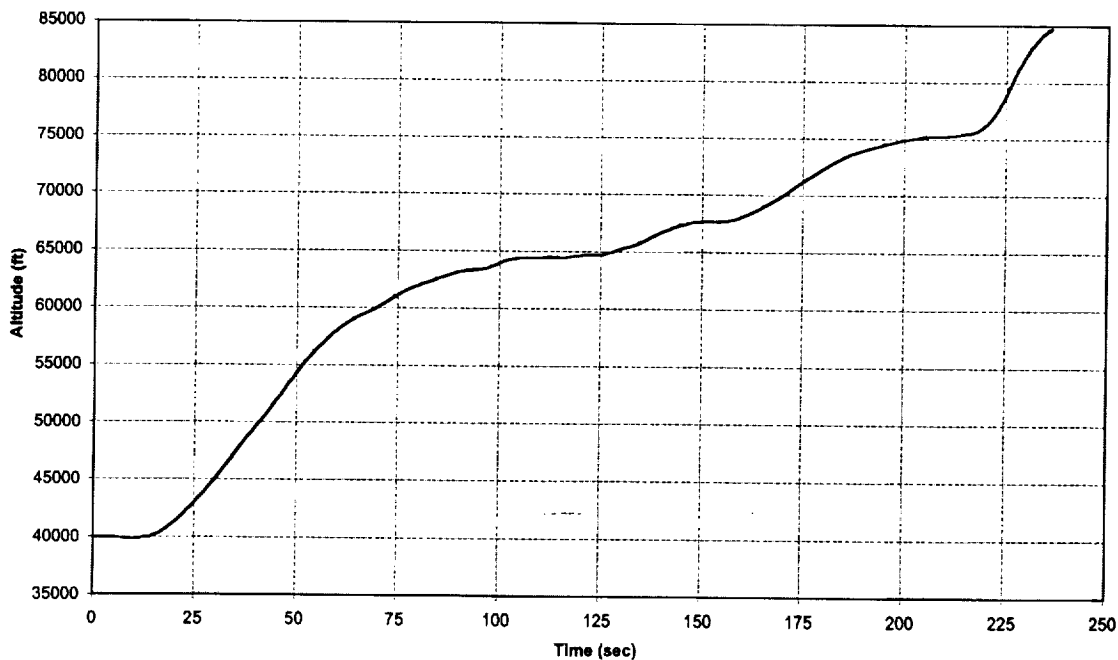
NASAE3CTLOXJPB4
Specific Impulse vs Time



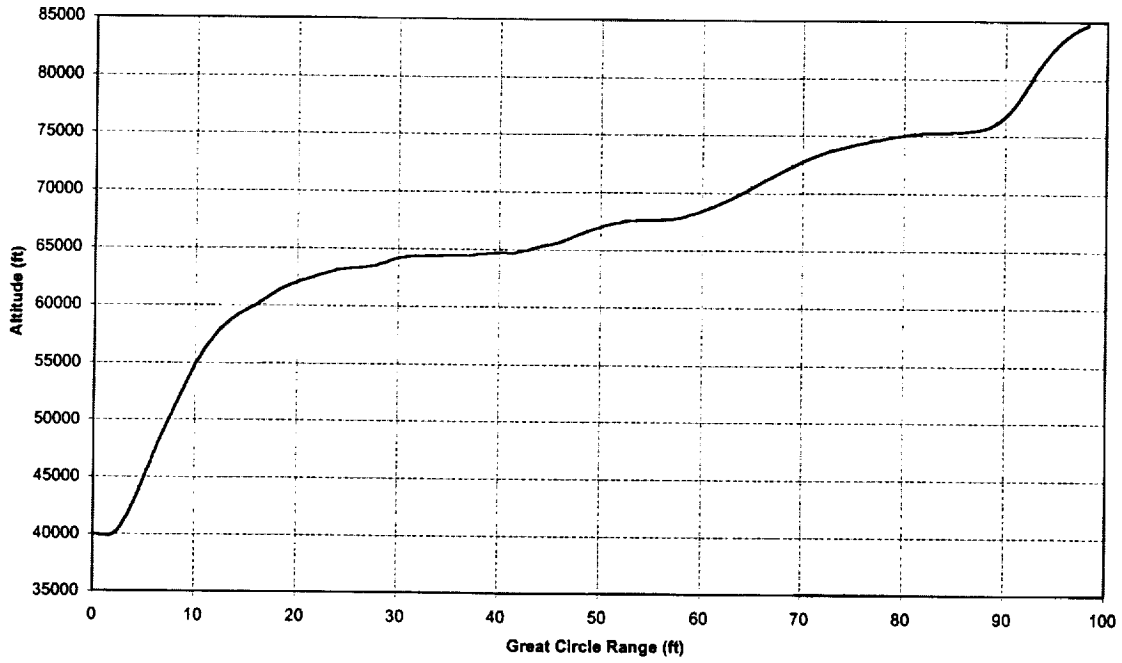
NASAE3CTLOX/JPB4
Thrust & Drag vs Time



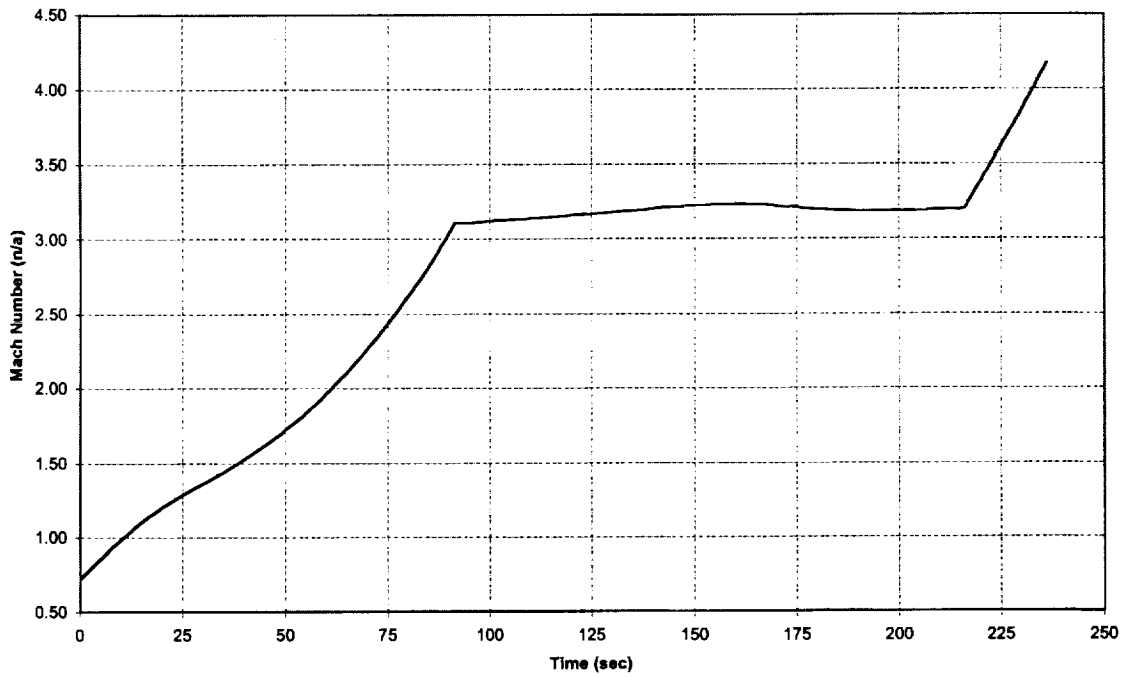
NASAE3CTLOX/JPB4
Altitude vs Time



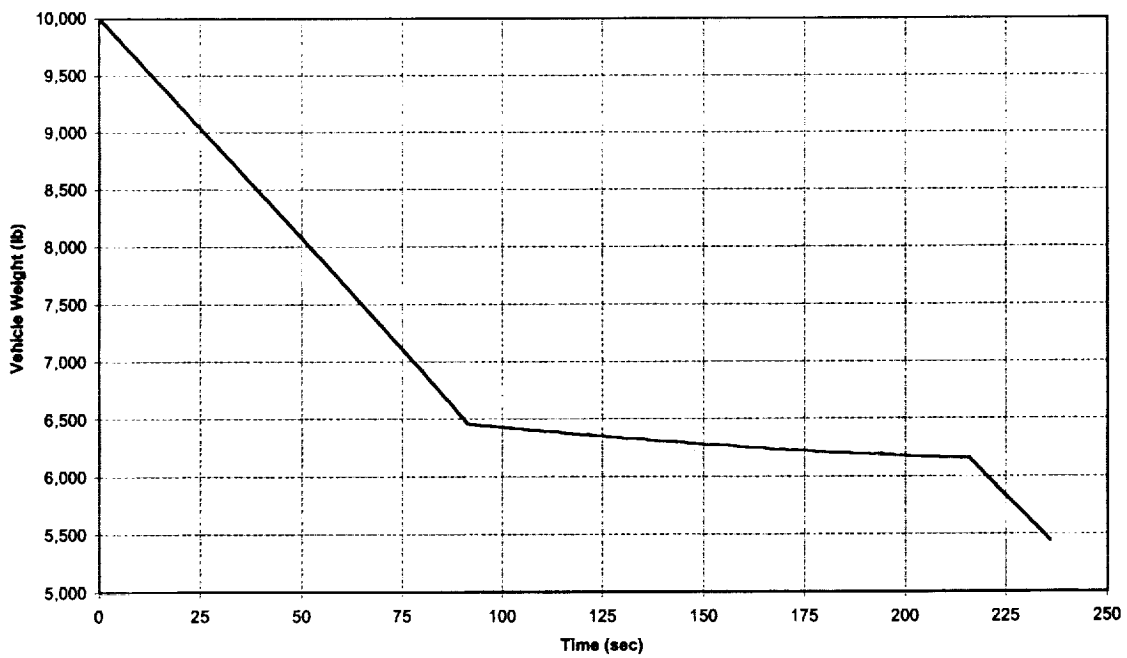
NASAE3CTLOXJPB4
Altitude vs Great Circle Range



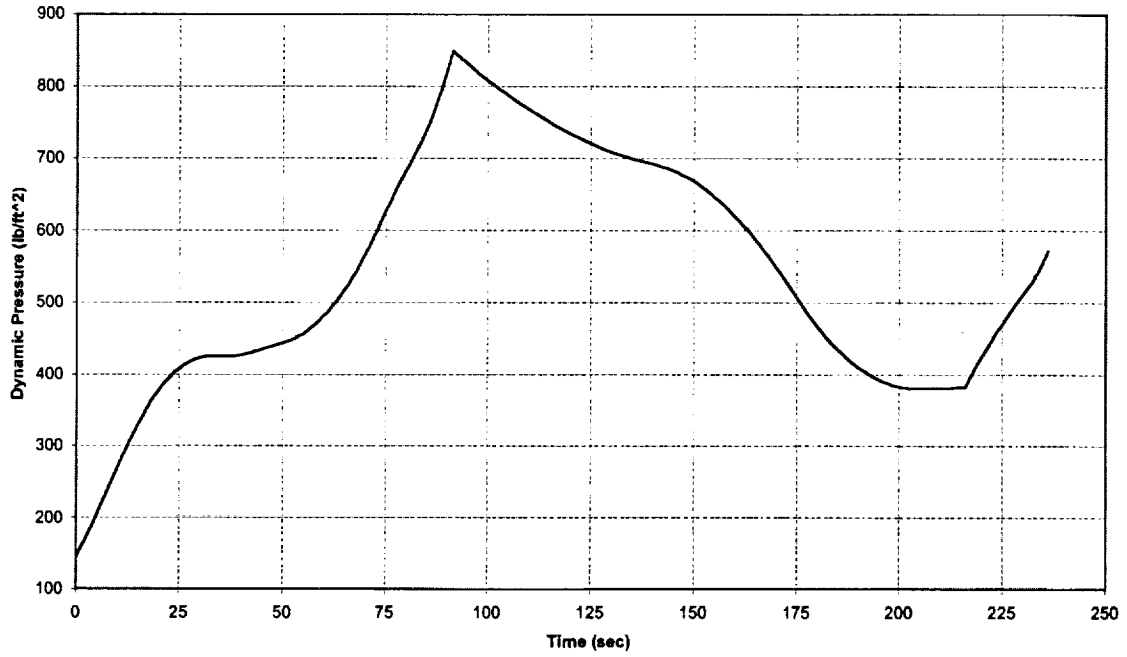
NASAE3CTH2O2/JPB4
Mach vs Time



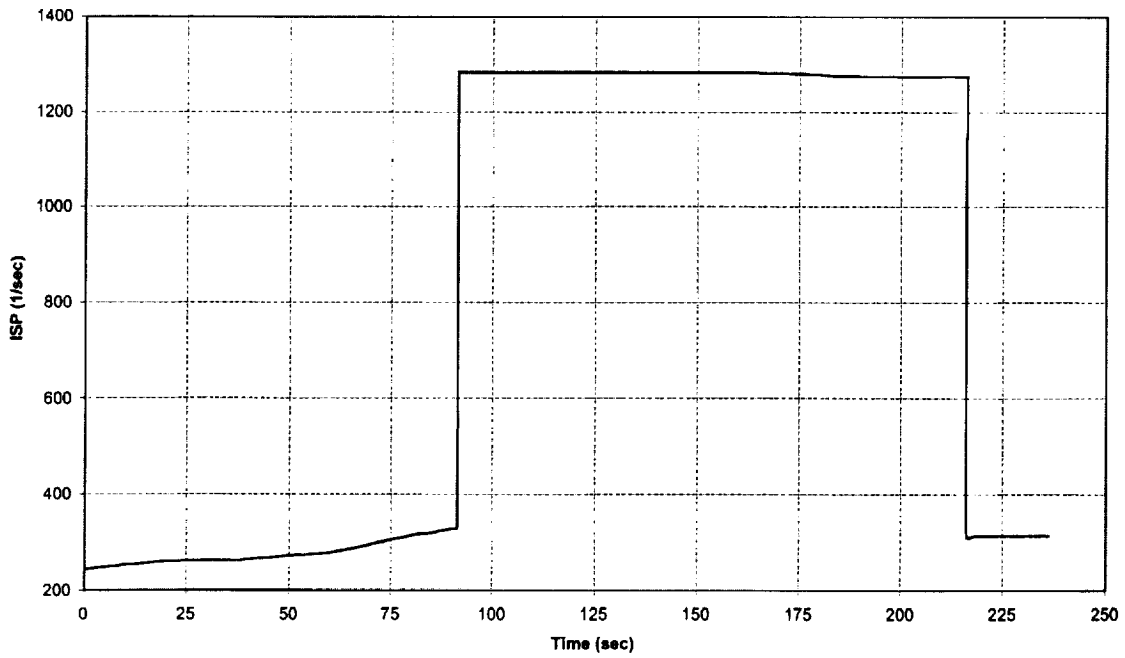
NASAE3CTH2O2/JPB4
Weight vs Time



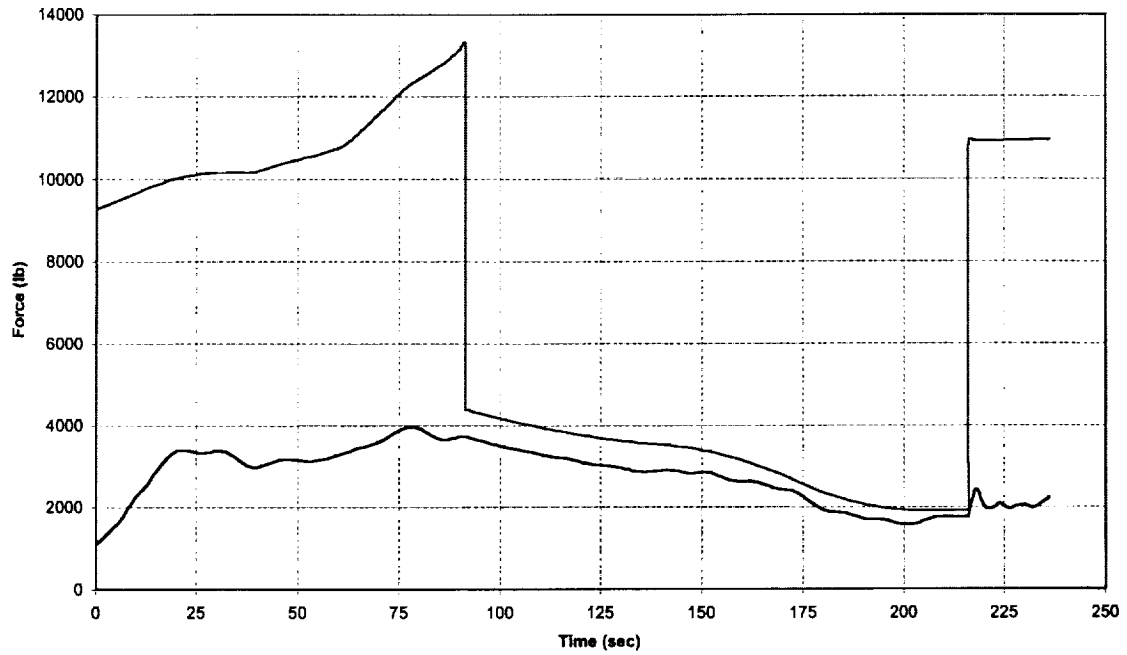
NASAE3CTH2O2/JPB4
Dynamic Pressure vs Time



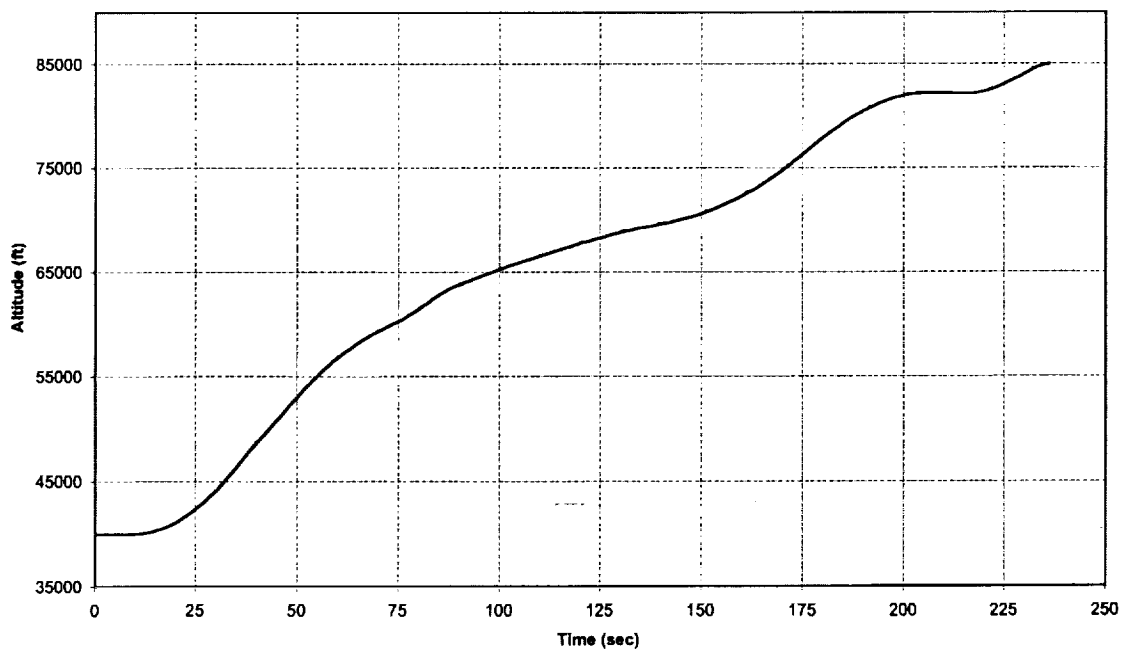
NASAE3CTH2O2/JPB4
Specific Impulse vs Time



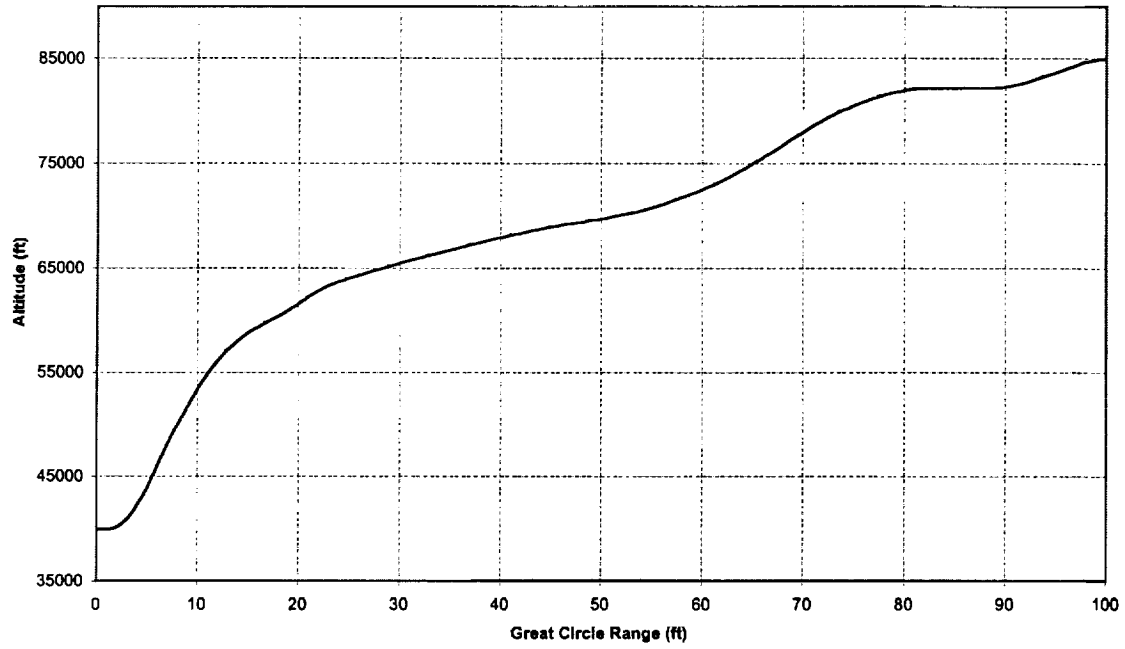
NASAE3CTH2O2/JPB4
Thrust & Drag vs Time



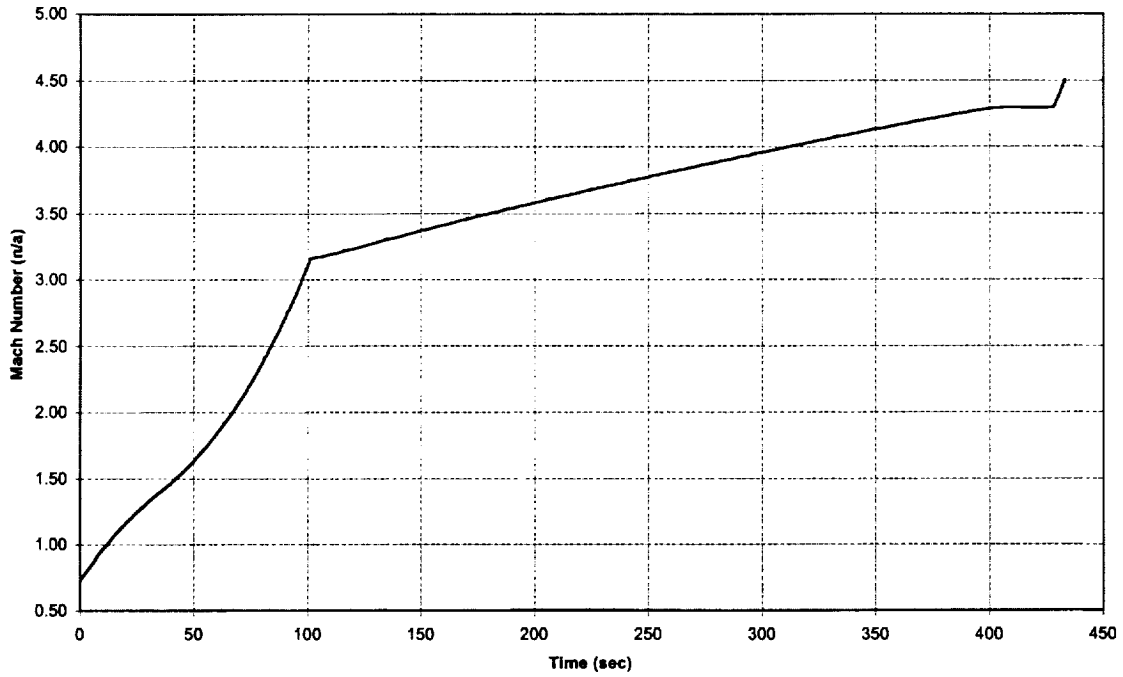
NASAE3CTH2O2/JPB4
Altitude vs Time



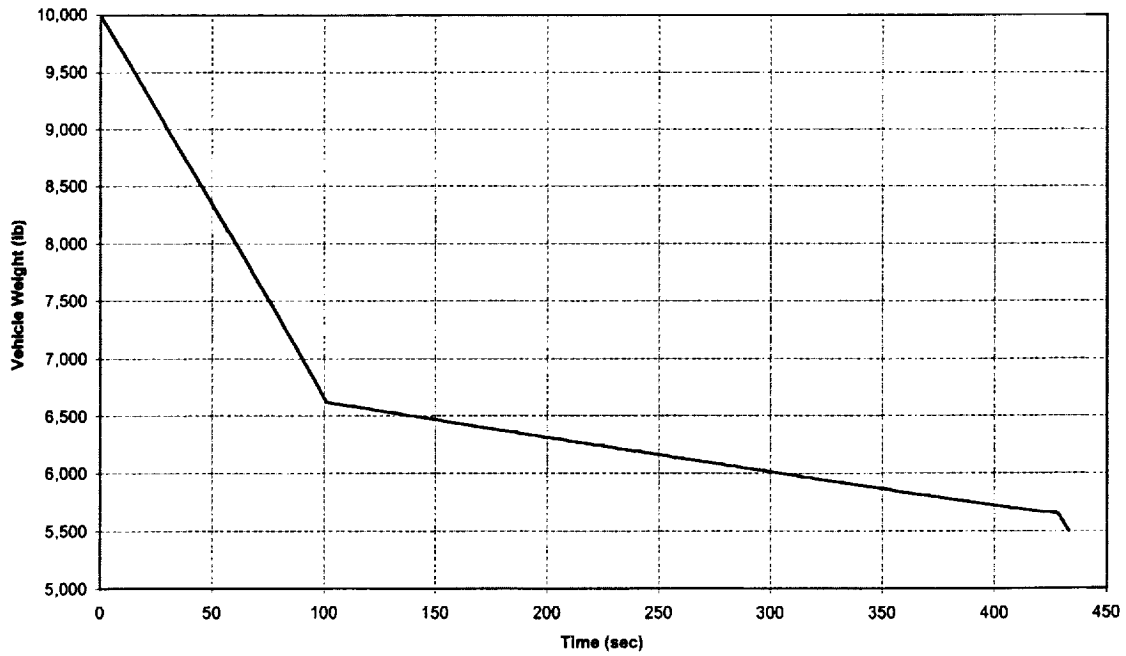
NASAE3CTH2O2/JPB4
Altitude vs Great Circle Range



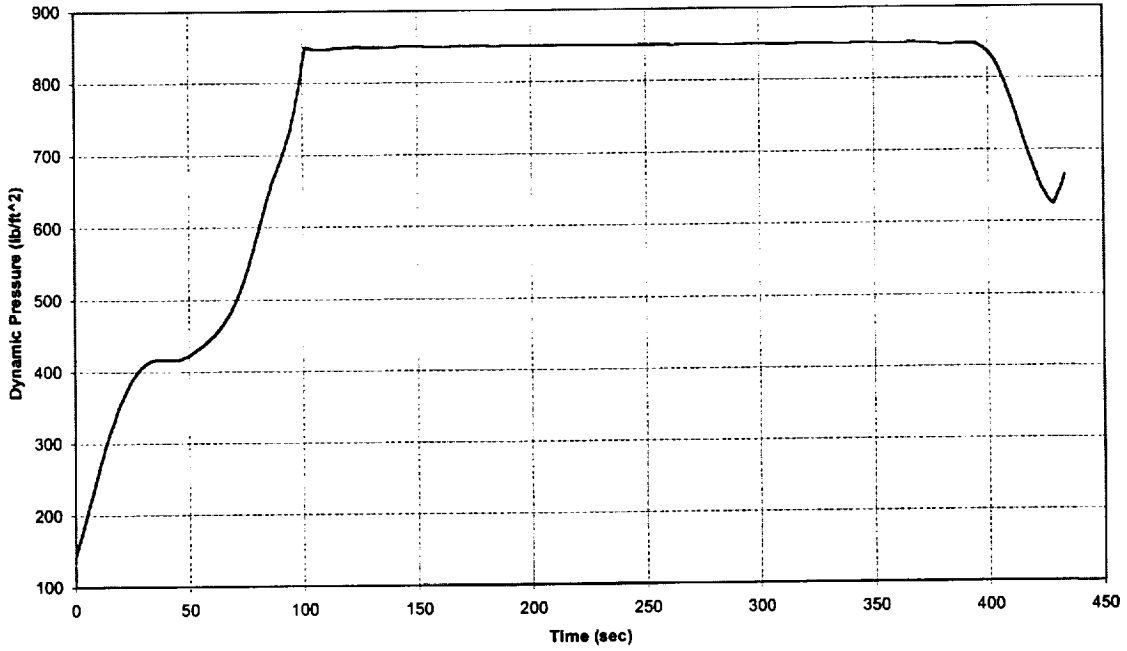
NASAE3CTLOX/ProC1
Mach vs Time



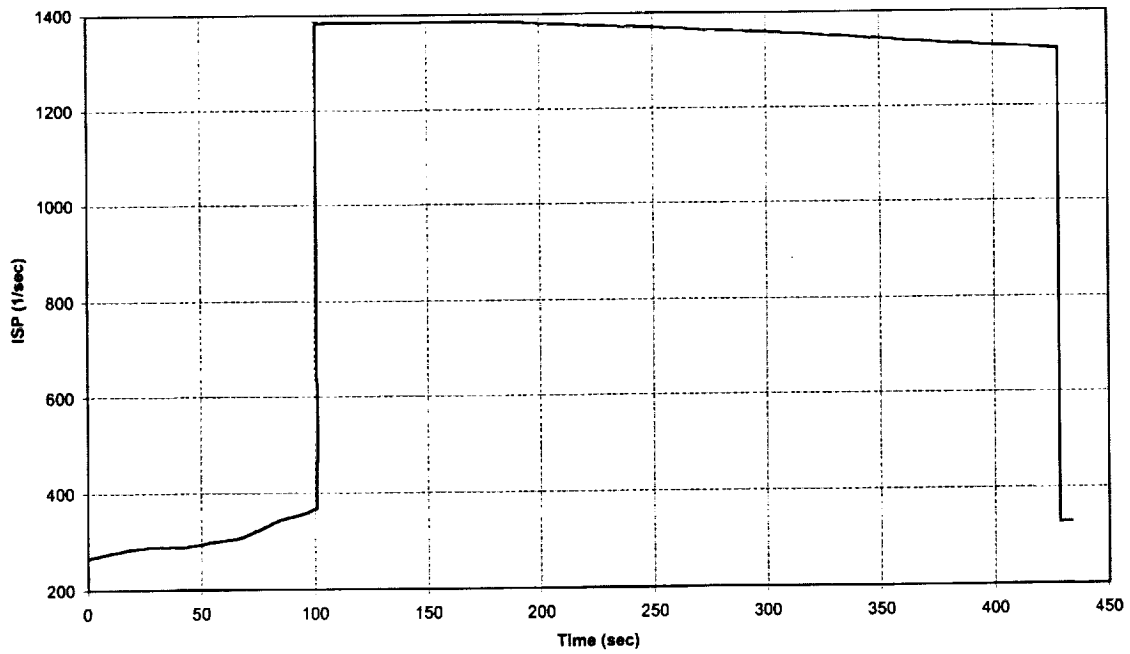
NASAE3CTLOX/ProC1
Weight vs Time



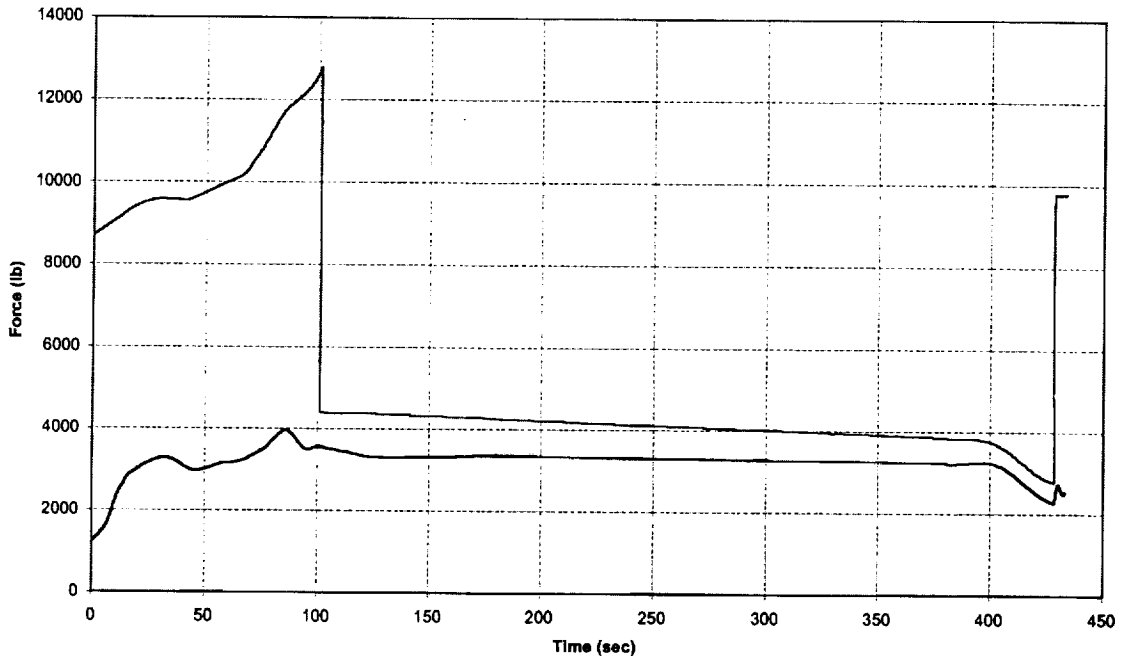
NASAE3CTLOX/ProC1
Dynamic Pressure vs Time



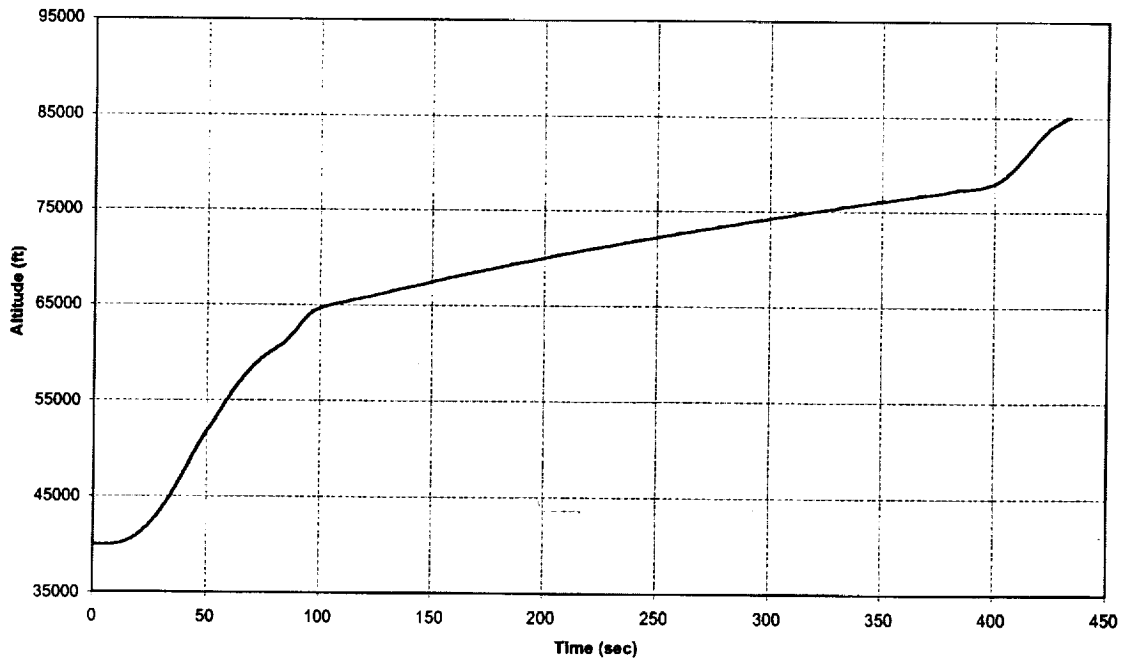
NASAE3CTLOX/ProC1
Specific Impulse vs Time



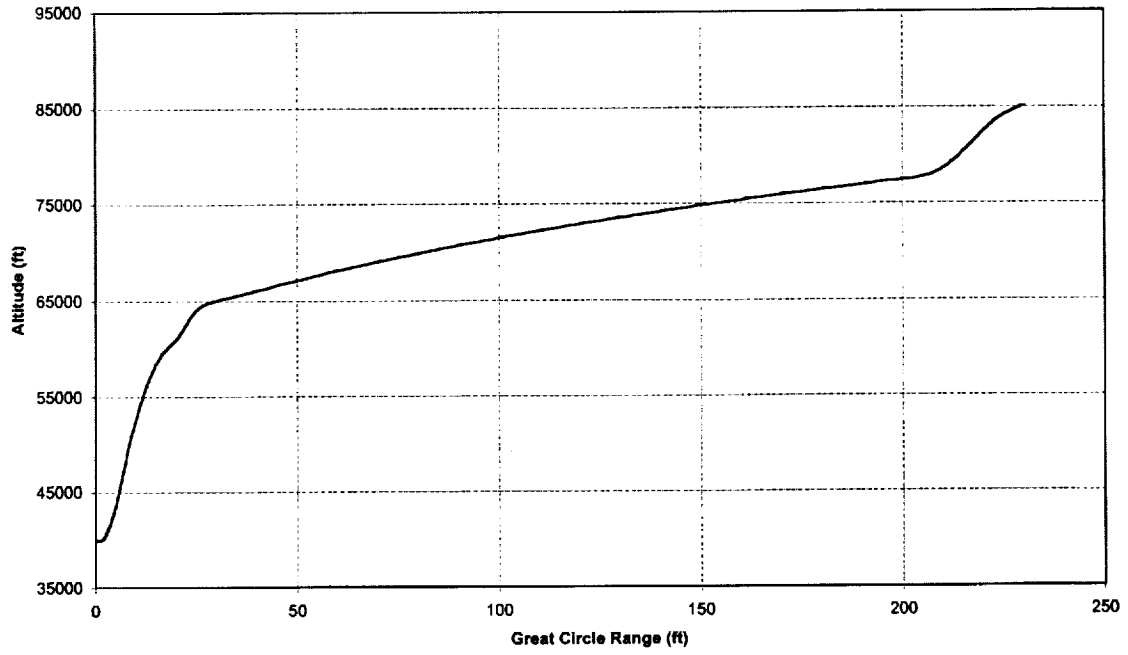
NASAE3CTLOX/ProC1
Thrust & Drag vs Time



NASAE3CTLOX/ProC1
Altitude vs Time

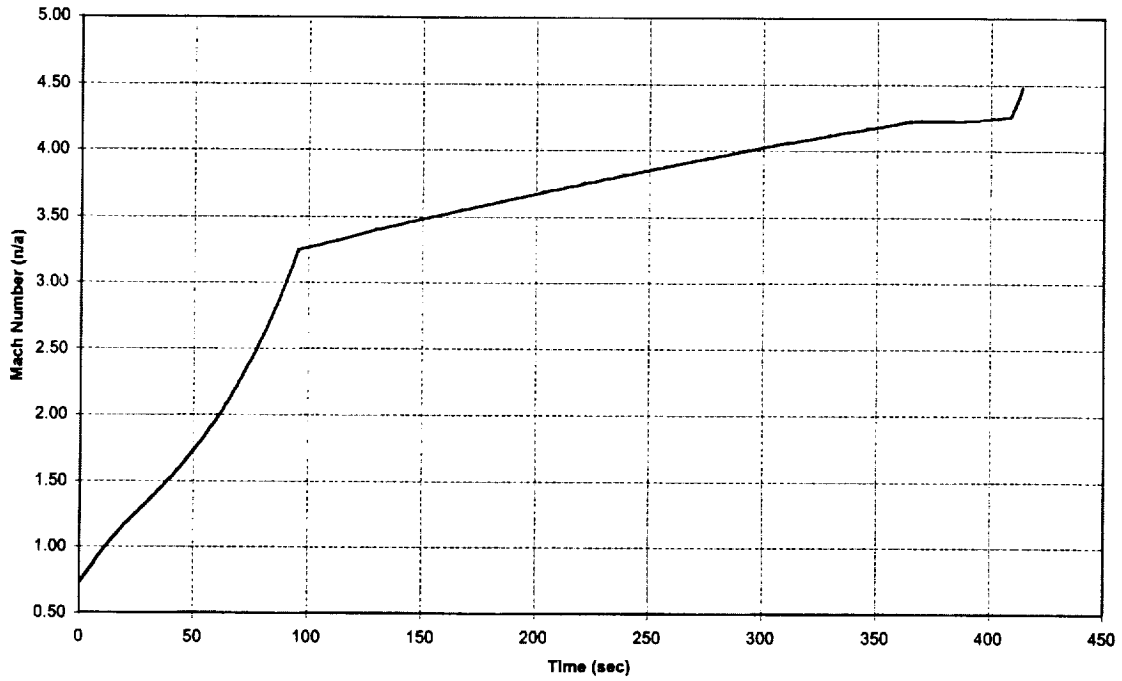


NASAE3CTLOX/ProC1
Altitude vs Great Circle Range

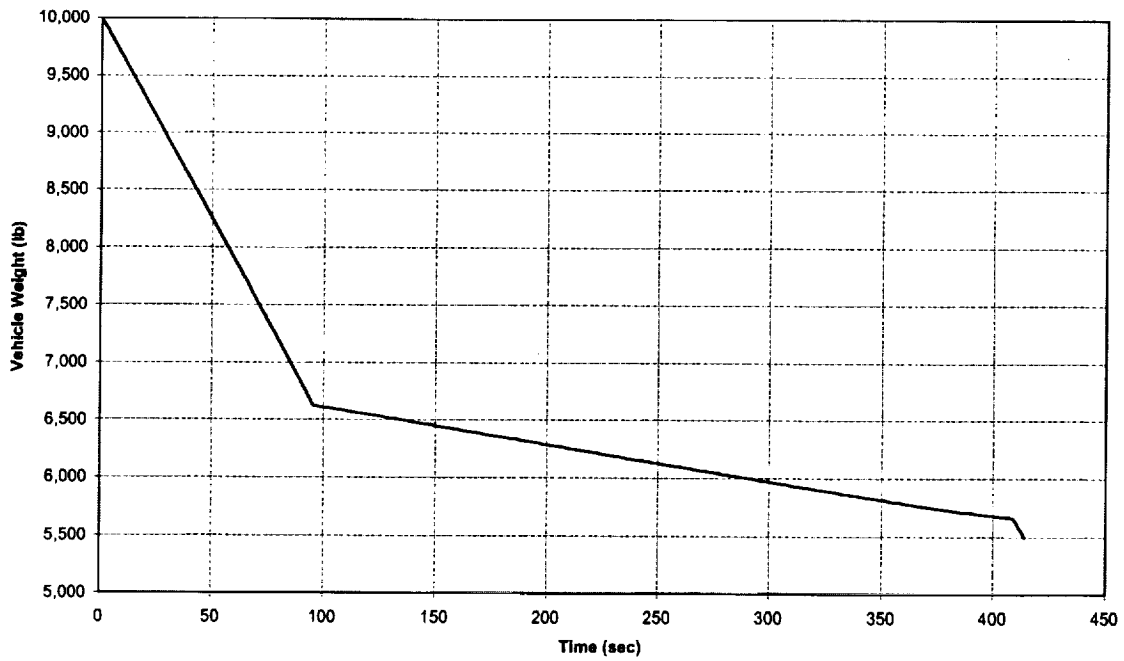


Appendix E8: NASA E3CTLOXJPC1

NASAE3CTLOX/JPC1
Mach vs Time

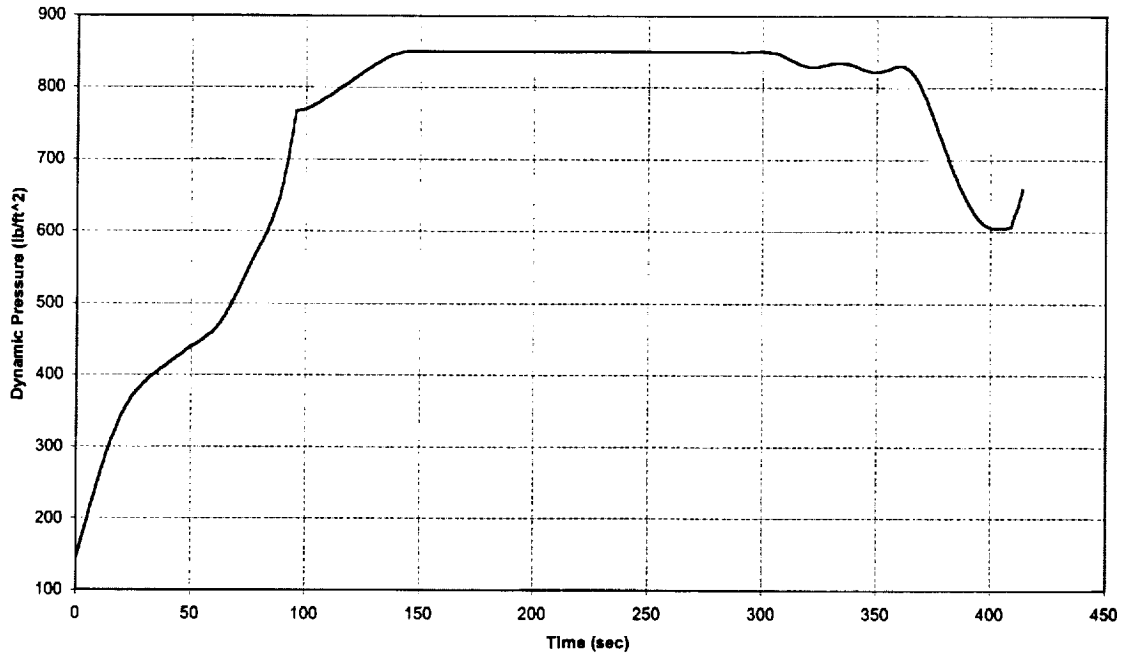


NASAE3CTLOX/JPC1
Weight vs Time

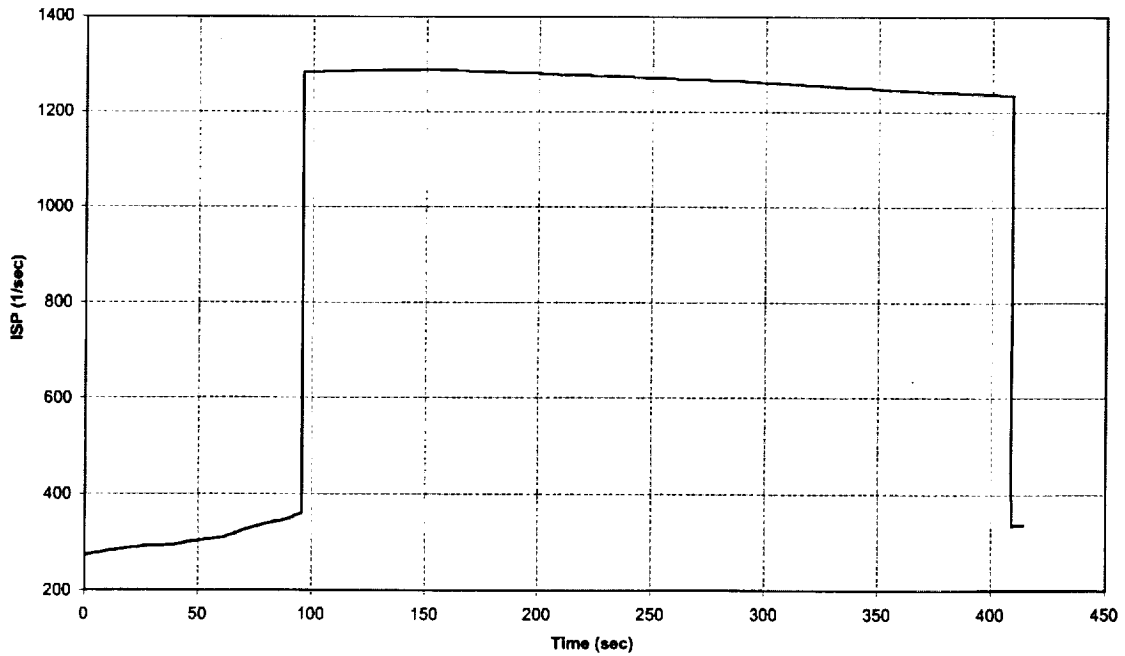


Appendix E8: NASA E3CTLOXJPC1

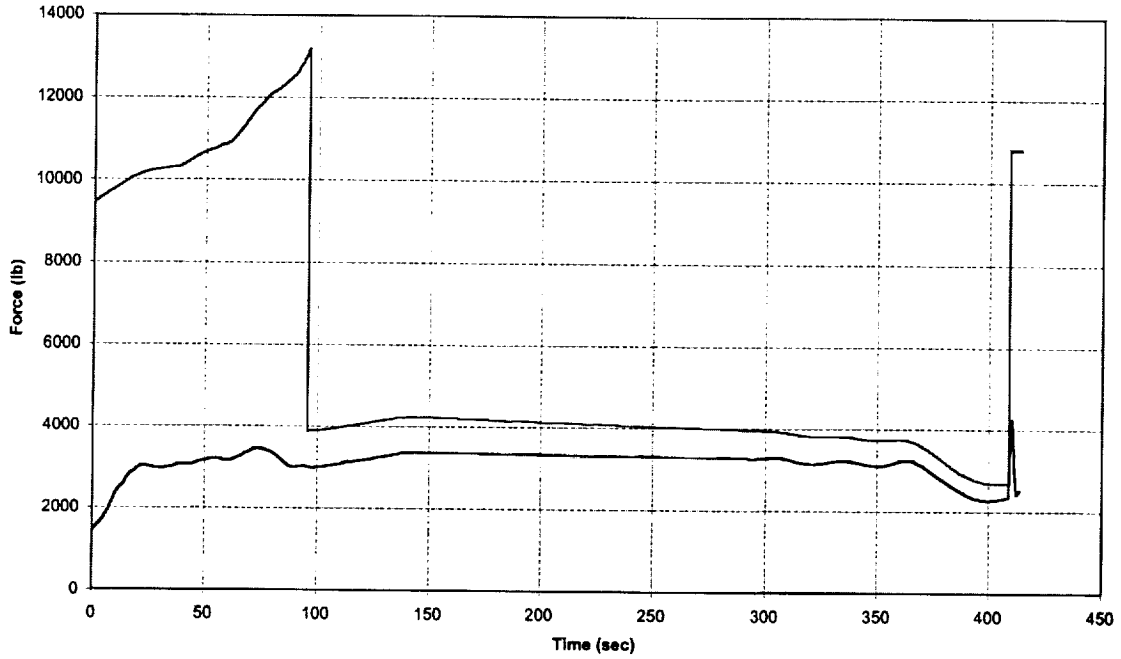
NASAE3CTLOX/JPC1
Dynamic Pressure vs Time



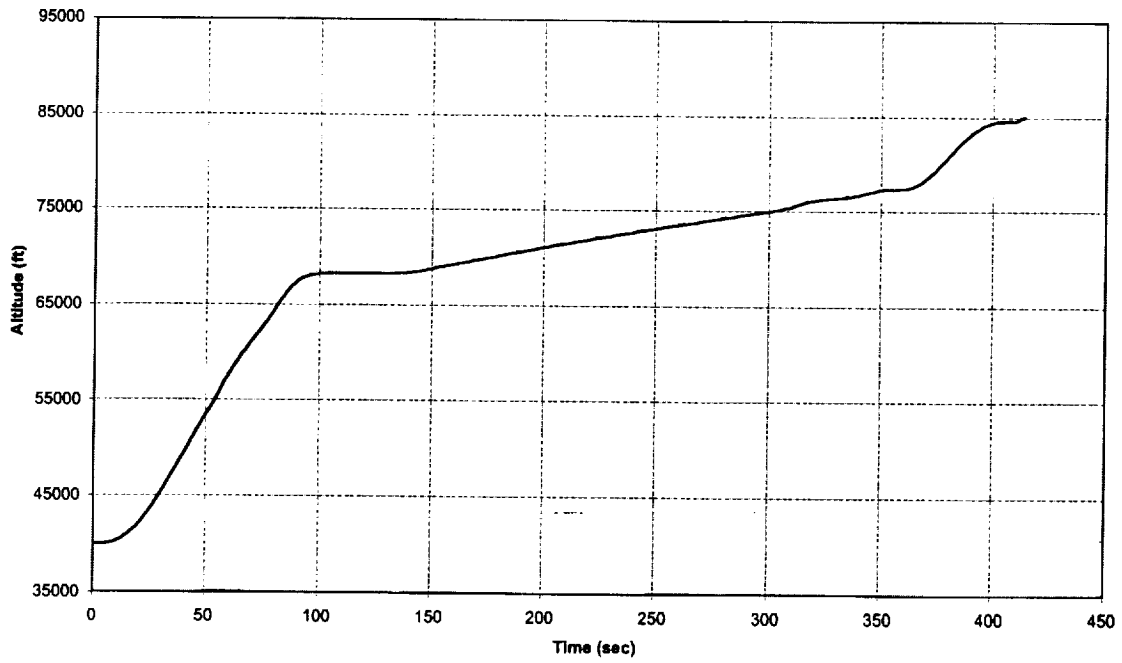
NASAE3CTLOX/JPC1
Specific Impulse vs Time



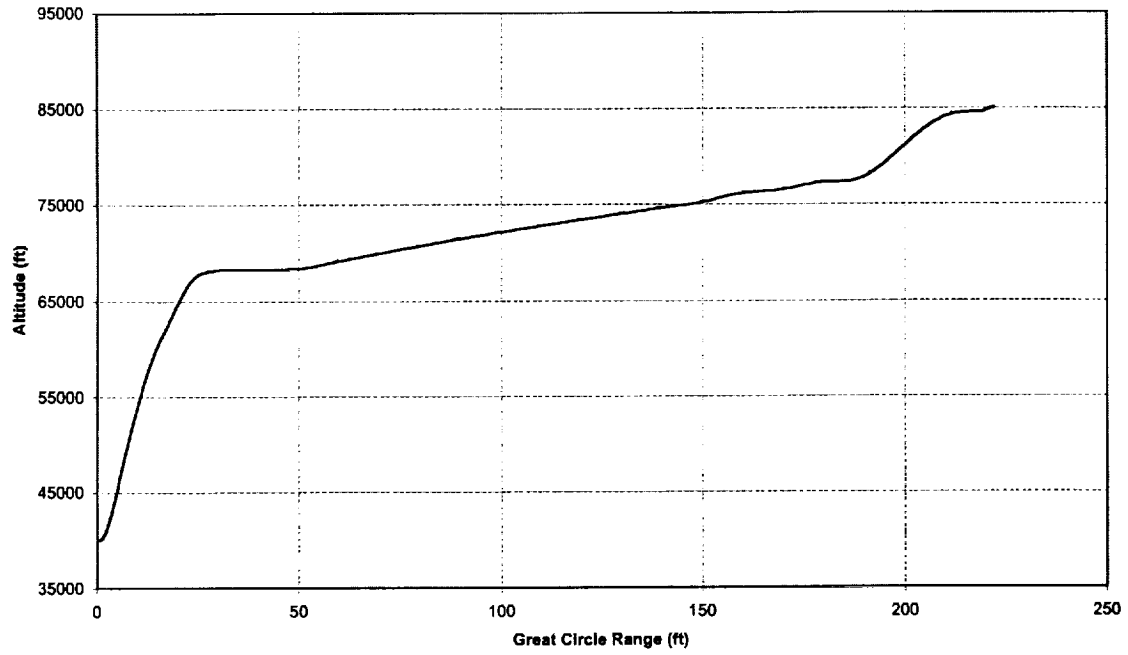
NASAE3CTLOX/JPC1
Thrust & Drag vs Time



NASAE3CTLOX/JPC1
Altitude vs Time

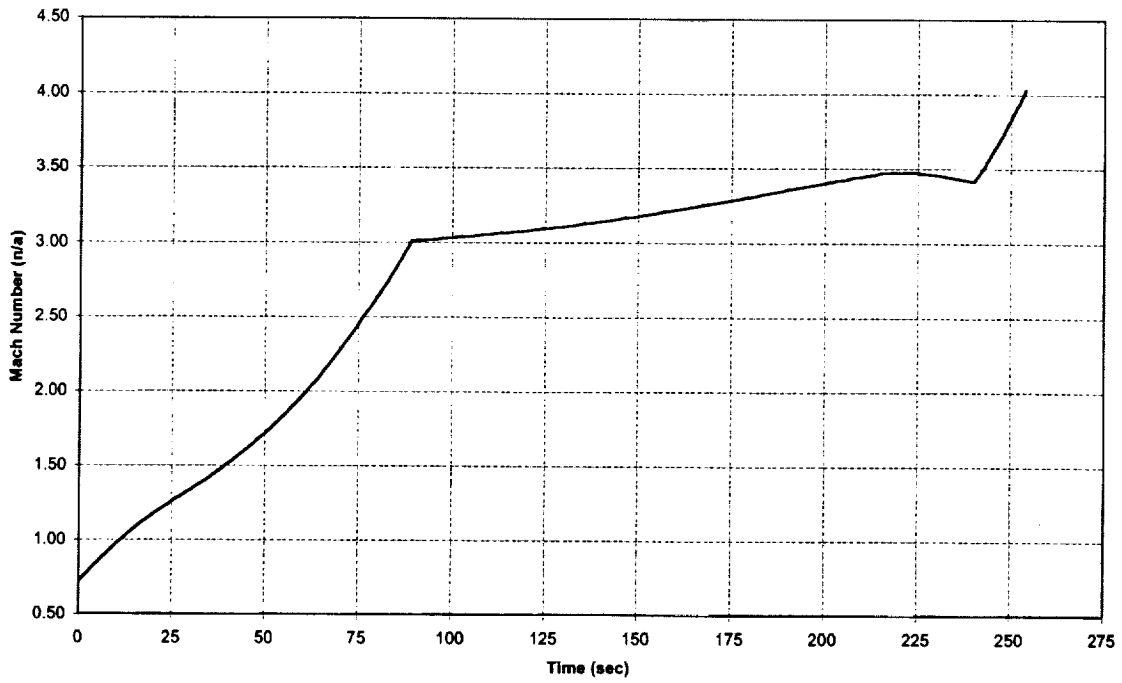


NASAE3CTLOX/JPC1
Altitude vs Great Circle Range

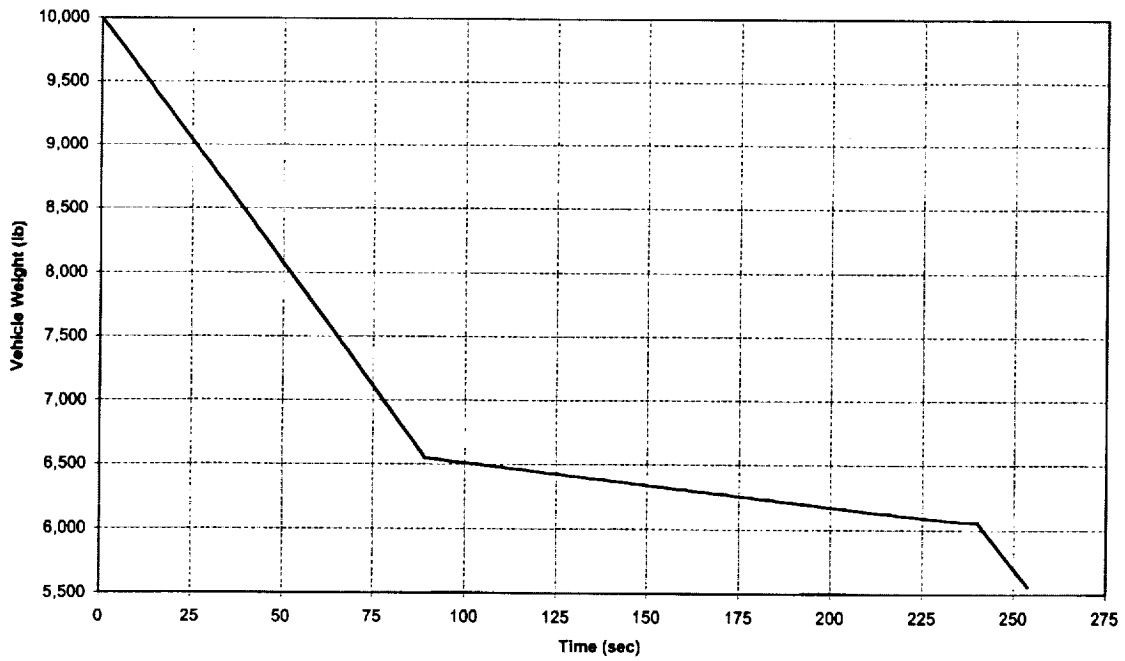


Appendix E9: NASA E3CTH2O2JPC1

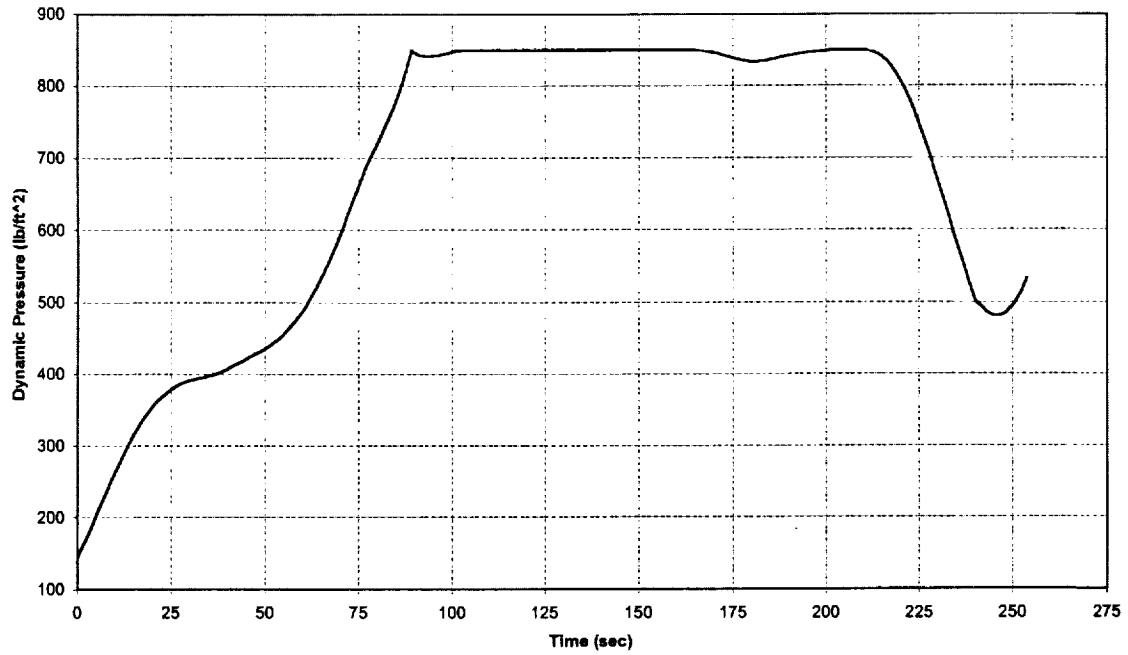
NASAE3CTH2O2/JPC1
Mach vs Time



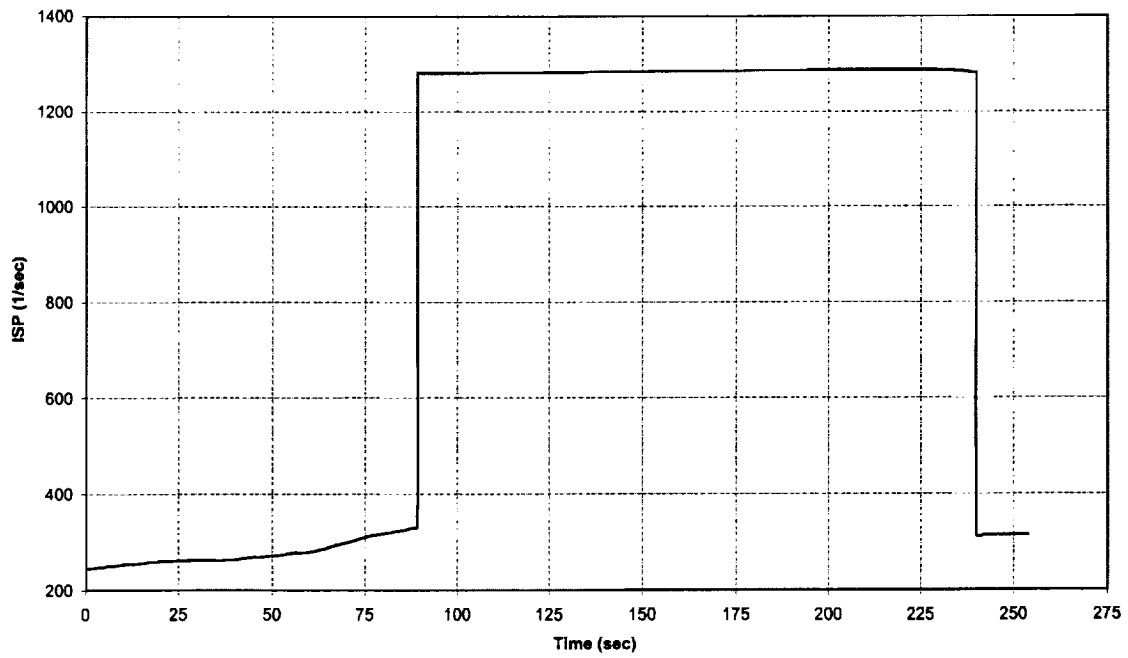
NASAE3CTH2O2/JPC1
Weight vs Time



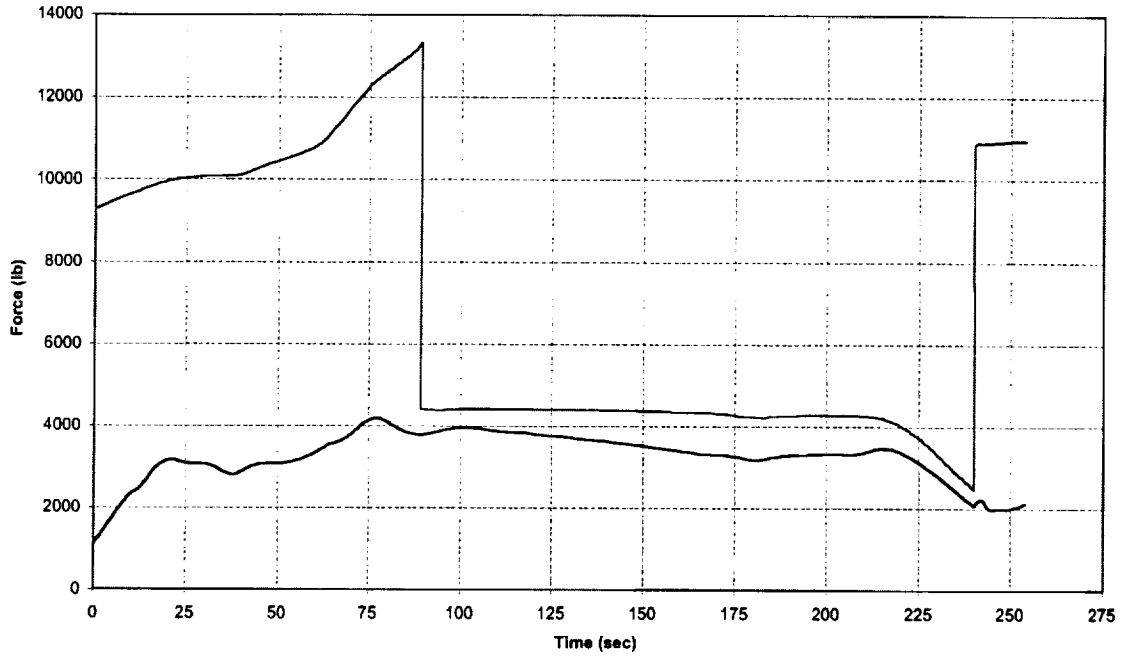
NASAE3CTH2O2/JPC1
Dynamic Pressure vs Time



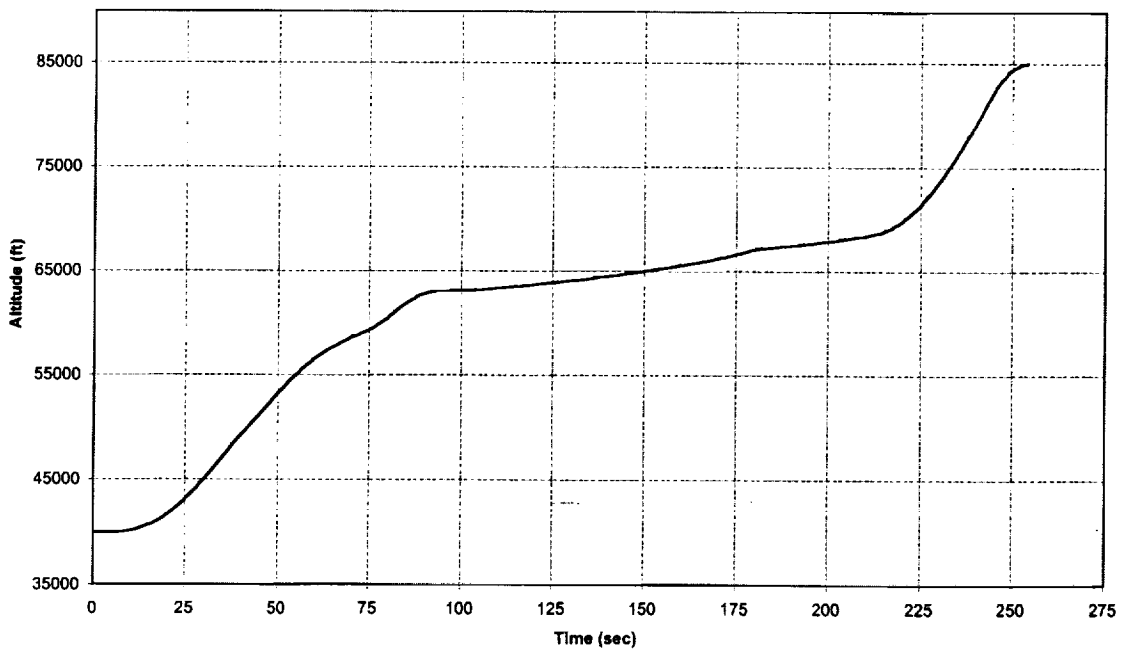
NASAE3CTH2O2/JPC1
Specific impulse vs Time



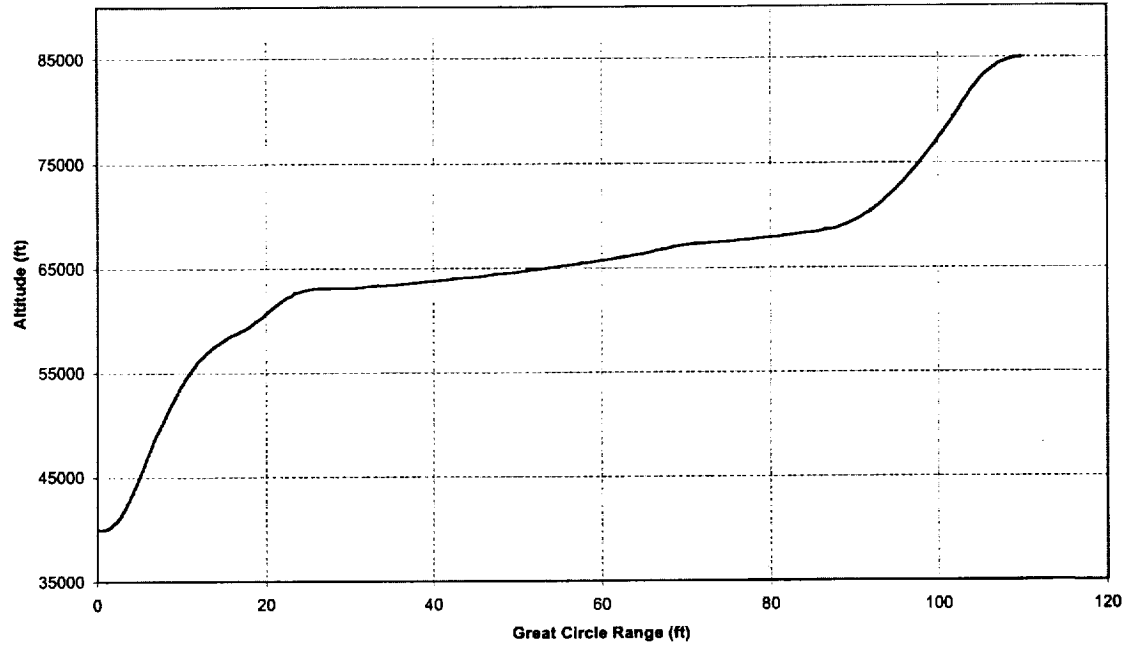
NASAE3CTH2O2/JPC1
Thrust & Drag vs Time



NASAE3CTH2O2/JPC1
Altitude vs Time



NASAE3CTH2O2/JPC1
Altitude vs Great Circle Range



Appendix F: FASTPASS Trajectory Results

F1:	H2O2/JP:	NASAF3CTH2O2/JP
F2:	LOX/JP:	NASAF3CTLOX/JP
F3:	LOX/Propane:	NASAF3CTLOX/Pr
F4:	H2O2/JP:	NASAF3GTH2O2/JP
F5:	LOX/JP:	NASAF3GTLOX/JP
F6:	LOX/Propane:	NASAF3GTLOX/Pr

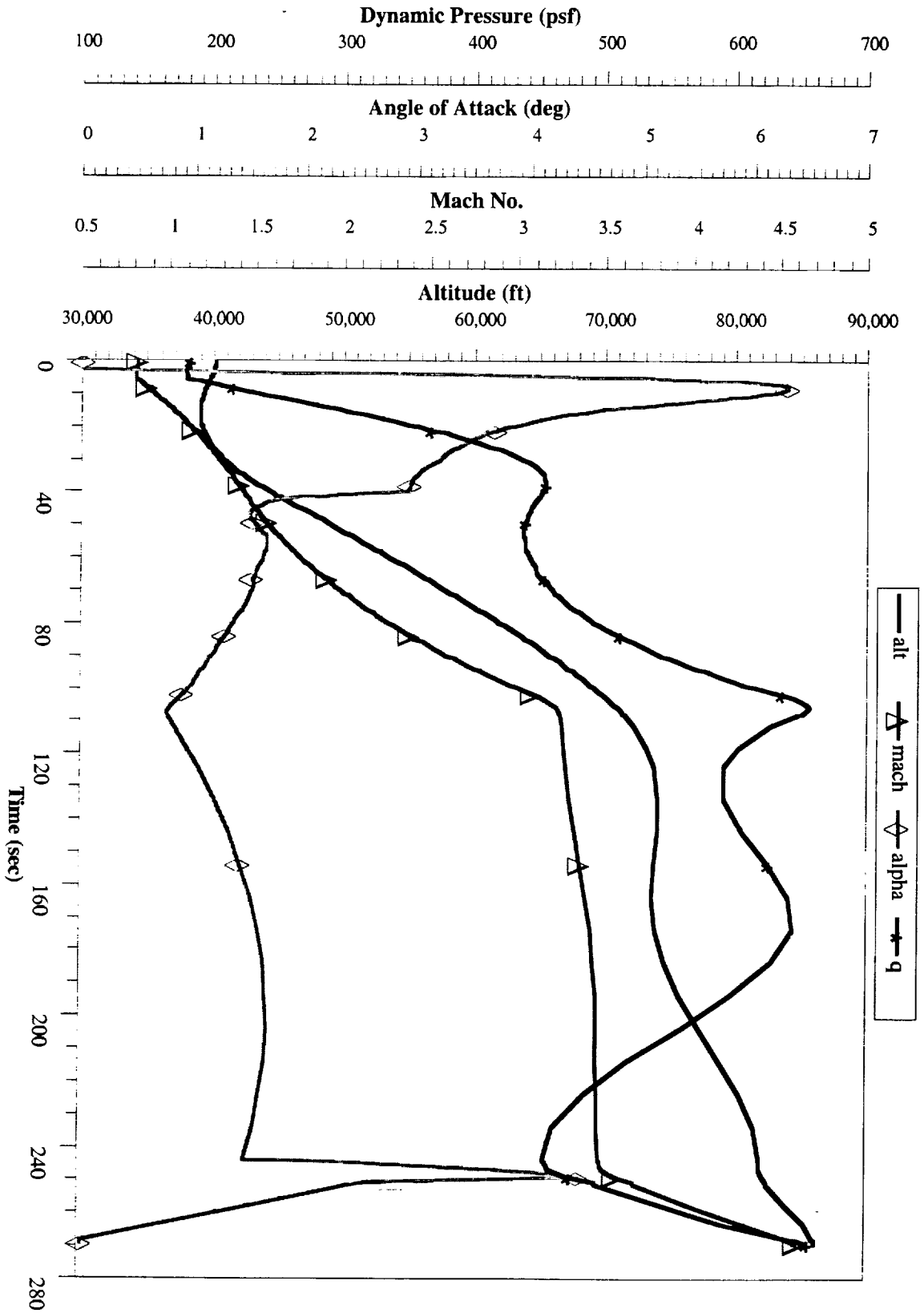
F1: NASA F1CTH2O2/JPA

Trajectory Constraints and Optimization Goals:

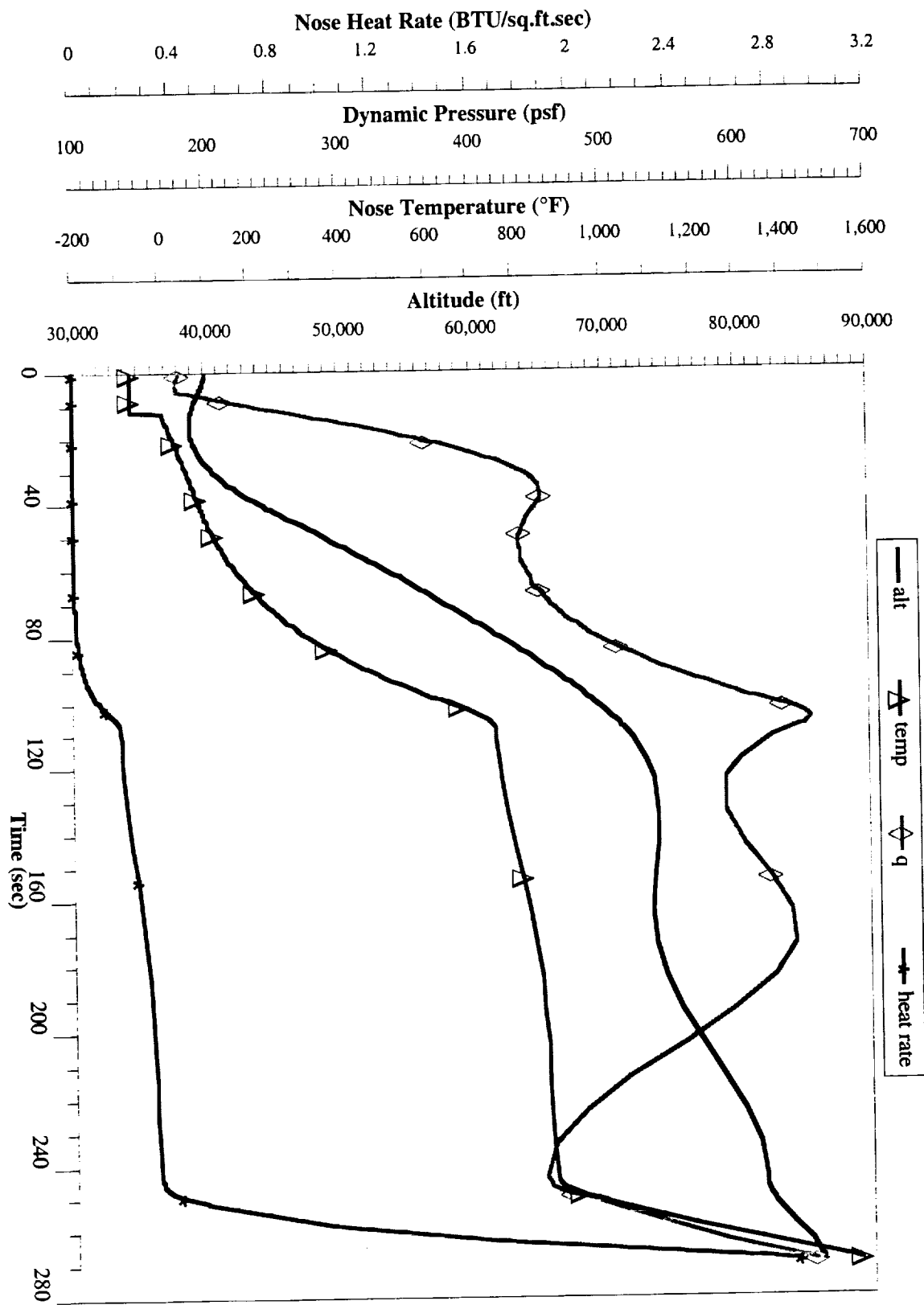
- Vehicle air-launched @ alt = 40,000 ft and Mach = 0.8
- Trajectory segmented into 5 engine operating modes
 - Air Augmented Rocket Mode $0.80 < M < 3.08$
 - AAR/Ramjet Transition Mode $3.08 < M < 3.24$
 - Ramjet Mode $3.24 < M < 3.47$
 - Ramjet Shutdown $3.47 < M < 3.67$
 - Rocket Startup $3.47 < M < 3.56$
 - Rocket Mode $3.56 < M < 4.60$
- Trajectory Goal: Maximize Ramjet Mode ΔV
- Angle of Attack limited to $-2^\circ < a < 12^\circ$ due to available data
- Maximum altitude limited to 120,000ft (to retain aerodynamic control effectiveness)
- Positive flight path angle required in final modes
- Time in rocket mode was fixed at 20 seconds

Trajectory Initial and Final conditions:

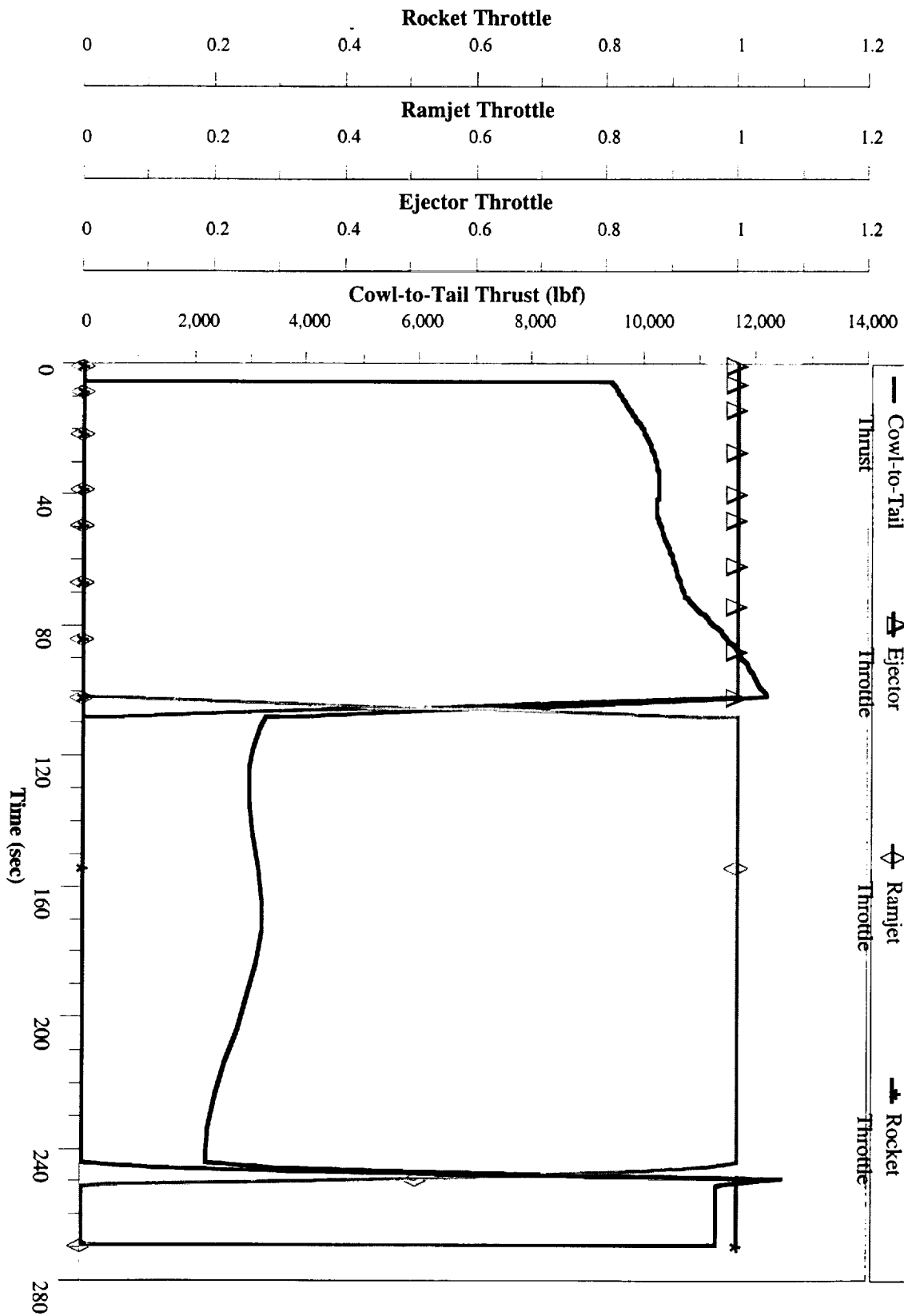
Vehicle Dry Mass	5,300 lbm
Added TPS Mass(estimate)	200 lbm
Oxidizer Mass	3817.2 lbm
Oxidizer Volume	44.75 cu.ft.
Fuel Mass	1133.6 lbm
Fuel Volume	22.95 cu.ft.
Gross Vehicle Mass	10450.8 lbm
Maximum Mach No.	4.6
Maximum Altitude	86,030.4 ft
Maximum Dynamic Pressure	654.4 psf
Maximum Nose Temp	1565.5 °F
Down Range at Rocket Termination	119.3 nm
Time in AAR Mode	96.4 sec
Time in AAR/Ram Transition	6.4 sec
Time in Ramjet Mode	134.7 sec
Time in Ramjet Shutdown	7.2 sec
Time in Rocket Startup	5.0 sec
Time in Rocket Mode	20.0 sec



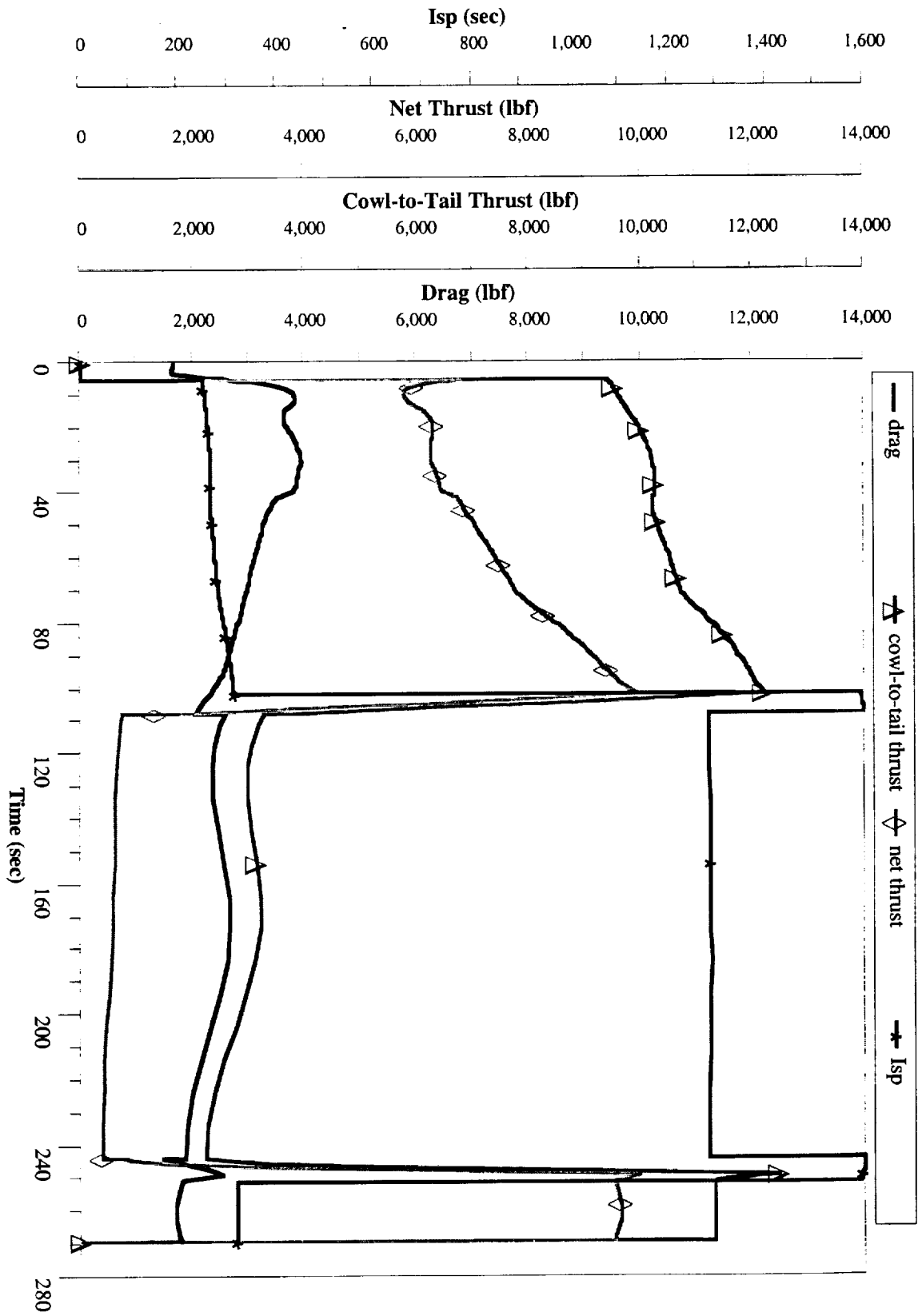
F1: NASA F1CTH2O2/JPA



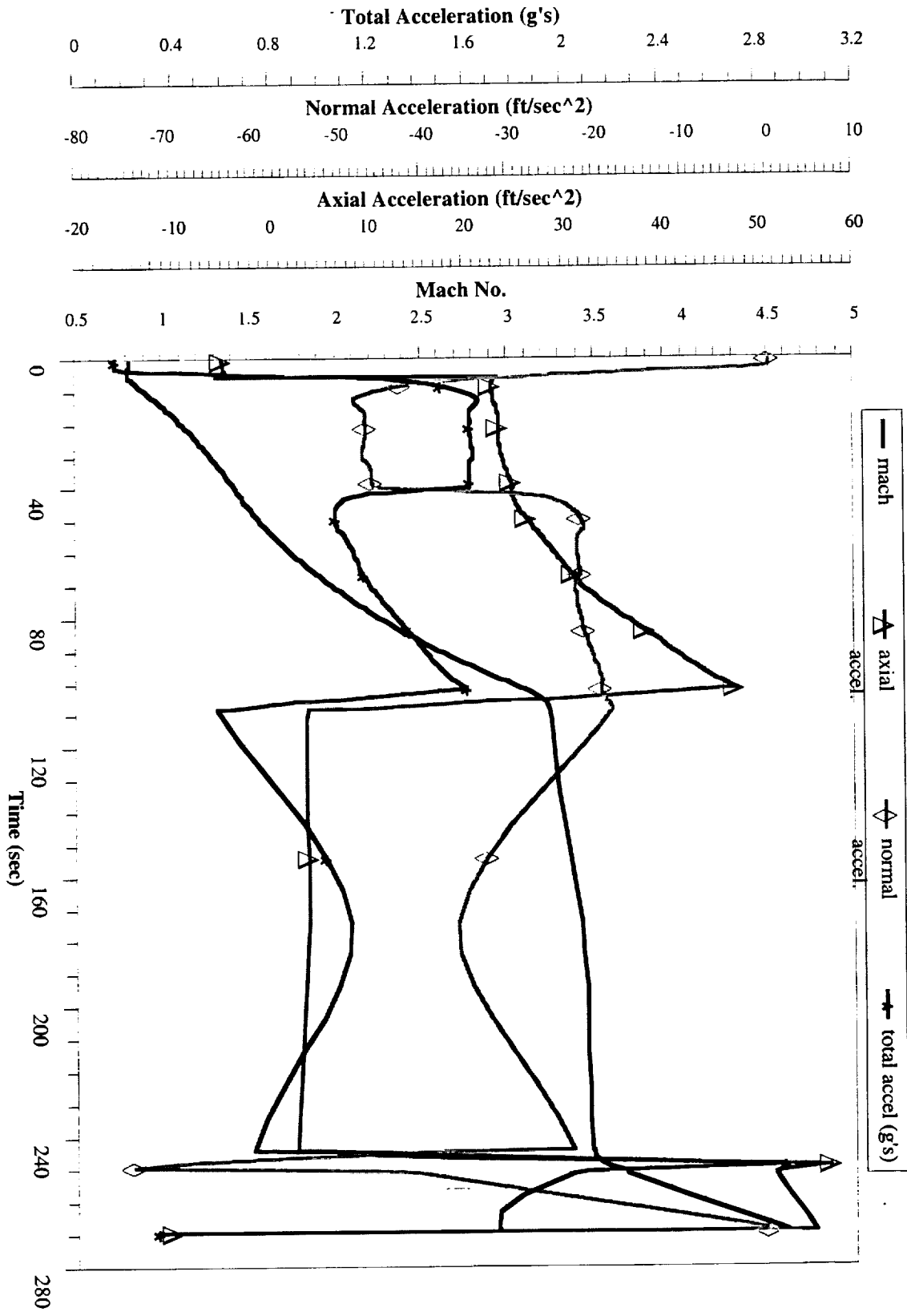
F1: NASA F1C TH202/JPA



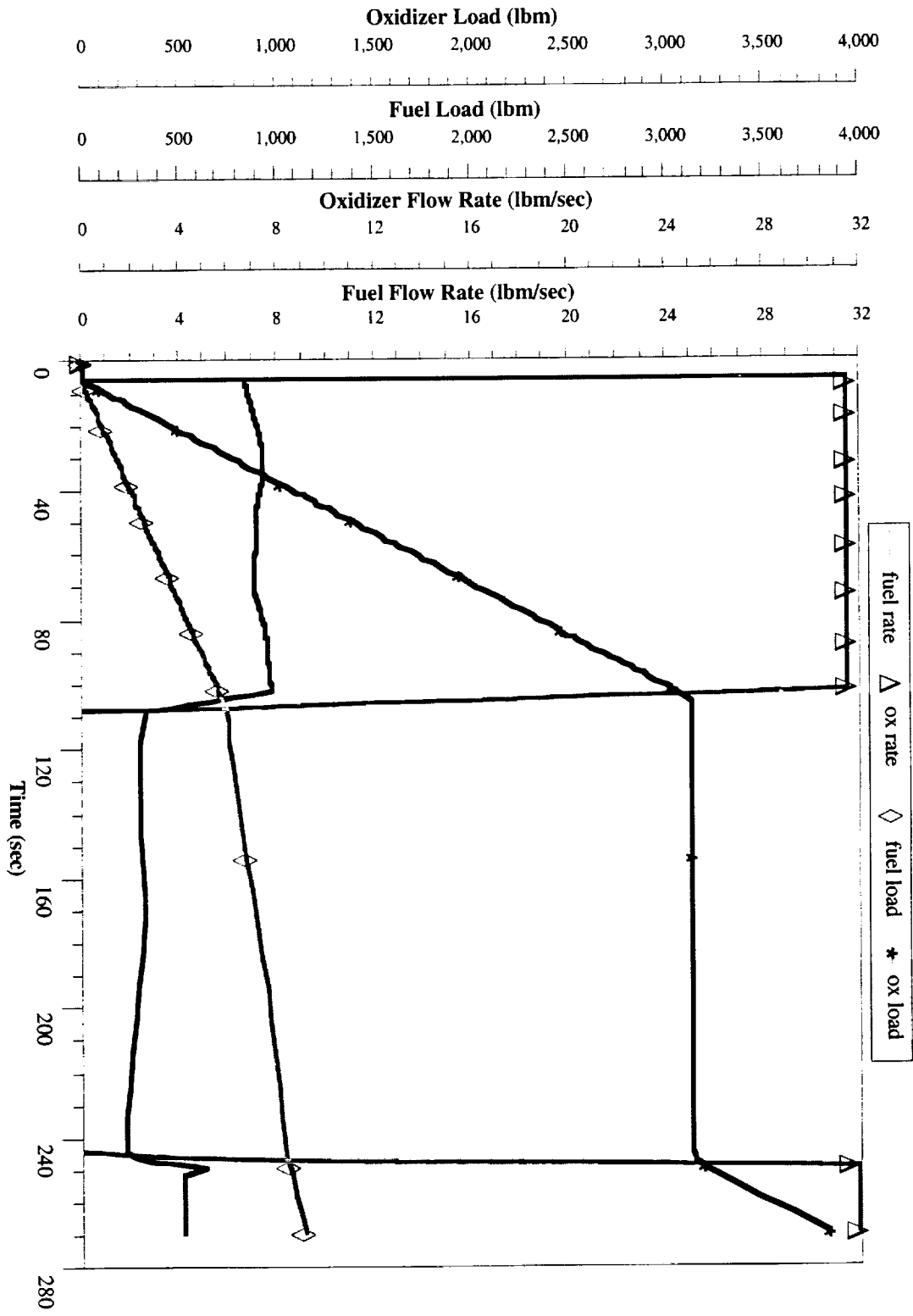
F1: NASA F1CTH2O2/JPA



F1: NASA F1CTH2O2/JPA



F1: NASA F1CTH202/JPA



F1: NASA F1CTH2O2/JPA

F2: NASA F2CTLOX/JPA

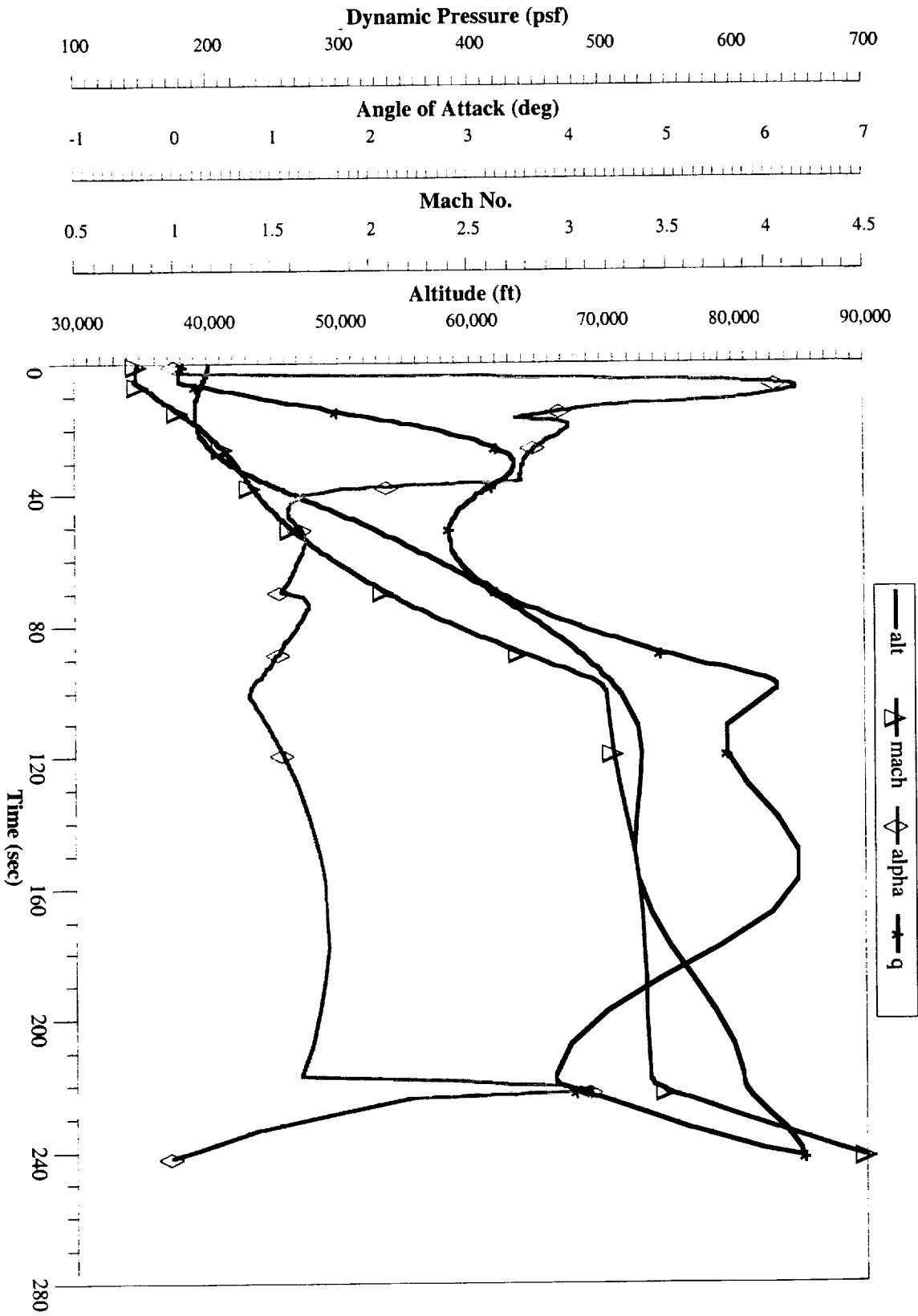
Trajectory Constraints and Optimization Goals:

- Vehicle air-launched @ alt = 40,000 ft and Mach = 0.8
- Trajectory segmented into 5 engine operating modes
 - Air Augmented Rocket Mode $0.80 < M < 3.03$
 - AAR/Ramjet Transition Mode $3.03 < M < 3.19$
 - Ramjet Mode $3.19 < M < 3.40$
 - Ramjet/ Shutdown $3.40 < M < 3.59$
 - Rocket Startup $3.40 < M < 3.49$
 - Rocket Mode $3.49 < M < 4.5$
- Trajectory Goal: Maximize Ramjet Mode ΔV
- Angle of Attack limited to $-2^\circ < \alpha < 12^\circ$ due to available data
- Maximum altitude limited to 120,000ft (to retain aerodynamic control effectiveness)
- Positive flight path angle required in final modes
- Time in rocket mode was fixed at 20 seconds

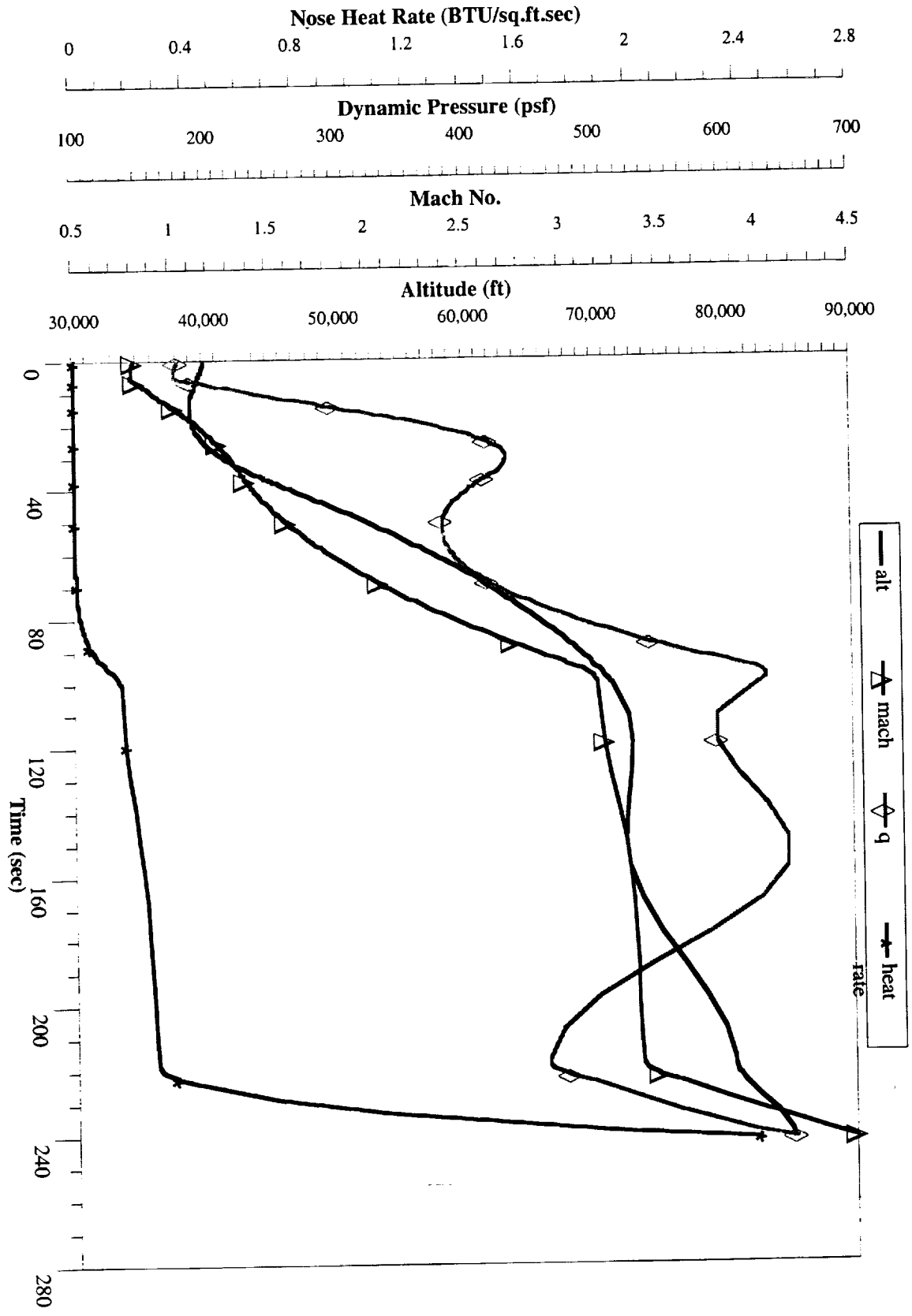
Trajectory Initial and Final conditions:

Vehicle Dry Mass	5,300.0 lbm
Added TPS Mass(estimate)	200.0 lbm
Oxidizer Mass	2,706.4 lbm
Oxidizer Volume	39.48 cu.ft
Fuel Mass	1,527.1
Fuel Volume	30.91 cu.ft.
Gross Vehicle Mass	9,733.5 lbm

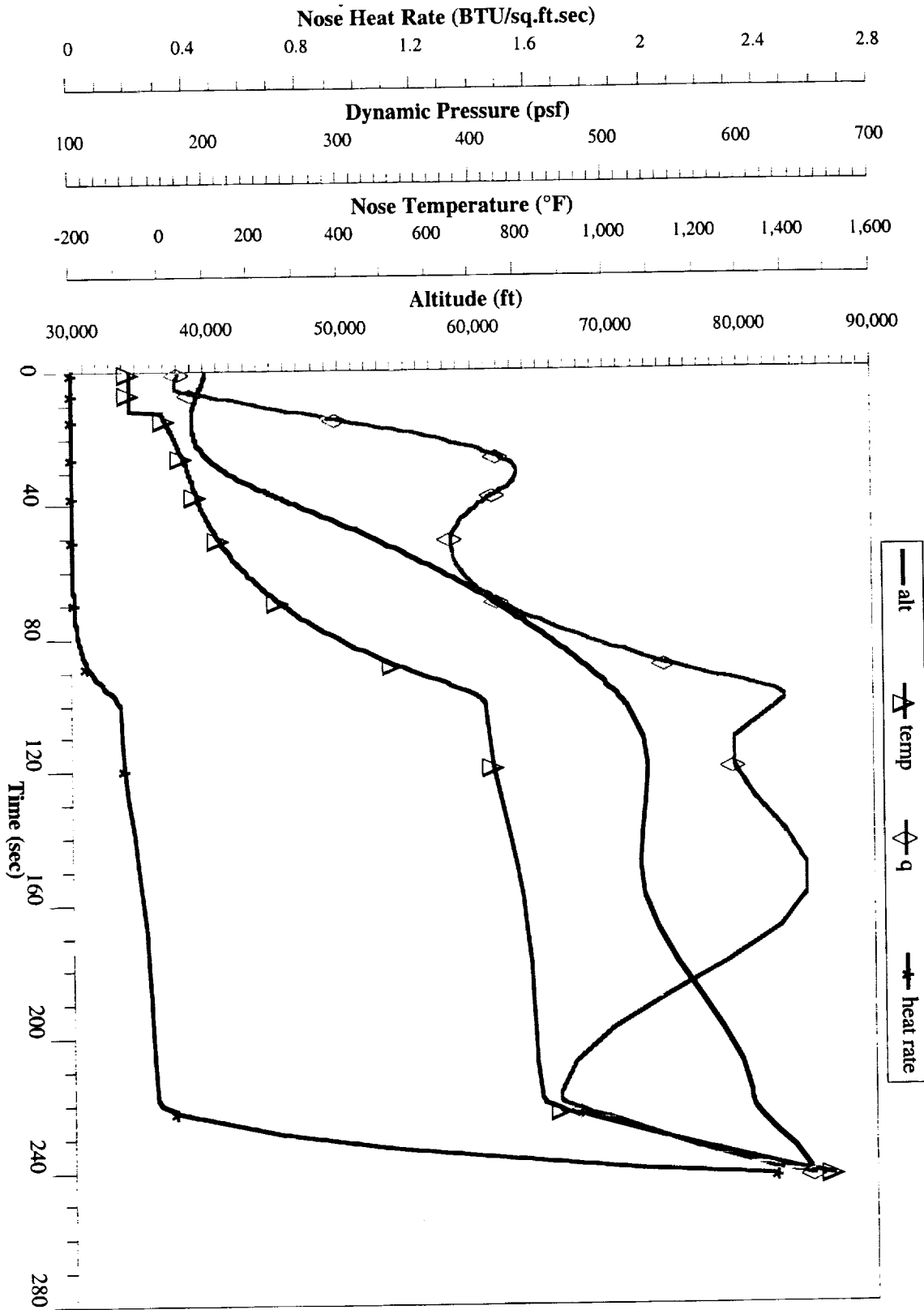
Maximum Mach No.	4.50
Maximum Altitude	85,124.2 ft
Maximum Dynamic Pressure	651.5 psf
Maximum Nose Temp	1498.6 °F
Down Range at Rocket Termination	104.6 nm
Time in AAR Mode	88.9 sec
Time in AAR/Ram Transition	6.3 sec
Time in Ramjet Mode	116.4 sec
Time in Ramjet Shutdown	7.1 sec
Time in Rocket Startup	5.0 sec
Time in Rocket Mode	20.0 sec



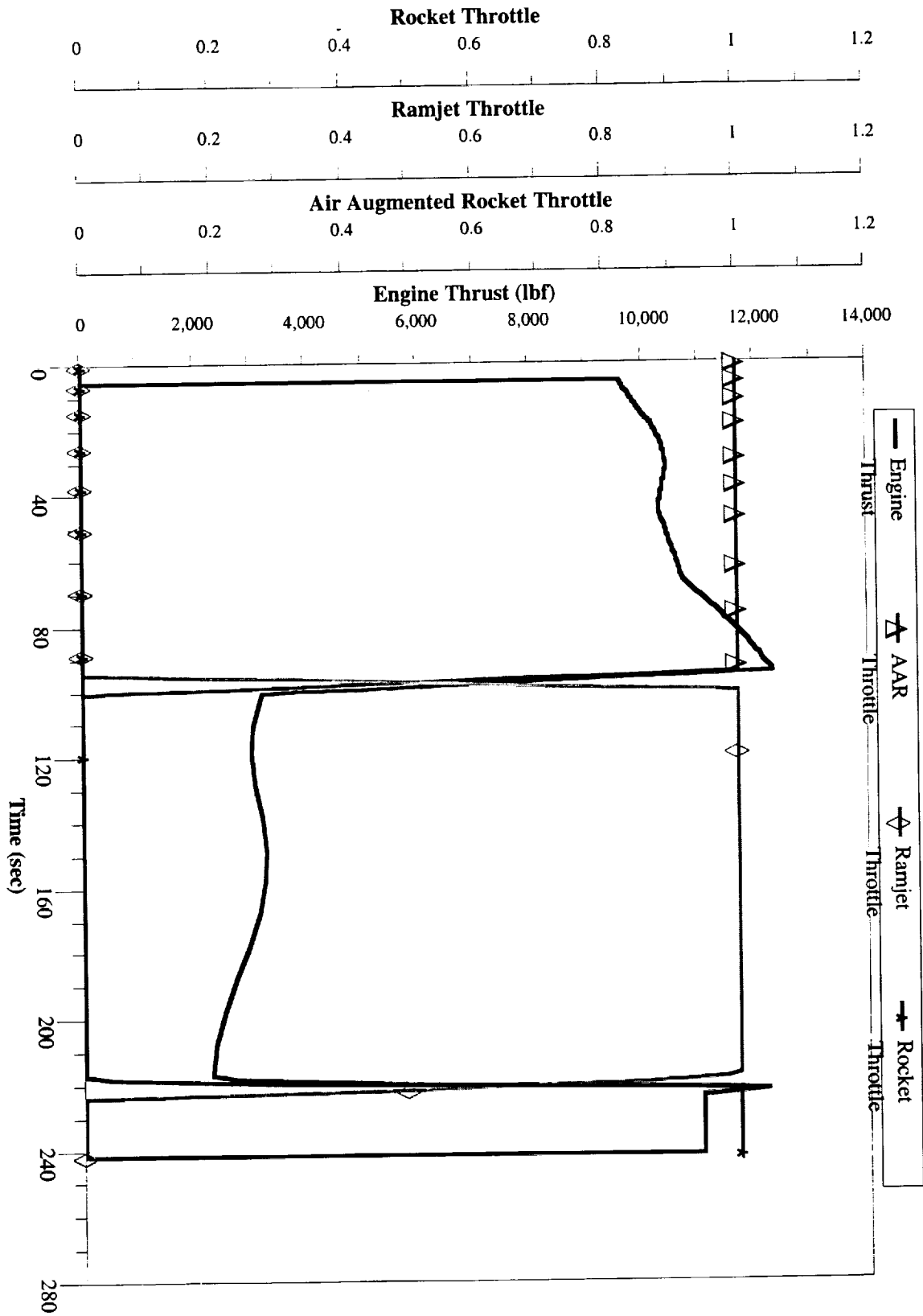
F2: NASA F2CTLOX/JPA



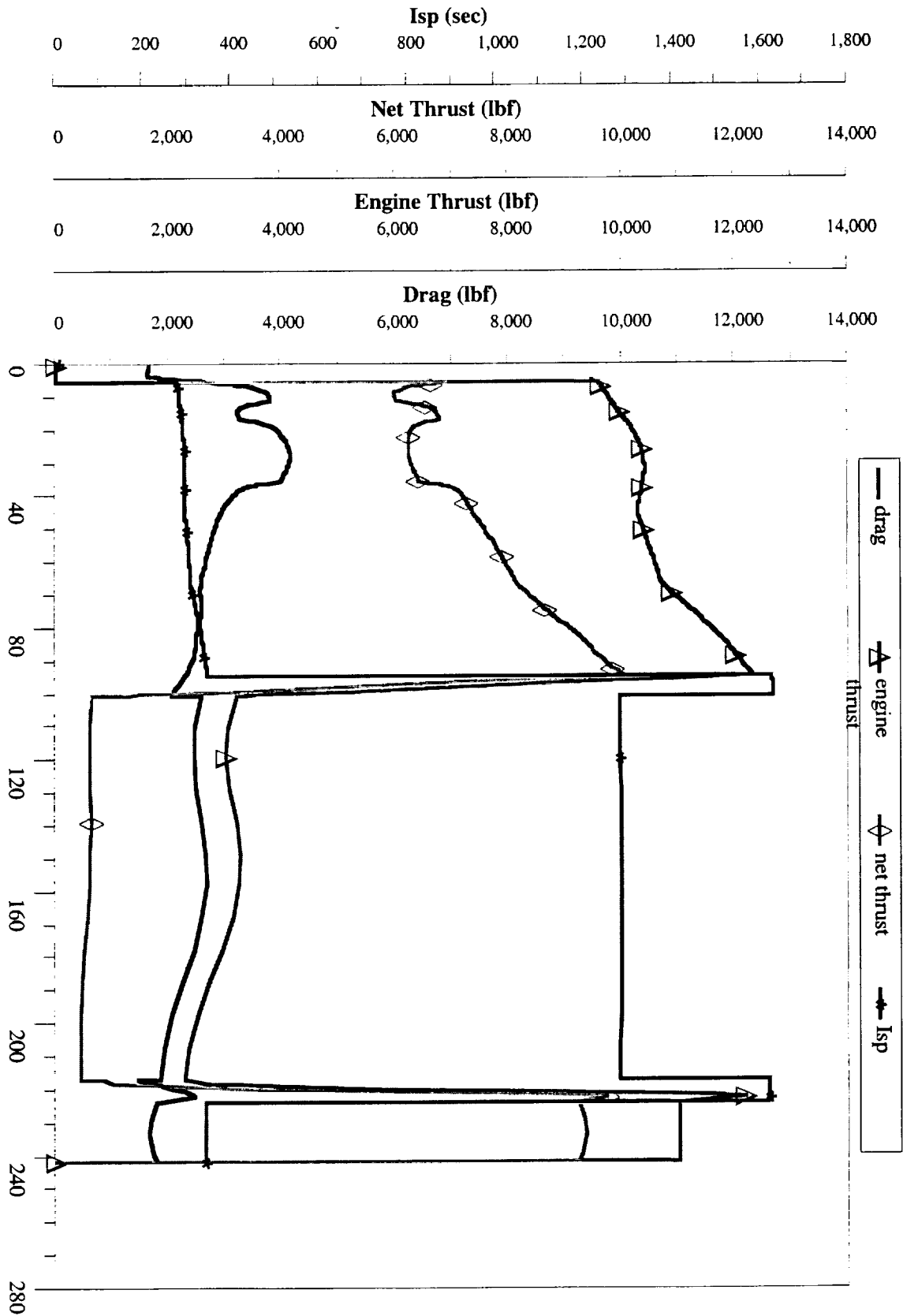
F2: NASA F2CTLOX/JPA



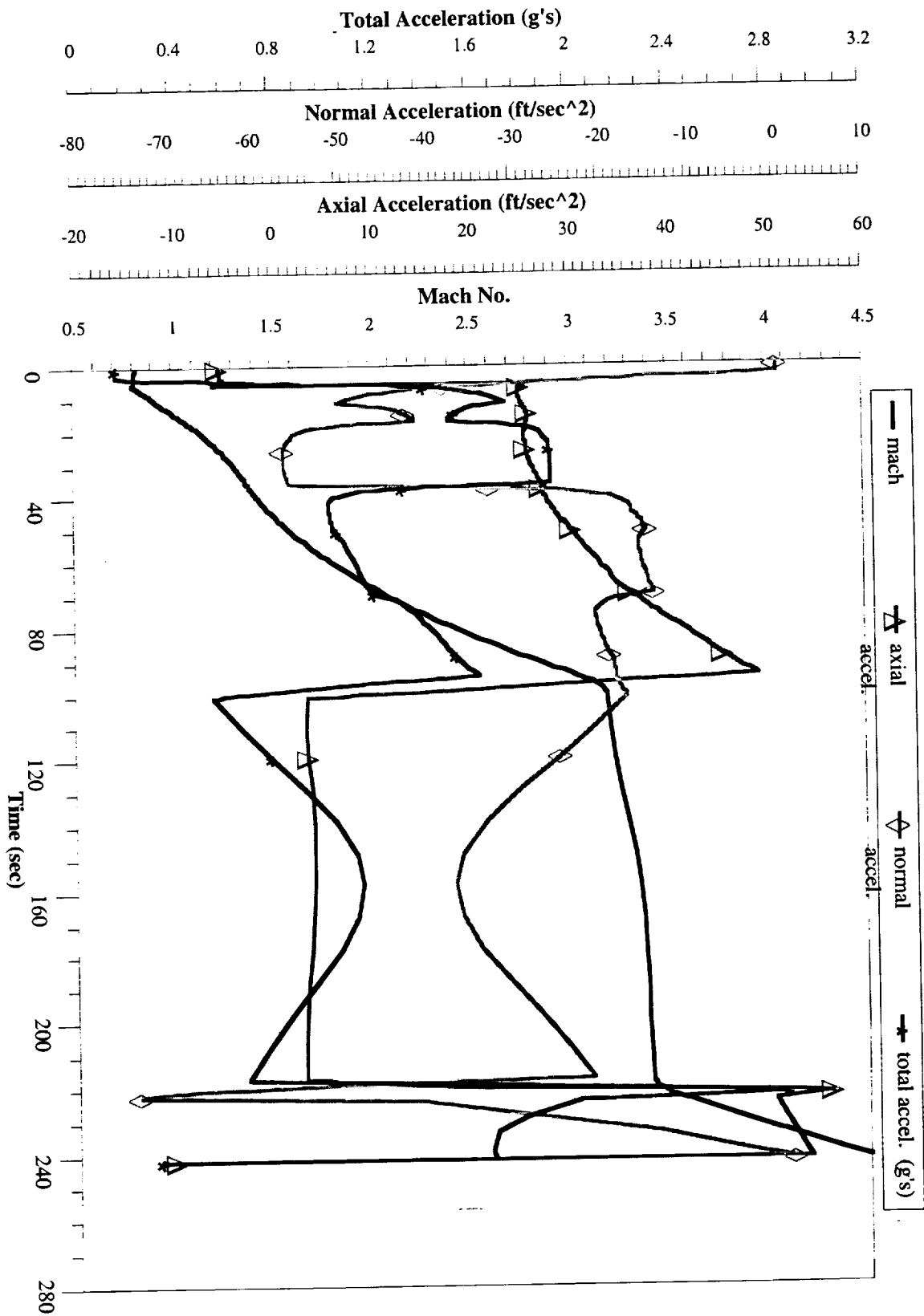
F2: NASA F2CTLOX/JPA



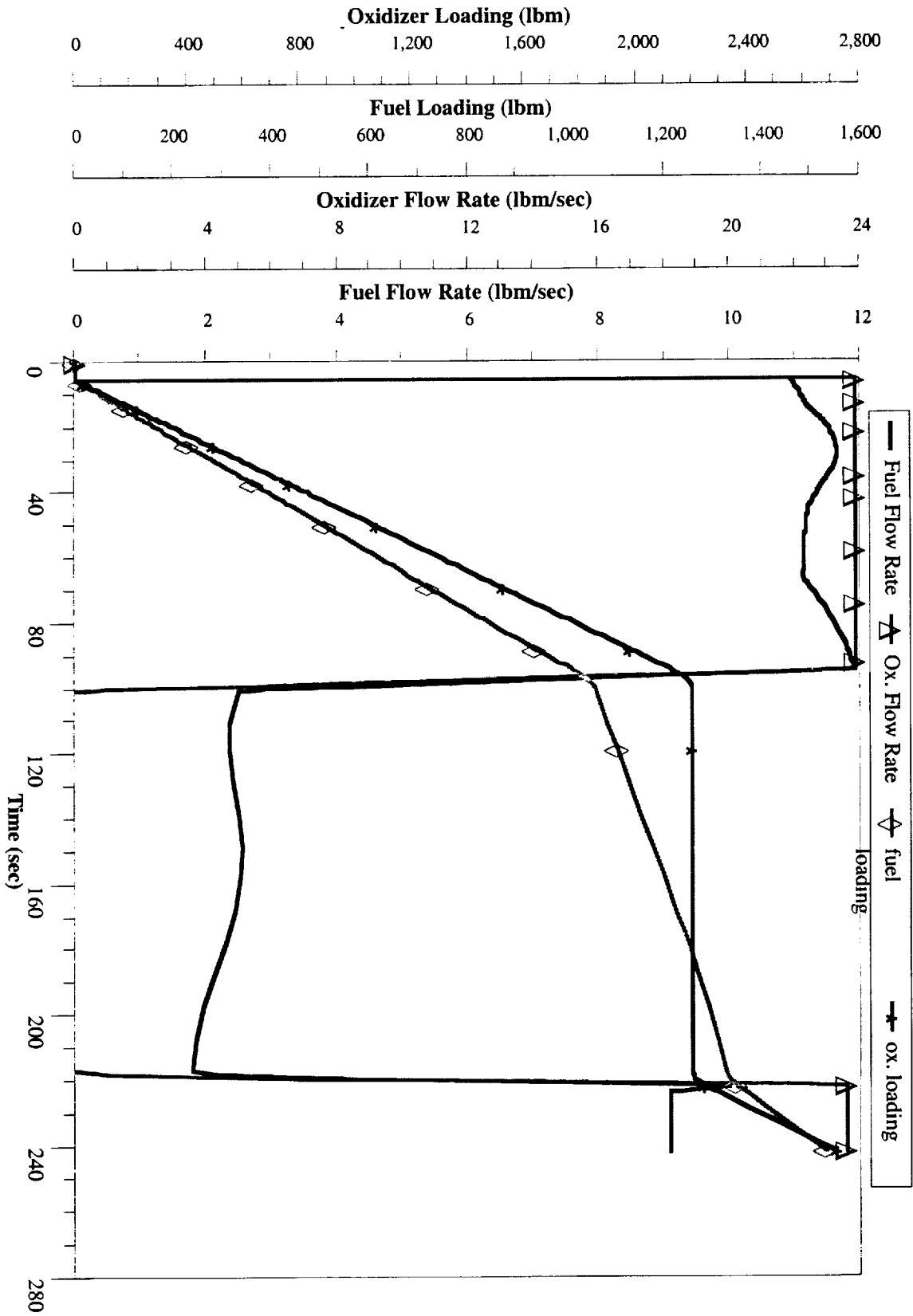
F2: NASA F2CTLOX/JPA



F2: NASA F2CTLOX/JPA



F2: NASA F2CTLOX/JPA



F2: NASA F2CTLOX/JPA

F3: NASA F3CTLOX/PROPANE A

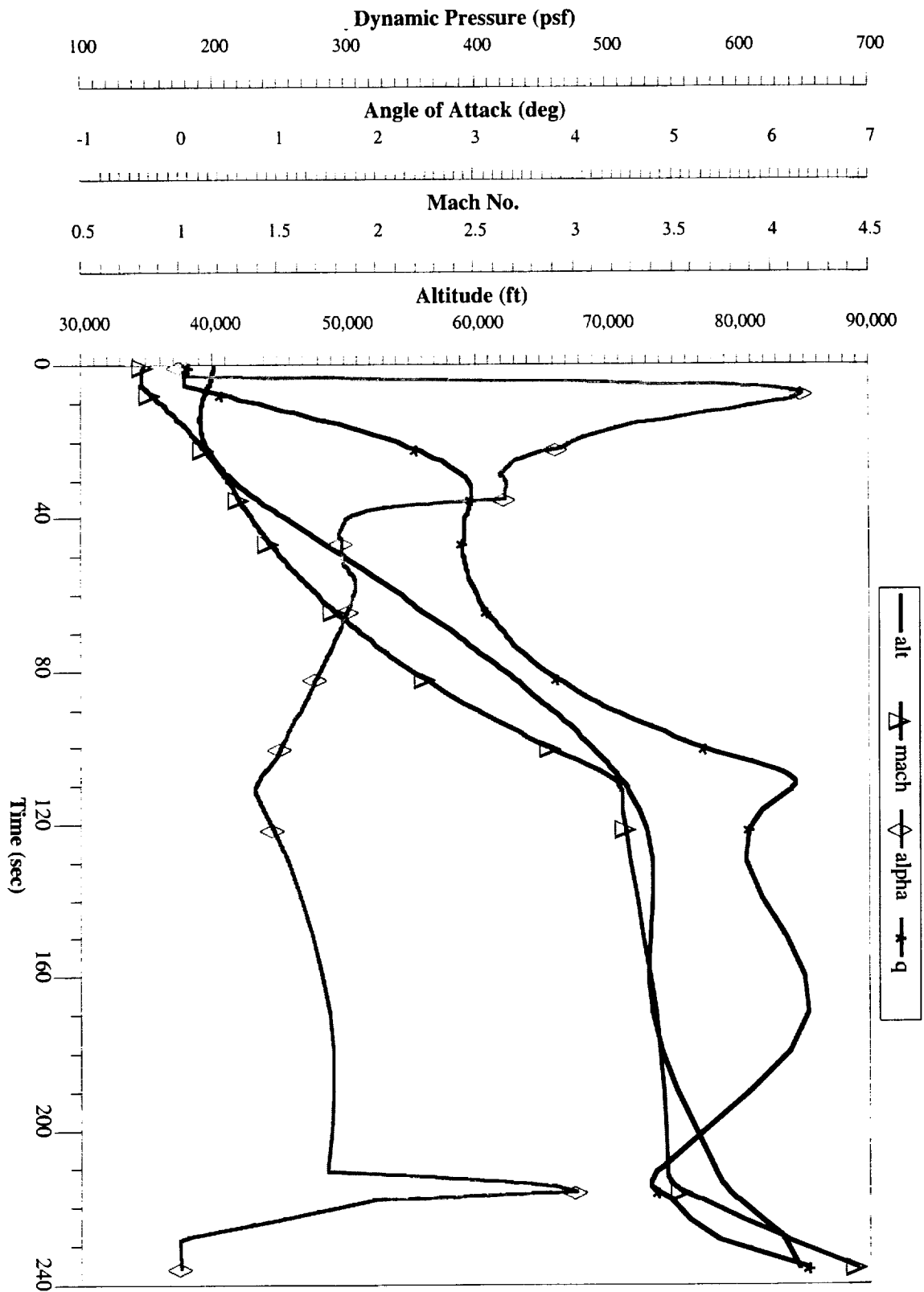
Trajectory Constraints and Optimization Goals:

- Vehicle air-launched @ alt = 40,000 ft and Mach = 0.8
- Trajectory segmented into 5 engine operating modes
 - Air Augmented Rocket Mode $0.80 < M < 3.08$
 - AAR/Ramjet Transition Mode $3.08 < M < 3.23$
 - Ramjet Mode $3.23 < M < 3.46$
 - Ramjet Shutdown $3.46 < M < 3.63$
 - Rocket Startup $3.46 < M < 3.54$
 - Rocket Mode $3.54 < M < 4.42$
- Trajectory Goal: Maximize Ramjet Mode ΔV
- Angle of Attack limited to $-2^\circ < \alpha < 12^\circ$ due to available data
- Maximum altitude limited to 120,000ft (to retain aerodynamic control effectiveness)
- Positive flight path angle required in final modes
- Time in rocket mode was fixed at 20 seconds

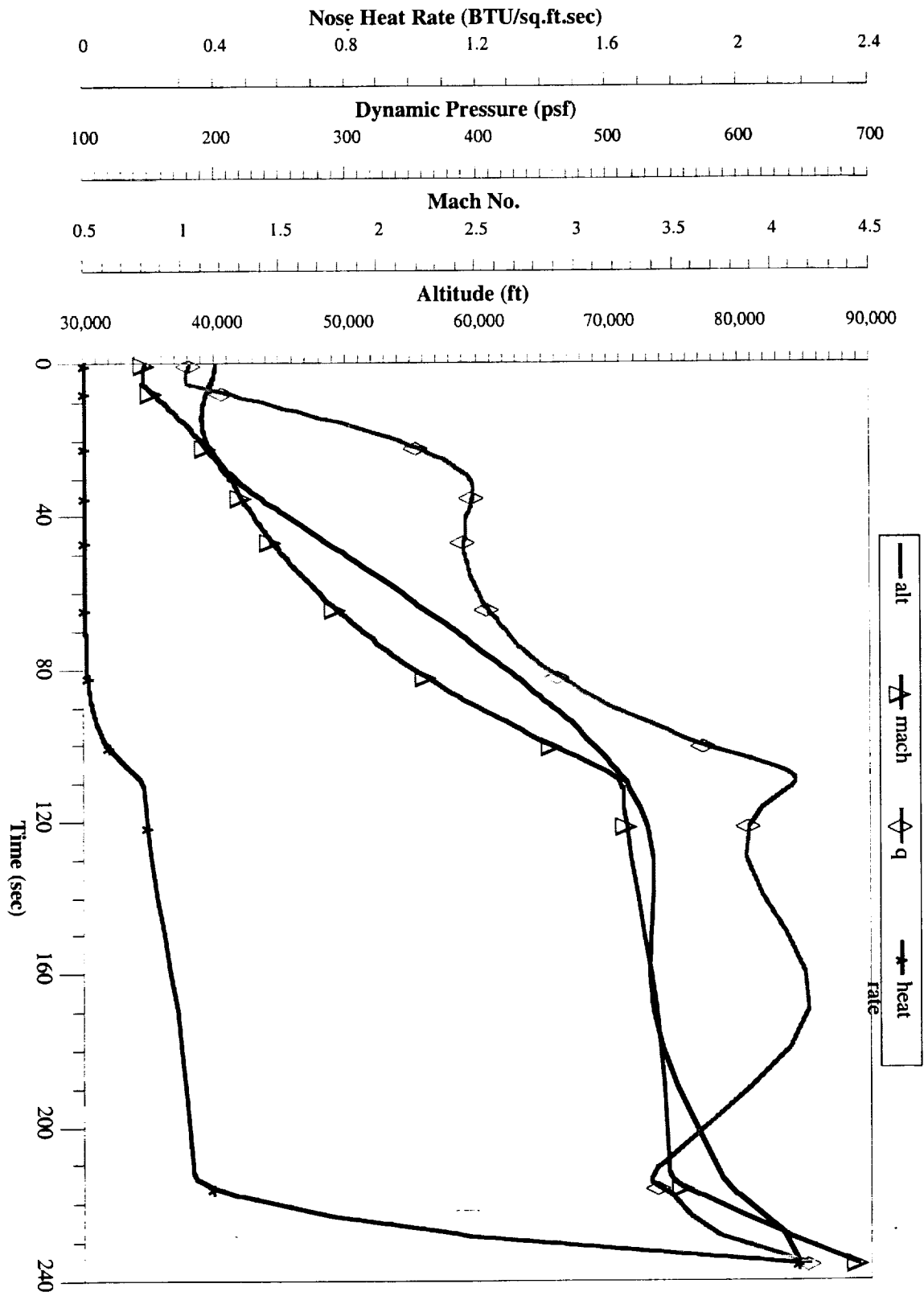
Trajectory Initial and Final conditions:

Vehicle Dry Mass	5,300.0 lbm
Added TPS Mass(estimate)	200.0 lbm
Oxidizer Mass	2,944.6 lbm
Oxidizer Volume	42.96 cu.ft.
Fuel Mass	1,364.4 lbm
Fuel Volume	36.88 cu.ft.
Gross Vehicle Mass	9,809.0 lbm

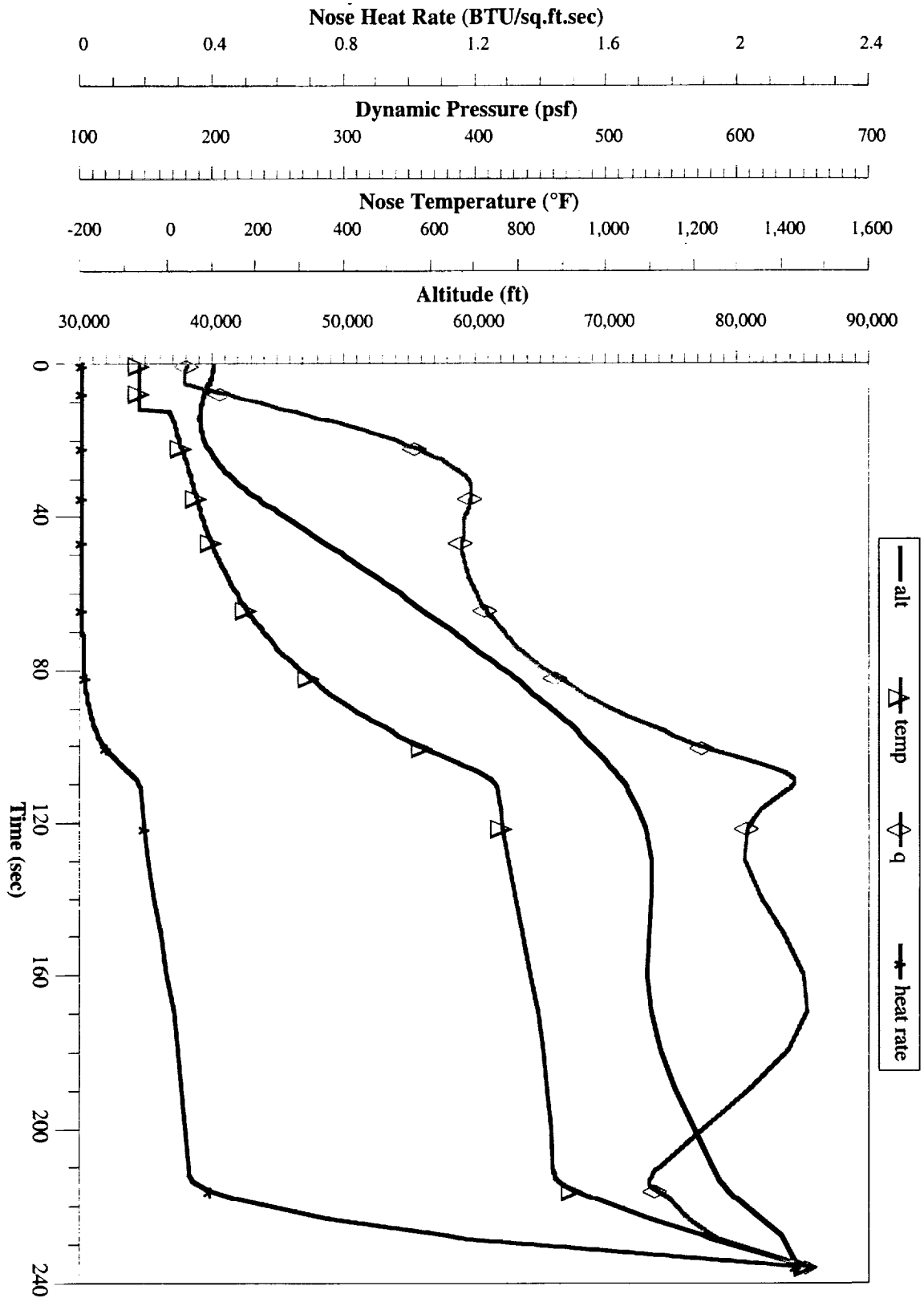
Maximum Mach No.	4.42
Maximum Altitude	84,471.0 ft
Maximum Dynamic Pressure	652.0 psf
Maximum Nose Temp	1452.6 °F
Down Range at Rocket Termination	99.6 nm
Time in AAR Mode	99.5 sec
Time in AAR/Ram Transition	6.4 sec
Time in Ramjet Mode	99.4 sec
Time in Ramjet Shutdown	7.2 sec
Time in Rocket Startup	5.0 sec
Time in Rocket Mode	20.0 sec



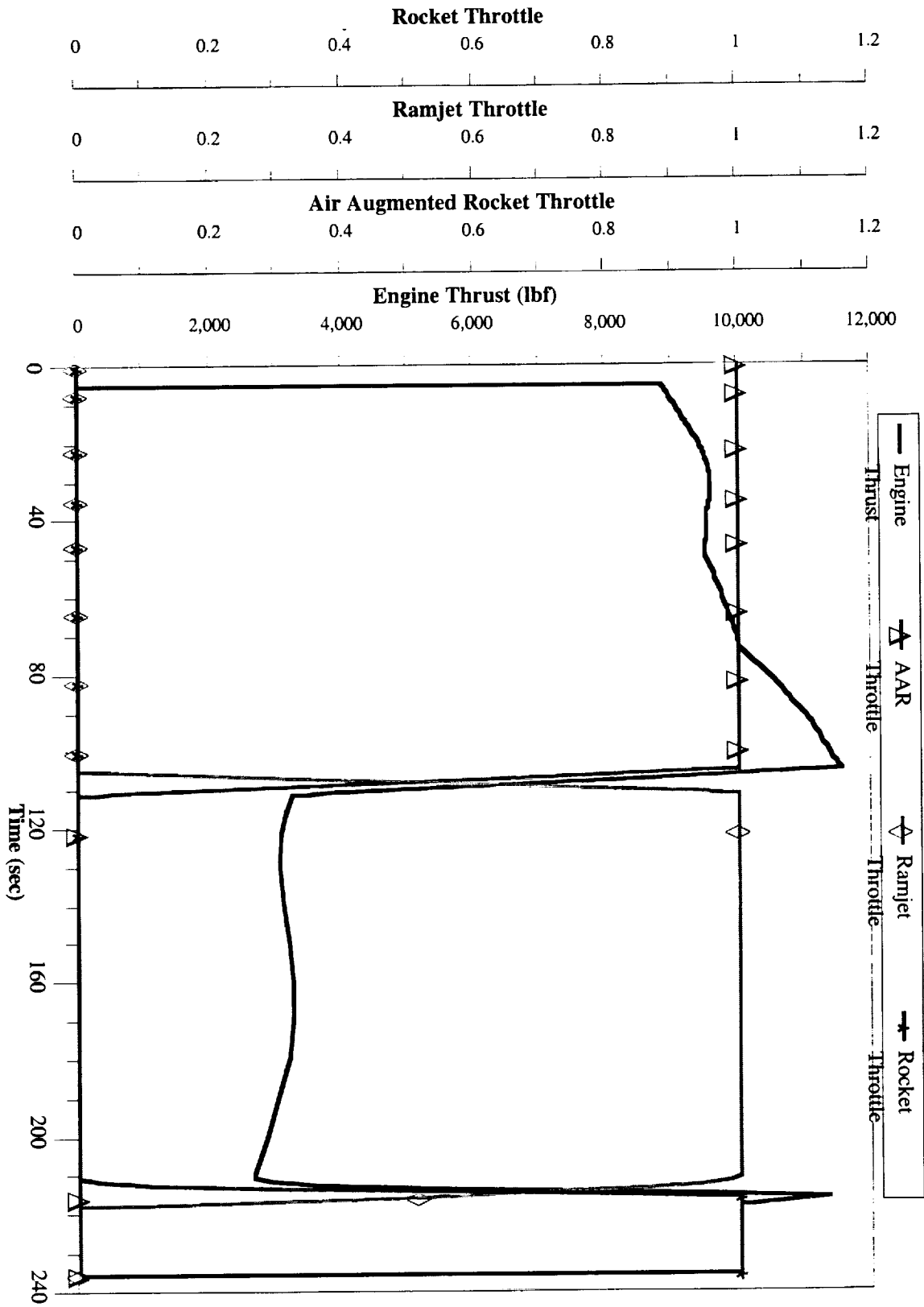
F3: NASA F3CTLOX/PROPANEA



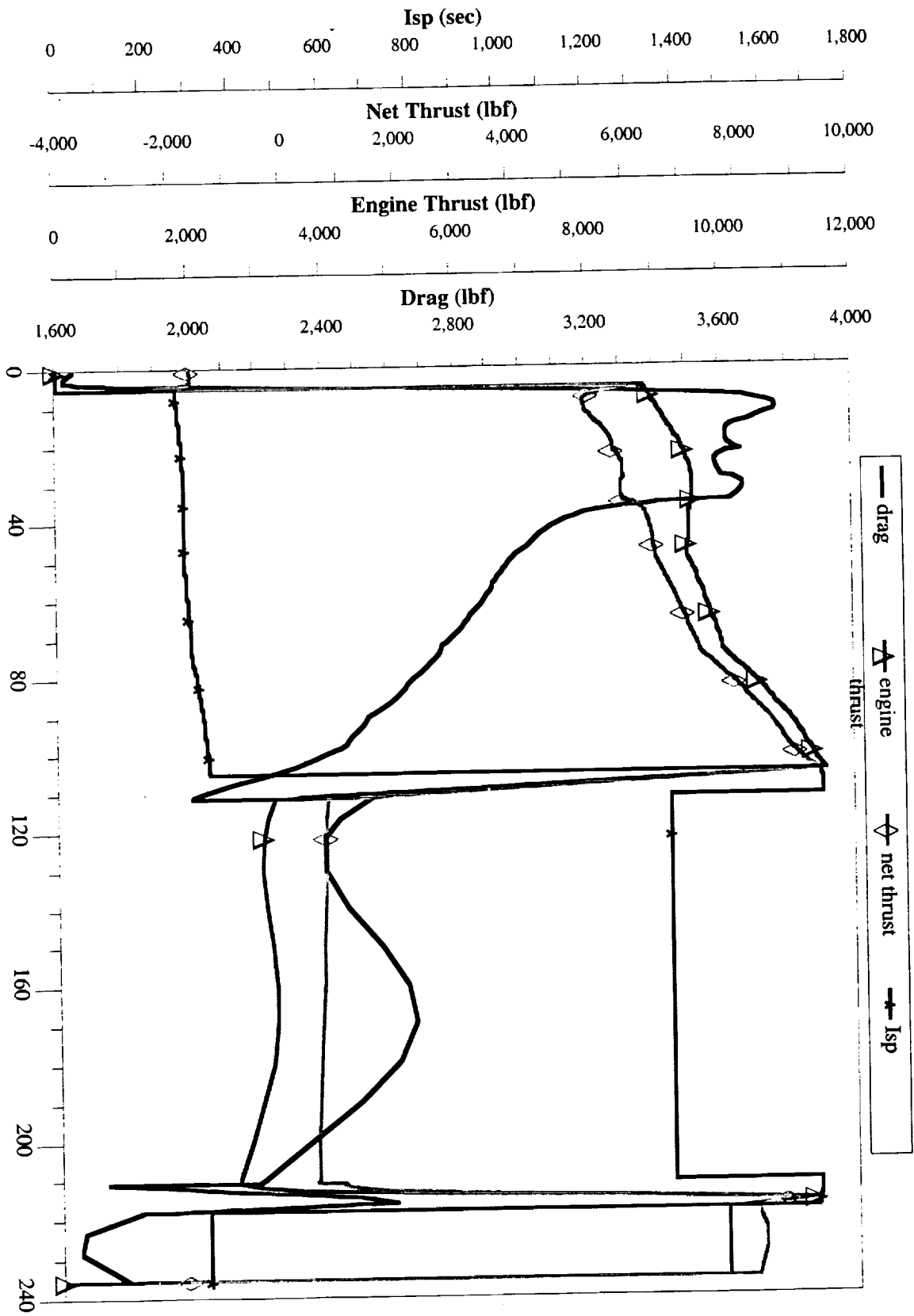
F3: NASA F3CTLOX/PROPANEA



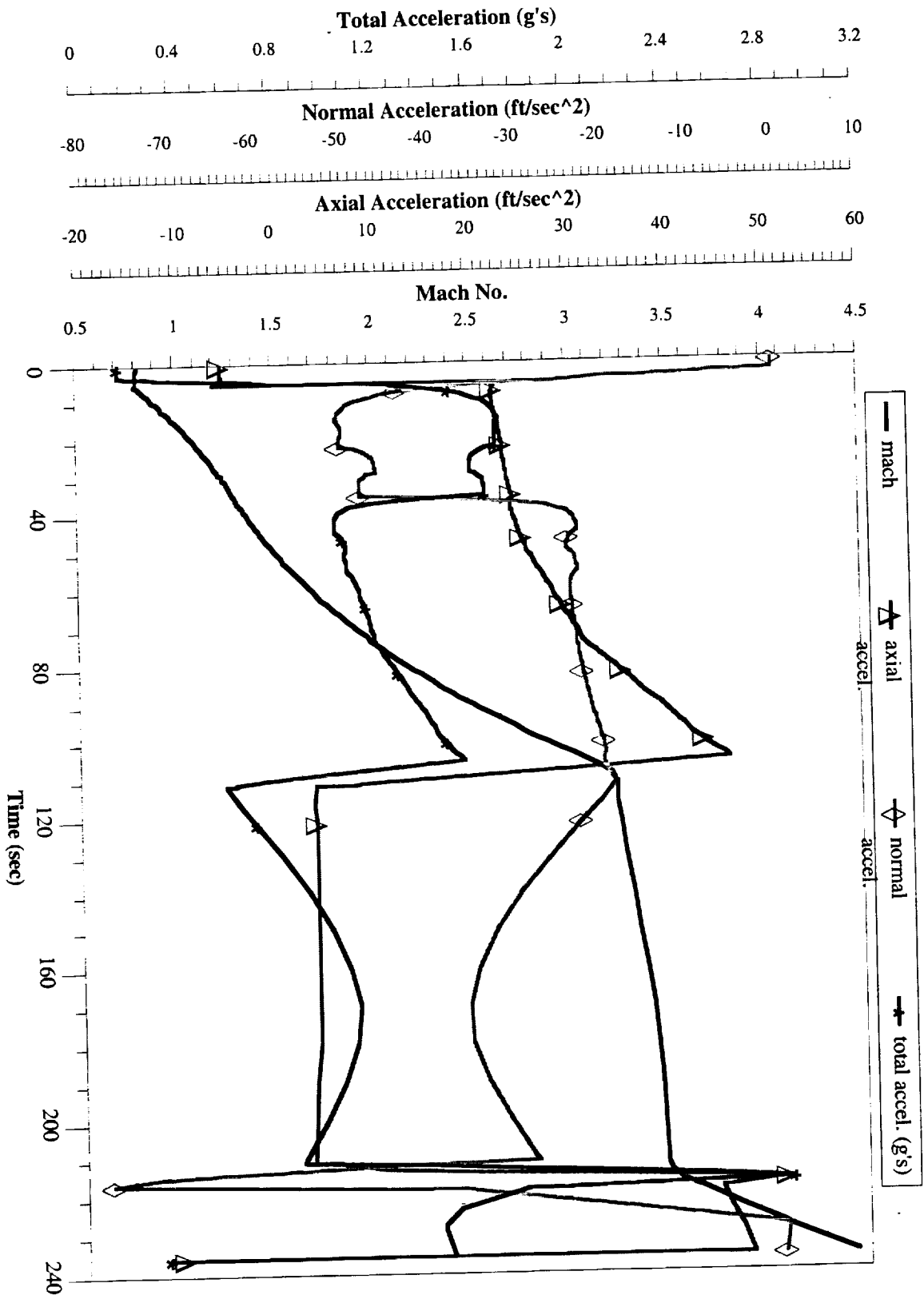
F3: NASA F3CTLOX/PROPANE



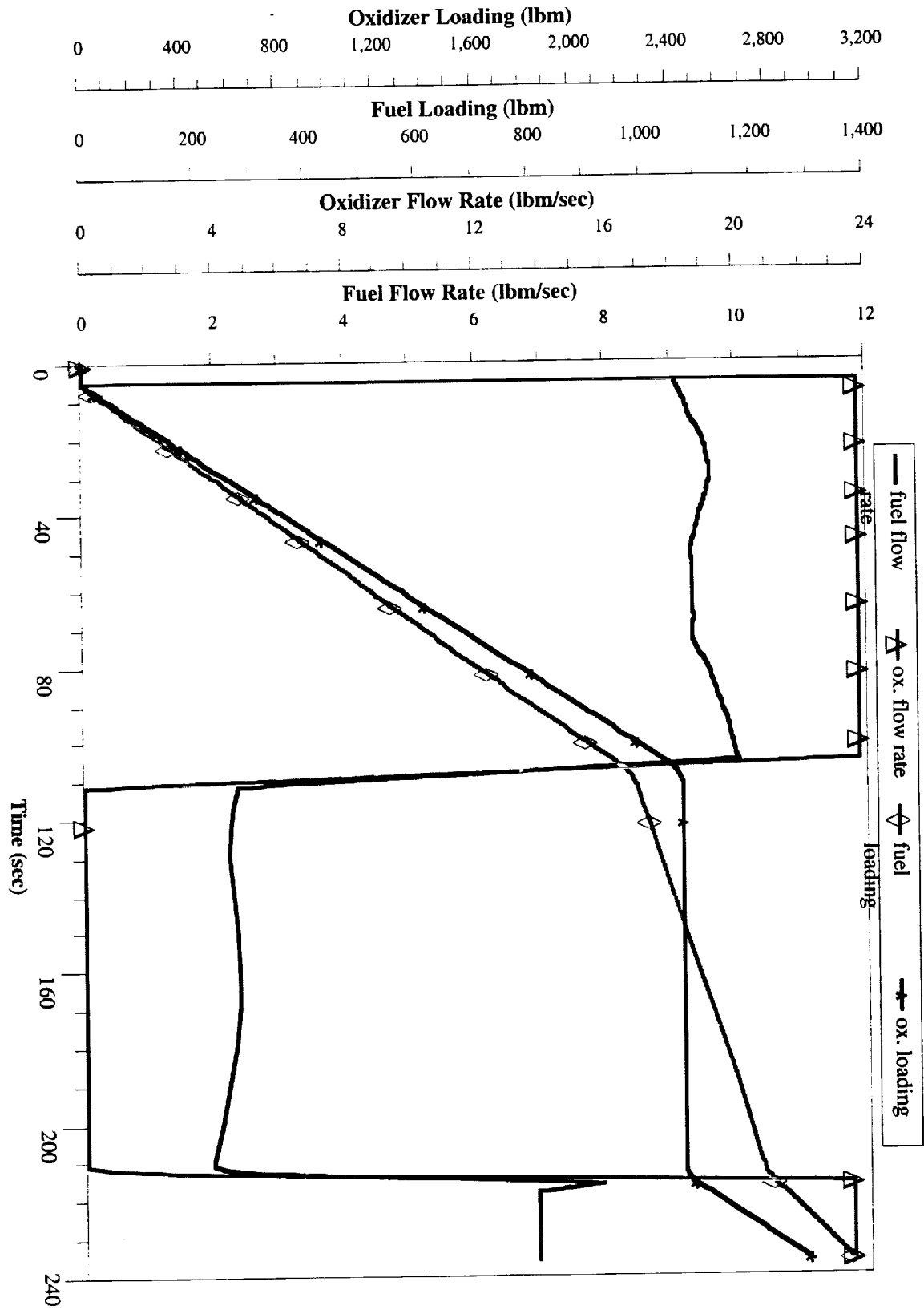
F3: NASA F3CTLOX/PROPANEA



F3: NASA F3CTLOX/PROPANEA



F3: NASA F3CTLOX/PROPANE A



F3: NASA F3 CTLOX/PROPANEA

F4: NASA F4GTH2O2/JPA

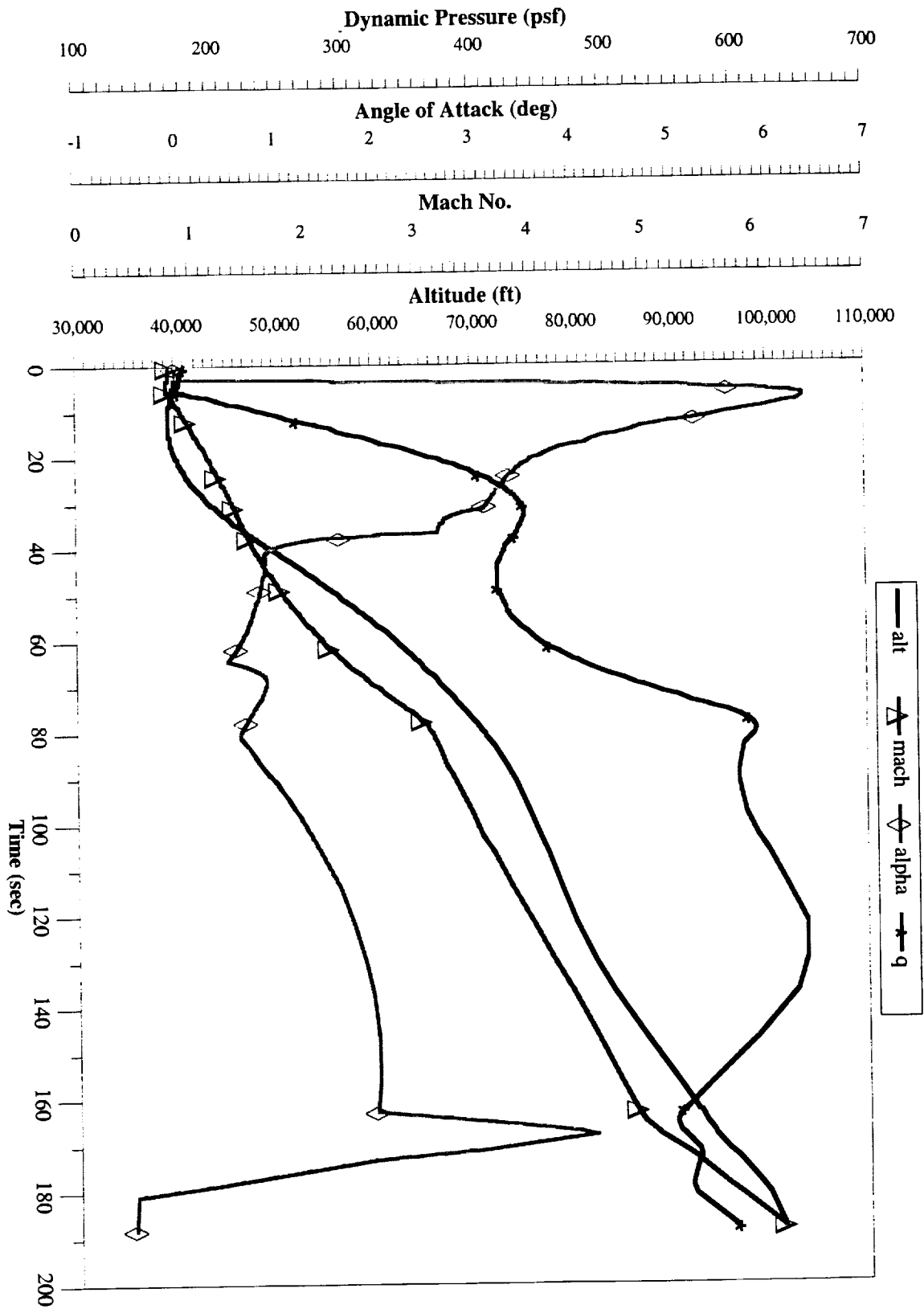
Trajectory Constraints and Optimization Goals:

- Vehicle air-launched @ alt = 40,000 ft and Mach = 0.8
- Trajectory segmented into 5 engine operating modes
 - Air Augmented Rocket Mode $0.80 < M < 2.90$
 - AAR/Ramjet Transition Mode $2.90 < M < 3.15$
 - Ramjet Mode $3.15 < M < 4.93$
 - Ramjet Shutdown $4.93 < M < 5.46$
 - Rocket Startup $4.93 < M < 5.12$
 - Rocket Mode $5.12 < M < 6.22$
- Trajectory Goal: Maximize Ramjet Mode ΔV
- Angle of Attack limited to $-2^\circ < \alpha < 12^\circ$ due to available data
- Maximum altitude limited to 120,000ft (to retain aerodynamic control effectiveness)
- Positive flight path angle required in final modes
- Time in rocket mode was fixed at 20 seconds

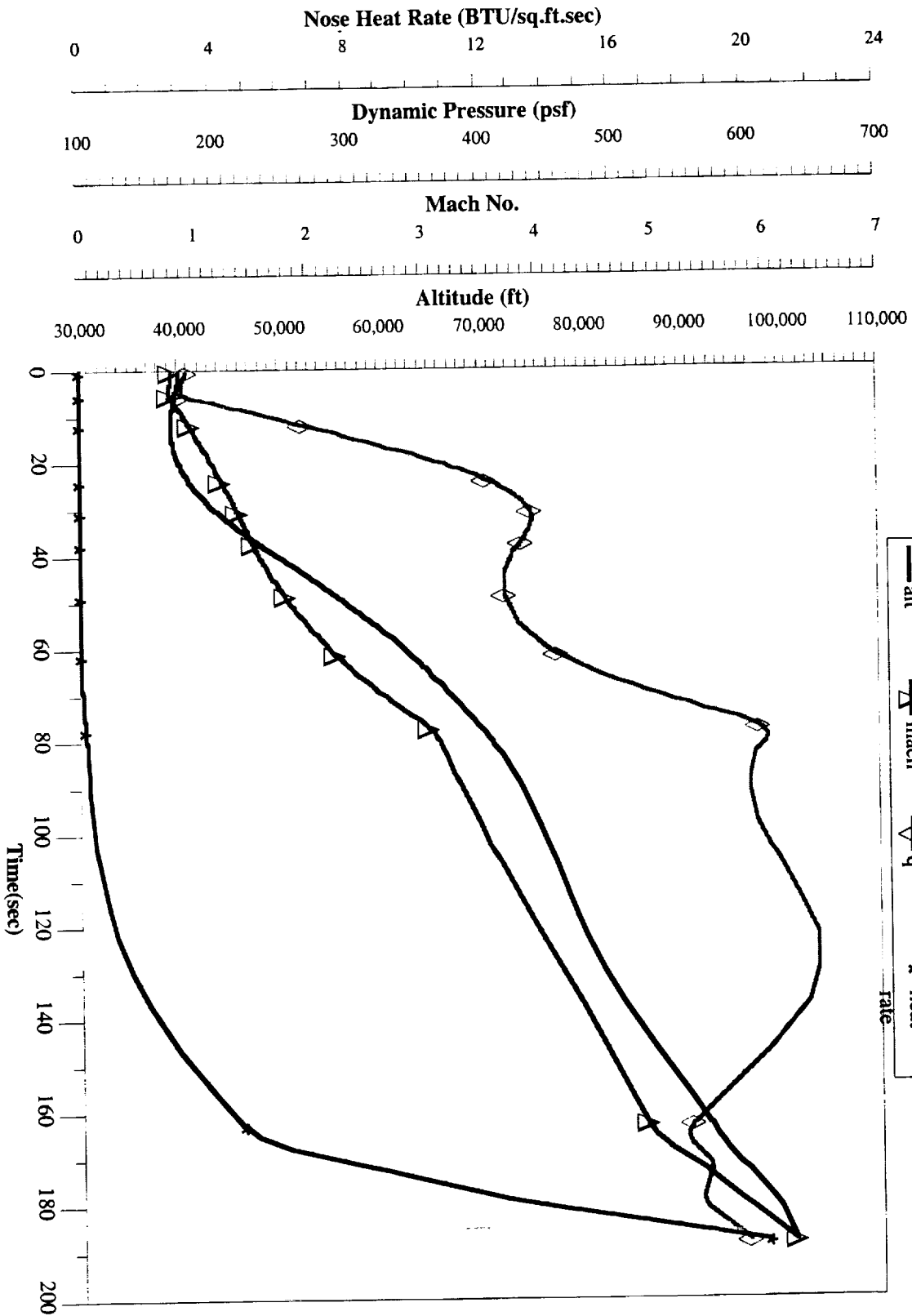
Trajectory Initial and Final conditions:

Vehicle Dry Mass	5,300 lbm
Added TPS Mass(estimate)	200 lbm
Oxidizer Mass	2,953.5 lbm
Oxidizer Volume	34.63 cu.ft.
Fuel Mass	783.2 lbm
Fuel Volume	15.85 cu.ft.
Gross Vehicle Mass	9,236.7 lbm

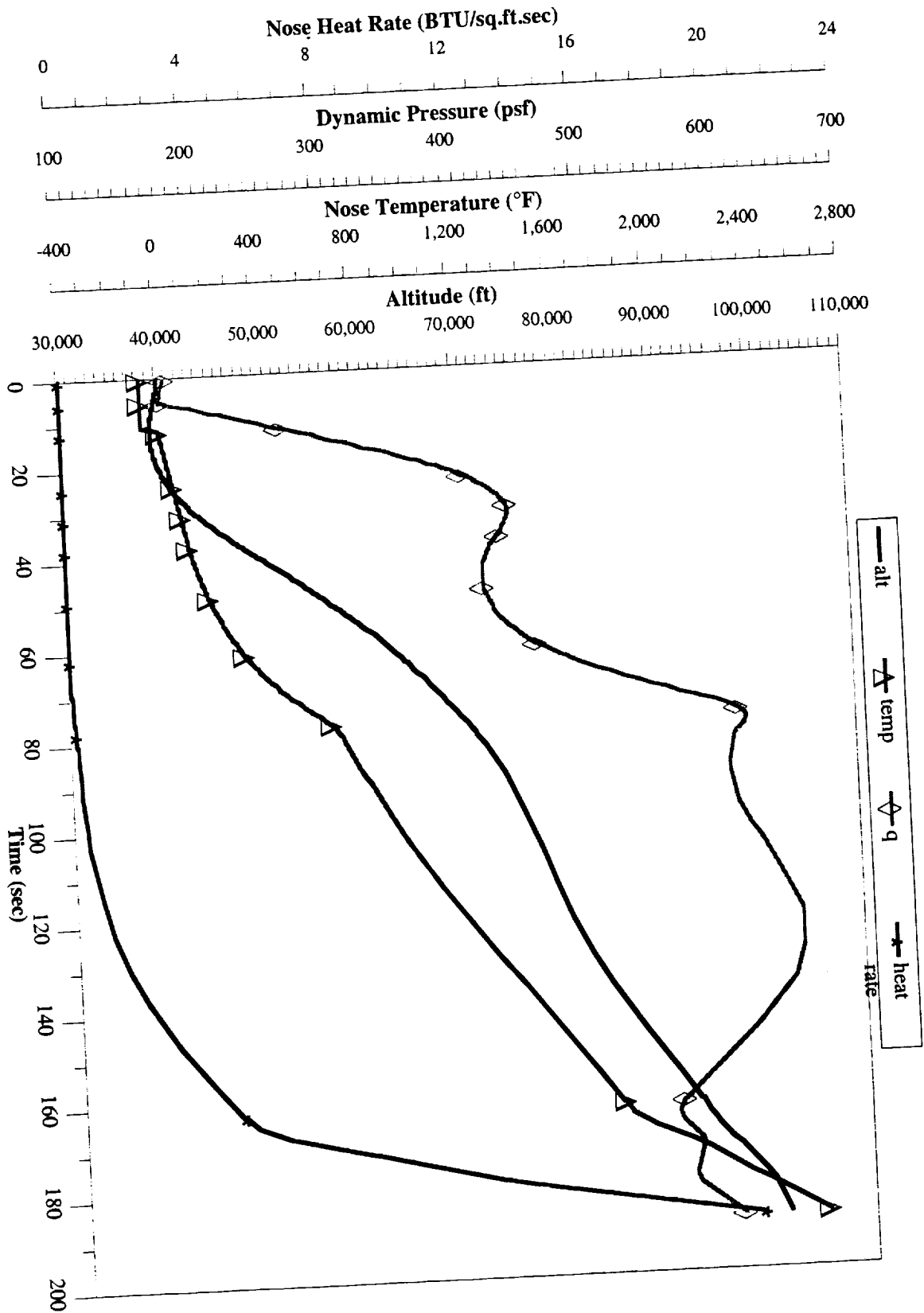
Maximum Mach No.	6.22
Maximum Altitude	101,178 ft
Maximum Dynamic Pressure	652.7 psf
Maximum Nose Temp	2600 °F
Down Range at Rocket Termination	96.5 nm
Time in AAR Mode	69.3 sec
Time in AAR/Ram Transition	6.1 sec
Time in Ramjet Mode	82.1 sec
Time in Ramjet Shutdown	10.4 sec
Time in Rocket Startup	5.0 sec
Time in Rocket Mode	20.0 sec



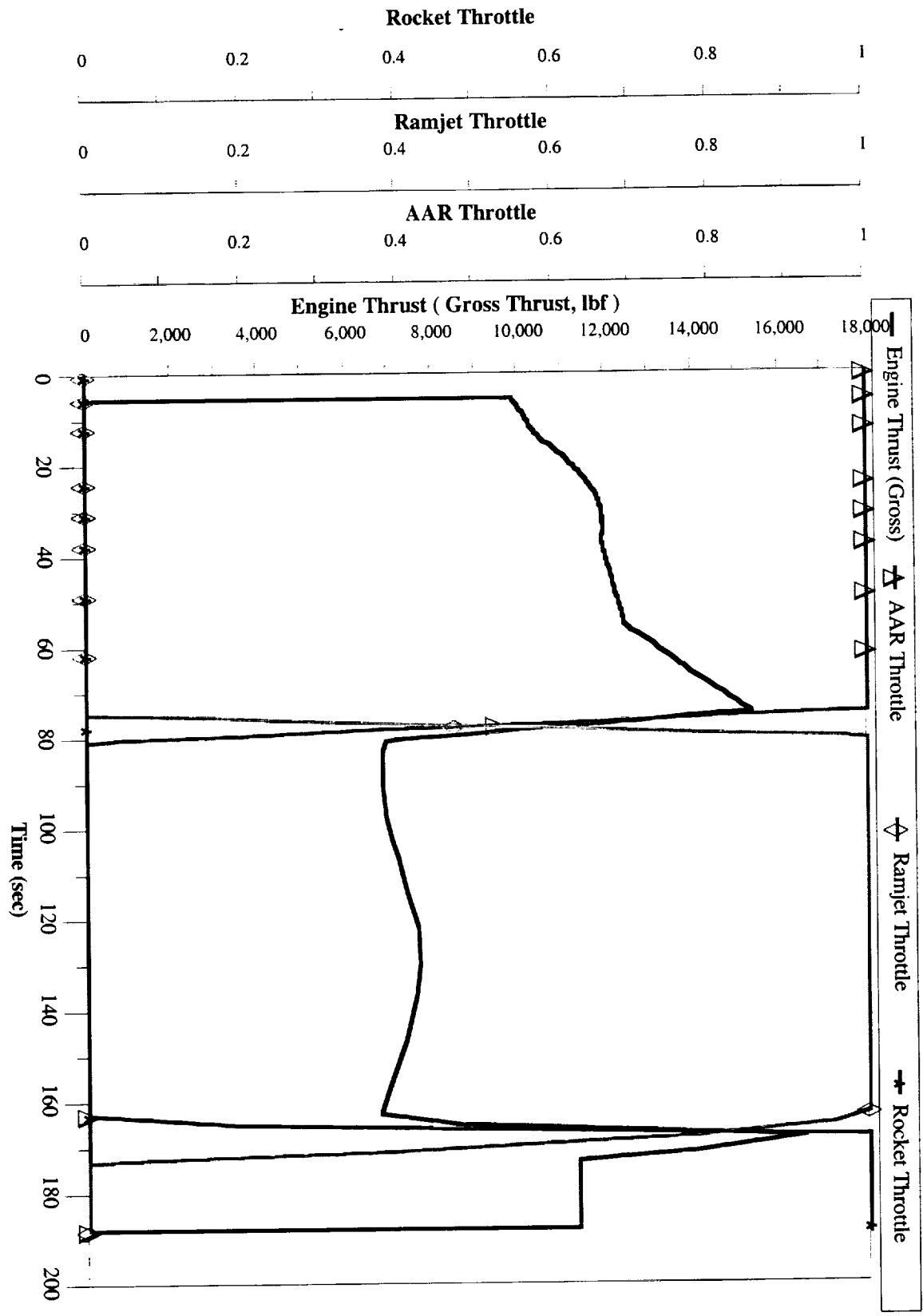
F4: NASA F4GTH2O2/JPA



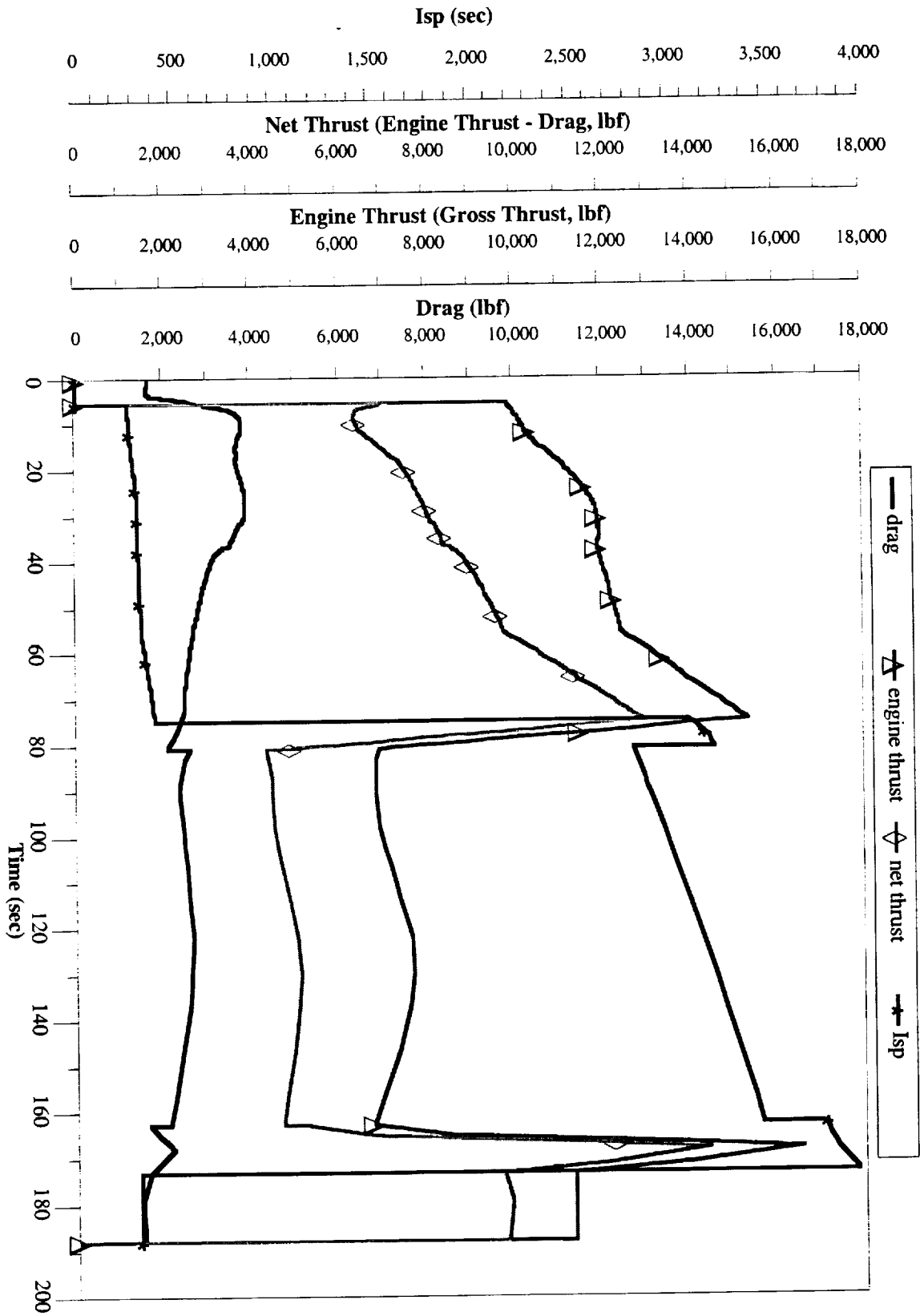
F4: NASA F4GTH2O2/JPA



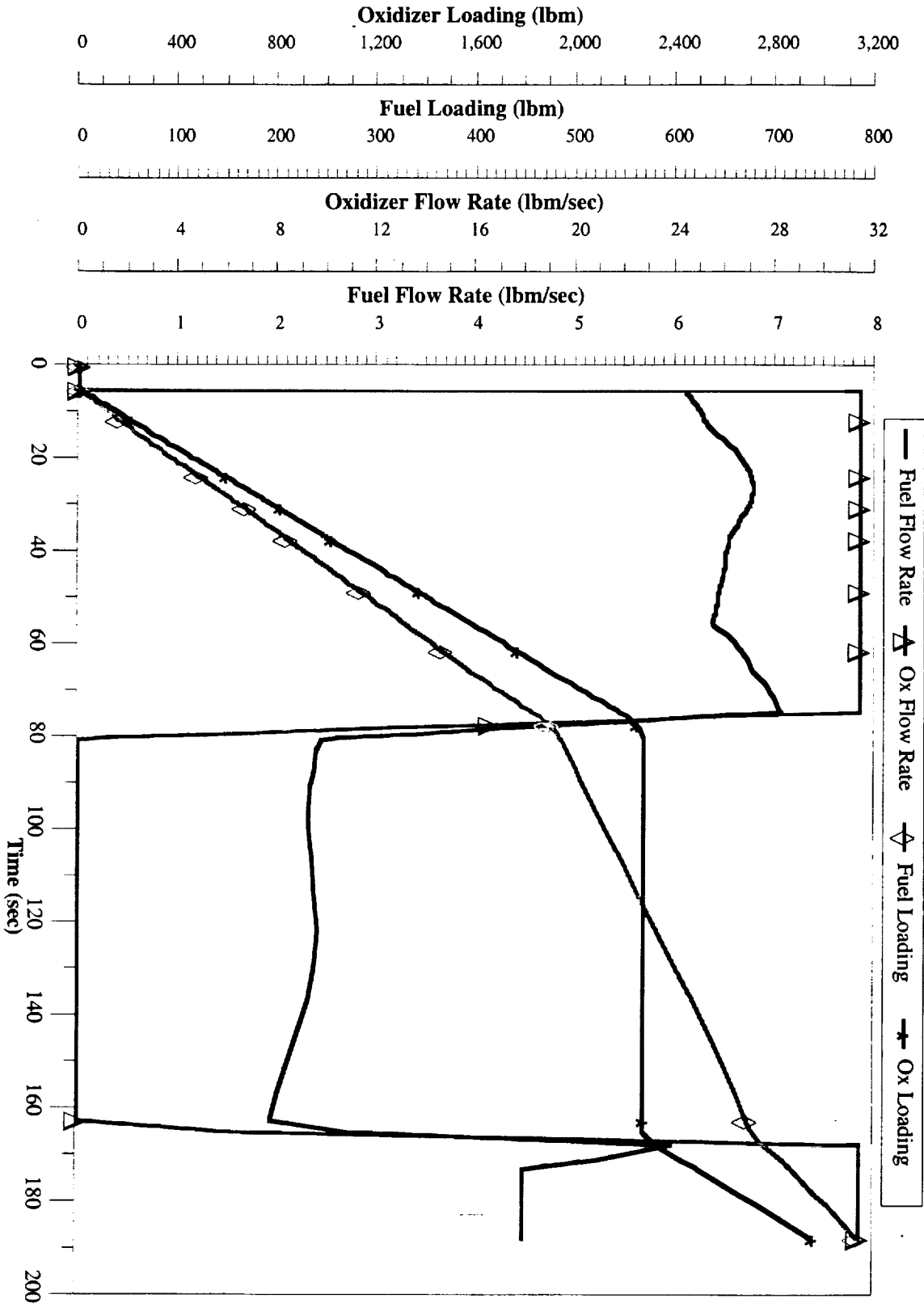
F4: NASA F4GTH2O2/JPA



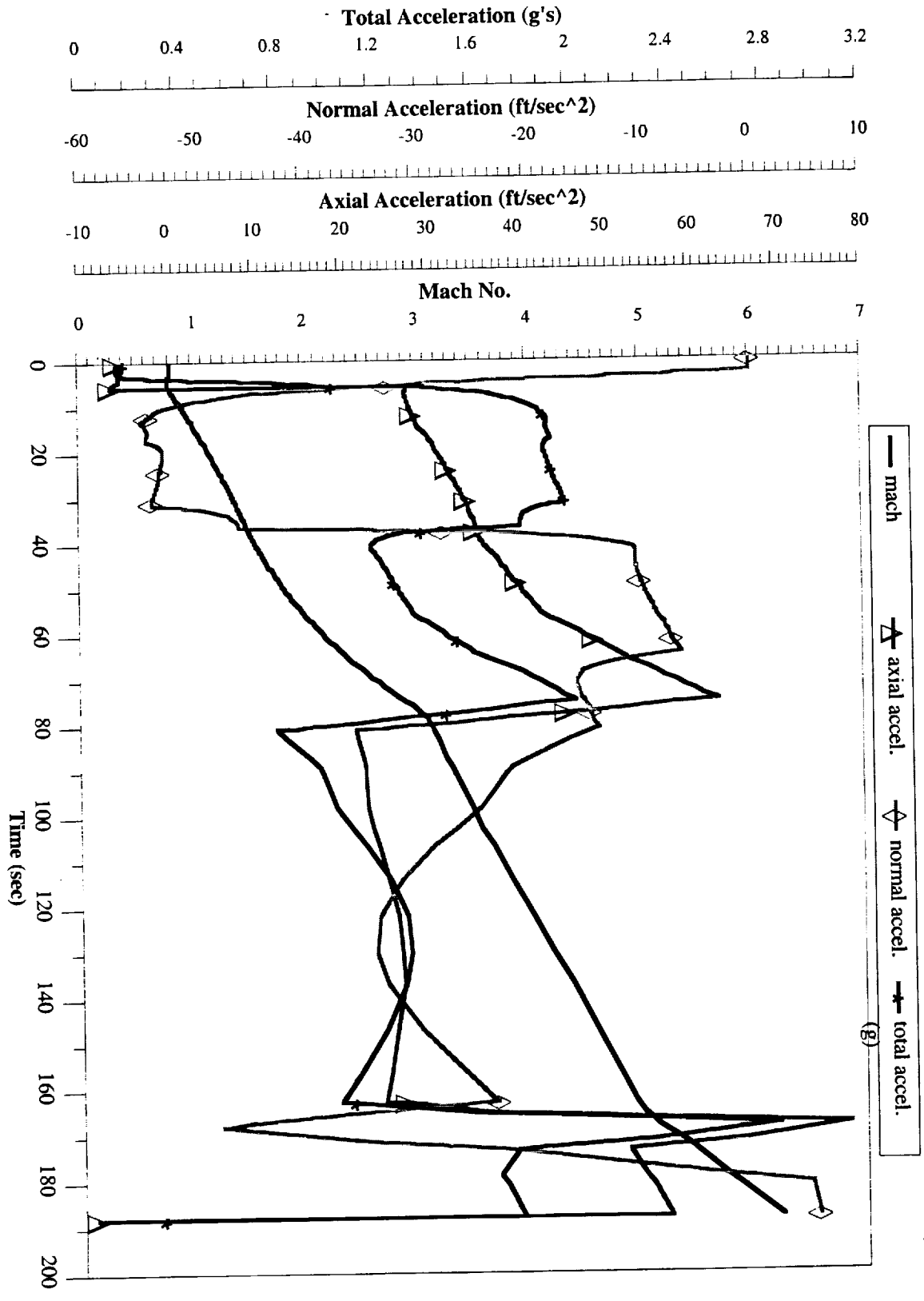
F4: NASA F4GTH2O2/JPA



F4: NASA F4GTH202/JPA



F4: NASA F4GTH2O2/JPA



F4: NASA F4GTH2O2/JPA

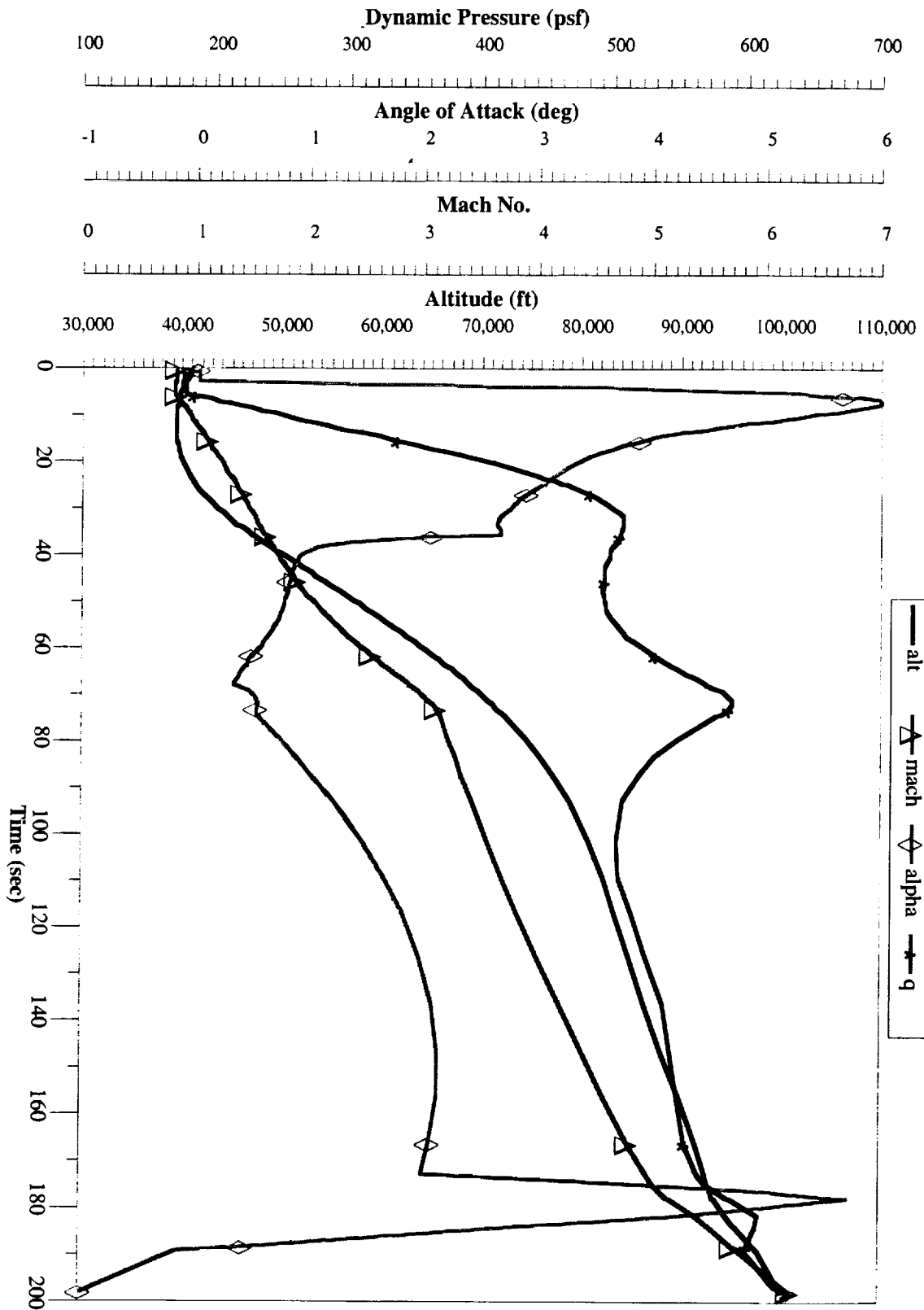
F5: NASA F5GTLOX/JPA

Trajectory Constraints and Optimization Goals:

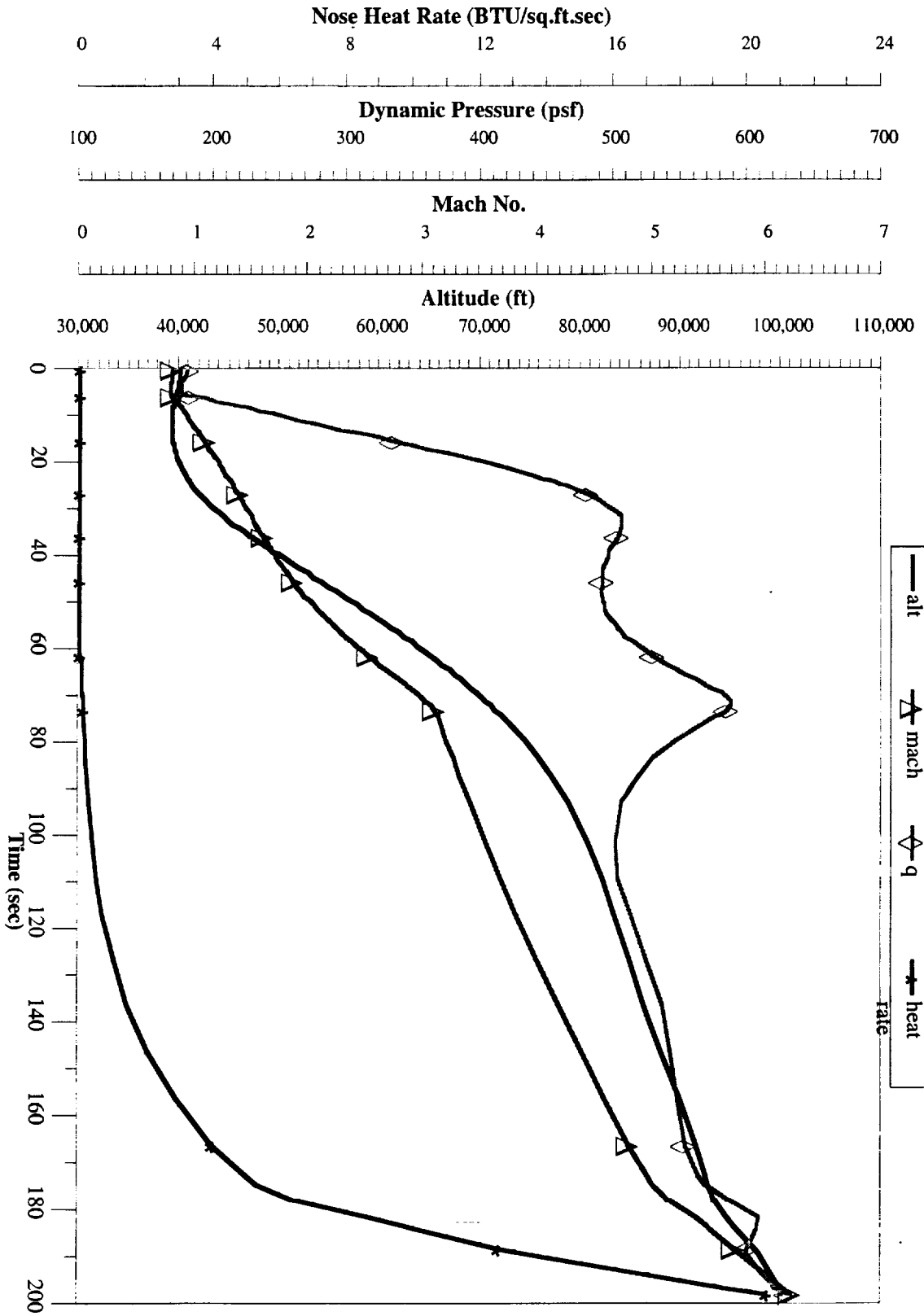
- Vehicle air-launched @ alt = 40,000 ft and Mach = 0.8
- Trajectory segmented into 5 engine operating modes
 - Air Augmented Rocket Mode $0.80 < M < 2.88$
 - AAR/Ramjet Transition Mode $2.88 < M < 3.12$
 - Ramjet Mode $3.12 < M < 4.95$
 - Ramjet Shutdown $4.95 < M < 5.50$
 - Rocket Startup $4.95 < M < 5.15$
 - Rocket Mode $5.15 < M < 6.22$
- Trajectory Goal: Maximize Ramjet Mode ΔV
- Angle of Attack limited to $-2^\circ < \alpha < 12^\circ$ due to available data
- Maximum altitude limited to 120,000ft (to retain aerodynamic control effectiveness)
- Positive flight path angle required in final modes
- Time in rocket mode was fixed at 20 seconds

Trajectory Initial and Final conditions:

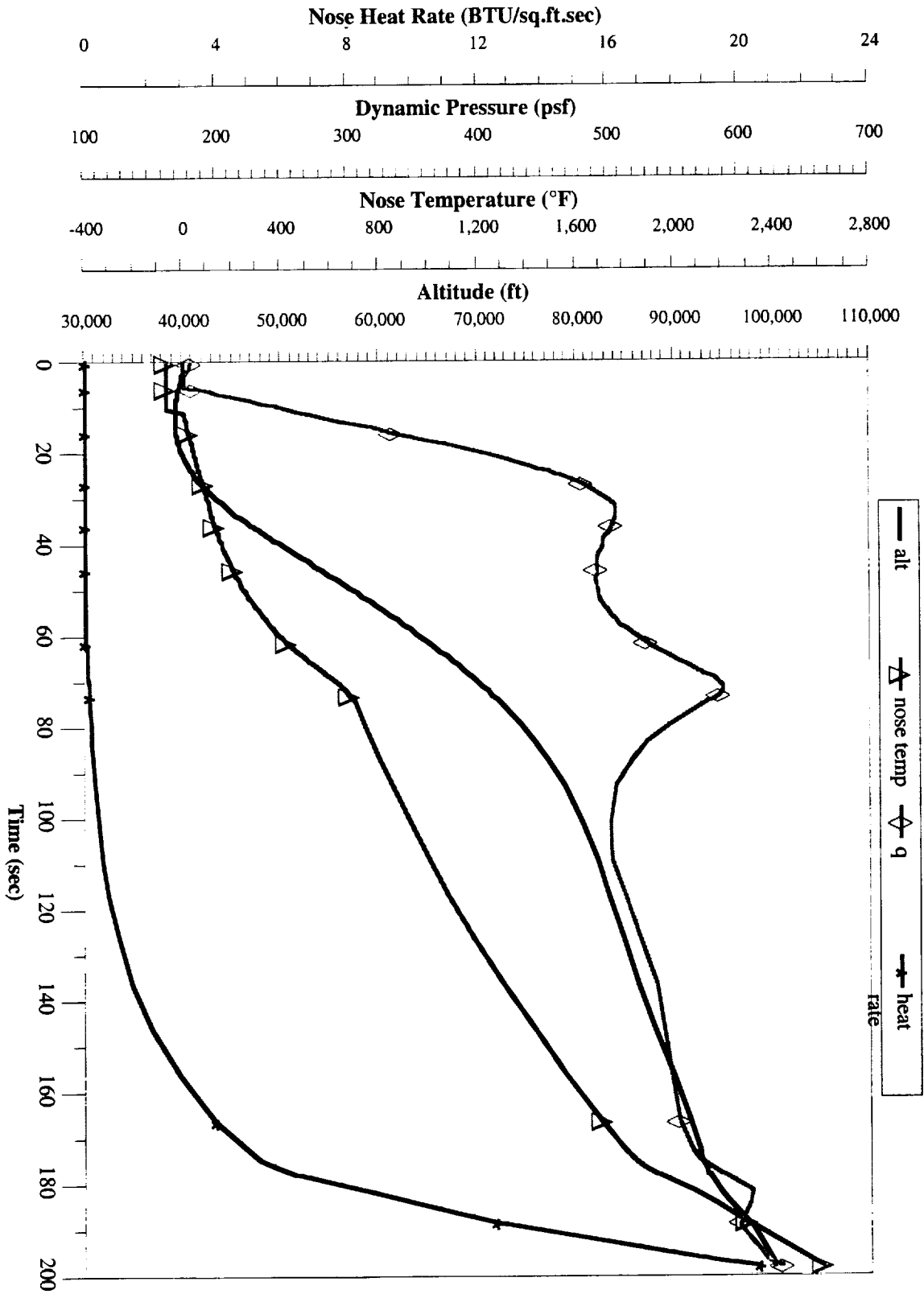
Vehicle Dry Mass	5,300 lbm
Added TPS Mass(estimate)	200 lbm
Oxidizer Mass	2,084.0 lbm
Oxidizer Volume	30.40 cu.ft.
Fuel Mass	1,150.3 lbm
Fuel Volume	23.29 cu.ft.
Gross Vehicle Mass	8,734.0 lbm
Maximum Mach No.	6.22
Maximum Altitude	100,038 ft
Maximum Dynamic Pressure	630.1 psf
Maximum Nose Temp	2600 °F
Down Range at Rocket Termination	105.0 nm
Time in AAR Mode	62.8 sec
Time in AAR/Ram Transition	6.3 sec
Time in Ramjet Mode	98.5 sec
Time in Ramjet Shutdown	10.9 sec
Time in Rocket Startup	5.0 sec
Time in Rocket Mode	20.0 sec



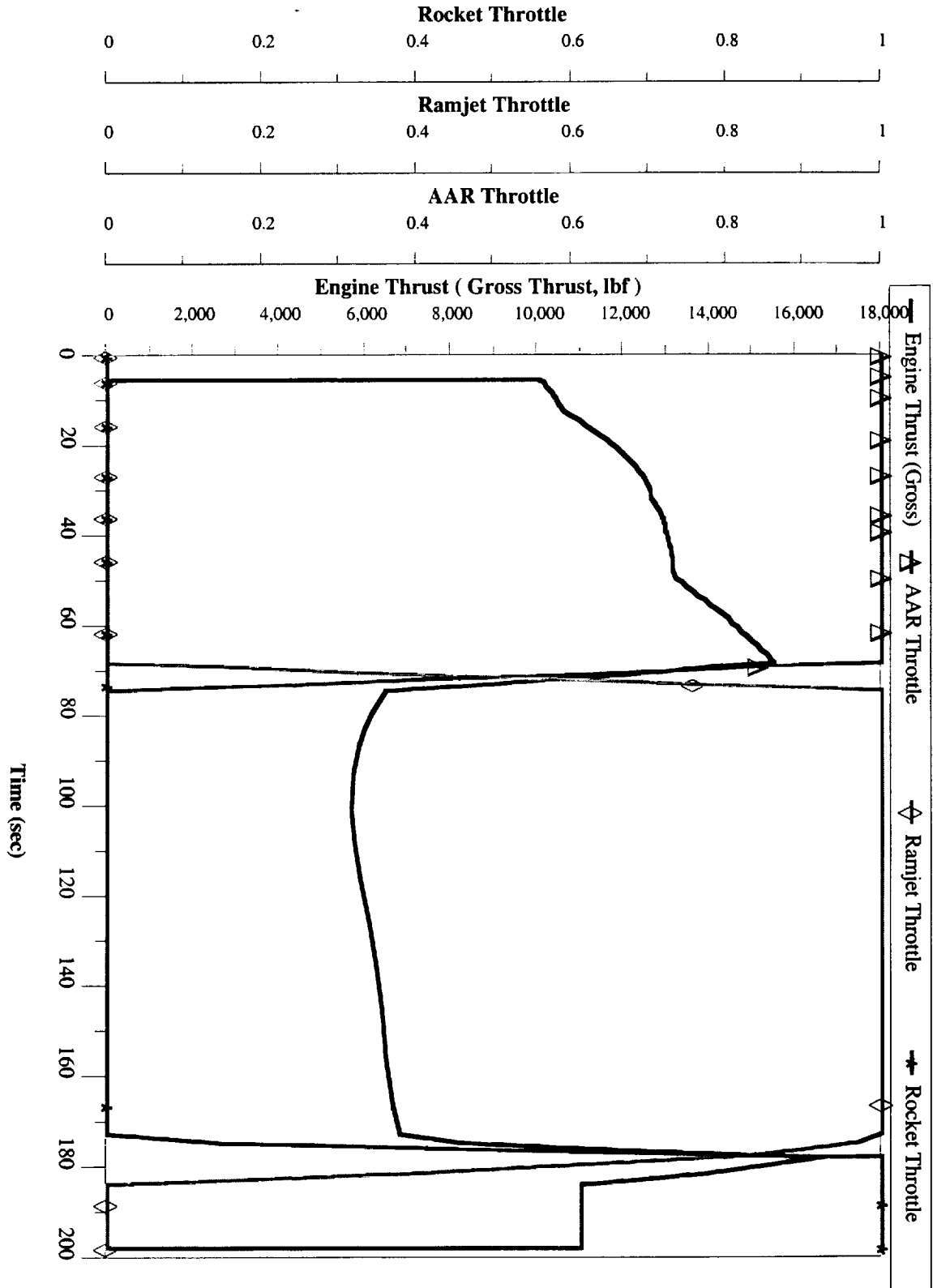
F5: NASA F5GTLOX/JPA



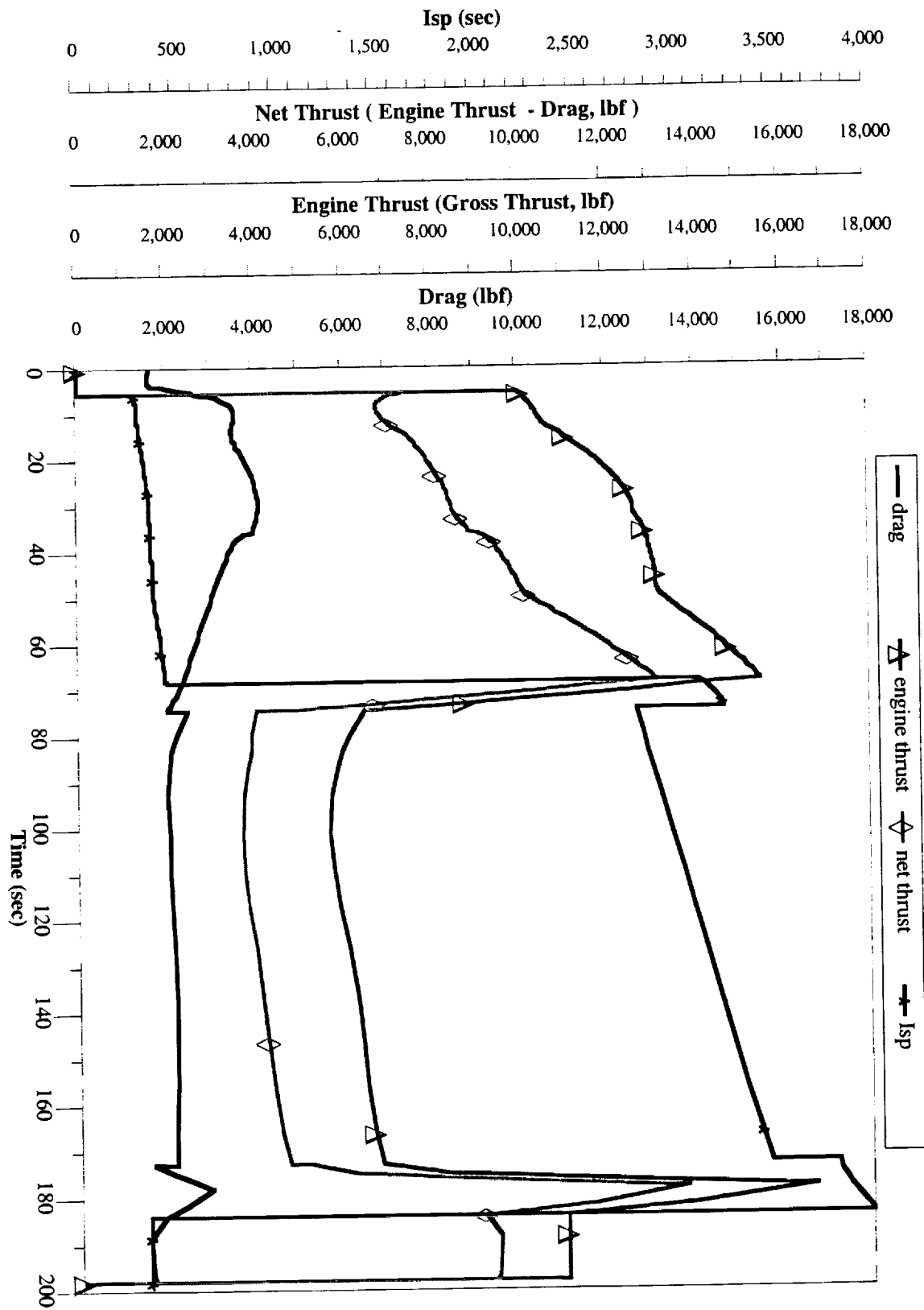
F5: NASA F5GTLOX/JPA



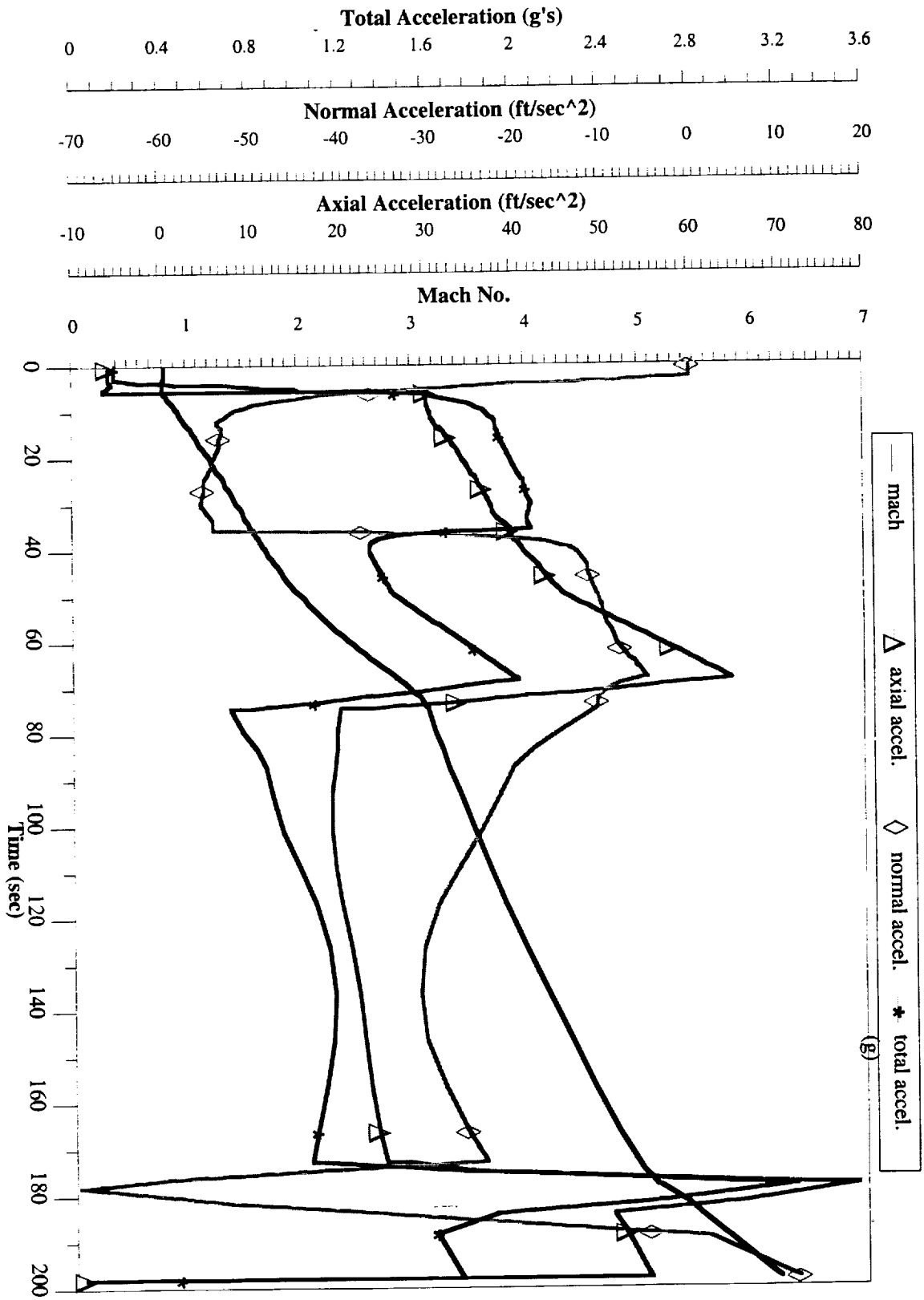
F5: NASA F5GTLOX/JPA



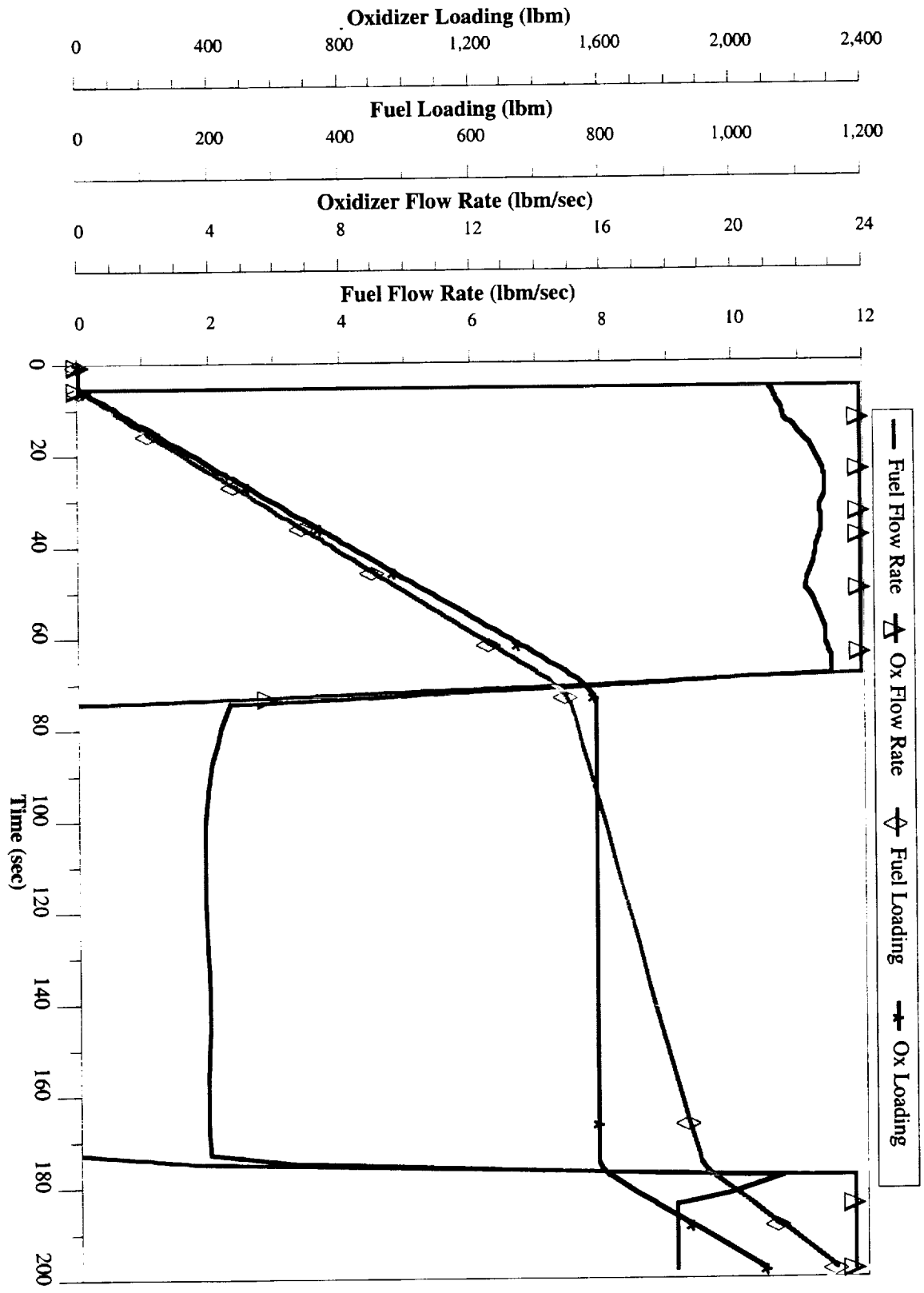
F5: NASA F5GTLOX/JPA



F5: NASA F5GTLOX/JPA



F5: NASA F5GTLOX/JPA



F5: NASA F5GTLOX/JPA

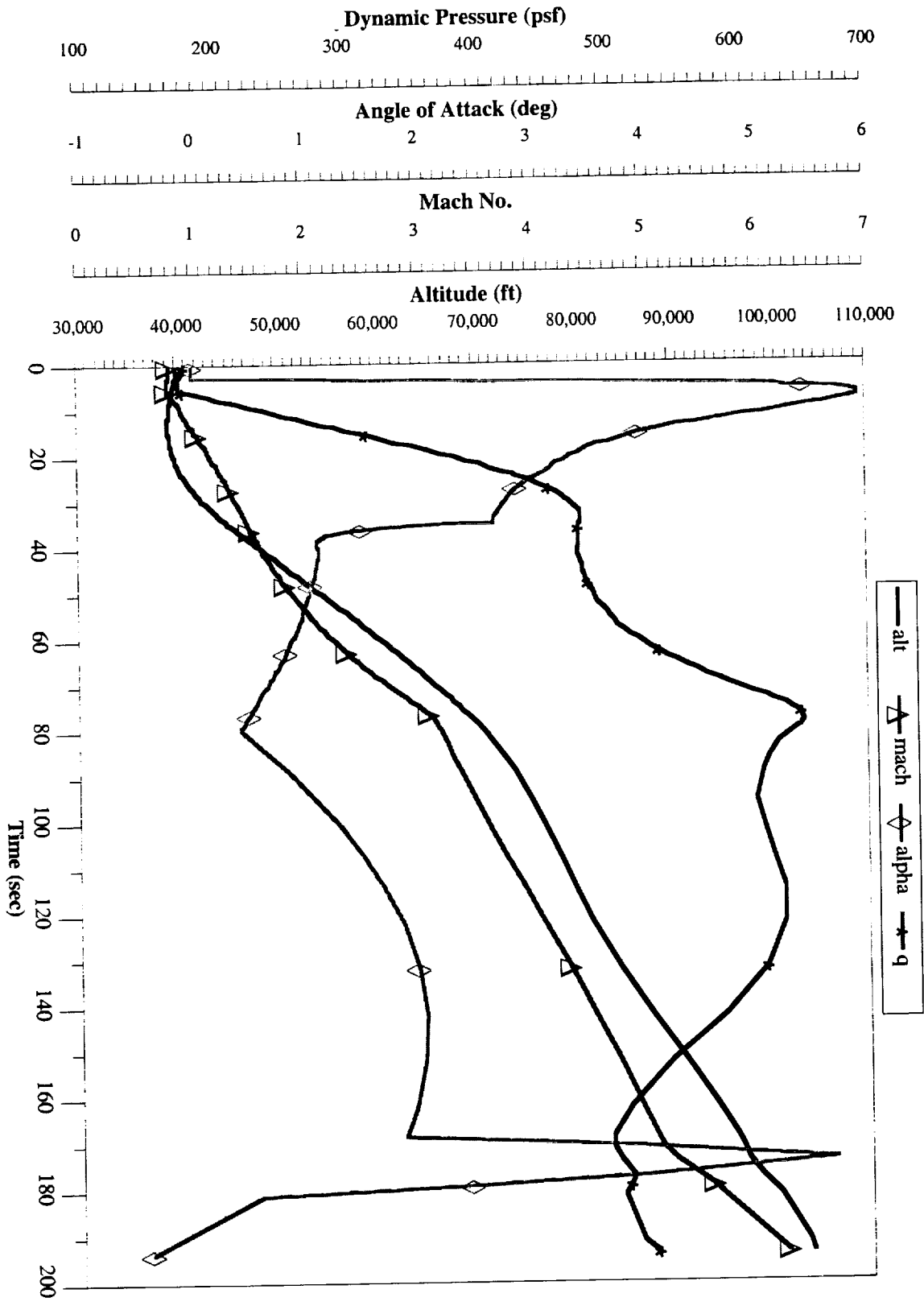
F6: NASA F6GTLOX/PropaneA

Trajectory Constraints and Optimization Goals:

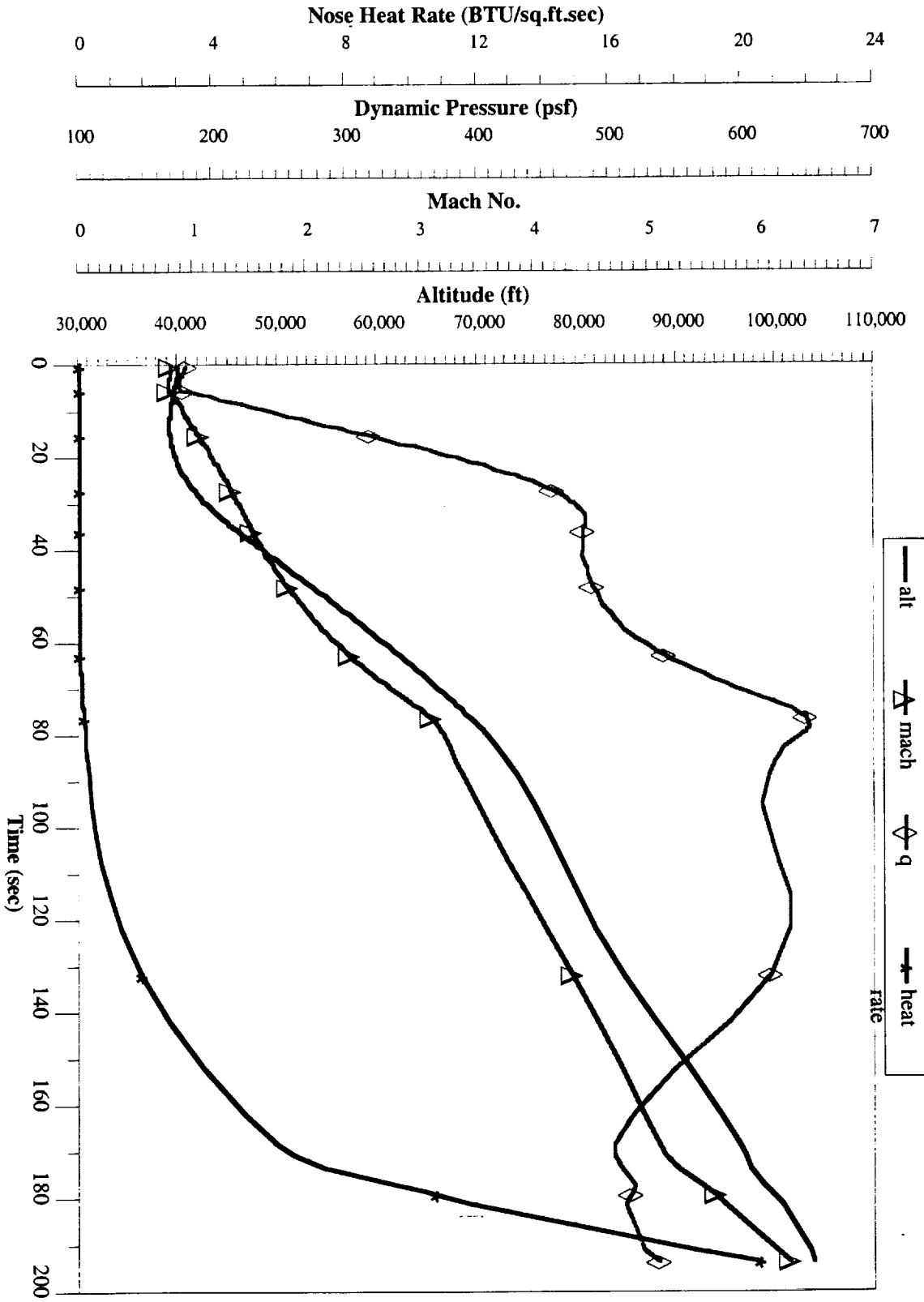
- Vehicle air-launched @ alt = 40,000 ft and Mach = 0.8
- Trajectory segmented into 5 engine operating modes
 - Air Augmented Rocket Mode $0.80 < M < 2.94$
 - AAR/Ramjet Transition Mode $2.94 < M < 3.19$
 - Ramjet Mode $3.19 < M < 5.08$
 - Ramjet Shutdown $5.08 < M < 5.58$
 - Rocket Startup $5.08 < M < 5.26$
 - Rocket Mode $5.26 < M < 6.24$
- Trajectory Goal: Maximize Ramjet Mode ΔV
- Angle of Attack limited to $-2^\circ < \alpha < 12^\circ$ due to available data
- Maximum altitude limited to 120,000ft (to retain aerodynamic control effectiveness)
- Positive flight path angle required in final modes
- Time in rocket mode was fixed at 20 seconds

Trajectory Initial and Final conditions:

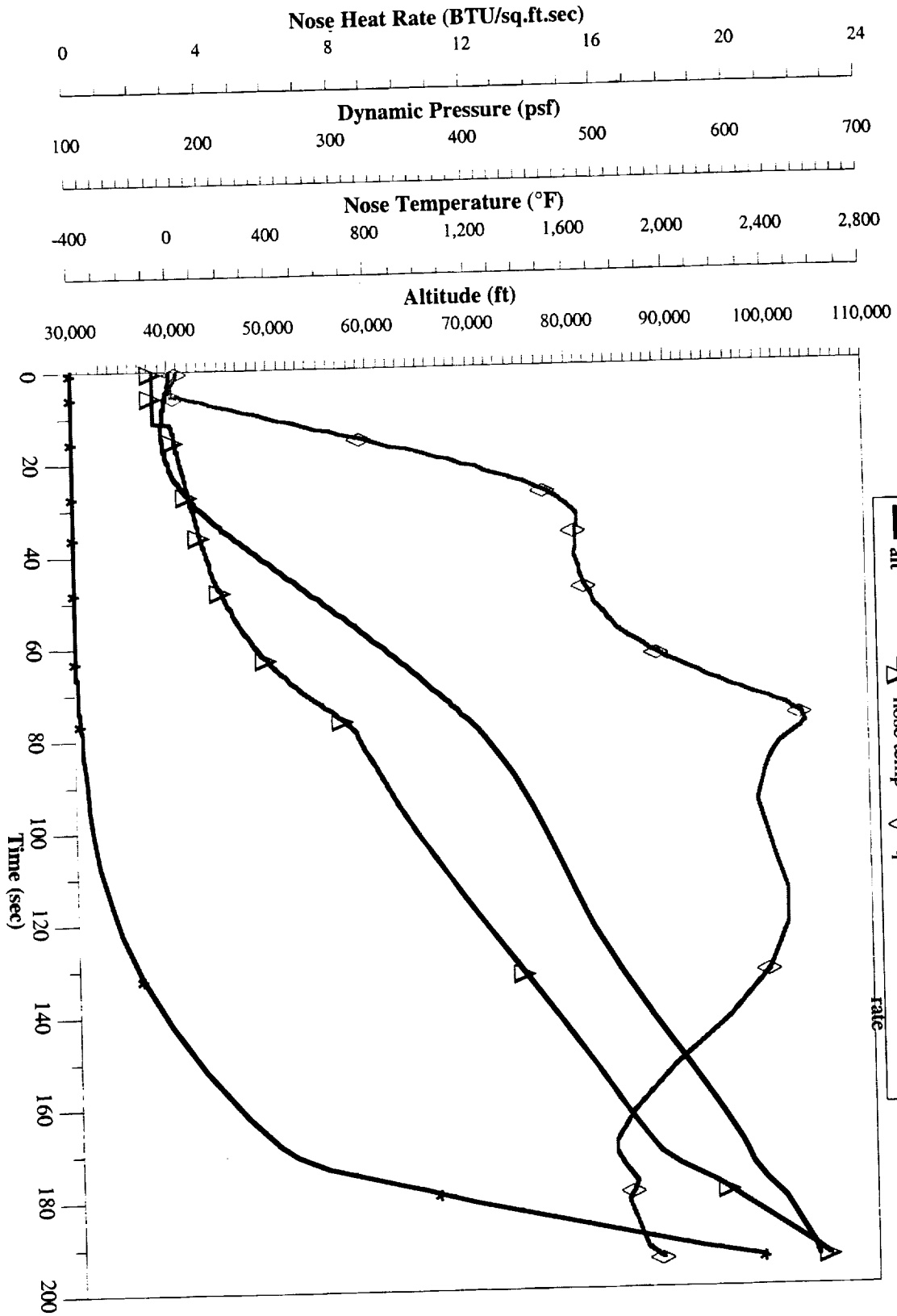
Vehicle Dry Mass	5,300 lbm
Added TPS Mass(estimate)	200 lbm
Oxidizer Mass	2,197.5 lbm
Oxidizer Volume	32.06 cu.ft.
Fuel Mass	1,014.2 lbm
Fuel Volume	27.41 cu.ft.
Gross Vehicle Mass	8711.7 lbm
Maximum Mach No.	6.24
Maximum Altitude	103,759 ft
Maximum Dynamic Pressure	650.1 psf
Maximum Nose Temp	2,599 °F
Down Range at Rocket Termination	103.2 nm
Time in AAR Mode	68.1 sec
Time in AAR/Ram Transition	6.2 sec
Time in Ramjet Mode	88.8 sec
Time in Ramjet Shutdown	10.8 sec
Time in Rocket Startup	5.0 sec
Time in Rocket Mode	20.0 sec



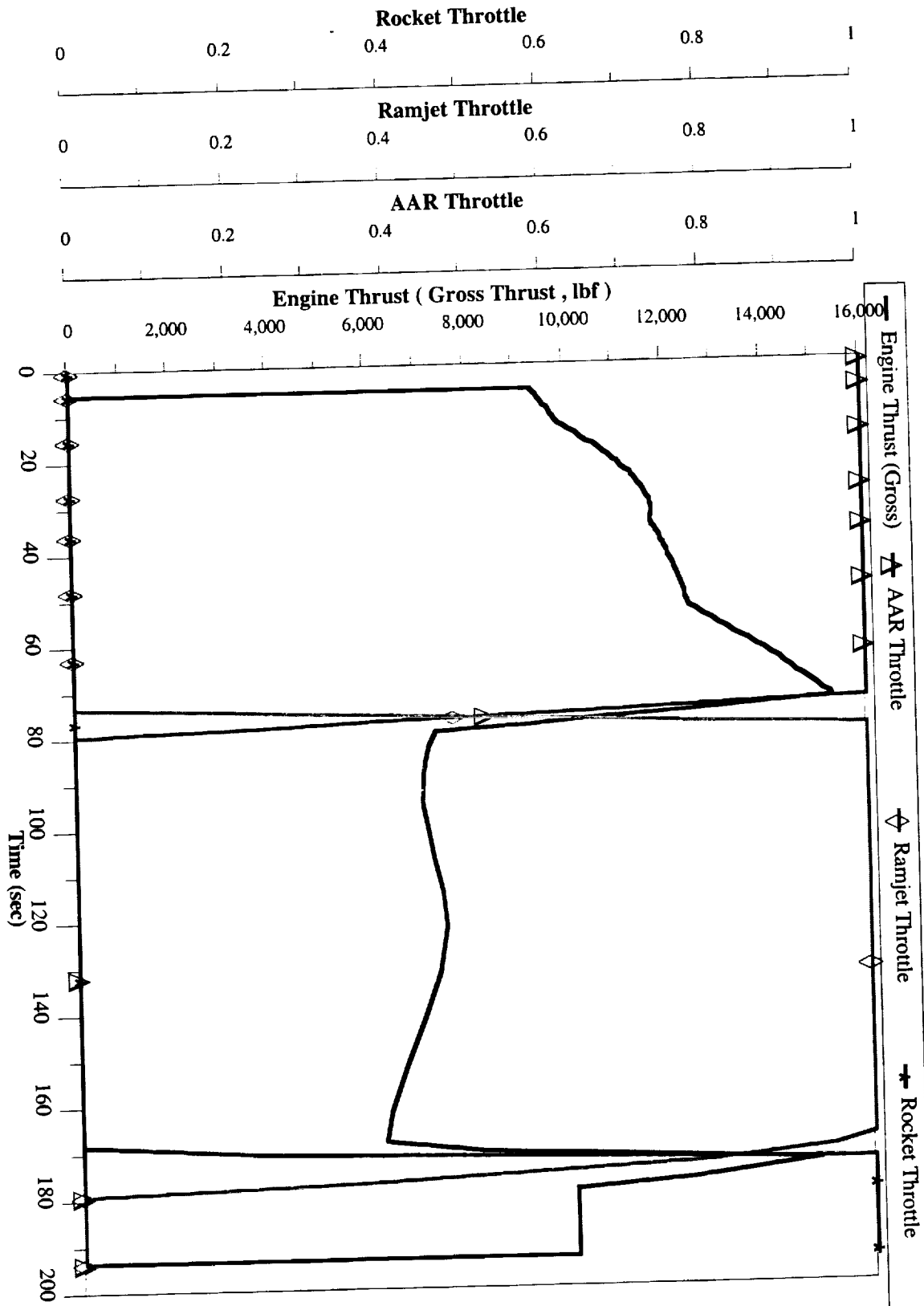
F6: NASA F6GTLOX/PropaneA



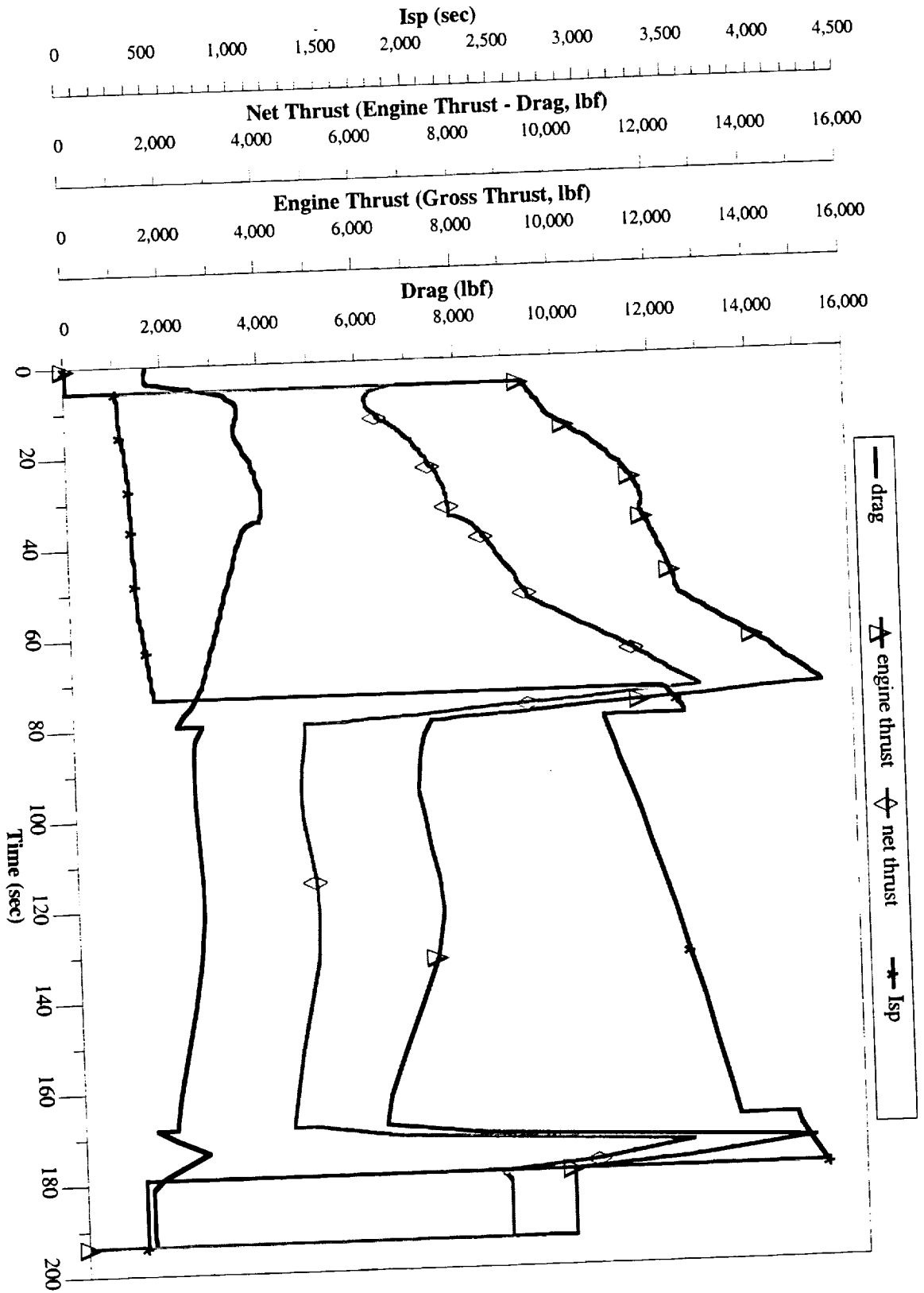
F6: NASA F6GTLOX/PropaneA



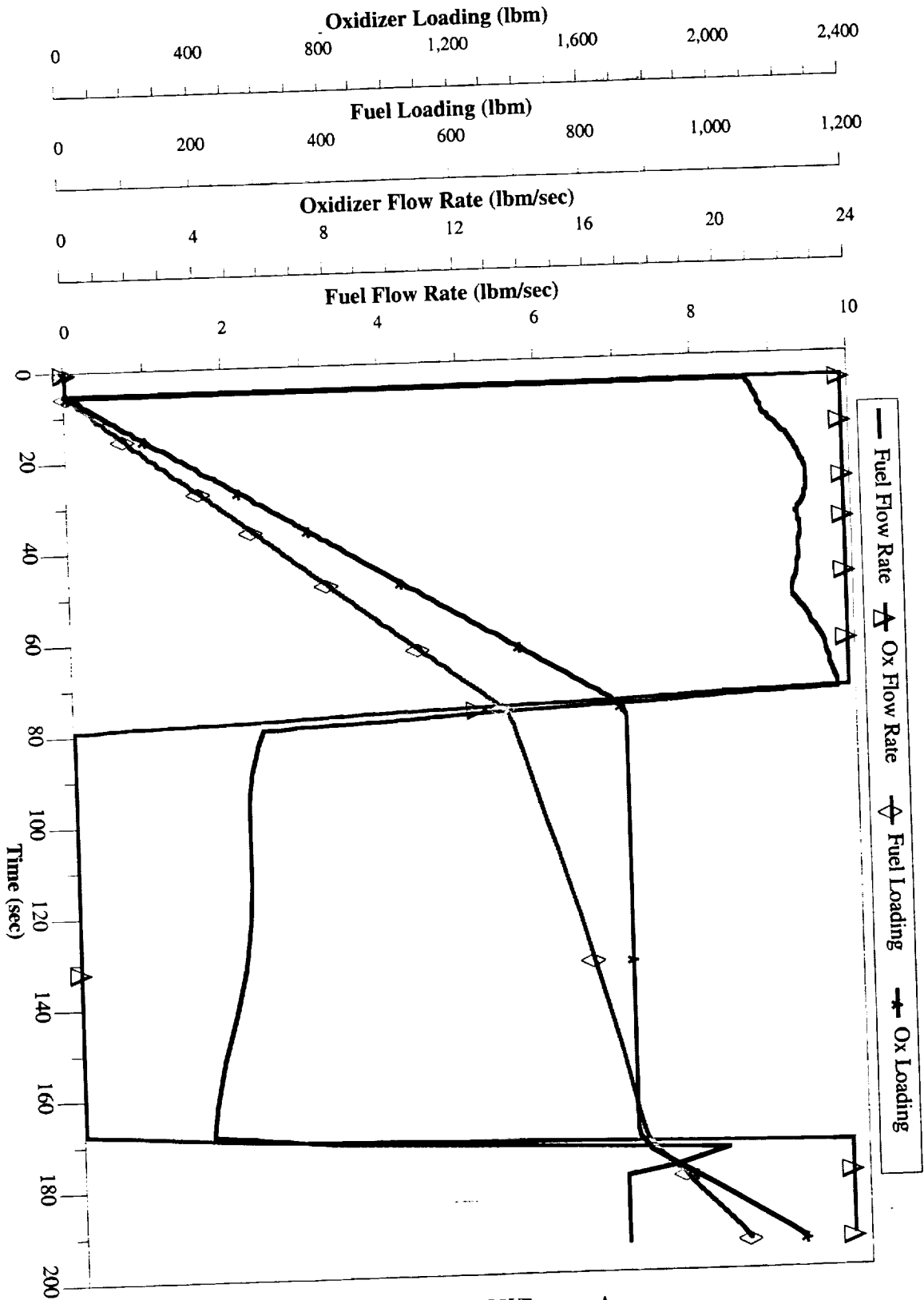
F6: NASA F6GTLOX/PropaneA



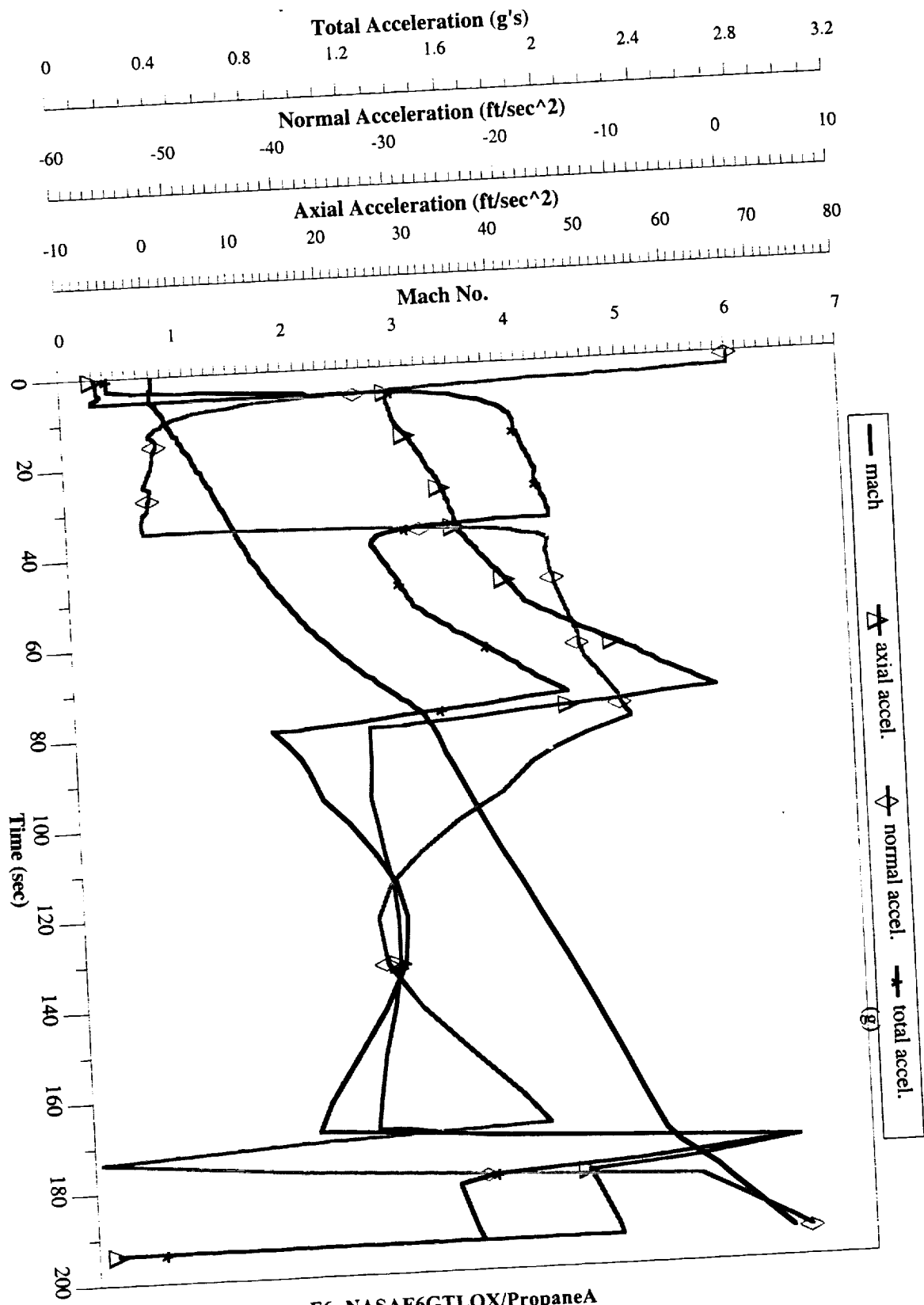
F6: NASA F6GTLOX/PropaneA



F6: NASA F6GTLOX/Propane A



F6: NASA F6GTLOX/PropaneA



F6: NASA F6GTLOX/Propane A